

APPLICATION OF IN-SITU REMEDIATION BY USING SOIL PHOSPHATE
AMENDMENTS AT THREE LEAD CONTAMINATED SOIL SITES
(RESIDENTIAL YARDS) IN NEW ORLEANS, LA.

by

DHARY SAAD ALKANDARY

Presented to the Faculty of the Graduate School of
The University of Texas at Arlington in Partial Fulfillment
of the Requirements
for the Degree of

DOCTOR OF PHILOSOPHY

THE UNIVERSITY OF TEXAS AT ARLINGTON

DECEMBER 2014

Copyright © by Dhary Alkandary 2014

All Rights Reserved



Acknowledgements

First, I would like to thank my advisor, Dr. Andrew Hunt for his effort, time and advice during these past four years. I have learned much from him. This work would not have been accomplished without his support. Second, I would like to thank the members of my graduate committee, Dr. Games Grover, Dr. John Weckham, Dr. Arne Winguth and Dr. Melanie Sattler for their knowledge and suggestions they have provided to improve this research.

I am grateful to the Department of Housing and Urban Development (HUD) for grant TXLHT0172-10, which funded our lab analysis. I would also like to thank Mr. Mel Chen for his support and interest in helping to protect our environment. I would like to thank the field operation manager Ben Shirtcliff for managing sites installation and samples collection in the last years in New Orleans.

My appreciation goes also for Kuwait University for their financial support especially the Department of Earth and Environmental Science and the head of the department, Dr. Mohammad Al Sarawi.

Finally, I would like to thank my parents, brothers and my friends for their help, encouragement and support during my studies over the past several years.

November 24, 2014

Abstract

APPLICATION OF IN-SITU REMEDIATION BY USING SOIL PHOSPHATE
AMENDMENTS AT THREE LEAD CONTAMINATED SOIL SITES
(RESIDENTIAL YARDS) IN NEW ORLEANS, LA.

Dhary Alkandary, PhD

The University of Texas at Arlington, 2014

Supervising Professor: Andrew Hunt

Lead (Pb) contamination of soil continues as a threat to public health. The problem exists, in part, due to the abundance of lead in soil in certain contexts which has the potential to cause adverse health effects in children at relatively low exposure levels. The dominant source of lead in soils in the city of New Orleans, in the older urban areas close to residences, is old deteriorated lead-based paint. A cost-effective intervention method to address the problem of lead in these soils is needed to reduce the Pb exposure risk for people in these areas.

Excavation and removal of lead (Pb) contaminated soils has been widely used as a remediation technique whereby the contaminated soil is removed, transported to a suitable landfill site, and clean soil is used to replace excavated soil. However, the cost of this "dig and dump" method is high, and the availability of an appropriate landfill may be problematic.

Several alternative, low-cost, and effective methods are now being used to remediate lead contaminated soils. *In situ* methods involve the treatment of soil in the contaminated locations. The treatment technique is based on adding a chemical stabilization agent to the soil in such manner as to immobilize the contaminants. A chemical stabilization amendment that is widely used phosphate, as it has the ability to combine with metal contaminants and form a stable mineral that is sparingly soluble, and stable in low pH conditions (such as in the human stomach).

The phosphate amendment is used in lead (Pb)-contaminated soils for several reasons. Namely, it combines with soluble Pb ions in the soil to form an insoluble crystalline lead phosphate mineral (pyromorphite). Also, pyromorphite has a low solubility product (K_{sp}) of approximately 10^{-80} so remains in the soil as immobile mineral. Apatite II is a biogenic phosphate, fish bones that can be applied to soil and it has been the focus of much attention because it is inexpensive, stable under various pH conditions, and it slowly and continuously supplies sufficient amount of phosphorous to form the mineral pyromorphite.

Here we propose to assess the suitability of Apatite II as an *in situ* soil amendment for lead in soil at urban residential sites. Specifically for the use on lead contaminated soils in New Orleans, LA. Three different sites have been chosen for this study to prove the effectiveness of Apatite II in treating lead contaminated soils. Also, other types of amendments will be used as phosphate

sources and a comparison will be made between each to show the effectiveness of Apatite II to the other phosphate agents. In our study, we propose to demonstrate that not only is Apatite II an effective intervention product, but is also an environmentally acceptable agent that does not excessively leach from the soil.

It was anticipated that Apatite II would be a better phosphate amendment agent than other types of phosphate. The potential problems associated with rapidly releasing phosphate agents involve phosphorus entering groundwater and then passing into standing water bodies and causing eutrophication. The work here will determine the advantage of Apatite II over other forms of phosphate agents in terms of leaching into the soil solution. In addition to evaluating the efficacy of Apatite II, the “Treat Lock and Cover” (TLC) approach that has been promulgated by the Artist Mel Chin (<http://www.fundred.org/about/operation-paydirt.php>), that involves capping the amended soil with clean layer of soil, is also to be tested by evaluating the action of Apatite II at depth in the soil. The advantage of TLC is that a barrier is put in place (the clean capping soil) for the time period over which conversion of the soil Pb to a sparingly soluble form occurs.

The principal idea of the study is to demonstrate that Apatite II can be presented as clean-up "method of choice" for lead contaminated soils in urban areas. By demonstrating this, we also propose to show that Apatite II can be used

as a remediation agent on a large urban scale as there is a recognized need for city wide remediation of lead contaminated soils in cities like New Orleans, LA.

Table of Contents

Acknowledgements.....	iii
Abstract.....	iv
List of Illustrations.....	xv
List of Tables.....	xx
Chapter 1 Introduction.....	1
1.1 Childhood Pb Exposure/Pb Poisoning.....	1
1.1.1 Exposure/Health Problems.....	2
1.1.2 Elevated Blood Pb Levels.....	3
1.1.3 Source of Pb.....	5
1.1.4 EPA/CDC Thresholds.....	6
1.1.5 History of Pb Use.....	8
Chapter 2 Background.....	14
2.1 Study of Lead in Soil.....	14
2.1.1 Speciation/ Nature of Pb in Soil.....	14
2.1.2 Pb Bioavailability.....	21
2.1.3 In vivo/In vitro Studies.....	22
2.2 Soil Remediation Methods.....	27
2.2.1 Soil Remediation Methods.....	27
2.2.1.1 In-Place Remediation without Permanent Soil Additions.....	27

2.2.1.2 Phytoremediation	29
2.2.1.3 Chemical Stabilization	30
2.2.1.4 Biosolids	30
2.2.1.5 Phosphate Amendments.....	31
2.2.1.5.1 Hydroxyapatite.....	33
2.2.1.5.2 Apatite II	35
2.2.1.5.3 Rock Phosphate.....	36
2.2.1.5.4 Bone Meal	37
2.2.1.5.5 Bone Char	38
2.2.1.5.6 Triple-Superphosphate (TSP)	39
2.2.1.5.7 Phosphorous Pentoxide.....	40
2.3 Research Objective and Hypotheses.....	40
Chapter 3 Experimental Design	44
3.1 Experimental Design.....	40
3.1.1 Reconnaissance survey and site selection	49
3.1.1.1 Phase 1	49
3.1.2 Site preparation and base line sampling	52
3.1.2.1 Phase 2	52
3.1.3 Amendment application	55
3.1.3.1 Phase 3	55
3.1.4 Post-treatment monitoring	59

3.1.4.1 Phase 4	59
3.1.5 Statistical Basis for Study Design	59
3.1.6 Quality Assurance Mechanisms	62
3.1.6.1 Field Quality Assurance.....	62
3.1.7 Standard Reference Materials	62
3.1.8 ICP-MS Quality Control (QC)	62
Chapter 4 Materials and Methods	64
4.1 Materials	64
4.1.1 A. Soil.....	64
4.1.2 B. Capping soil	64
4.1.3 C. Equipment.....	65
4.1.4 D. Water	65
4.1.5 E. Lysimeters.....	66
4.1.6 F. Fencing.....	67
4.1.7 G. Amendments.....	67
4.1.8 G. Ground barrier	69
4.2 Methods	70
4.2.1 pH, Moisture content, Loss on ignition (LOI).....	72
4.2.2 Total Pb in soil	74
4.2.3 Soil relative bioaccessibility (RBA) lead content	75

4.2.4 Scanning Electron Microscopy (SEM) with Energy- Dispersive X-Ray Spectroscopy (EDS)	81
4.2.5 Extended X-ray Absorption fine structure (EXAFS) spectroscopy	82
4.2.6 Phosphorous content of soil pore water	84
Chapter 5 Results	87
5.1.Results.....	87
5.1.1 Soil Analysis.....	87
5.1.1.1 Total Soil Pb	87
5.1.1.1.1 Reconnaissance Samples	87
5.1.1.1.2 Weak Acid Digest.....	92
5.1.1.1.3 Strong Acid Digest.....	93
5.1.1.2 Pb Bioaccessibility.....	93
5.1.1.2.1 Comparison of Zero and Twelve Months Bioaccessibility Results	93
5.1.1.3 Soil pH, Loss On Ignition (LOI), and Moisture content.....	105
5.1.1.4 Extended X-ray Absorption Fine Structure Spectroscopy (EXAFS).....	117
5.1.1.5 Water phosphorous content data (Lysimeters) by Induced Coupled Plasma Mass Spectroscopy (ICP-MS).....	121
5.1.1.7 Scanning Electron Microscope (SEM) Analysis	132

5.1.1.7.1 Zero Month Soil Samples: Individual Particle Analysis (IPA)	132
5.1.1.7.2 Summary of results obtained from IPA analysis of Pb in the soils sampled at zero month at 1613 St. Roche Ave.....	133
5.1.1.7.3 Twelve Months Soil Samples: Individual Particle Analysis (IPA)	133
5.1.1.7.1.2 1613 St. Roche Ave. plots (1A, 2A, 3A, 4A).....	133
5.1.1.7.4 Summary of results obtained from IPA analysis of Pb in the soils sampled at twelve months at 1613 St. Roche Ave.	134
5.1.1.7.5 Zero Month Soil Samples: Individual Particle Analysis (IPA)	134
5.1.1.7.1.3 1818 Dumaine St. plots (1A, 2A, 3A, 4A).....	134
5.1.1.7.6 Summary of results obtained from IPA analysis of Pb in the soils sampled at zero month at 1818 Dumaine St.	135
5.1.1.7.7 Twelve Months Soil Samples: Individual Particle Analysis (IPA)	136
5.1.1.7.1.4 1818 Dumaine St. plots (1A, 2A, 3A, 4A).....	136
5.1.1.7.8 Summary of results obtained from IPA analysis of Pb in the soils sampled at twelve month at 1818 Dumaine St.	137

5.1.1.7.9 Zero Month Soil Samples: Individual Particle Analysis (IPA)	137
5.1.1.7.1.5 2224 N. Prieur St. plots (1A, 2A, 3A, 4A)	137
5.1.1.7.10 Summary of results obtained from IPA analysis of Pb in the soils sampled at zero month at 2224 N.Prieur St.	137
5.1.1.7.11 Twelve Months Soil Samples: Individual Particle Analysis (IPA)	138
5.1.1.7.1.6 2224 N. Prieur St. plots (1A, 2A, 3A, 4A)	138
5.1.1.7.12 Summary of results obtained from IPA analysis of Pb in the soils sampled at twelve months at 2224 N.Prieur St.	138
Chapter 6 Discussion and Conclusions	140
6.1 Discussion	140
6.2 Conclusions	154
6.2.1 Conclusions	154
6.2.2 Areas for Future Study	156
Appendix A SEM Images and X-Ray Spectra of Amendments	157
Appendix B SEM Images and X-Ray Spectra of Zero Month 1613 St. Roche Samples	163
Appendix C SEM Images and X-Ray Spectra of Twelve Months Post Treatment 1613 St. Roche Samples	184

Appendix D SEM Images and X-Ray Spectra of Zero Month 1818	
Dumaine St. Samples	201
Appendix E SEM Images and X-Ray Spectra of Twelve Months Post	
Treatment 1818 Dumaine St. Samples.....	220
Appendix F SEM Images and X-Ray Spectra of Zero Month 2224	
N.Prieur St. Samples	236
Appendix G SEM Images and X-Ray Spectra of Twelve Months Post	
Treatment 2224 N.Prieur St. Samples.....	253
Appendix H 1613 St. Roche Ave. General Site Images	270
Appendix I 1818 Dumaine St. General Site Images	282
Appendix J 2224 N. Prieur St. General Site Images.....	298
References.....	348
Biographical Information.....	396

List of Illustrations

Figure 1-1 Median blood Pb vs. median soil Pb.....	9
Figure 1-2 Part A, census tract median blood Pb distribution in grades of shaded gray for pre-Katrina. Part B, census tract median blood Pb distribution for post-Katrina.....	12
Figure 2-1 Level on maximum effect of soil pH on Pb, Cu, Zn, and Ni retention by Dekalb and Hagerstown A and B horizons. N1 and N2 refer to maximum apparent sorption.....	16
Figure 2-2 pH-Eh diagram of the stability of Pb-bearing minerals in ecosystems	19
Figure 4-1 Bonnet Carré Spillway cap soil.....	65
Figure 4-2 Lysimeter installation.....	66
Figure 4-3 Fencing.....	67
Figure 4-4 Ground barrier.....	70
Figure 4-5 WDXRF Benchtop Supermini Rigaku.....	71
Figure 4-6 Fisher Scientific accumet basic AB15pH meter	73
Figure 4-7 TCLP Extractor	77
Figure 4-8 Filtering system.....	79
Figure 4-9 Image of Scanning Electron Microscopy-Energy Dispersive Spectroscopy ASPEX® SEM-EDS.....	82
Figure 4-10 Pb XANES spectra standards for fitting	83

Figure 4-11 Sample recovery from the filter media. Figure from Campbell Monoflex Lysimeter.....	85
Figure 5-1 Comparison of average IVBA (%) between zero and twelve months apatite II un-capped 1613 St. Roche soil	99
Figure 5-2 Comparison of average IVBA (%) between zero and twelve months apatite II capped 1613 St. Roche soil.....	100
Figure 5-3 Comparison of average IVBA (%) between zero and twelve months apatite II capped and un-capped 1613 St. Roche soil	100
Figure 5-4 Comparison of average IVBA (%) between zero and twelve months rock phosphate un-capped 1613 St. Roche soil	101
Figure 5-5 Comparison of average IVBA (%) between zero and twelve months rock phosphate capped 1613 St. Roche soil.....	101
Figure 5-6 Comparison of average IVBA (%) between zero and twelve months rock phosphate capped and un-capped 1613 St. Roche soil	102
Figure 5-7 Comparison of average IVBA (%) between zero and twelve months TSP un-capped 1613 St. Roche soil.....	102
Figure 5-8 Comparison of average IVBA (%) between zero and twelve months TSP capped 1613 St. Roche soil.....	103
Figure 5-9 Comparison of average IVBA (%) between zero and twelve months TSP capped and un-capped 1613 St. Roche soil.....	103

Figure 5-10 Comparison of average IVBA (%) between zero and twelve months control un-capped 1613 St. Roche soil	104
Figure 5-11 Comparison of average IVBA (%) between zero and twelve months control capped 1613 St. Roche soil.....	104
Figure 5-12 Comparison of average IVBA (%) between zero and twelve months control capped and un-capped 1613 St. Roche soil	105
Figure 5-13 Average pH at both t = 0 and t = 12 months for un-capped soils at 1613 St. Roche Ave. site.....	107
Figure 5-14 Average pH at both t = 0 and t = 12 months for capped soils at 1613 St. Roche Ave. site.....	107
Figure 5-15 Average LOI (%) for un-capped and capped soils at 1613 St. Roche Ave. site.....	108
Figure 5-16 Average moisture content (%) for un-capped and capped soils at 1613 St. Roche Ave. site.....	108
Figure 5-17 Average pH at both t = 0 and t = 12 months for un-capped soils at 1818 Dumaine St. site.....	111
Figure 5-18 Average pH at both t = 0 and t = 12 months for capped soils at 1818 Dumaine St. site.....	112
Figure 5-19 Average LOI (%) for capped and un-capped soils for 1818 Dumaine St. site.....	112

Figure 5-20 Average moisture content (%) for capped and un-capped soils at 1818 Dumaine St. site	113
Figure 5-21 Average pH at t = 0 and t = 12 months for capped soils at 2224 N. Prieur St. site	115
Figure 5-22 Average pH at t = 0 and t = 12 months for un-capped soils at 2224 N. Prieur St. site	115
Figure 5-23 Average LOI (%) for capped and un-capped soils for 2224 N. Prieur St. site	116
Figure 5-24 Average moisture content (%) for capped and un-capped soils at 2224 N. Prieur St. site	116
Figure 5-25 Lysimeter data of water Phosphorous content leach into the soil treated with Apatite II at 1613 St Roche Ave. site	122
Figure 5-26 Lysimeter data of water Phosphorous content leach into the soil treated with Roch Phosphate at 1613 St Roche Ave. site	123
Figure 5-27 Lysimeter data of water Phosphorous content leach into the soil treated with TSP at 1613 St Roche Ave. site	123
Figure 5-28 Lysimeter data of water Phosphorous content leach into the Un- treated soil at 1613 St Roche Ave. site	124
Figure 5-29 A twelve months average Lysimeter data of water Phosphorous content leach into the soil at 1613 St. Roche Ave. site.....	124

Figure 5-30 Lysimeter data of water Phosphorous content leach into the soil treated with Hydroxyapatite at 1818 Dumaine St. site	126
Figure 5-31 Lysimeter data of water Phosphorous content leach into the soil treated with Phosphorous Pentoxide at 1818 Dumaine St. site	126
Figure 5-32 Lysimeter data of water Phosphorous content leach into the soil treated with Apatite II at 1818 Dumaine St. site.....	127
Figure 5-33 Lysimeter data of water Phosphorous content leach into the Untreated soil at 1818 Dumaine St. site	127
Figure 5-34 A twelve months average Lysimeter data of water Phosphorous content leach into the soil at 1818 Dumaine St. site	128
Figure 5-35 Lysimeter data of water Phosphorous content leach into the Untreated soil at 2224 N. Prieur St. site	130
Figure 5-36 Lysimeter data of water Phosphorous content leach into the soil treated with Bone Char at 2224 N. Prieur St. site.....	130
Figure 5-37 Lysimeter data of water Phosphorous content leach into the soil treated with Apatite II at 2224 N. Prieur St. site.....	131
Figure 5-38 Lysimeter data of water Phosphorous content leach into the soil treated with Bone Meal at 2224 N. Prieur St. site	131
Figure 5-39 A twelve months average Lysimeter data of water Phosphorous content leach into the soil at 2224 N. Prieur St. site	132

List of Tables

Table 1-1 Comparison of Total Black and White Population Based on HMCT and LMCT 1990 Census Tracts Demographic Data in New Orleans Metropolis	10
Table 2-1 Solubility Products of Pb Phosphate Minerals at 298 K.	19
Table 3-1 Sample Sizes Required to Detect the Assumed Difference with 70% Power with 0.05 One-Sided and Two-Sided α	61
Table 4-1 Description of Used Amendments, Quantities, Source, and Costs in Three Locations	68
Table 5-1 Total Pb of 1613 St. Roche Ave. Reconnaissance Samples with DMS Coordinates	88
Table 5-2 Total Pb of 1818 Dumaine St. Reconnaissance Samples with DMS Coordinates	89
Table 5-3 Total Pb of 2224 N. Prieur St. Reconnaissance Samples with DMS Coordinates	91
Table 5-4 Calculated <i>In Vitro</i> Bioaccessibility of Pb as a Percentage of Total Pb in Zero and Twelve Months Un-capped Soil at 1613 St. Roche Ave.....	94
Table 5-5 Calculated <i>In Vitro</i> Bioaccessibility of Pb as a Percentage of Total Pb in Zero and Twelve Months Capped Soil at 1613 St. Roche Ave	97

Table 5-6 Average LOI, Average pH at both t = 0 and t = 12 Months and Average Moisture Content Data per Plot for Uncapped Soils for 1613 St. Roche Ave. Site.....	106
Table 5-7 Average LOI, Average pH at both t = 0 and t = 12 Months and Average Moisture Content Data per Plot for Capped Soils for 1613 St. Roche Ave. Site.....	106
Table 5-8 Average LOI, Average pH at both t = 0 and t = 12 Months and Average Moisture Content Data per Plot for Uncapped Soils for 1818 Dumaine St. Site.....	109
Table 5-9 Average LOI, Average pH at both t = 0 and t = 12 Months and Average Moisture Content Data per Plot for Capped Soils for 1818 Dumaine St. Site	110
Table 5-10 Average LOI, Average pH at both t = 0 and t = 12 Months and Average Moisture Content Data per Plot for Capped Soils for 2224 N.Prieur St. Site	113
Table 5-11 Average LOI, Average pH at both t = 0 and t = 12 Months and Average Moisture Content Data per Plot for Uncapped Soils for 2224 N.Prieur St. Site	114
Table 5-12 Weighted Speciation Distribution Percent EXAFS Data for St. Roche, Dumaine St., and N. Prieur St. Soils at Time Zero and Twelve Months	120

Table 5-13 Phosphorous Water Content at 1-, 2-, 3-, 4-, 5-, 6- and 12- Months at 1613 St. Roche Ave. Site	121
Table 5-14 Phosphorous Water Content at 1-, 2-, 3-, 4-, 5-, 6- and 12- Months at 1818 Dumaine St. Site	125
Table 5-15 Phosphorous Water Content at 1-, 2-, 3-, 4-, 5-, and 6- Months at 2224 N. Prieur St. Site	128

Chapter 1

Introduction

1.1 Childhood Pb Exposure/Pb Poisoning

There has been much concern that childhood lead (Pb) exposure can cause various adverse health effects at relatively low levels. Extensive studies were done on Pb exposure, pathways, poisoning and elevated blood lead levels in children because they are more vulnerable to Pb exposure than adults due to their activity behavior and the greater rates of incidental ingestion (direct contact) of soil or re-suspension of Pb dust (inhalation) (Abdel *et al.* 2010; Belluck *et al.* 2003; Laidlaw *et al.*, 2005, 2012; Mielke and Reagan, 1998; Mukerjee, 1998; Reagan and Silbergeld, 1990). The USEPA Consolidated Human Activity Database (CHAD) provides data

based on children's cohort activities which suggests the prediction of children's Pb ingestion to be more reasonable by determine the children's life style and activities in home, school, and park (Abel *et al.* 2012). The prediction of potential toxicity of Pb to children can be estimated by calculating the fraction of soil lead concentration (Schoof *et al.* 1995).

In the United States, the National Health and Nutrition Examination Surveys (NHANES) published data showed that the Pb poisoning cases is not equally distributed (Gould 2009). The study demonstrated the reduction of 84 % overall prevalence of blood lead levels $\geq 10 \mu\text{g/dL}$ in U.S. children from 8.6 % in

1988-1991 to 1.4 % in 1999-2004 (Jones *et al.* 2009). This prevalence is much less than previously reported (CDC, 2005); however the prediction of susceptible children's to Pb exposure between age 1 to 4 years is challenging due to lack of data (Abdel *et al.* 2010).and disparities still exist. The possible exposure of contaminated Pb soils can cause adverse health effects to children due to hand-to-mouth activities (Laperche 2000). A correlation between the Pb contaminated hand and blood Pb levels was shown in the literature (Clark *et al.*, 1991) with the greatest Pb exposure from direct contaminated urban soils ingestion (Chaney and Ryan, 1994; Chaney *et al.*, 1989).

1.1.1 Exposure/Health Problems

The adverse health effects of the pediatric population resulting from lead exposure are huge and the weakness of neurological development considered to be "critical effect" (USEPA 2006, CDC 2009, Bellinger 2008, Lanphear *et al.* 2005). Recent studies show that the decrement in intelligence quotient score in children's blood lead that increase from 1 to 10 µg/dL is larger than increases from 10 to 20 µg/dL, or from 20 to 30 µg/dL (Lanphear *et al.* 2005; Canfield *et al.* 2003; Schwartz 1994).

Several recent studies (Canfield *et al.*, 2003, Chiodo *et al.*, 2004, Jusko *et al.*, 2008, Lanphear *et al.*, 2005, Miranda *et al.*, 2007, Surkan *et al.*, 2007, Téllez-Rojo *et al.*, 2006) have documented adverse effects and childhood decrements in intelligence quotient (IQ) at blood lead concentrations less than 10 µg/dL. Also,

some newer studies have identified an association between early lead exposure and increased incidence of attention deficit hyperactivity disorder (ADHD) (Nigg *et al.*, 2008, 2010), ADHD coupled with other behavior problems (Roy *et al.*, 2008), and other behavioral problems (Chen *et al.*, 2007). However, different studies suggested that no lower bound threshold is mandatory to determine impairment of neurological development (Chiodo *et al.* 2004) and other organs such as kidney, the gastrointestinal tract, and immune system can be affected in relatively low Pb exposure (Skerving and Bergdahl, 2007; Goyer, 1996).

1.1.2 Elevated Blood Pb Levels

A study showed the relationship between the soil Pb and elevated blood lead levels in children in Marion County, Indianapolis, Indiana (Filippelli *et al.* 2005). A higher blood lead levels were recorded in children aged 6-30 months than the 0-5 month- old children for low income Hispanic or non-Hispanic blacks living in older houses (Deborah *et al.* 2013). Also, a study of the association of elevated blood lead levels and Mental Development Index (MDI) of the Bayley scales between 9,489 infants born between 1979 and 1981 at Brigham and Women's Hospital in Boston has been done (Bellinger *et al.* 1985). The infants were divided into three groups of low $< 3 \mu\text{g/dL}$, medium 6 to 7 $\mu\text{g/dL}$, and high $\geq 10 \mu\text{g/dL}$ blood Pb concentrations. It has been suggested that infants with higher blood Pb levels had lower MDI (Bellinger *et al.* 1985). One study in Michigan, Detroit has identified the relationship between seasonal variation and

blood Pb levels in children where Pb in urban soils are re-suspended in the air dust due to precipitation, humidity, and wind which may be inhaled or ingested by children (Zahran *et al.*, 2013).

The absorption and retention of Pb ingested with food as a source of lead exposure has been calculated by using urine samples of twelve infants in age 14 to 746 days in Iowa (Ziegler *et al.* 1978). This study determined that the retention of Pb was highly correlated with lead absorption which increases the prevalence Pb intoxication for children (Ziegler *et al.* 1978). Thus, the long term of environmental exposure to Pb may affect the intellectual development (Landsdown *et al.*, 1986 Harvey *et al.*, 1988).

The major route of lead exposure for children is hand-to-mouth activities for Pb in soil or dust (RCEP, 1983, Davies *et al.*, 1990). According to Culbard *et al.* (1988), the average soil Pb concentration was 5,610 µg/g in Derbyshire villages in U.K. related to historic lead mining and the average house dust was 1,870 µg/g. Baltrop *et al.* (1975) demonstrated that the average blood lead levels for young children were 25 µg/dL. Several models have been constructed to predict the children's blood Pb levels related to high concentration of Pb in soil and dust (Duggan, 1983, Duggan and Inskip, 1985, Laxen *et al.*, 1987, Davies *et al.*, 1990) where an increase of 5 µg/dL in blood level refers to 1,000 µg/g increase in soil or dust Pb concentration (Cotter-Howells *et al.* 1991).

1.1.3 Source of Pb

Undoubtedly, some fraction of lead in soil comes from historic gasoline emissions and a major source of lead in soil is old lead-based paint once applied to the exterior of houses. Also, different studies have determined that indoor dust is one of major exposure pathway for infants (Hunt *et al.* 1993; Simon *et al.* 2007) and exposure can be considerably huge when the soil particle fraction is less than 250 μm that adhere to children's hands (Juhasz *et al.* 2011).

In recent years, many studies have been conducted to assess the distribution of surface soil Pb in New Orleans, LA due to hurricanes Katrina and Rita (Abel *et al.* 2012). A spatial distribution model has been constructed by Abdel *et al.* (2010) and a correlated spatial map for Mielke *et al.* (1999) suggested that no change in the surface soil Pb was occurred after hurricanes Katrina and Rita (Abel *et al.* 2012).

However Zaharan *et al.* (2010) have mentioned that the soil lead levels in New Orleans dropped down by approximately 125 mg/kg after Hurricane Katrina and this was consistent with children's blood lead levels reduction. However, different studies argue that the concentration of soil lead is insignificant for pre- and post-Hurricane Katrina (Abdel *et al.*, 2010a; 2010b).

Some areas in New Orleans have alarming soil Pb content. The average Pb soil content in the yard was set as 1,200 mg/kg by the Environmental Protection Agency (EPA) and a level of 400 mg/kg of lead in soil was determined as lead

hazard for children. This level has been determined based on a blood lead level of concern (from Centers for Disease Control and Prevention (CDC)) of 10 µg/dL blood lead.

1.1.4 EPA/CDC Thresholds

Currently, the EPA's lead hazard standard permits a level of 400 mg/kg of lead in bare soil in children's play areas or 1,200 mg/kg average for bare soil in the rest of the yard. The level of 400 mg/kg is based on a blood lead level of concern (from CDC) of 10 µg/dL blood lead and 44% lead bioavailability. It has been suggested in EPA circles (S. Calanog, USEPA Region 9, pers. comm.) that if the blood lead level of concern was to be reduced to 5 µg/dL and no other parameters were changed (i.e., soil lead bioavailability) then the acceptable level would drop from 400 mg/kg to 150 mg/kg.

Significantly, the California Office of Environmental Health Hazard Assessment (OEHHA) has recently developed a 1 µg/dL benchmark for source-specific incremental change in blood lead levels for protection of school children and fetuses (OEHHA, 2007).

The resultant revised California human health screening level for lead in soil that has been proposed (OEHHA, 2009), would be 80 mg/kg. In the wake of the California EPA's proposed revision it has been suggested the USEPA might revise its hazard standard down to 80 mg/kg also. A revised USEPA hazard

standard of 80 mg/kg or even 150 mg/kg would greatly increase the urban land area with soil considered as hazardous in terms of its lead content.

In the literature, the average soil Pb concentration in the soil is 8,550 $\mu\text{g/g}$ which is considered to be alarming and blood Pb testing is the tool for soil remediation targets (Moodie and Evans, 2011; USEPA, 2005, 2000). Pb surface soil (<5 cm) contamination was measured to estimate children Pb exposure. As a result of massive soil Pb contamination and insidious public health threat, the CDC recommends actions to be taken to for public health protection for child's blood lead level exceeds the recommended threshold which is 5 $\mu\text{g/dL}$ based on the 97.5th percentile of blood Pb levels in the U.S. children aged between 1 and 5 years (CDC, 2012).

The approximate amount of Pb exposed to children was > 33.5 $\mu\text{g/dL}$ which exceeded the updated blood Pb level of concern of the Center for Disease Control and Prevention (CDC) (Abel *et al.* 2012). A reduction in children's blood Pb levels in the U.S. has been noticed in the last sixty years (Chiodo *et al.* 2004) however, elevated Pb poisoned population still exists (Mielke and Reagan, 1998). The accumulation and spread of historic Pb in surface soil due to heavy use in the old cities (lead in paint and gasoline) make it exposed to children in urban areas even with the United States Environmental Protection Agency (USEPA) elimination (Abel *et al.* 2012, Skerving and Bergdahl, 2007).

1.1.5 History of Pb Use

The problem of elevated blood lead levels has long been known in New Orleans with two major sources of lead in soil: old lead-based paint and historic gasoline emission. The high Pb concentrations in neighborhood soils may increase the child blood Pb to a levels which exceed the lead level of concern (Mielke *et al.*, 2007; Zahran *et al.*, 2010, 2011).

For the general population of children, the global monitoring prevalence of elevated blood lead was about 11.8% $\geq 10\mu\text{g/dL}$ (Mielke *et al.*, 1997). The potential source of lead exposure for children is contaminated soil and it has been well documented for New Orleans area (Mielke *et al.*, 2006; Higgs *et al.*, 1999; Mielke *et al.*, 1997; Mielke 1994).

The relationship between soil lead levels and children blood lead levels for the years 2000-2005 has been evaluated by Mielke *et al.* in 2007 within residential communities. A consistent relationship identified between soil lead levels and blood lead levels with an increase in blood lead levels of 1.4 $\mu\text{g/dL}$ per 100 mg/kg lead with less than 100 mg/kg lead containing soil and with an increase in blood lead levels of 0.32 $\mu\text{g/dL}$ per 100 mg/kg lead with greater than 300 mg/kg lead in soil.

Several studies have indentified the association between soil Pb and elevated blood Pb levels in children especially in Minnesota and New Orleans (Mielke and Reagan, 1998; Mielke *et al.*, 1997, 1999, 2007a; Zahran *et al.*, 2011).

Also, other comparable studies in Syracuse, New York (Johnson and Bretsch, 2002) and Los Angeles, California (Wu *et al.*, 2010) have shown same trend in soil Pb and children's blood Pb levels which support the evidence of children's blood Pb levels response and dust contamination in urban cities (Laidlaw website; Mielke *et al.*, 2011a).

Furthermore, Mielke *et al.* (1999) has determined the non linear increase relationship between median blood Pb and median soil Pb to compare Higher Metal Census Tract (HMCT) and Lower Metal Census Tract (LMCT) by applying Atomic Absorption Spectrometry (AAS) methods on 173 census tracts data (Mielke *et al.*, 1997) and ICP-AES analysis on 175 census tracts model (Figure 1.1).

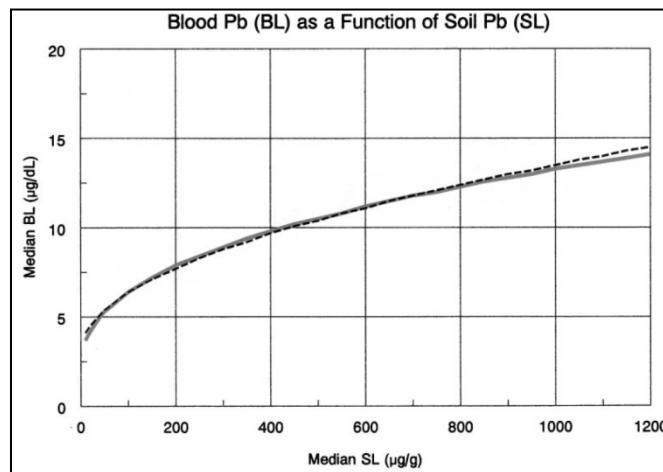


Figure 1.1 Median blood Pb vs. median soil Pb (After Mielke *et al.*, 1999).

In 1990, most of the population (750,551) lived in low metal census tract regions, majority of white people, and around 144,491 people lived in high metal

census tracts regions where the majority are black (Mielke *et al.*, 1999). The black people lived in older houses built in 1940's surrogate for Pb-based paint which consider to be high soil Pb contamination unfavorable conditions for homeowners inhabits (Table 1.1).

Table 1.1 Comparison of Total Black and White Population Based on HMCT and LMCT 1990 Census Tracts Demographic Data in New Orleans Metropolis (After Mielke *et al.*, 1999).

Demographic characteristics	Higher metal census tracts (n=72)	Lower metal census tracts (n=214)
Total population	144,491	750,551
Black population	86,607	273,566
White population	53,813	456,418
Total children		
≤6 years	14,233	77,982
Black children		
≤6 years	10,723	37,751
White children		
≤6 years	3,080	37,996

The major concern of childhood Pb exposure that the health problems in adulthood is still present (Bellinger, 2011) such as learning and self-control disabilities (Cecil *et al.*, 2008, 2011; Mielke and Zahran, 2012; Wright *et al.*, 2008). For instance, several studies of lead exposure for children in New Orleans have identified the reduction in the performance of standardized tests for students at district elementary schools and elevated toxic metals concentrations in soils

around them (Mielke *et al.*, 2005a; Mielke PW and Berry, 2007) and elevated blood lead levels associated with low student achievements tests because of the Pb neurotoxicity (Zahran *et al.*, 2009).

The social and racial differences between populations in New Orleans are associated with high or low Pb contaminated soils. For instance, poor African American or Hispanic people live in high soil Pb areas while rich white people with few exceptions live in low soil Pb neighborhoods (Campanella and Mielke, 2008). Undoubtedly, children from poor inhabits will be more exposed to soil Pb and dust. The concentration of Pb in inner city of New Orleans seems to be higher than the outlying areas due to large traffic flow, older housing, and the immediate vicinity of play yards to houses and streets (Mielke *et al.*, 2013).

Accordingly, recent extended study of soil Pb and blood Pb in children has identified the prevalence blood Pb greater than 5µg/dL was 58.5 % for high Pb inner city areas (> 100 mg/kg) and 25% for low Pb areas (<100 mg/kg) pre-Katrina. However, an opposite situation occurred in post- Katrina where the prevalence blood Pb greater than 5µg/dL was 30 % in high soil Pb content areas and 7.5 % in low soil Pb content areas. This study has been accomplished with 5,467 soil samples, 55,551 pre- Katrina blood Pb samples, and 7,384 post-Katrina blood Pb samples retrieved from the Louisiana Childhood Lead Poisoning Prevention Program (LACLPPP) (Mielke *et al.*, 2013) (Figure 1.2).

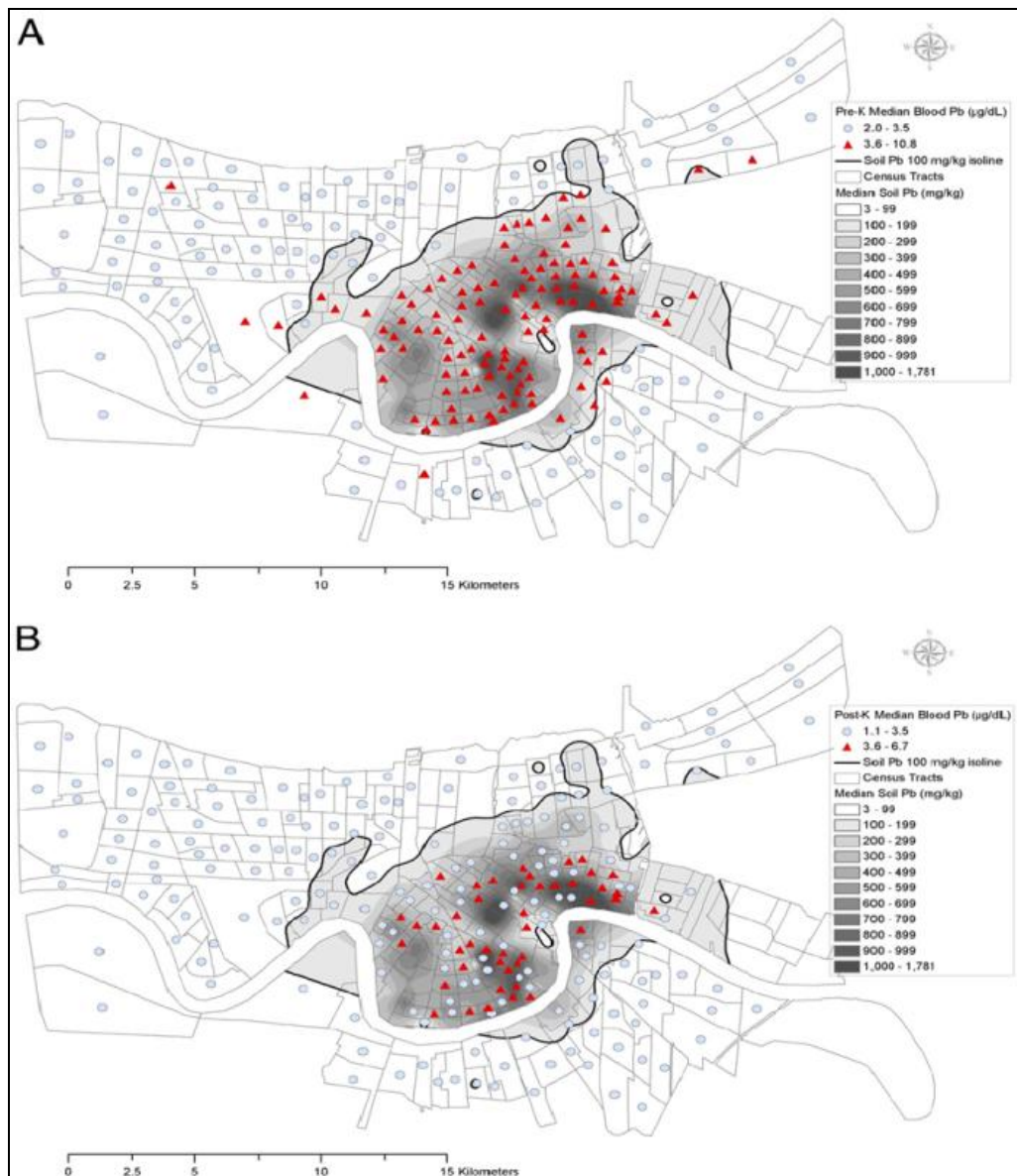


Figure 1.2 Part A, census tract median blood Pb distribution in grades of shaded gray for pre-Katrina. Part B, census tract median blood Pb distribution for post-

Katrina (After Mielke *et al.*, 2013).

As a comparison of public and private properties in inner and outlying areas within 800 meter radii from the center of public housing census tracts New Orleans, 224 soil samples were collected from ten public housing properties and 363 soil samples were collected from residential private properties. This study showed that the inner-city public properties median soil Pb concentration is 290 mg/kg and the medial soil Pb for the outlying properties is 84 mg/kg.

Mielke *et al.* (2011) concluded that the children's blood Pb prevalence greater than 10 $\mu\text{g/dL}$ is much more for those who live inner-city than outlying areas. He also included in his study the same conclusions for the inner-city and outlying areas residential private properties Mielke *et al.* (2011). He also mentioned that the soil Pb in the housing authority public properties is 202 mg/kg where in residential private properties the soil Pb is about 434 mg/kg. He also connected that to the children's blood Pb prevalence $\geq 10 \mu\text{g/dL}$ to be higher in residential private properties (25%) than in housing authority public properties (18.5%).

Chapter 2

Background

2.1 Study of Lead in Soil

2.1.1 Speciation/ Nature of Pb in Soil

The speciation of Pb, a toxic naturally occurring metal, is difficult to predict in soils because of different factors and parameters such as pH, moisture content, and diffusion rates (deTreville, 1964, Ruby *et al.*, 1994; Berti and Cunningham, 1997). Pb can be characterized by different forms due to the conversion to other compounds, such as Pb when it was present in gasoline converted to Pb sulfate in the atmosphere, and was deposited in relatively low-soluble particles in soils (Olson and Skogerboe, 1975, Zimdahl and Skogerboe, 1977). Pb residency in soil can be controlled by its speciation (i.e., how it is bound to the various soil phases). It can be precipitated as a sparingly soluble phase, it can be adsorbed onto clays, and Pb can form organic matter complexes (Davis 1995; Bradl, 2004).

The mobility of Pb in the soil profile depends on the solubility of the Pb in the soil, therefore the lack of mobility of Pb in soil is a result of how it is bound in the soil (Zimdahl and Skogerboe, 1977; Sauve *et al.*, 2000, Zimdahl and Skogerboe, 1977, Tornabene and Edwards, 1972). Other Pb mobility controlling factors include soil pH, low organic matter content of soil, sandy soil texture, concentration of mineral type in soil, and presence of water (Zimdahl and

Skogerboe, 1977; Cao *et al.*, 2008). Soil has a large capacity for Pb immobilization due to common small pH ranges in soil, cation exchange of the organic matter, and sorption by hydrous oxides (Zimdahl and Skogerboe, 1977).

Also, particle size distributions affect the Pb particles fixation processes (Berti *et al.*, 1998). Pb can also form a stable complex in the presence of dissolved organic matter (McLean and Bledsoe, 1992). The chemisorption of Pb is affected by the complex dependency on the amount and form of Pb introduced and present in the soil, soil properties, reduction-oxidation reactions, soil solution chemistry, amount of ligands and pH (McLean and Bledsoe, 1992; Ruby *et al.*, 1994).

Lowering the pH results in the liberation of Pb from various soil phases and, happily for the purposes of this study, phosphorus (P) goes into solution in the soil pore water and can form (with the Pb) Pb-phosphate minerals (Xu and Schwartz, 1994).

Harter (1983) concluded that the adsorption of Pb and other metals like zinc, nickel and copper did not require very low pH levels but increased with pH levels ranging from approximately 4.3 to 8.3 (Figure 6).

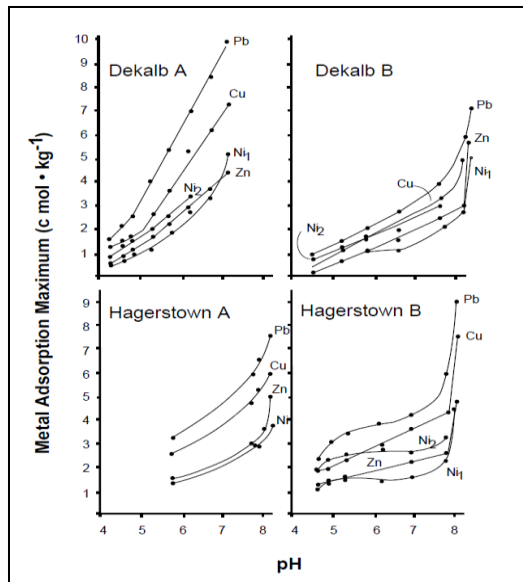


Figure 2.1 Level on maximum effect of soil pH on Pb, Cu, Zn, and Ni retention by Dekalb and Hagerstown A and B horizons. N1 and N2 refer to maximum apparent sorption (After Harter, 1983).

Clearly, Pb reacts with clays, phosphates, sulfates, carbonates, hydroxides, and organic matter, when present in soluble form, in soil, and the formation any thermodynamically stable Pb compounds reduces its solubility (McLean and Bledsoe, 1992). Pb Oxides and Pb Carbonates are common forms that are stable forms in the environment (Ruby *et al.*, 1994).

Following introduction of Pb into the soil and its dissolution, and entry into the soil pore water solution, Pb is highly adsorbed onto clay surfaces or precipitates as Pb carbonate in soils at pH greater than 6 (McLean and Bledsoe, 1992). This process can be modified, and it has been shown that Pb shows less

sorption in the presence of complexing ligands and competing cations because of the high affinity of Pb for ligands (McLean and Bledsoe, 1992, Puls *et al.*, 1991; Koutby-Amacher and Gambrell, 1988).

Although soil processes are dynamic and never at equilibrium, the idea of Pb sorption and reactions in soils can be determined by performing equilibrium kinetic studies in order to understand the transport of Pb in soils over certain time intervals (McLean and Bledsoe, 1992).

Cao *et al.* (2008) demonstrated that the kinetic dissolution of different Pb phases, such as PbO, PbCO₃, and PbSO₄, is pH dependent and is a function of reaction time where low pH (<3) and absence of P the dissolution follow the order PbO > PbCO₃ > PbSO₄. When pH increased to 7, the order of dissolution Pb phase was PbSO₄ > PbO > PbCO₃ regardless of P. In the presence of P at low pH (<3), the Pb solubility followed the order of PbCO₃ > PbO > PbSO₄.

Pb fractionation (the quantity bound to specific soil components) has been widely studied to understand the mechanism of Pb transformation in soils induced by phosphate amendments (the focus of this study) (Melamed *et al.*, 2003). It is known that Pb in soil has an affinity for iron (Fe) and Manganese (Mn) oxides both in crystalline and amorphous forms (Kabata-Pendias, 1980; McKenzie, 1980; Aualiitia and Pickering, 1987). Bound with iron/manganese oxide phases; Pb binding was decreased after phosphoric acid addition, This was considered as the result of the dissolution of the oxides and release of the bound Pb as a function

of the lower pH, followed by the precipitation of phosphorus with soluble Pb (Hayes and Katz, 1996, Zhang *et al.*, 1997).

Pb can be found in three primary phases, these are: Pb-oxide (PbO), Pb-carbonate (PbCO₃), and Pb-sulfate (PbSO₄) (Cao *et al.*, 2008). The addition of a potentially soluble phosphate to a soil containing any of the Pb phases and with adequate chlorine (Cl) availability, will result in an insoluble PbP phosphate mineral, chloropyromorphite (Pb₅(PO₄)₃Cl) precipitating, which, with is the most stable among Pb minerals (Ma *et al.*, 1993; Ryan *et al.*, 2001, Lindsay., 1979). At lower pH values (pH<4), the dissolution rate of PbCO₃ rapidly corresponds to chloropyromorphite precipitation (Zhang and Ryan, 1999a, b). The dissolution of PbSO₄ is fast under high pH conditions (pH>5) (Zhang and Ryan, 1999b).

In various studies the stability of environmentally insoluble pyromorphite (which has a log K_{sp} value of -84) and kinetics between soluble Pb and P in the aqueous systems has been extensively studied (Nriagu, 1974; Cotter-Howells and Thornton, 1991; Ma *et al.*, 1993; Cotter-Howells *et al.*, 1994; Ruby *et al.*, 1994; Cotter-Howells, 1996; Laperche *et al.*, 1997; Zhang *et al.*, 1998; Traina and Laperche, 1999; Hettiarachchi *et al.*, 2000; Pearson *et al.*, 2000; Ryan *et al.*, 2001; Eusden *et al.*, 2002; Cao *et al.*, 2003) (Figure 7 and Table 3).

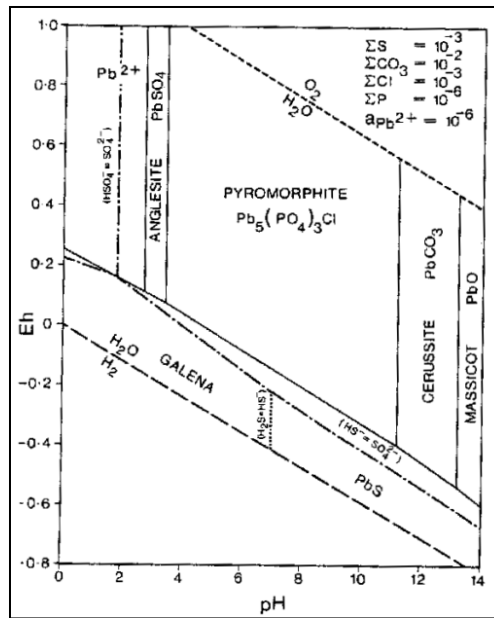


Figure 2.2 pH-Eh diagram of the stability of Pb-bearing minerals in ecosystems

(After Nriagu and Moore, 1984).

Table 2.1 Solubility Products of Pb Phosphate Minerals at 298 K (After Nriagu,

1974).

Mineral	$\log K_{sp}$
$Pb_5(PO_4)_3Cl$	-84.4
$Pb_5(PO_4)_3OH$	-82.3
$Pb_5(PO_4)_3F$	-71.6

The formation rates of phosphate minerals in soils are extremely difficult to define. Although, the pyromorphite precipitation from soluble Pb in aqueous systems in laboratory conditions, with pH 5 to 7, takes less than ten minutes, they are much slower in a soil environment (Ruby *et al.*, 1994, Ma *et al.*, 1993; Xu and Schwartz, 1994). The pyromorphite formation process appears to be limited by

presence of various mineral constituents, such as Al, Ca, Fe and Mn, which are less soluble and have high sorption affinity with phosphorous materials, especially Al and Fe oxyhydroxides in phyllosilicate mineral like kaolinite (Hashimoto *et al.*, 2009).

One classification of Pb-bearing grains was established on urban roadside soils based on the chemical association of those grains by using X-ray window file to P-rich (Pb phosphate), S-rich (Pb sulfate), Fe-rich co-precipitation with adsorption onto iron oxides and hydroxides, and a no other element group (PbO or PbCO₃) (Cotter-Howells, 1996).

Other techniques have also been used to identify the Pb-bearing minerals and possible Pb-phosphate phases of soil constituents, such as Analytical Transmission Electron Microscopy (ATEM) (Zhang *et al.*, 1998; Zhang and Ryan, 1999a; Mavropoulos *et al.*, 2004; Srinivasan *et al.*, 2006), Extended X-ray Absorption Fine Structure (EXAFS) (Cotter-Howells *et al.*, 1994; Ryan *et al.*, 2001), X-ray Diffraction (XRD) (Ma *et al.*, 1993, 1994a; Zhang and Ryan, 1999b; Mavropoulos *et al.*, 2002), Scanning Electron Microscope (SEM) (Laperche *et al.*, 1997; Chen *et al.*, 1997b; Zhang and Ryan, 1999a; Ryan *et al.*, 2001; Arnich *et al.*, 2003). The latter was being used to identify Ca-rich pyromorphite in a mine-waste soil (Cotter-Howells *et al.*, 1994).

2.1.2 Pb Bioavailability

Pb is now widely dispersed in urban soils due to the heavy use in old Pb paints, Pb as an additive (anti-knock agent) in gasoline and subsequent release in exhaust emissions, and through mining activities (Hunt *et al.*, 1992; Levin *et al.*, 2008; Mielke *et al.*, 1983). Oral ingestion of contaminants such as Pb, whose major environmental reservoir is soil, is considered a major route of exposure, more so than dermal and respiratory pathways.

Therefore, it is pertinent to study the bioavailability and bioaccessibility of Pb in media such as soil. *In vivo* models (juvenile swine are physiologically most appropriate), can be extremely costly, so low cost alternatives have been developed such as the *in vitro*, Physiologically Based Extraction Test (PBET) method (Zia *et al.*, 2011, Chaney *et al.*, 1989; Davies *et al.*, 1990; Johnson and Bretsch, 2002; Paustenbach, 2000; Thornton *et al.*, 1990, 1995).

The *in vitro* approach mimics the conditions of fasting human gastrointestinal tract based on a simulated gastric fluid (SGF) that maintains the human body temperature, stomach pH, and soil volume to SGF ratio (Hooda, 2010; Hettiarachchi and Pierzynski, 2004; Ruby, 2004; Wragg and Cave, 2002; Ruby *et al.*, 1999). The U.S. Environment Protection Agency (EPA) definition of bioavailability is "The fraction of an ingested dose that crosses the gastrointestinal epithelium and becomes available for distribution to internal target tissues and organ" (U.S. EPA, 2007). The bioavailable Pb is also the fraction of soil Pb, or

dust that can be absorbed into the blood stream after ingestion of the soil (Wixson and Davies, 1994; Casteel *et al.*, 1997).

Commonly, the fractional dose is referred to as absolute bioavailability and the comparison between them is called relative bioavailability. Thus, it is important to know the relative bioavailability in order to know the extent of absolute bioavailability of Pb as an exposure to humans (U.S. EPA, 2007). Relative bioavailability is defined as "The ratio of the bioavailability of a metal in one exposure context (i.e., physical chemical matrix or physical chemical form of the metal) to that in another exposure context" (U.S. EPA, 2007).

2.1.3 *In vivo/In vitro* Studies

Historically, Pb bioavailability has been determined by experimental studies on animals like rats and juvenile swine because their metabolisms are similar to those of a human (Casteel *et al.*, 2006; Weis and LaVelle, 1991). By way of example, a group of juvenile swine were dosed for 15 days with different concentrations of soil Pb or Pb acetate (Ruby *et al.*, 1999). Swine were dosed two times per day and blood samples were collected regularly.

Samples were reported for high Pb bioavailability especially ones with Pb carbonate. Furthermore, several studies have been established in a weanling rat models to assess the bioavailable Pb from mining and smelting sites (Dieter *et al.*, 1993; Schoof and Freeman, 1995). In 2003, a strong relationship between *in vivo* and *in vitro* data was presented in an EPA workshop in Tampa, Florida between a

standardized *in vitro* extraction method and the EPA Region VIII juvenile swine model.

Due to the high cost of *in vivo* tests, an *in vitro* technique was developed to substitute for the *in vivo* tests, which resulted in a test that cost less, was faster and contained easier procedures (Miller and Schricker 1981; Ruby *et al.*, 1993, 1996; Medlin 1997; Rodriguez *et al.*, 1999). The EPA identified validated *in vitro* procedures for a site-specific Pb bioavailability calculation and extrapolated it to *in vivo* (experimental studies on animals) results or the measurement of bioaccessibility. This is the maximum amount absorb by target organ, however, not all *in vitro* results produce identical *in vivo* results (U.S. EPA, 1997).

The *in vitro* technique basically measures the rate and extent of Pb solubility from solid phase to fluid that represent human gastric juice (Drexler and Brattin, 2007). The *in vitro* tests mimic the temperature, pH and acid gastric fluid in order to estimate the bioaccessible Pb. The Pb uptake by a human's gastrointestinal tract is complex because of its physical and chemical properties, and Pb particle size, which imparts the degree of bioavailable Pb that is dependent on the ingested Pb dissolution that passes through systemic circulation (Wixson and Davies, 1994; Ruby *et al.*, 1996).

According to the EPA, "The bioavailability and toxicity of metals depend strongly on the exact physical and chemical form of the metal and on the species affected" (11, p. 96). Additionally, the solubility of Pb, and leaching through the

soil profiles, are major sources of bioavailable Pb (Bubb and Lester, 1991). This bioavailable Pb is primarily controlled by stomach pH, residence time, Pb mineralogy and soil type (Ruby et al., 1996; Davis *et al.*, 1993).

Additional factors, such as iron deficiency and a calcium/phosphate diet, can reduce Pb absorption (Wixson and Davies, 1994). Some studies have showed that food consumption can reduce Pb toxicity by increasing stomach acidity (Chaney *et al.*, 1989). However, there are different health risks associated with soil Pb toxicity than those that are present in the consumption of Pb contaminated paint, food or drink.

The EPA established recommended absorption factors of environmental Pb exposure for children by using the Integrated Exposure Uptake Biokinetic (IEUBK) Model to predict the Pb concentration in children and adult's blood (U.S. EPA, 1994a, b; White *et al.*, 1998). This model calculates the relative bioavailability of low-intake rates, 60 percent for Pb in soil or dust, compared to soluble Pb in water or food for children, based on the assumption that the absolute bioavailability of Pb in soil and dust at low-intake rates is 30 percent for children and 50 percent for soluble Pb in food or water (U.S. EPA, 1997).

However, different assumptions are set for adults, who have an absolute availability of soluble Pb in water of 20 percent and the relative bioavailability of Pb in soil of 60 percent. Although the default absorption factors estimate the relative bioavailability of Pb in soil, any site-specific data may provide

significantly better metal absorption or bioavailable results because of the known physical and chemical nature of Pb in soil and soil characteristics (pH, moisture content, texture, etc.).

Locked mineral phases can prove problematic when evaluating bioavailability. Solid phase Pb speciation that involves the Pb component bound in a relatively insoluble matrix will have a much lower bioavailability than a Pb component bound in an easily soluble matrix. A study was conducted to test the bioavailable Pb from encapsulated Pb by Clapp *et al.* (1991).

The Pb-carbonate pigment fed to young Sprague-Dawley rats had a high oral bioavailable Pb at between two and four weeks at an amount of 1056 µg/l and 1432 µg/l respectively. However, less oral bioavailable Pb was determined for a Pb-chromate phase. Generally, it has been shown that the solubility of Pb compounds, except for Pb-sulfate, decrease with high pH (Davis *et al.*, 1993). Also, Davis *et al.* (1993) demonstrated that Pb bioavailability decreases in soil when it is encapsulated by phosphate and ferromanganese.

In New Orleans, decreasing the Pb bioavailability for children is of primary concern when dealing with Pb contaminated soils (Martin & Ruby, 2004). The goal of *in situ* remediation for Pb contaminated soils is the immobilization of Pb, such that Pb no longer represents an exposure risk (Martin & Ruby, 2004). This technique relies on altering soil chemistry in order to

immobilize metals and enhance certain reactions that immobilize the contaminant in the soil matrix (Martin & Ruby, 2004).

One major advantage of this technique is that it does not change the soil characteristics because they are present in such low concentrations and do not decrease the permeability of the soil matrix (Martin & Ruby, 2004). As discussed below, much of the research that has been done in the area of chemical stabilization has focused on the use of phosphate amendments in bench-scale laboratory investigations.

Phosphate has been shown to be an effective mineral in immobilization of Pb in soil (Nriagu, 1974). It has been shown that the addition of phosphate to a Pb contaminated soil results in the formation of highly insoluble Pb phosphate mineral forms such as the pyromorphites. The sparing solubility of this phase can produce a significant decrease in the bioavailability and mobility of Pb in soil (Ruby *et al.*, 1994).

Phosphate amendments are commercially available in different forms such as apatite II and phosphate rocks (Berti & Cunningham, 1997; Boisson *et al.*, 1999a, b; Chen *et al.*, 1997; Cotter-Howells & Caporn, 1996; Hettiarachchi & Pierzynski, 2002; Ma *et al.*, 1993, 1995; Mosby, 2000; Pierzynski & Schwab, 1993; Rabinowitz, 1993; Vangronsveld & Cunningham, 1998; Xenidis *et al.*, 1999; Zhang *et al.*, 1998).

2.2 Soil Remediation Methods

2.2.1 Soil Remediation Methods

The excavation and removal of Pb contaminated soil in New Orleans has been proposed as a useful method of removing the soil Pb exposure threat (Abel *et al.*, 2010a). However, the extensiveness of the Pb contamination and the nature of the soil locations would suggest that excavation and removal would be an exceedingly expensive exercise. An alternative, economically viable, and efficient method would be better suited to treat Pb contaminated soil in urban New Orleans yards. An *in situ* soil Pb chemical stabilization method suggests itself as the most appropriate.

2.2.1.1 *In-Place Remediation without Permanent Soil Additions*

There are various strategies that have been employed *in situ* to reduce the contaminant threat posed by various soil constituents. For example, *in situ* vitrification (ISV), which is an isolation technique for soil remediation through the application of a high voltage electric current that immobilizes the soil by converting it to a glass matrix.

This is achieved by the application of high temperatures (1,600 to 2,000 °C) that melt the soil's inorganic materials and volatilizes any organic contaminants in the soil (Martin & Ruby, 2004). ISV is an effective but high-cost method that can be applied to nonvolatile contaminants with less than 25 wt%

(Evanko & Dzombak, 1997; U.S. EPA, 2000a). But the soil is no longer able to be used for its original purpose.

Electrokinetic remediation (ER) is an *in situ* technique that involves the installation of electrodes that carry low-intensity direct current into the subsurface. This current desorbs metals from the soil matrix through stimulation of an electrochemical process toward the electrodes (FRTR, 2001). This electrochemical process stimulates acid/base chemical reactions that supports desorption and dissolution of metals from the soil matrix (U.S. EPA, 1997b).

This process concentrates solubilized contaminants around the electrodes that allow them to be eliminated through processes involving binding with ion exchange resins, pumping water near electrodes, precipitation at the electrode, excavation, and electroplating at electrode (FRTR, 2001). Again, this is an very high cost remediation method that is capable of treating only small areas of soil at one time.

A soil-flushing remediation method that has been employed *in situ* uses water to extract Pb from the soil matrix (FRTR, 2001). Extraction fluid is injected into the contaminated soil matrix to treat the contaminant (Martin & Ruby, 2004). This fluid can be recycled to enhance the cost-effectiveness of this procedure (U.S. EPA, 1997b). The treatment depth that this procedure can be used for is moderate to low depending on the extraction fluid used and the level of contamination (Martin & Ruby, 2004).

The removal rate of contaminants relies on surface contacts between the extraction fluid and soil matrix, Pb solubility in the fluid, and Pb sorption to the matrix when it dissolves in the extraction fluid (Martin & Ruby, 2004). Again this is not a low-cost approach, and the nature of the extraction fluid can potentially have a deleterious effect on the soil.

2.2.1.2 *Phytoremediation*

Phytoextraction is a removal process that operates *in situ* (Martin & Ruby, 2004). Phytoextraction employs the planting of specific types of plants that can accumulate metals into their tissues. These metals are subsequently removed through harvesting and recovering of the plant tissue (Brown *et al.*, 1994a, b). Plant species that can accumulate high amount of metals through absorption from contaminated soils (hyperaccumulator species) have been investigated as to their cost effectiveness and removal efficiencies (Martin & Ruby, 2004).

The Phytoremediation technique may require extended removal times (over many years), and the possibility exists that accumulator plant species may experience growing deficiencies in contaminated soils (ESTCP, 2006). There are several factors that can determine the effectiveness of phytoextraction remediation. These include: plant growing rates, plant resistance to environmental stress, concentration of contaminants of interest, and mineralogy of the metal contaminant (Martin & Ruby, 2004).

It has been found that concentrations of contaminants such as Pb, Zn, and Cd can result in high plant uptake of these metals (Davis *et al.*, 1995; Dudka *et al.*, 1996; Salt *et al.*, 1995; Xiong, 1997). However, Pb can resist plant uptake, even in soils with high concentrations of Pb due to its relative insolubility (Blaylock *et al.*, 1997). The potential for facilitating phytoextraction through the addition of a chelating agent like ethylenediaminetetraacetic acid (EDTA) to the soil has been advocated. However, the potential adverse effects associated with EDTA addition to soil remain unclear.

2.2.1.3 Chemical Stabilization

In situ chemical stabilization methods have been developed to replace expensive methods such as excavation, vitrification, Electrokinetic removal, and soil flushing. *In situ* remediation is a useful method that can chemically immobilize Pb in the soil, thus reducing the Pb bioavailability to children.

2.2.1.4 Biosolids

The application of biosolids as an alternative technique of soil remediation has been studied by Brown *et al.* (2003). Biosolids have been used for treating Pb contaminated urban soils with more than 800 mg/kg Pb. As a result of the high concentrations of iron, manganese, phosphorous, and organic matter in biosolids they have been shown to be a very effective amendment product (Brown *et al.*, 2004; Farfel *et al.*, 2005). The transformation mechanism from Pb in soil to

pyromorphite has been suggested to be either adsorption or precipitation (Li *et al.*, 2000).

High iron and manganese levels in biosolids can facilitate the precipitation of Pb in crystalline Pb-bearing iron oxide (Scheinost *et al.*, 2001). The use of biosolids has, however, become problematic with concerns that the potential presence of pathogens in them makes them unsuitable for residential soils.

2.2.1.5 Phosphate Amendments

The addition of phosphorus to soil by applying a phosphate amendment has been shown to several positive effects. Phosphorus is a basic soil nutrient and a component of N, P, and K fertilizers. In addition to Pb, phosphorus has been shown to bind with Cd and Zn in soils (Boisson *et al.*, 1999a, b; Chanery *et al.*, 1997; Chlopecka & Adriano, 1997; Hamon *et al.*, 2002; Laperche *et al.*, 1997; Phosphate Induced Metal Stabilization [PIMS], 2000), hence reducing the bioaccessibility of these metals. The effectiveness of phosphate addition can be increased by the sufficient amounts of iron and manganese oxides in soils facilitating the reduction of Pb bioavailability (Hettiarachchi & Pierzynski, 2002).

In addition phosphate other types of specific element/mineral additions have been used to modify soil Pb solubility. Iron and manganese additions, in the form of: hydrous oxides, steel shot, and steel sludge, have been used to decrease the bioaccessibility, leachability, and phytoavailability of Pb and other minerals (Berti & Cunningham, 1997; Chen *et al.*, 2000; Chlopecka & Adriano, 1997;

Hettiarachchi & Pierzynski, 2002; Mench *et al.*, 1994; Pierzynski & Schwab, 1993; Sappin-Didier *et al.*, 1997; Shuman, 1997).

Zeolites, because of their high cation-exchange capacity, have also been considered as a soil metal sequestration medium (Weber *et al.* 1984). The majority of studies investigating *in situ* soil amendment possibilities for reducing metal bioaccessibility have focused on various phosphorous additions, such as apatite II, hydroxyapatite, rock phosphate and others (Ma *et al.*, 1993, 1995; Ruby *et al.*, 1994; Cotter-Howells and Caporn, 1996; Basta *et al.*, 2001; McGowen *et al.*, 2001; Ryan *et al.*, 2001; Yang *et al.*, 2001; Mavropoulos *et al.*, 2002; Cao *et al.*, 2004; Hettiarachchi and Pierzynski, 2004).

This *in situ* treatment endeavors to increase soil Pb chemical stability by combining it with phosphorus to form a different sparingly soluble mineral form. This treatment technique has been shown to be both inexpensive and effective (Ma *et al.* 1993; Ma *et al.* 1994; Conca *et al.* 2000). The application of phosphate in the form of apatite ($\text{Ca}_{10}(\text{PO}_4)_6(\text{OH})_2$) has been shown to be a successful and cost-effective method to immobilize Pb in contaminated soils because of the low cost of apatite (Zhang *et al.* 1998; Conca *et al.* 2000; Giammar *et al.* 2000; Chen *et al.* 2006; Berti and Cunningham 1997).

Apatite, a calcium phosphate mineral, precipitates Pb in the soil matrix as the poorly soluble mineral pyromorphites. The formation of pyromorphite is a

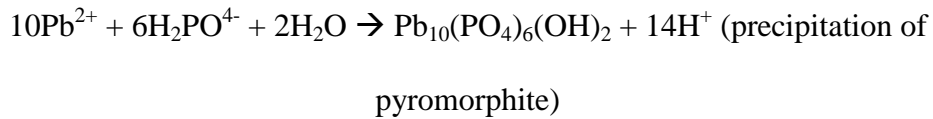
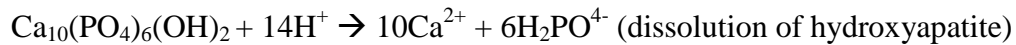
significant buffer mechanism that minimizes migration and enhances fixation of Pb in the contaminated soils (Shevade *et al.* 2001).

2.2.1.5.1 Hydroxyapatite

Hydroxyapatite has been shown to be an effective form of phosphorus amendment in reducing the bioavailability of Pb in soils (Fransworth, 2003). Hydroxyapatite $[\text{Ca}_5(\text{PO}_4)_3\text{OH}_{(s)}]$ is the main structural component vertebrate bone (Giammar *et al.* 2000) and makes up the matrix of teeth (Ma *et al.* 1993). Hydroxyapatite dissolved in low acidic medium (pH = 6) forms a phosphate that reacts with Pb in solution (Arnich *et al.* 2003).

As shown in equation 1, when apatite dissolves in a solution, ion exchange interactions occur between Pb^{2+} and Ca^{2+} , causing pyromorphite to precipitate (Arnich *et al.* 2003; Chen *et al.* 2007).

Equation 1: Ion Exchange between Pb^{2+} and Ca^{2+}



Through this reaction, Pb adsorbs on the surface of apatite with subsequent cation exchange between the Ca^{2+} and Pb^{2+} ions in the solution by diffusion (Equation 2) (Shashkova *et al.*, 1999):

Equation 2: Cation exchange between the Ca^{2+} and Pb^{2+} ions



The combination of Pb^{2+} ions and Hydroxyapatite ($\text{Ca}_5(\text{PO}_4)_3\text{OH}$) forms insoluble pyromorphite [$\text{Pb}_{10}(\text{PO}_4)_6(\text{OH})_2$] immobilized in the soil matrix (Arnich *et al.* 2003) along with chloropyromorphites ($\text{Ca}_5(\text{PO}_4)_3\text{Cl}$) or hydroxypyromorphite ($\text{Pb}_{10}(\text{PO}_4)_6(\text{OH})_2$) insoluble forms (Giammar *et al.* 2000). It has been suggested that the application of hydroxyapatite to soil Pb can be applicable as a 3/5 molar ratio of P/Pb, which is typical pyromorphite molar ratio (Ma *et al.*, 1993; Laperche *et al.*, 1996). However, the presence of calcium carbonate (CaCO_3) can consume H^+ that leads to a reduction in soil pH, which enhances the dissolution of soil Pb and affects the pyromorphite formation process (Laperche *et al.*, 1996; Zhang *et al.*, 1998; Knox *et al.*, 2003).

The formation of pyromorphite has been introduced by two mechanisms; first, hydroxyapatite dissolution is followed by phosphate reaction with aqueous Pb (Ma *et al.*, 1993; Xu and Schwartz, 1994; Chen *et al.*, 1997a, b; Zhang and Ryan 1999a, b; Zhang *et al.*, 1998; Lower *et al.*, 1998). Second, ion exchange between Pb^{2+} and Ca^{2+} has been confirmed by the hydroxyapatite lattice (Suzuki *et al.*, 1981; Takeuchi and Arai, 1990; Shashkova *et al.*, 1999).

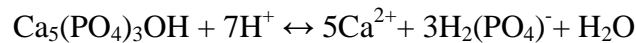
A mix of pyromorphite has been recorded due to the adsorption of Pb or the dissolution of hydroxyapatite followed by co-precipitation of pyromorphite (Laperche and Traina, 1998). Both mechanisms are affected by pH and pore solution chemistry (Chrysochoou *et al.*, 2007).

2.2.1.5.2 Apatite II

Phosphate-induced metal stabilization (PIMS™) using Apatite II (fish bones) to remediate Pb contamination problems in a variety of contexts has proved very successful. For instance, PIMS has been used to remediate various types of firing range soils at several sites and to address contamination of groundwater (Wright *et al.*, 2004; Conca *et al.*, 2000). Apatite II has been recognized as an environmentally sound product which holds promise for the stabilization of a variety of heavy metals as its crystals are attractive to ionic replacement of Ca^{2+} by Ba^{2+} , Sr^{2+} , Cd^{2+} and Pb^{2+} where P^{5+} and is a possible substitute for V^{5+} , Cr^{5+} and As^{5+} (Srinivasan *et al.*, 2006).

Several studies have been conducted to prove the pyromorphite formation between Pb in soil or aqueous solutions and Apatite II in solid phase (Ma *et al.*, 1993, 1994a, b; Xu and Schwartz, 1994; Laperche *et al.*, 1996, 1997; Chen *et al.*, 1997a, b; Zhang and Ryan, 1999a, b; Zhang *et al.*, 1998; Ryan *et al.*, 2001; Seaman *et al.*, 2001; Mavropoulos *et al.*, 2002, 2004; Knox *et al.*, 2003). The transformation mechanism involves the dissolution of the Apatite II followed by precipitation of pyromorphite (Equation 3, Equation 4).

Equation 3: Apatite dissolution



Equation 4: Pb Precipitation

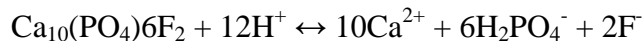


2.2.1.5.3 Rock Phosphate

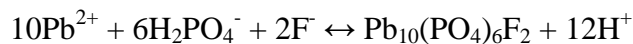
Rock phosphate, that is, fluoroapatite [$\text{Ca}_{10}(\text{PO}_4)_5\text{F}_2$], has been tested for previously as Pb immobilization phosphate in contaminated soils. This phosphate has less of an impact on soil pH reduction (Miretzky and Fernandez-Cirelli, 2008) and the leaching of P, which can pose potential eutrophication problems (Chen *et al.*, 2003; Melamed *et al.*, 2003).

The addition of rock phosphate to immobilize Pb in soil has been the subject of a number of studies (Laperche *et al.*, 1997; Ma and Rao, 1999; Hettiarachchi *et al.*, 2000; Basta *et al.*, 2001; Cao *et al.*, 2002; Lin *et al.*, 2005). The stabilization of Pb in soil associated with the addition involves the formation of fluoropyromorphite [$\text{Pb}_{10}(\text{PO}_4)_6\text{F}_2$]. The reactions are set out in equations 5 and 6 (Miretzky and Fernandez-Cirelli, 2008):

Equation 5: Dissolution



Equation 6: Precipitation



It has been suggested that the rock phosphate ability to immobilize Pb in soil becomes restricted in alkaline soils ($\text{pH} > 7$) due to low solubility of Pb and P (Laperche *et al.*, 1997; Zhang *et al.*, 1997; Melamed *et al.*, 2003). However, in acidic soils ($\text{pH} < 4$), the pyromorphite formation is spontaneous (Miretzky and

Fernandez-Cirelli, 2008). In a different principle, the grain size of the rock phosphate plays an important role in Pb immobility.

Chen *et al.* (2006) has been suggested that the small rock phosphate grains (in the Chen *et al.* study $<35\mu\text{m}$) are more effective for immobilizing Pb than large particles. However, rock phosphate particles, in general, are not typically of a size to readily facilitate Pb transformation in soils to deliver to Pb (Liu and Zhao, 2007). Rock phosphate has been shown to compare favorably in terms of reduced Pb solubility in stomach digestion models with to triple super phosphate (TSP) and phosphoric acid, as sources of P (Hettiarachchi *et al.*, 2001).

2.2.1.5.4 Bone Meal

Bone meal is a poorly crystalline structured material that is a mixture of finely and coarsely ground animal bones and animal protein. It contains chloride, sodium, potassium, magnesium with high level of phosphate (56 wt.%) and calcium (31 wt.%), two major constituents of bone, mainly as a mixture of $\text{Ca}_{10}(\text{PO}_4)_6(\text{OH})_2$ and $\text{Ca}_3(\text{PO}_4)_2$ phases (Deydier *et al.*, 2005). Bone meal has attracted attention as potential source of phosphorous for spoil metal immobilization (Miretzky and Fernandez-Cirelli, 2008). A significant decrease in Pb solution has been identified due to P addition via bone meal supplementation. However, the Pb transformation mechanism has not yet been determined (Hodson *et al.*, 2001; Sneddon *et al.*, 2006).

Bone meal amendments are a more expensive, natural phosphate source than hydroxyapatite (Hodson *et al.*, 2001). Unfortunately, the cattle bone meal as a feed product is no longer generally used because of possible transmission of bovine spongiform encephalopathy disease (Miretzky and Fernandez-Cirelli, 2008). Consequently, bone meal may be considered by the public to be an undesirable amendment to apply to urban contaminated soils.

2.2.1.5.5 Bone Char

Bone char [$\text{Ca}_{10}(\text{PO}_4)_6(\text{OH})_2$], is a poorly crystalline apatite, with a low cost and low phosphorous release (Chen *et al.*, 2006; Ma *et al.*, 1995; Ma and Rao, 1997). It has been identified as a high adsorption capacity amendment composed of ten percent carbon and 90 percent calcium phosphate and is a carbonization product of animal bones (Choy and McKay, 2005).

The calcium phosphate part of animal bones has a hydroxyapatite structure form (Girgis *et al.*, 1997). The production of bone char involves heating up animal bones to 600°C. A principal use for this product has been for decolorizing sugar solution during manufacturing (Abdel Raouf and Daifullah, 1997; Choy and McKay, 2005).

Additionally, bone char can be used to adsorb radioisotopes of antimony and has been widely tested for Cr, Pb, Cu, Hg, and Co ion sorption (Bennet and Abram, 1967; Cheung *et al.*, 2001; McKay and Bino, 1990). Bone char was used as a smelter-contaminated soil treatment in the Hunan Providence in south China

(Chen *et al.*, 2006). Several studies have determined sorption mechanism of bone char to immobilize Pb and other metals exchanges (Netzer and Hughes, 1984, McKay and Bino, 1987; Gabaldon *et al.*, 1996; Namasivayam and Kadirvelu, 1997; Danny *et al.*, 2004).

2.2.1.5.6 Triple-Superphosphate (TSP)

Triple-Superphosphate (TSP) contains a soluble form of P and is an agricultural fertilizer derived from rock phosphate and orthophosphoric acid reactions (Hettiarachchi *et al.*, 2001). TSP has been tested previously as a Pb stabilizing agent in contaminated soils (Chen *et al.*, 2007; Moseley *et al.*, 2008). The main components of TSP are; monocalcium phosphate ($\text{Ca}(\text{H}_2\text{PO}_4)_2 \cdot \text{H}_2\text{O}$); gypsum, calcium biphosphate (CaHPO_4); iron oxide, silica, aluminum, and water (Budavari, 1996).

Moseley *et al.* (2008) concluded that TSP can reduce the Pb bioaccessibility faster than rock phosphate. However, accessible Pb remained bound to aluminosilicate clays and adding large amounts of TSP has suggested a decrease in Pb bioaccessibility by around 25 percent is possible. Rapid solubilization of P from applied TSP may not be considered desirable as leached P may pose a eutrophication risk if excess P is transported to surface water bodies (Hettiarachchi *et al.*, 2000; Hettiarachchi *et al.*, 2001; Tang *et al.*, 2004; Scheckel and Ryan, 2004).

2.2.1.5.7 Phosphorous Pentoxide

Phosphorous pentoxide is widely used in agriculture and is a well known fertilizer. No research is available on using phosphorous pentoxide as a P amendment for immobilizing Pb in contaminated soil.

2.3 Research Objective and Hypotheses

The immobilization of Pb in soil has shown a potential for *in situ* remediation by applying a phosphate amendment. Nriagu (1974) suggested, “...the interaction of Pb and phosphorus in soils to form pyromorphite (a sparingly soluble Pb-phosphate mineral) ...is an important buffer mechanism controlling the migration and fixation of Pb in the environment”.

Similarly, Davis *et al.* (1993) concluded that pyromorphite was identified as a weathering product of galena (PbS), cerussite (PbCO₃) and anglesite (PbSO₄) in mine-waste contaminated soil in Butte, Montana. Also, Cotter-Howells *et al.* (1994) found pyromorphite to be a weathering product in mine-waste soils in Derbyshire, England. Pyromorphite was also found in urban Derbyshire soils (Cotter-Howells, 1996).

Phosphorus amendments have also been documented to change the chemistry of soil Pb (Rabinowitz, 1993; Ma *et al.*, 1993; Ruby *et al.*, 1994). Pyromorphite [Pb₁₀(PO₄)₆(OH)₂] is a suitable conversion product because it is extremely stable. The solubility constant (K_{sp}) for pyromorphite is approximately 10⁻⁸⁴, which is considered a highly insoluble mineral and relatively insoluble

form of Pb in the acid environment of the human stomach. Once ingested, the Pb is not mobilized or retained by the body, rather it passes through the gastrointestinal tract and is excreted relatively unchanged.

Extensive literature exists on the immobilization of Pb in soil after phosphate treatment. The formation of pyromorphite has been recognized in a purely theoretical way to reduce biosolubility in experimental laboratory conditions and in field trials (Shevade *et al.*, 2001; Porter *et al.*, 2004; Scheckel and Ryan, 2002; Bostick, 2003; Zhang *et al.*, 1998; Brown *et al.*, 1999; Cao *et al.*, 2003; Scheckel and Ryan 2004).

The appropriate form of phosphate to use as a soil addition has also been explored in various studies. These include: phosphoric acid (H_3PO_4) (Cao *et al.*, 2003), potassium phosphate monobasic (KH_2PO_4) (Berti and Cunningham, 1997) and rock phosphate/apatite (Chen *et al.*, 1997).

Problems with slow or fast release rates of the phosphorus have been discussed in the literature (Ma *et al.*, 1993; Cotter-Howells and Caporn, 1996; Laperche *et al.*, 1996). A waste product from the commercial fish industry known as Apatite II, a calcium phosphate, has also been found to have desirable properties such as low trace metal concentrations, poor crystallinity (>90% amorphous), high microporosity and high reactivity. Apatite II [$\text{Ca}_{10-x}\text{Na}_x(\text{PO}_4)_6-x(\text{CO}_3)_x(\text{OH})_2$ where $x < 1$], has been found to be an effective Pb immobilization additive under various conditions.

In this study it was proposed to evaluate an effective, low-impact, inexpensive, *in situ*, soil Pb immobilization methodology. The stabilization technique relied on changing Pb chemistry in soil by adding soil amendments, which employ phosphate as a soil amendment to reduce the bioaccessibility (the solubility under stomach acid conditions) of soil Pb. The use of phosphate compounds for this purpose has been investigated extensively.

Here we propose to test the suitability of one specific phosphate form commonly known as Apatite II™. Apatite II has been shown to be an effective agent under various environmental conditions for supplying phosphorus to various media. This includes soils and groundwater that are highly contaminated with Pb (Wright *et al.*, 2004, Conca *et al.*, 2000). However, Apatite II has not been used to remediate Pb contaminated urban soils in humid subtropical locations such as New Orleans, Louisiana.

The aim of this study was to show that Apatite II can potentially be developed as a cleanup amendment "method of choice" for Pb contaminated soils in residential New Orleans areas. A wide-scale remediation of Pb contaminated soil is needed in low income residential areas such as those found in New Orleans. And, this problem can best be addressed by an effective and low cost intervention strategy. The specific objectives of the study were:

- To examine the remediation protocol, treat, lock, and cover (TLC), by applying a Phosphate Induced Metal Stabilization (PIMS)

method, which uses apatite II to treat and lock Pb in soil, then cover it with a clean soil cap soil. To assess the effectiveness of the conversion of the existing soil Pb to a non-bioaccessible form, at certain depths, by covering the treated soil with a clean soil cap. We assume that the treated soil will not be affected by a covering of clean soil.

- To illustrate that Apatite II is an environmentally acceptable remediation agent. Based on previous studies it was hypothesized that Apatite II is a limited source of phosphorus when added to soil and does not pose a threat in terms of excessive leaching down through the soil, causing rapid percolation to groundwater and possible subsequent eutrophication problems.

Chapter 3

Experimental Design

3.1 Experimental Design

This study was designed to test the hypothesis that bio-available lead in residential soil can be limited by efforts that involve adding an inexpensive phosphate product (Apatite II) to lead contaminated soil at a number of urban test sites. The protocol to be adopted consists of three elements, treat, lock and cover (TLC). The treatment and locking elements employed the phosphate-induced metal stabilization (PIMS™) methodology.

The PIMS method involved nothing more adding phosphate to the soil in the form of Apatite II, this calcium phosphate efficiently releases phosphorus that combines with, and “locks-up”, the soil lead in the form a sparingly soluble lead-phosphate mineral. The cover portion of the experiment involved covering the treated soil with a surface layer of imported clean soil.

The study had, in part, been conceived to provide the theoretical underpinning for large-scale remediation work, which was projected to be undertaken by OPERATION PAYDIRT. PAYDIRT was conceived by the artist Mel Chin (http://en.wikipedia.org/wiki/Mel_Chin), whose concern with elevated soil lead levels in New Orleans prompted him to develop PAYDIRT.

The ultimate goal of PAYDIRT was envisaged, after gaining sufficient financial backing, to render lead-contaminated soils in New Orleans safe by

verified scientific method. The proposed scope of PAYDIRT is considerable in that its aim is to remediate lead contaminated soils across much of suburban New Orleans. The funding initiative (still underway) to support PAYDIRT had been designated, “THE FUNDRED DOLLAR BILL PROJECT” (<http://www.fundred.org/>).

It is expected that this study would improve on current methods for mitigating urban residential soil lead in several ways. First, the application of Apatite II directly converts the lead in the soil to poorly-bioaccessible form. Second, this is in many respects a green technology; no manufactured chemicals are used in the phosphate treatment of soil. Soil amendment with Apatite II (which is basically ground fish bones) makes use of a waste product from one industry and puts it to valuable use in the soil “clean-up” industry. So, the recycling element is strong in this type of project.

It was anticipated that the TLC approach would potentially gain wide acceptance for several reasons. In terms of phosphate treatment of the soil, the application of Apatite II is inexpensive. At a cost of approximately \$2.00/lb, it is expected that it will prove to be the most effective immobilizing agent available at its price point.

The cost of clean soil used for capping treated soils is also cost-effective, especially for New Orleans where clean alluvium from the Mississippi deposited in the Bonnet Carré Spillway from where it is inexpensively dredged. The

spillway is a flood control mechanism for the Lower Mississippi; it is located in St. Charles Parish, approximately about 12 miles west of New Orleans. In addition, the relative ease of implementation of the TLC approach makes it a desirable alternative to “high-impact” interventions such as excavation and removal.

It was posited that the TLC approach would improve on other approaches because Apatite II has a history of success in remediating soils heavily contaminated with lead and other metals, whereas other approaches have had mixed success. An early effort to address the soil lead problem was undertaken under the Urban Soil Lead Abatement Demonstration Project (USLADP), also known as the “Three City Study” (conducted in Cincinnati, Baltimore and Boston).

This study had the advantage of measuring blood lead levels in the children in the abatement areas before and after the implementation of the abatement. The overarching hypothesis of the USLADP was to test whether a reduction of lead in residential soil accessible to children would result in a decrease in their blood lead concentrations. In each city, abatement involved soil excavation and removal, as well as dust abatement (USEPA 1993). This was an essentially a contaminant removal project.

A small decline in the mean blood lead of children was observed following soil abatement at one of the three study cities. The relative lack of

success of USLADP inevitably meant that no further major abatement trials using other approaches followed. More recent interventions have been small scale and have avoided costly excavation and removal. Most of these efforts have involved *in situ*, cost-effective, strategies. Interventions have included: fencing to limit access, covering (capping) with uncontaminated soil (Mielke *et al.*, 2006), dilution by roto-tilling with uncontaminated soil (Elias, 1989), and vegetation barrier interventions such as promotion of grass growth or planting of bushes (Binns *et al.*, 2004).

Variations on these methods have been proposed by the USEPA's "Lead-Safe Yards" program (USEPA 2001a; Litt *et al.*, 2002) to contend with different levels of residential soil lead contamination. These types of intervention do not remove the lead or render it harmless, the lead remains as a potential threat to some degree, at some future point.

In situ chemical stabilization involves treating the soil in such a manner as to render the metal contaminants inert (i.e., nontoxic or non-bioaccessible) and/or immobile. Adding phosphate to soil is widely viewed as a chemical stabilization technique of much promise.

Here it was proposed that the following hypotheses be tested. (1) The soil lead remediation protocol (employing Apatite II) significantly stabilizes the lead in soil at the test sites in New Orleans. The null hypothesis would be stated as: no significant difference in the amount of bio-accessible lead in Apatite II treated soil

compared to untreated soil (control). (2) Apatite II is demonstrably better at stabilizing the lead in soil than other phosphorus-based amendments. The null hypothesis would be stated as: there is no significant difference in the amount of bio-accessible lead in Apatite II treated soil at the test sites compared to soils treated with other types of phosphorus products. (3) Apatite II does not leach excessive phosphorus down through the soil profile. The null hypothesis would be stated as: there is no significant difference in levels of phosphorus transported down through the soil compared to that leached from the soils treated with other phosphorus amendments.

In the broadest sense the principal issue to be addressed is whether the lead in urban residential soils in NOLA can be effectively stabilized (i.e., rendered non-bioaccessible) through the application of phosphate-based amendments.

Apatite II has been shown to be a highly effective remediation practice under various conditions; however, this methodology has yet to be applied to contaminated urban residential soils. While Apatite II is the soil amendment of choice here, to judge its effectiveness with respect to other phosphate forms, the intention was to undertake several side-by-side comparisons. To assess the level of bioaccessible lead in the soil, a Relative Bioaccessibility (RBA) assay that simulates stomach acid digestion was used.

To address the study objectives, a comprehensive field trial was conducted in urban New Orleans. It was proposed that a comparison of different forms of phosphate amendment be made at three locations across the city. It was hypothesized that the three sites would reveal if there were any site differences across the city that might affect the experimental results. A phased study design was proposed.

Phase 1: Reconnaissance survey and site selection

Phase 2: Site preparation and base line sampling

Phase 3: Amendment application

Phase 4: Post-treatment monitoring

3.1.1 Reconnaissance survey and site selection

3.1.1.1 Phase 1

The New Orleans Redevelopment Authority (NORA) previously assisted OPERATION PAYDIRT in order to identify appropriate experimental sites. Here, NORA and project personnel toured potential sites, over which NORA (post-hurricane Katrina) had authority in an effort to select sites of appropriate dimensions (and other criteria for this study). Under the proposed experimental design, individual sites needed to be a minimum 26'x62' in size. During the reconnaissance phase surface soil samples (top 2 cm) were collected from sites meeting the inclusive size criterion.

The concentration of lead and other elements in the reconnaissance samples (that is soils collected from potential study sites of the appropriate size) were determined by X-ray fluorescence (XRF) analysis using a bench top wavelength XRF system. XRF analysis was performed after the soils had been dried overnight at 40 °C, ground, homogenized and screened through a 250 µm nylon mesh.

Since lead levels vary across urban yards, it was determined that, in addition to the site size requirements, a soil lead concentration target should be least 800 mg/Kg (Macher and Hosick, 2004). This value is within the US EPA guideline range. The US EPA soil lead guidelines, which are set to protect young children, are 400 mg/kg for bare soil in children's play areas and an average of 1,200 mg/kg across a grassed area where children have regular access, such as a residential yard or a school play ground (US Federal Register, 2001). The reconnaissance phase of surface soil sampling proceeded as follows.

In the case of a yard at the rear of a property, it was determined that in the first instance, five evenly spaced drip line soil samples would be collected for testing. If these soil samples proved to have elevated lead levels, then five follow-up samples across a second line one meter away from the drip line would be collected. Then, a third line of five samples approximately at mid yard was sampled.

In the case of a front yard, it was again proposed that, in the first instance, five evenly spaced drip line soil samples would be collected for testing. Should these soil samples prove to have elevated lead levels, then a follow-up of five samples across a second line close to the road would be sampled. Next a third line of samples approximately at mid yard would be collected.

In the case of yard space between the sides of two properties, it was proposed that in the first instance five evenly spaced drip line soil samples from the drip line of each property would be collected. If the lead in these samples proved to be elevated, then five follow-up samples across a third line midway between the two properties would be collected.

Eligibility criteria based on soil lead levels are: (1) Overall soil lead concentration (on a dry weight basis) of ≥ 800 mg kg⁻¹ for the yard. The cut-off value of 800 mg kg⁻¹ was chosen for two reasons. It is in line with the value (700 mg/kg) defined elsewhere for detection of change in soil Pb bioaccessibility following in situ remediation (Farfel et al., 2002). Also, it is the midpoint for the two EPA action levels for bare and vegetation covered soil promulgated by the EPA. (2) Lead concentration (on a dry weight basis) of ≥ 700 mg/kg for most sampling lines.

An eligibility requirement that related to site conditions was the stipulation that no extensive addition to, or removal of, topsoil (construction activities or landscaping should be absent) would be acceptable.

3.1.2 Site preparation and base line sampling

3.1.2.1 Phase 2

The second phase of the project was initiated with site clearance and preparation. As a prelude to dividing a site into test plots, all extraneous material was removed (stones, branches, etc.), and vegetation was mown close to the surface. Once a site was cleared, it was then divided into a grid of test plots. Eight 10'x10' test plots were laid out in two parallel rows of five plots with a border 2' wide bounding each plot.

A high-density polyethylene geomembrane liner of 2.5 mm in thickness to prevent flooding out of, or into, the plots was installed to reduce cross-contamination. Each test plot was then divided into four 5'x5' sub-areas. A surface (scrape) soil sample of approximately 75 grams was then sampled from each sub area. With 8 test plots, each divided into 4 areas; soil collection yielded 32 samples from each site (96 in total from all sites). These soil samples and those subsequently collected were dried overnight at 40 °C, ground, homogenized and screened through a 250 µm nylon mesh.

The second set of data that was obtained related directly to the concentration of lead in the soil determined by, Inductively Coupled Plasma Optical Emission Spectroscopy (ICP-OES), and basic soil parameters, including:

- Soil pH (by laboratory pH meter).
- Soil moisture content (loss of weight upon drying).

- Organic matter content (by loss on ignition).

The solid phase speciation of the lead in the soil was determined by:

- Scanning Electron Microscopy (SEM) with Energy-Dispersive X-Ray Spectroscopy (EDS) analysis to identify and visualize the forms of lead particles in the soil (see below).
- Extended X-ray Absorption fine structure (EXAFS) spectroscopy.

Total Soil Lead: The total soil lead concentrations provided a basis for calculating the percentage of the soil lead that was bioaccessible obtained from the RBA assay results. The Metal content of the of the soil samples was determined by ICP-OES. Total soil Pb was determined from the amount of soil taken into solution by a combined strong acid and microwave digestion method.

Soil pH: Soil lead stabilization by the formation of pyromorphite is mediated through the soil solution. Under alkaline soil conditions, the process is slowed. Soil pH measurement provided an indicator of whether the soil needed to be more acidic (e.g., adding another amendment such as iron sulfate to lower the pH).

RBA Lead: The potential bioaccessibility of lead in the soils was assessed by an *in vitro* procedure intended to mimic the dissolution of the lead in soil during residence in the human stomach. Many such procedures have been proposed, but the one adopted here followed the draft *in vitro* bioaccessibility extraction procedure developed by Drexler. The methodology used was based

upon the Solubility/Bioavailability Research Consortium (SBRC), SOP 110499, Rev #8, and was measured at pH 2.2 and with an original pH of 1.5 (Ruby *et al.*, 1996 and Ruby *et al.*, 1999 Brown *et al.*, 2003a S.L. Brown, R.L. Chaney, J.G. Hallfrisch and Q. Xue).

Brown *et al.* (2003) reported that extraction at a pH of 1.5 gave problematic results due to conversion during the assay. Contrary to rat and pig tests, human feeding tests showed significant reduction in the bioavailable Pb (Ryan *et al.*, 2004). The assay involves:

1. Sample preparation involved oven drying of the soil at $\sim 40\text{ }^{\circ}\text{C}$; dried sample was sieved to select $< 500\text{ }\mu\text{m}$ size fraction.
2. Buffered extraction medium (60.06 g glycine in 2-L solution, adjusted to either pH 2.2 or pH 1.5).
3. Phase contact: $1.00 + 0.005\text{ g}$ dried test substrate was added to $100 \pm 5\text{ mL}$ of buffered extraction medium at $37 \pm 2\text{ }^{\circ}\text{C}$. The phases were contacted by tumbling in a TCLP extractor at $30 \pm 2\text{ rpm}$ for 1 hour, with temperature maintained at $37 \pm 2\text{ }^{\circ}\text{C}$. At the end of phase contact, an aliquot of liquid was filtered through $0.45\text{-}\mu\text{m}$ pore cellulose acetate filter.
4. The filtered solution was then analyzed for by Inductively Coupled Plasma–Optical Emission Spectroscopy (ICP-OES) to determine its lead content.

SEM analysis: A Computer Controlled Scanning Electron Microscope (CCSEM) was used to search through thousands particles in the soil samples in order to find lead-bearing particles. This allowed particles to be relocated for manual examination (i.e, imaging and element composition data collection). This analysis provided data on the forms of the particulate lead in the soil.

Extended X-ray Absorption fine structure spectroscopy (EXAFS): EXAFS spectroscopy had the potential to differentiate the various possible structural solutions previously envisaged for the location of lead into pyromorphite. Its greater sensitivity allowed for a differentiation between incorporation into pyromorphites versus adsorption onto apatite surfaces.

3.1.3 Amendment application

3.1.3.1 Phase 3

The third phase, the amendment addition phase of the project, followed after the base-line sampling. The study design called for different phosphate amendments on the test plots plus a control plot at three sites. Soil phosphorus was available for lead phosphate formation, and was presented as free phosphate (H_nPO_4 n-3) in the soil solution. A variety of a soil phosphate amendment was employed to introduce free phosphate into the soil, and in this study, we tested some of those that showed to be effective.

At each site, side-by-side plots were amended in the same fashion as three plots amended and one left as control. The amendments took the following forms

at Site 1613 St. Roche Ave. (29° 58' 27.2418" N, 90° 3' 8.7264" W) (Appendix H, Figure H.20):

- One plot pair was amended with Apatite II at 5% w/w added in granular form.
- One pair with Triple Super Phosphate ($\text{Ca}(\text{H}_2\text{PO}_4)_2 \cdot \text{H}_2\text{O}$) (TSP) added at 5,000 mg/kg.
- One pair with rock phosphate ($\text{Ca}_5(\text{PO}_4)_3\text{F}$), added at 1% w/w basis.
- One pair left untreated as a control.

In the above figure, TSP was chosen because it has shown previously to be capable of immobilizing soil lead (Owenby *et al.*, 2005). Similarly, rock phosphate is capable of *in situ* lead stabilization (Chen *et al.*, 2006; Chen *et al.*, 2007).

At Site 1818 Dumaine St. (29° 57' 58.7448" N, 90° 4' 24.8016" W) (Appendix I, Figure I.29):

- (i) One plot pair was amended with Apatite II at 5% w/w.
- (ii) One pair with fertilizer grade phosphoric acid (phosphorus pentoxide) in powder form added at a rate of 10g of phosphorus per kg of soil.
- (iii) One pair with hydroxyapatite (calcium apatite; $\text{Ca}_{10}(\text{PO}_4)_6(\text{OH})_2$) added at 1% w/w basis.

(iv) One pair left untreated as a control.

Based on Yang *et al.* (2001), Phosphoric acid is effective at stabilizing soil lead and roto-tilling of dry phosphorus pentoxide seems to be the most effective method of amendment (Yang and Mosby, 2006). Hydroxyapatite ($\text{Ca}_{10}(\text{PO}_4)_6(\text{OH})_2$) has also been shown to be effective at immobilizing lead in soil (Ma *et al.*, 1994, Chen *et al.*, 2007).

At Site 2224 N. Prieur St. (29° 58' 36.0552" N, 90° 3' 23.8644" W)

(Appendix J, Figure J.97):

- (i) One plot pair was amended with Apatite II at 5% w/w basis.
- (ii) One pair with bone-char fertilizer (poorly crystalline apatite, $[\text{Ca}_{10}(\text{PO}_4)_6\text{OH}_2]$) added at a ratio of 1:50.
- (iii) One pair with bone-meal fertilizer (typically, 90% hydroxyapatite and 10% carbon) added at a ratio of 1:50.
- (iv) One pair left untreated as a control.

Bone-char fertilizer is efficient at immobilizing soil lead (Chen *et al.*, 2006). Bone-meal addition to soil (calcium phosphate) is also a useful treatment for lead contaminated (Hodson *et al.*, 2000; Hodson *et al.*, 2001). It has been argued that bone-char is no more effective than bone-meal at immobilizing soil lead (Hodson *et al.*, 2000). However, concern over the safety of skeletal tissue of cattle may favor the incineration of bone-meal prior to use.

Potassium chloride (as muriated potash) was also added to the treated plots at a rate of 500 mg Cl per Kg of soil to provide a Cl source for chloropyromorphite formation (the application rate was suggested by Yang and Mosby, 2006).

Once the amendments were added to each plot, the plot was thoroughly watered (approximately 1.5" of water). Next, one plot of each amendment type was capped with a 6" layer of clean soil. The clean soil capping will utilize Mississippi River alluvium obtained at the Bonnet Carré Spillway following the procedures described by Mielke *et al.* (2006).

In the 4 plots not covered with clean soil at each site, a shallow, ceramic cup, lysimeter was installed to a depth of 3'. The lysimeter was located at the center of the plot, in an augured hole. Samples of soil pore-water were extracted using the lysimeter at monthly intervals until the sixth month after the installation, and then again at the 12 month sampling event. The pore-water was tested for its phosphorus content. The goal of this testing was to evaluate the potential for down-profile transport of phosphorus that had entered the soil solution from the phosphate amendments. The phosphorus content of the pore water was determined by ICP-AES analysis.

3.1.4 Post-treatment monitoring

3.1.4.1 Phase 4

The soil at each plot was sampled at 12 months post amendment. Approximately 25g of soil were collected (from different locations in plot) from each of the sub-areas on each un-capped plot. In the case of the plots with the clean soil cap, core samples were taken at each time interval and soil from a depth greater than 6” was sampled. The soils sampled at the post-amendment time interval were submitted for the following previously described tests:

- Total Soil Lead
- Soil pH
- Soil RBA Lead
- Scanning Electron Microscopy (SEM) with Energy-Dispersive X-Ray Spectroscopy (EDS)
- Extended X-ray Absorption fine structure (EXAFS) spectroscopy

3.1.5 Statistical Basis for Study Design

The basis for the design of this study was to test how significant the reduction in soil lead bio-accessibility would be in the Apatite II treated plots compared to the control plots after one year. In a study presented by Ryan *et al.* (2004) the bio-accessible lead in phosphorus treated soil (amended with 1 % phosphorus) at 3, 18, and 32 months post treatment was almost uniformly about 20%, while at the same time intervals, the bio-accessible lead in the controls was

almost uniformly about 60%. We have used soil lead concentration data (values only >800 mg/kg) from some yards tested by OPERATION PAYDIRT selected by NORA (n: 27; mean: 1,903 mg/kg; range: 893-7,091 mg/kg) to calculate how many test plots would be needed with phosphate.

Our calculations were for a 50% reduction in relative bio-accessibility of lead (at 12 month), based on a t-test for two independent groups, for 70% power and both a one and two sided alpha of 0.05. We started with soil lead concentrations in the range of 1,000-7,000 mg/kg, and the control plots with an RBA of 80% and treatment plots with an RBA of 30% at the end of the experiment. The plots were paired, so the experimental difference in mg/kg calculated was tested to see if it was different from a null value of zero.

We assumed that the main source of experimental variability is inherent variability in lead among samples, and used the standard deviation of the numbers in the test list to estimate that variability that was; errors in the lead and bioavailability determinations were small compared to inherent variability. The following table shows the sample sizes required to detect the assumed difference with 70% power (Table 3.1). These were larger for plots with smaller initial lead, because the percentage differences specified worked out to be smaller absolute differences in lead.

Table 3.1 Sample Sizes Required to Detect the Assumed Difference with 70% Power with 0.05 One-Sided and Two-Sided α .

Initial Pb (mg/Kg)	Control Bioavailable (mg/Kg)	Treated Bioavailable (mg/Kg)	Experimental reduction (mg/Kg)	N for paired 2-tail	N for paired 1-tail
1000	800	300	500	44	34
2000	1600	600	1000	13	10
3000	2400	900	1500	7	6
4000	3200	1200	2000	5	4
5000	4000	1500	2500	4	4
6000	4800	1800	3000	4	3
7000	5600	2100	3500	4	3

Thus, for the six sample plots designated in this study (6 for paired 1-tail test), an initial soil value of approximately 3,000 mg/kg was required, which would be the target for this study. The use of a standard deviation of the lead measurements was used rather pessimistically due to the variability. Pairing usually reduces the variability of the difference below the variability of the starting point. So, it probably wasn't quite as difficult, as this analysis suggested, to identify a significant difference (i.e., soils with lead concentrations < 3,000 mg/kg would likely work).

3.1.6 Quality Assurance Mechanisms

3.1.6.1 Field Quality Assurance

Assessment of field contamination (Blanks): Equipment blank samples involved the collection of equipment rinsate blanks that collected to evaluate field sampling and decontamination procedures.

Field Blanks: Field blanks were collected to evaluate whether contaminants been introduced into the samples during soil sampling because cross contamination. Leachate test water blank was collected during each phosphorous water sampling event.

Sample Replicates: For site assessment, duplicate sample analysis was at a rate of 5%. Duplicate samples were prepared independently of other samples using the same sample preparation procedure. Duplicates provided a check on heterogeneity of the sample matrix, consistency of sample preparation, and precision of the analysis, and should be within $\pm 20\%$.

3.1.7 Standard Reference Materials

There is a soil SRM (2587) that is available from the National Institute of Standards and Technology. Each is certified for more than 25 elements. Acid-washed sand was used to provide a zero concentration (clean matrix) sample.

3.1.8 ICP-MS Quality Control (QC)

A 1 g portion from each soil sample selected for ICP-MS analysis was digested for total lead content using a modified U.S. EPA nitric acid hotplate

digestion method SW 846 Method 3050 (USEPA, 1986). QC samples of various types were included in the ICP analysis. Each batch of 14 samples prepared for total lead analysis were included the following types of QC samples: 1 g of NIST SRM 2587 and stock solution spike and spike triplicate samples prepared with 0.5 ml of Spec Pure standard. For, bioaccessible lead analysis, each batch will include 1 g of NIST SRM 2587, a stock solution spike, a spike triplicates, and a reagent blank.

Chapter 4

Materials and Methods

4.1 Materials

4.1.1 A. Soil

For the purposes of the experimental design, thirty grams of soil were used from each plot (subsampled by coning and quartering from original sampled material) collected at starting time zero and twelve months (total of 480 grams of soil for each site) to determine the variability in soil characteristics (e.g. pH, moisture content, and loss on ignition) and to perform relative bioaccessibility test, EXAFS, and SEM analysis.

4.1.2 B. Capping soil

A reliable source for Bonnet Carré Spillway soil was identified in order to deliver the required soil from the spillway to cap four of the eight plots in each site. Since soil could only be delivered in intervals of 6 cubic yards, the per plot coverage of soil was modified from 1.85cy to 1.5, or approximately 12.7 cm (5 inches) of soil per plot. Plots were capped to establish whether the geochemical conversion process that produces pyromorphite takes place at depth in the soil and so making the “cover” part of the TLC concept viable(Figure 4.1).



Figure 4.1 Bonnet Carré Spillway cap soil.

4.1.3 C. Equipment

Equipment rentals were scheduled one week prior to site installation day. Installation is the term used here for the work done on site entailing: application of phosphate products, capping with clean soil, installing the lysimeters, and collection of soil samples for analysis.

An auger was rented that was capable of drilling a 0.914 m (3 foot), 15.24 cm (6 inch) deep hole and a 4 horsepower rototiller capable of tilling soil to a depth of 15.24 cm (6 inches). Also, shovels, rakes, hoses, water volume meter, wheel barrows, and a 30.48 cm (12”) 3.5 millimeter plastic barrier held by 45.72 cm (18”) wooden stakes were used to prevent cross flow contamination between plots were brought to the site on installation day.

4.1.4 D. Water

It was recommended that 3.81 cm (1.5”) of water be used for saturating the plots after installation. At no site was there an available source of water on the

site itself. Consequently, water had to be used from a home neighboring the site. Although any water that was used was paid for, establishing a positive relationship with a neighbor whose water was important. Neighbors were reimbursed for approximately 2,271.25 liter (600 gallons) of water per site and water flow was monitored by flow meters.

4.1.5 E. Lysimeters

Lysimeter well head assembly, shallow sampling lysimeter, vacuum pressure hand pump, external case PVC 33 cm (1 1”) diameter, and polyethylene tubing were ordered through the Ben Meadows company. Lysimeters were installed after the amendments to prevent damage when the phosphate products were roto-tilled into the soil (Figure 4.2).



Figure 4.2 Lysimeter installation.

4.1.6 F. Fencing

A 1.524 m (5') fence was installed at the openings at all sites after installation was complete to serve as a barrier to access by the public and prevent interference with the lysimeters (Figure 4.3). Fortunately, the lysimeters were not maliciously damaged or stolen, and it took hurricane "Isaac" (8/29/12) to destroy the lysimeters of one of the sites.



Figure 4.3 Fencing.

4.1.7 G. Amendments

Three different phosphate amendments were roto-tilled (separately) into six of the test plots at each with one test plot left untouched as a control. A variety of soil phosphate amendments were employed to introduce free phosphate into the soil, and the goal being to test the relative effectiveness of each. In each yard, side-by-side plots in the two rows were marked out. The amendments distributed

in the forms as described previously in the experimental design chapter. The powder products were hand broadcast over the test plots on to the surface, following the deigned plot allocations.

An iron-sulfate product was considered as additional amendment as a pH modifying agent. It was to be used if the original pH measurements indicate that soil is basic. Pyromorphite mineral is suggested to form at pH 5 than at pH 6 or 7 with different Pb and phosphorous concentrations (Laperche *et al.*, 1996). The pH of the entire sets soils can close to neutral, so no soil acidification through the addition of iron-sulfate was attempted. It is known that generally lead accumulates within the top few centimeters of a soil (Swaine and Mitchell, 1960), therefore the amendments were tilled by hand-held, gas powered, roto-tiller into the soil to a depth of 15.24 cm (6 inches).

The following table illustrates the amendments, quantities, source, and costs for the entire project. While iron-sulfate was not added to the solid, 2 pounds of muriate potash was added to each plot.

Table 4.1 Description of Used Amendments, Quantities, Source, and Costs in Three Locations.

Description	Quantity	Ratio (amendment/soil)	Source	Cost
APATITE II	1,200 lbs	5% weight/weight	NA	\$2,145
TRIPLE SUPER PHOSPHATE	40 lbs	5,000 mg/kg	Local Farm and Feed	\$100

Table 4.1 - continued

ROCK PHOSPHATE	80 lbs	1% w/w	Superior Growers	\$125.00
BONE CHAR	200 lbs	1:50	Buy Activated Charcoal	\$300
BONE MEAL	160 lbs	1:50	Local Farm and Feed	\$150
HYDROXYAPATITE	100 lbs	1% w/w	ScienceLab	\$918
PHOSPHOROUS PENTOXIDE	60 lbs	10 g/kg	Midwest Supply	\$200
MURIATE POTASH	36 lbs	500 mg/kg	Local Farm and Feed	\$55
IRON SULFATE	24 lbs	based on pH	Ace Hardware	\$60

4.1.8 G. Ground barrier

As the specific odor was associated with the Apatite II (a fish-like aroma accompanied the processed Apatite II), a protective barrier was placed over the plots to prevent animals such as cats, from digging up treated plots. A 25 cm open weave, plastic net was used as a barrier on all plots. Thus netting was also placed on the capped plots for practical purposes. When samples were collected at 12-months from the capped soil, which required the surface cap to be dug-up to find the layer of amended soil beneath, the net provided a marker to distinguish the treated soil from the capping soil (Figure 4.4).



Figure 4.4 Ground barriers.

4.2 Methods

All sites were prepared prior to installation for the soil amendments following the procedures outlined previously (e.g., site clearance of extraneous material, and close mowing of surface vegetation). Minor deviations from the experimental design were made at the time of installation as needed (e.g., if something like an old tree stump, or a concrete surface was found to be present beneath the top of the soil). The following is the sequence of events that describes the process followed for establishing the suitability of a site for the study.

All the reconnaissance samples (collection described previously) were analyzed for total lead concentration using a bench top Rigaku X-ray Fluorescence system (Figure 4.5). After the soils were dried overnight at 40 °C, they were ground, homogenized, screened through a 250 µm nylon mesh and

three grams were pressed into boric acid pellets (the boric acid being in powder form).



Figure 4.5 WDXRF Benchtop Supermini Rigaku.

Once suitable sites were identified, (see experimental design chapter), and a one-year lease was negotiated with NORA for the property installation proceeded. One of the initial difficulties experienced by the project (which caused a considerable time delay) was the acquisition of suitable sites. Likely, as a result of communication problems with NORA, reconnaissance samples were initially taken at a number of sites, and several proved to meet the inclusion criteria for the project, but these sites were never used in the study. For some reason(s), that still remain unclear, even though a communication of interest was sent to NORA about site suitability, the potential sites identified were subsequently disrupted by NORA associated contractors.

Buildings on the properties would be demolished, and any deep depression left in the yard following the use of heavy equipment to demolish the property were simply filled in with sand. In subsequent discussions with NORA, it was made clear that we tried to take out leases on sites that had not been altered since the original reconnaissance soil lead survey. After this discussion leases were obtained on undisturbed properties.

4.2.1 pH, Moisture content, Loss on ignition (LOI)

Soil samples were collected at both time zero and twelve months, were dried overnight at 40 °C, ground, homogenized and screened through a 500 µm mesh. Multiple tests were performed on each soil. First, pH analysis was done following the EPA 9045D protocol in order to check the acidity of the soil and to determine whether iron sulfate should be used to acidify soil and improve soil lead transformation (Martin & Ruby, 2004).

Twenty grams of each sample were added to a twenty mL of DI water into 50 mL beaker, stirred for five minutes and was left to settle for one hour. The pH meter accumet basic AB15 was then calibrated by using three buffering solutions with value of pH 4, 7, and 10, and the soil pH was measured for all samples (Figure 4.6).



Figure 4.6 Fisher Scientific accumet basic AB15pH meter.

Next, soil moisture and organic matter content of the soils was calculated by drying samples in an oven and performing sample drying in two stages. Dry crucibles were weighed and 1 gram of soil added to each. Then, each crucible was placed in the oven at approximately 40°C overnight to dry the soil. After that the initial drying, the crucibles was placed in dessicator for 6 hours and re-weighed providing by difference a determination of the soil water content. The soil containing crucibles were then placed in a furnace at 450°C for 4 hours before removal and placement in dessicator for cooling.

Finally, the crucible was weighed and the organic matter was calculated based loss (of mass) On Ignition (LOI).

The moisture content of soil then calculated by the formula:

$$\text{Soil Moisture (\%)} = 100 \times \frac{\text{Weight of crucible and soil (g)} - \text{Weight of crucible and soil after drying at } 105^{\circ}\text{C (g)}}{\text{Weight of crucible and soil after drying at } 105^{\circ}\text{C (g)} - \text{Weight of crucible (g)}}$$

Equation (1)

Following the organic matter removal (after furnace heating), the loss on ignition mass was calculated by the following formula:

$$\text{LOI (\%)} = 100 \times \frac{\text{Weight of crucible and soil after drying at } 105^{\circ}\text{C (g)} - \text{Weight of crucible and soil after heating at } 450^{\circ}\text{C (g)}}{\text{Weight of crucible and soil after drying at } 105^{\circ}\text{C (g)} - \text{Weight of crucible (g)}}$$

Equation (2)

The purpose of measuring the organic matter is to estimate the mineral portion in the soil after all the organic matter has been removed. This was of interest, as soil lead can bind to organic matter in soil.

4.2.2 Total Pb in soil

The total soil lead concentrations provide a basis for calculating the percentage of the soil lead that is in a bioaccessible from the RBA assay results. It should be noted that soil lead determinations to be used in the RBA calculations were measured by ICP-OES, the phosphorus content of lysimeter extracted pore water measured by ICP-mass spectrometry (ICP-MS) which has much better low concentration detection limits.

For the purposes of Extended X-Ray Absorption Fine Structure (EXAFS) analysis (performed at the Argonne national laboratory), one gram of soil from each uncapped plot quadrant was combined to make up individual 4 gram soil composites that were sent for Extended X-Ray Absorption Fine Structure (EXAFS) analysis.

4.2.3 Soil relative bioaccessibility (RBA) lead content

The potential bioaccessibility of lead in the soils was assessed using an *in vitro* procedure intended to mimic the dissolution of lead in soil during residence time in the human gut. This process was accomplished based on the US EPA OSWER 9200.3-51 method. The *in vitro* bioavailability (IVBA) of Pb in soil depends on the minerals phase of Pb, which might have low (e.g. Anglesite), medium (e.g. Minium), or high (e.g. Cerussite) bioavailability. The IVBA protocol, described by Drexler and Brattin (2007), is a time-efficient and cost-effective method for RBA determination, compared to more accurate, but in comparison, much more expensive *in vivo* methods that typically use juvenile swine models (US EPA, 2007).

The extraction procedure was done by adding soil samples, in batches of 1 gram for each soil, taken at time zero and twelve months, to 100 mL of SGF (glycine added to pH 2.5 HCl stock solution) in 125 mL high-density polyethylene (HDPE) bottles. The buffered stock solution was prepared by adding 60 grams of glycine to 2 liters of deionized (DI) water, and then HCl was added to

adjust the stock solution to the desired pH value of 2.5. For quality assurance, the pH of the fluid was tested in samples in order to monitor the buffering capacity of the soil (potentially altering the pH of the simulated gastric fluid (SGF)).

The *in vitro* assay was completed in batches of 13 soil samples with separate extraction bottles containing only the SGF added as reagent blanks. The HDPE bottles were placed into a large water tank with temperature-controls (Figure 4.7). The extraction bottles were completely immersed in the water, which was maintained at a temperature of 37 °C to mimic the temperature of the human stomach.

An electric motor tumbled the extraction bottles, end-over-end, for one-hour at a speed of 28 RPM (U.S. EPA, 2008). After one hour of extraction in the tank, a 15 mL aliquot of fluid was removed by syringe filtering. A Luer-Lok attachment fitted with 0.20 µm cellulose acetate disk filter that was connected to a syringe and fluid was withdrawn of an HDPE bottle by pulling back on the syringe. The filtered solutions were then analyzed by ICP-OES for total Pb in solution. This is the lead that has gone into solution after, essentially weak acid digestion mimicking dissolution conditions in the stomach.



Figure 4.7 TCLP Extractor.

After the digestion procedure, the remaining SFG and soil residue in each HDPE bottle was decanted into a large filter system chimney, and under vacuum the soil residue was collected onto a qualitative Whatman 41 filter (Figure 4.8). In addition the luer-lok was cut open and the 0.20 μm cellulose acetate disk filter inside, which had collected a small mass of soil during fluid extraction, was removed.

For soil residue lead content analysis, both filters (with soil residue) were folded together and retained for strong acid digestion. These samples were subsequently sent in batches to a contract analysis lab for strong acid digestion and included in each batch with standard soils (National Institute of Standards and

Testing (NIST) Standard Reference Material (SRM) 2587). It should be noted that there are no reference values for weak acid extracted lead for SRM 2578. This SRM was included to monitor the consistency of the weak acid extraction and subsequent strong acid digestion between batches.

The contact lab that soils were sent to is housed in the chemistry department of the State University of New York College of Environmental Science and Forestry (SUNY-CESF) in Syracuse, NY. The hot acid digest of the soils (and filters) involved the addition of an Aqua regia solution (4:1 HCl to HNO₃ by vol) to Teflon tube containing the soil and filters. The tubes were then subsequently placed in a microwave block digester (manufactured by Grant Instruments, Cambridge, Scienco Western, Cambridge). In detail the process involved adding the sample to 8ml HCl and 2ml HNO₃ and this was left to digest for 2-3 hours at 60°C.

The mixture was then placed in the digestion block at 105°C for 1 hour and then sample was dried at 140°C. Following cooling 12.5 ml of 20% v/v HCl was added and the solution re-warmed for 20 minutes at 80°C. Then, sample was filtered through a 40 whatman filter paper and made up to volume (50 ml) with DIW. The solutions were later analyzed by ICP-OES. The digestion process and solution analysis follow the method of McGrath and Cunliffe (1985).



Figure 4.8 Filtering system.

The weight of soil collected on the filters was determined by difference following the weighing of the Whatman 41 filters before the filtering step and then weighing the dried filter and collected soil. In the case of the small filters in the luer-lok holders, no initial weight could be determined as the filters were sealed in the holders. So, an average weight of ten blank luer-lok cellulose acetate filters was used for a filter weight correction. The removed cellulose acetate filters were dried and then weighed. The weight of soil on the Whatman 41 filters and on the cellulose acetate filters was combined to give a mass of soil recovered from the weak acid digest.

To estimate what the contribution to the sample Pb was made by the reagent and (weak-acid extraction) process, HDPE bottles containing a reagent

blank were included with site- and SRM-soil samples in each weak acid extraction batch.

Solutions from the weak- and the strong-acid digestions were analyzed for lead using a Perkin Elmer Optima 3300DV ICP-OES. Small quantities of solution were injected into argon plasma. The solutions were atomized in the plasma (thermally exciting the valence electrons of elements present in the sample). From the plasma electro-magnetic radiation at characteristic wavelengths is produced which are recorded by a spectrometer and converted to Pb concentrations.

The ICP-OES was calibrated at the 220 nm Pb emission line, and the calibration standards were prepared in a 1% nitric acid matrix from single element 1000 mg/L Pb standards. These standards ranged in concentration from 10 to 100 mg/L and gave a standard curve with a correlation coefficient > .9999.

The percentage IVBA lead in the soil samples was calculated as follows:

The weak acid extracted Pb was calculated as follows:

$$\text{Weak acid extracted Pb (mg/g)} = 100 \times \frac{\text{Weak acid concentration (mg/L)} \times 0.1}{\text{Weight of sample (g)}}$$

Equation (4)

After that, the strong acid extracted Pb was calculated as follows:

$$\text{Pb from soil and filter digest (mg/g)} = 100 \times \frac{\text{Strong acid concentration (mg/L)} \times 0.1}{\text{Weight of sample (g)}}$$

Equation (5)

Then, total soil Pb was calculated as follows:

Total soil Pb (mg/g) = Weak acid extraction (mg/g) + Pb from soil and filter
digest (mg/g)

Equation (6)

Finally, the percentage *in vitro* bioaccessibility was calculated as follows:

$$\text{IVBA (\%)} = \frac{\text{Weak acid extraction (mg/g)}}{\text{Total soil Pb (mg/g)}} \times 100$$

Equation (7)

4.2.4 Scanning Electron Microscopy (SEM) with Energy-Dispersive X-Ray Spectroscopy (EDS)

A personal computer controlled PSEM (ASPEX@ SEM) was used to search through particles in the soil samples to find lead-bearing particles (Figure 4.9). This analysis provided data on the forms of the solid phase particulate lead in the soil. In detail the analysis involved the following: Imaging of particles accomplished using the backscattered electron (BE) signal which essentially provides a particle density.

Backscattered electrons were collected by a four-quadrant detector located at the base of the SEM column. The measurement of sample characteristic X-rays provided element composition information for each particle. Characteristic X-rays were collected using an OmegaMax EDX system with a silicon drift detector with

a 10mm² active area and ultra-thin window. Particle examination was conducted in variable pressure mode (no conducting coating needed to be applied to the samples).

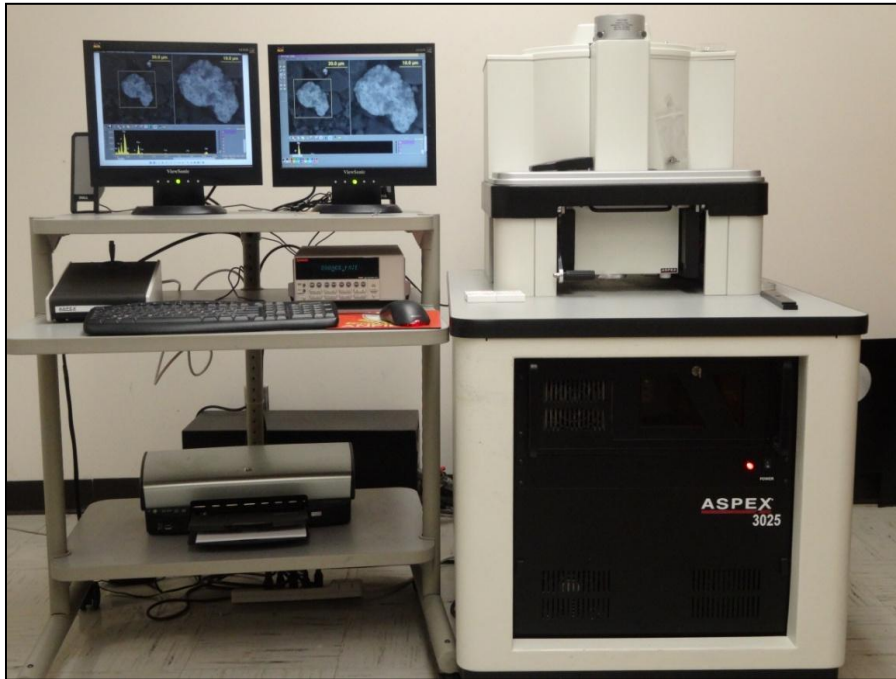


Figure 4.9 Image of Scanning Electron Microscopy-Energy Dispersive Spectroscopy ASPEX[®] SEM-EDS.

4.2.5 Extended X-ray Absorption fine structure (EXAFS) spectroscopy

EXAFS has the potential to differentiate the various possible structural solutions previously envisaged for the location of lead into pyromorphite (Figure 4.10). Also, its greater sensitivity should allow for differentiation between incorporation into pyromorphites versus adsorption onto apatite surfaces. EXAFS

was used to determine the presence of pyromorphite when SEM and X-ray Diffraction (XRD) cannot confirm it (Schofield *et al.*, 2001).

X-ray absorption spectroscopy refers to the interaction of how X-rays are absorbed by an atom at energies near and above the core-level binding energies of that particular atom. XAS is the modulation of an atom's X-ray absorption probability due to the chemical and physical state of the atom. XAS spectra are especially sensitive to the formal oxidation state, coordination chemistry, and the inter-atomic distances, coordination number and species of the atoms in the surrounding proximity of the selected element of interest. As a result, XAS provides a practical and simple way to determine the chemical state and local atomic structure for a selected atomic species.

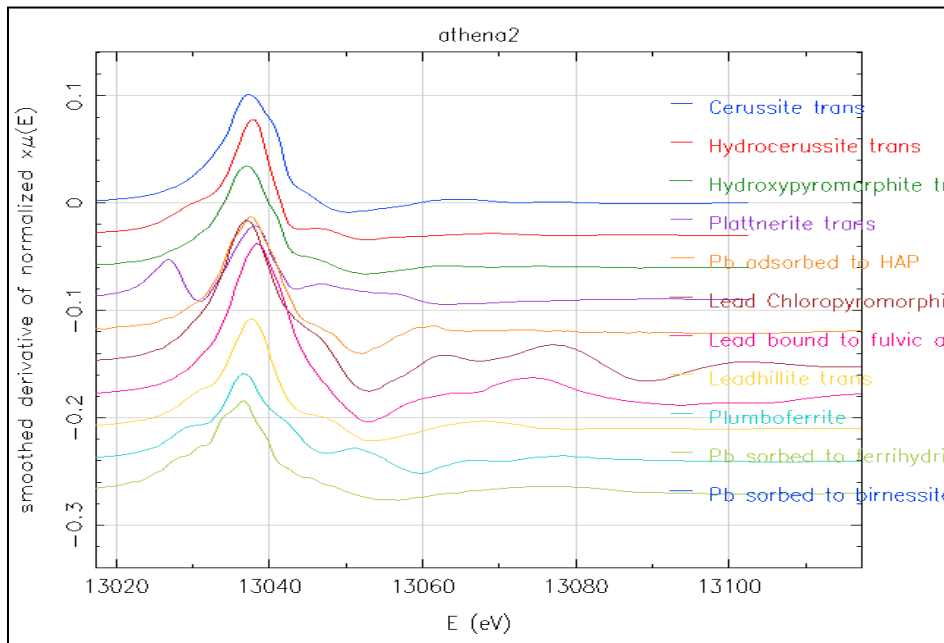


Figure 4.10 Pb XANES spectra standards for fitting.

4.2.6 Phosphorous content of soil pore water

Lysimeter samples were collected at four plots at each site during a time period of 6 or 12 months. Samples were collected per manufacturer's instructions as specified in Campbell Monoflex Porous Cup Lysimeter Instruction Manual by using the following flask-activation method: The pressure valve was sealed on the well head and the sample recovery valve was opened. Flexible Teflon tubing was then inserted into the push-to-connect fitting on the sample recovery valve on one end and into a hole in a two-hole plastic rubber stopper on top of a 125ml Nalgene Graduated Erlenmeyer Polycarbonate Flask. A separate piece of flexible Teflon tubing was inserted into the other hole on the stopper so the tubing was flush with the bottom of the stopper and the other into the vacuum end of a hand pump.

A gentle vacuum was applied to the system and soil pore-water samples were collected from the porous ceramic base of the Lysimeter. The lysimeter well-heads were then reactivated by applying a gentle vacuum until a reading of 18-21" of mercury was reached on the vacuum/pressure gauge on the head-assembly. All valves were closed and a protective cap was placed over the well-head assembly. Repeatedly, samples were transferred from the field to sanitized and pre-labeled 4 ounce Wheaton, HDPE Leak Resistant Wide Mouth Bottles and the Flexible Teflon tubing was discarded after every sample and flasks and stoppers sanitized between collection periods on the day of collection (Figure 4.11).

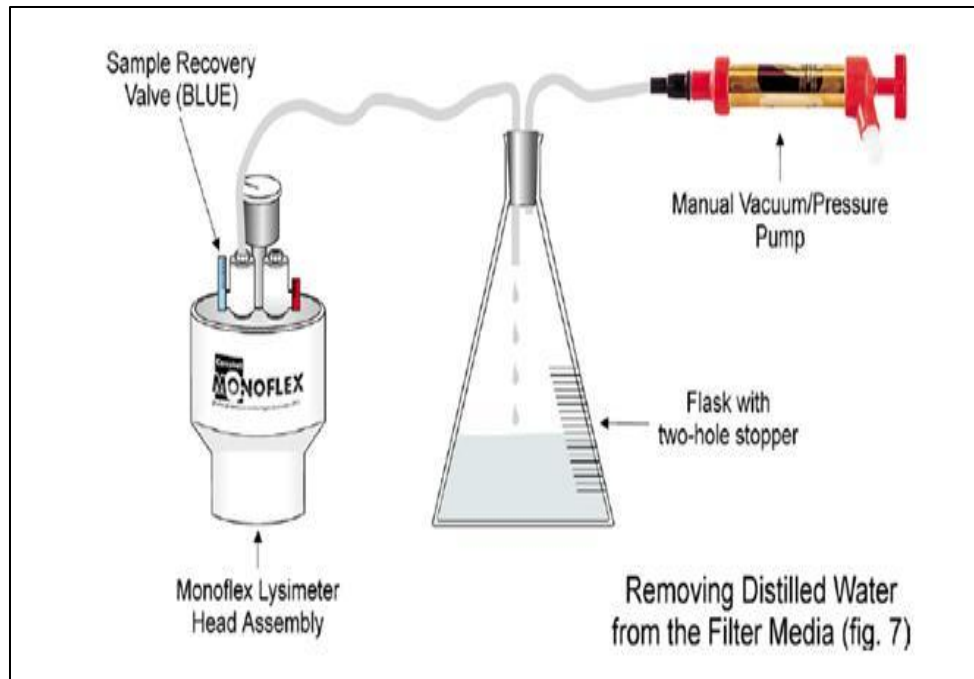


Figure 4.11 Sample recovery from the filter media. Figure from Campbell Monoflex Lysimeter.

The soil pore-water samples were analyzed using A Perkin Elmer Sciex Elan DRC-e quadruple ICP-MS for phosphorous concentration at m/z 31 with Quartz concentric nebulizer, Perkin Elmer quartz cyclonic spray chamber, 1.06L/min nebulizer flow set for < 2.7% oxides (CeO^+/Ce^+), and 1500W power instrument operating conditions following the US EPA 365.4 method. Standards were made in deionized water with single element 1000 mg/L standards. The range of standard concentrations was 5 to 200 ug/L with curves and correlations coefficients of at least 0.999.

ICP-OES was used to verify the accuracy of ICP-MS by measuring 3 samples with relatively high P content. The ICP-OES was calibrated at 214 nm with the same standards as above, but in the range of 25 to 100 ug/L with a correlation coefficient > 0.999.

Samples of soil pore-water were extracted using the lysimeter at monthly intervals until the sixth month after the installation, and then again at the 12 month sampling time. The pore-water was tested for its phosphorus content, using ICP-OES/ICP-MS analysis, with the aim of evaluating the potential for phosphorus transportation into the soil solution from the phosphate amendments.

The Elan DRC-e Inductively Coupled Plasma Mass Spectrometer (ICP-MS) was used to measure Pb by argon plasma, which evaporates the solvent, vaporizes and atomizes the sample. Plasma conditions are optimized to ionize the sample. The ions are calculated by mass analyzer according to their mass to charge ratio. The intensity of the signal at the Pb mass is converted to an elemental concentration by comparison with concentration standards.

Chapter 5

Results

5.1 Results

The results presented in this study were obtained using a bench top wavelength X-ray fluorescence spectroscopy (WDXRF), pH meter to determine the soil acidity, Extended X-ray Absorption Fine Structure Spectroscopy (EXAFS), Induced Coupled Plasma Mass Spectroscopy and Optical Emission Spectroscopy (ICP-MS and ICP-OES), and a Personal Scanning Electron Microscopy (PSEM).

5.1.1 Soil Analysis

5.1.1.1 Total Soil Pb

5.1.1.1.1 Reconnaissance Samples

For the site selection, random soil samples were collected and analyzed by WDXRF to determine the total Pb in soil and confirm the specific USEPA criteria for the selected contaminated site (see chapter three for details). The following tables show the total Pb for the reconnaissance samples with the Global Positioning System (GPS) coordinates for each data point. The wide range of soil Pb concentrations at each site reflect on the heterogeneity of the Pb content of contaminated soils (Pb levels can vary considerably over short distances).

Table 5.1 Total Pb of 1613 St. Roche Ave. Reconnaissance Samples with DMS

Coordinates.

Sample ID	Total Pb (mg/Kg)	Latitude	Longitude
1613_1	2064	29° 58' 27.339"	-90° 3' 7.6206"
1613_2	2421	29° 58' 27.3504"	-90° 3' 7.2966"
1613_3	1585	29° 58' 27.3756"	-90° 3' 7.0236"
1613_4	3640	29° 58' 27.6162"	-90° 3' 7.077"
1613_5	2775	29° 58' 27.5844"	-90° 3' 7.326"
1613_6	2245	29° 58' 27.555"	-90° 3' 7.4982"
1613_8	2672	29° 58' 27.4038"	-90° 3' 7.344"
1613_9	3274	29° 58' 27.4182"	-90° 3' 7.1742"
1613_10	2221	29° 58' 27.4332"	-90° 3' 7.0236"
1613_11	2349	29° 58' 27.555"	-90° 3' 7.0518"
1613_12	2532	29° 58' 27.5406"	-90° 3' 7.1958"
1613_13	2817	29° 58' 27.5298"	-90° 3' 7.3542"
1613_14	3377	29° 58' 27.5088"	-90° 3' 7.4982"

Table 5.2 Total Pb of 1818 Dumaine St. Reconnaissance Samples with DMS

Coordinates.

Sample ID	Total Pb (mg/Kg)	Latitude	Longitude
1818-1	1017	29° 57' 59.3892"	-90° 4' 24.492"
1818-2	186	29° 57' 59.1444"	-90° 4' 24.708"
1818-3	95	29° 57' 58.8846"	-90° 4' 24.927"
1818-4	99	29° 57' 58.6722"	-90° 4' 25.1148"
1818-5	1993	29° 57' 58.41"	-90° 4' 25.3416"
1818-6	2004	29° 57' 58.2294"	-90° 4' 25.0968"
1818-7	3329	29° 57' 58.572"	-90° 4' 24.7908"
1818-8	3489	29° 57' 58.7514"	-90° 4' 24.6252"
1818-9	3636	29° 57' 58.935"	-90° 4' 24.459"
1818-10	1312	29° 57' 59.1912"	-90° 4' 24.2322"
1818-11	386	29° 57' 59.2776"	-90° 4' 24.3366"
1818-12	2301	29° 57' 59.1834"	-90° 4' 24.4092"
1818-13	4394	29° 57' 59.0904"	-90° 4' 24.4848"
1818-14	2323	29° 57' 58.989"	-90° 4' 24.5712"

Table 5.2 - continued

1818-15	1349	29° 57' 58.896"	-90° 4' 24.639"
1818-16	375	29° 57' 58.809"	-90° 4' 24.7296"
1818-17	579	29° 57' 58.716"	-90° 4' 24.801"
1818-18	204	29° 57' 58.6254"	-90° 4' 24.8916"
1818-19	2140	29° 57' 58.5354"	-90° 4' 24.9744"
1818-20	1067	29° 57' 58.4526"	-90° 4' 25.0356"
1818-21	1419	29° 57' 58.377"	-90° 4' 25.1184"
1818-22	1837	29° 57' 58.284"	-90° 4' 25.2042"
1818-23	1055	29° 57' 58.3488"	-90° 4' 25.2834"
1818-24	1023	29° 57' 58.4712"	-90° 4' 25.176"
1818-25	114	29° 57' 58.5858"	-90° 4' 25.0674"
1818-26	285	29° 57' 58.7052"	-90° 4' 24.9708"
1818-27	95	29° 57' 58.8378"	-90° 4' 24.8442"
1818-28	278	29° 57' 58.971"	-90° 4' 24.7296"
1818-29	94	29° 57' 59.1048"	-90° 4' 24.6174"
1818-30	255	29° 57' 59.2194"	-90° 4' 24.5166"
1818-31	842	29° 57' 59.3136"	-90° 4' 24.441"

Table 5.3 Total Pb of 2224 N. Prieur St. Reconnaissance Samples with DMS

Coordinates.

Sample ID	Total Pb (mg/Kg)	Latitude	Longitude
2224-1	1983	29° 58' 35.9106"	-90° 3' 23.5584"
2224-2	1590	29° 58' 35.6298"	-90° 3' 23.529"
2224-3	5419	29° 58' 35.31"	-90° 3' 23.5038"
2224-4	1849	29° 58' 35.0508"	-90° 3' 23.4894"
2224-5	1518	29° 58' 35.022"	-90° 3' 23.745"
2224-6	599	29° 58' 35.2992"	-90° 3' 23.7918"
2224-7	14674	29° 58' 35.601"	-90° 3' 23.8134"
2224-8	1550	29° 58' 35.8572"	-90° 3' 23.796"
2224-9	89	29° 58' 35.9142"	-90° 3' 23.6226"
2224-10	1204	29° 58' 35.634"	-90° 3' 23.6046"
2224-11	1560	29° 58' 35.331"	-90° 3' 23.583"
2224-12	5524	29° 58' 35.2302"	-90° 3' 23.58"
2224-13	2157	29° 58' 35.1264"	-90° 3' 23.5686"
2224-14	1637	29° 58' 35.043"	-90° 3' 23.5614"
2224-15	2074	29° 58' 35.0256"	-90° 3' 23.6838"

Table 5.3 - continued

2224-16	2338	29° 58' 35.3166"	-90° 3' 23.6874"
2224-17	3214	29° 58' 35.4828"	-90° 3' 23.7024"
2224-18	1482	29° 58' 35.6154"	-90° 3' 23.7054"
2224-19	921	29° 58' 35.7522"	-90° 3' 23.7168"
2224-20	183	29° 58' 35.9034"	-90° 3' 23.7234"

Soil samples were collected at time zero and twelve months from three different sites, St. Roche, Dumaine, and N. Prieur, and were analyzed by SEM analysis to determine the change in Pb particles pre and post treatment.

5.1.1.1.2 Weak Acid Digest

The measurement of the simulated gastric fluid (SGF) extracted (A.K.A. weak acid digest) Pb employed US EPA 6010B method with Pb quantification by Inductively Coupled Plasma-Optical Emission Spectrometry (ICP-OES). The weak acid digest was used to determine in triplicate the soluble Pb content of the soil in each quadrant, of each plot, at each site. A Toxicity Characteristics of Leaching Procedure (TCLP) extractor (see chapter four) was used to perform the weak acid extraction.

Soils samples were analyzed in triplicate to overcome the problem of the heterogeneity of Pb levels in soil. This problem is demonstrated by the variations in Pb levels in soil samples initially analyzed and whose data is presented in

Tables 5.1-5.3. The triplicate analyses were averaged to provide a single soil Pb concentration value for each quadrant. The weak acid digest results of 1613 St. Roche, was used to calculate the IVBA.

5.1.1.1.3 Strong Acid Digest

The determination of the Pb concentration of the soil that was retained after the TCLP weak acid digest was involved in microwave digestion and strong acid dissolution (see chapter four). The strong acid digest results of 1613 St. Roche was used to calculate the IVBA.

5.1.1.2 *Pb Bioaccessibility*

Once the soil was digested for total Pb and the provided data on the total Pb for time zero and twelve months was used to determine the relative bioaccessibility of Pb in the soil for the three sites (Table 5.4 & 5.5).

5.1.1.2.1 Comparison of Zero and Twelve Months Bioaccessibility Results

The forthcoming results from the *in vitro* SGF bioaccessibility test for 1613 St. Roche Ave. sampled at zero and twelve months are presented in Figures 5.1 - 5.11. At this site it was clear that the bioaccessibility of Pb in the soil was not high. In this *in vitro* extraction procedure approximately half of the Pb initially presents in the soil was in a stable non-bioaccessible soluble form. Thus Pb bioaccessibility reduction efforts by phosphate addition would not yield very large changes (i.e., >50%) in this soil.

For the un-capped apatite II treated soil it appears that the bioaccessible Pb slightly decreased in soil (Approximately 3%) and it showed around 10% of Pb bioaccessible reduction in the capped soil. The rock phosphate has shown reduction for the un-capped soils of 13% and 19% decrease in bioaccessible Pb for the capped plot. Also, un-capped soil treated with TSP amendment shows 16% reduction in mobilized Pb and 19% represents Pb bioaccessible decline in capped TSP treated soil.

Clearly, the general trend indicates that some initially bioaccessible Pb in the soil had become less soluble after addition of the amendments. The capped control plot has 1% Pb bioaccessible change where it is 8% difference between time zero and twelve months.

Table 5.4 Calculated *In Vitro* Bioaccessibility of Pb as a Percentage of Total Pb in Zero and Twelve Months Un-capped Soil at 1613 St. Roche Ave.

Sample Name	0-month IVBA (%)	12-month IVBA (%)	Average IVBA (%)	Amendment	Plot
1613 St. Roche 1Aa1	58.2	50.1		Apatite II	Un-capped
1613 St. Roche 1Aa2	50.4	41.5	44.4	Apatite II	Un-capped
1613 St. Roche 1Aa3	49.8	41.7		Apatite II	Un-capped
1613 St. Roche 1Ab1	49.8	34.6		Apatite II	Un-capped
1613 St. Roche 1Ab2	50.3	46.5	45.0	Apatite II	Un-capped
1613 St. Roche 1Ab3	50.0	54.0		Apatite II	Un-capped
1613 St. Roche 1Ac1	50.1	46.8		Apatite II	Un-capped
1613 St. Roche 1Ac2	49.1	50.6	47.3	Apatite II	Un-capped

Table 5.4 - continued

1613 St. Roche 1Ac3	50.2	44.3		Apatite II	Un-capped
1613 St. Roche 1Ad1	49.2	52.6		Apatite II	Un-capped
1613 St. Roche 1Ad2	52.2	53.3	53.3	Apatite II	Un-capped
1613 St. Roche 1Ad3	50.6	53.8		Apatite II	Un-capped
Average	50.8	47.5			Change 3.3%
std	2.3	5.8			
min	49.1	34.6			
max	58.2	54.0			
range	9.1	19.4			
1613 St. Roche 2Aa1	45.9	35.6		Rock Phosphate	Un-capped
1613 St. Roche 2Aa2	47.5	33.7	35.6	Rock Phosphate	Un-capped
1613 St. Roche 2Aa3	48.9	37.6		Rock Phosphate	Un-capped
1613 St. Roche 2Ab1	50.0	34.6		Rock Phosphate	Un-capped
1613 St. Roche 2Ab2	50.4	31.1	32.1	Rock Phosphate	Un-capped
1613 St. Roche 2Ab3	48.8	30.6		Rock Phosphate	Un-capped
1613 St. Roche 2Ac1	50.0	40.7		Rock Phosphate	Un-capped
1613 St. Roche 2Ac2	50.1	40.9	40.3	Rock Phosphate	Un-capped
1613 St. Roche 2Ac3	49.9	39.2		Rock Phosphate	Un-capped
1613 St. Roche 2Ad1	48.6	36.5		Rock Phosphate	Un-capped
1613 St. Roche 2Ad2	47.8	35.7	37.1	Rock Phosphate	Un-capped
1613 St. Roche 2Ad3	51.0	39.1		Rock Phosphate	Un-capped
Average	49.1	36.3			Change 12.8%
std	1.4	3.3			
min	45.9	30.6			
max	51.0	40.9			
range	5.1	10.3			
1613 St. Roche 3Aa1	48.7	35.6		TSP	Un-capped
1613 St. Roche 3Aa2	49.0	36.3	35.5	TSP	Un-capped
1613 St. Roche 3Aa3	47.5	34.6		TSP	Un-capped

Table 5.4 - continued

1613 St. Roche 3Ab1	49.7	35.3		TSP	Un-capped
1613 St. Roche 3Ab2	48.7	31.6	33.8	TSP	Un-capped
1613 St. Roche 3Ab3	48.2	34.4		TSP	Un-capped
1613 St. Roche 3Ac1	45.9	26.5		TSP	Un-capped
1613 St. Roche 3Ac2	47.6	29.0	28.0	TSP	Un-capped
1613 St. Roche 3Ac3	48.3	28.6		TSP	Un-capped
1613 St. Roche 3Ad1	47.0	29.9		TSP	Un-capped
1613 St. Roche 3Ad2	48.6	34.1	30.5	TSP	Un-capped
1613 St. Roche 3Ad3	45.5	27.4		TSP	Un-capped
Average	47.9	31.9			Change 15.9%
std	1.2	3.4			
min	45.5	26.5			
max	49.7	36.3			
range	4.2	9.8			
1613 St. Roche 4Aa1	48.0	44.8		CONTROL	Un-capped
1613 St. Roche 4Aa2	48.5	46.7	44.4	CONTROL	Un-capped
1613 St. Roche 4Aa3	47.2	41.6		CONTROL	Un-capped
1613 St. Roche 4Ab1	54.4	43.2		CONTROL	Un-capped
1613 St. Roche 4Ab2	47.2	44.2	43.0	CONTROL	Un-capped
1613 St. Roche 4Ab3	45.1	41.7		CONTROL	Un-capped
1613 St. Roche 4Ac1	47.9	38.1		CONTROL	Un-capped
1613 St. Roche 4Ac2	49.8	32.6	35.6	CONTROL	Un-capped
1613 St. Roche 4Ac3	50.1	36.1		CONTROL	Un-capped
1613 St. Roche 4Ad1	48.0	38.7		CONTROL	Un-capped
1613 St. Roche 4Ad2	44.1	37.1	36.5	CONTROL	Un-capped
1613 St. Roche 4Ad3	46.2	33.6		CONTROL	Un-capped
Average	48.0	39.9			Change 8.2%
std	2.5	4.3			
min	44.1	32.6			

Table 5.4 - continued

max	54.4	46.7
range	10.3	14.1

Table 5.5 Calculated *In Vitro* Bioaccessibility of Pb as a Percentage of Total Pb
in Zero and Twelve Months Capped Soil at 1613 St. Roche Ave.

1613 St. Roche 1Ba1	63.3	52.8		Apatite II	Capped
1613 St. Roche 1Ba2	64.6	52.4	53.5	Apatite II	Capped
1613 St. Roche 1Ba3	67.7	55.2		Apatite II	Capped
1613 St. Roche 1Bb1	63.4	53.0		Apatite II	Capped
1613 St. Roche 1Bb2	65.5	56.1	54.5	Apatite II	Capped
1613 St. Roche 1Bb3	64.9	54.5		Apatite II	Capped
1613 St. Roche 1Bc1	56.6	45.7		Apatite II	Capped
1613 St. Roche 1Bc2	59.9	47.2	47.0	Apatite II	Capped
1613 St. Roche 1Bc3	59.5	48.2		Apatite II	Capped
1613 St. Roche 1Bd1	61.4	50.4		Apatite II	Capped
1613 St. Roche 1Bd2	64.2	53.5	53.4	Apatite II	Capped
1613 St. Roche 1Bd3	65.1	56.2		Apatite II	Capped
Average	61.9	51.2			Change 10.7%
std	4.9	4.6			
min	48.0	39.9			
max	67.7	56.2			
range	19.6	16.3			
1613 St. Roche 2Ba1	51.6	35.5		Rock Phosphate	Capped
1613 St. Roche 2Ba2	50.2	32.6	34.2	Rock Phosphate	Capped
1613 St. Roche 2Ba3	51.0	34.6		Rock Phosphate	Capped
1613 St. Roche 2Bb1	49.1	31.2		Rock Phosphate	Capped
1613 St. Roche 2Bb2	54.4	32.1	32.0	Rock Phosphate	Capped
1613 St. Roche 2Bb3	55.0	32.7		Rock Phosphate	Capped
1613 St. Roche 2Bc1	53.9	35.6		Rock Phosphate	Capped

Table 5.5 - continued

1613 St. Roche 2Bc2	53.5	35.1	34.5	Rock Phosphate	Capped
1613 St. Roche 2Bc3	52.2	32.7		Rock Phosphate	Capped
1613 St. Roche 2Bd1	53.1	32.9		Rock Phosphate	Capped
1613 St. Roche 2Bd2	53.9	32.2	32.2	Rock Phosphate	Capped
1613 St. Roche 2Bd3	51.9	31.7		Rock Phosphate	Capped
Average	52.5	33.2			Change 19.3%
std	1.7	1.5			
min	49.1	31.2			
max	55.0	35.6			
range	5.9	4.4			
1613 St. Roche 3Ba1	46.9	26.3		TSP	Capped
1613 St. Roche 3Ba2	47.8	28.2	26.1	TSP	Capped
1613 St. Roche 3Ba3	44.4	23.8		TSP	Capped
1613 St. Roche 3Bb1	43.1	30.3		TSP	Capped
1613 St. Roche 3Bb2	43.3	28.2	30.4	TSP	Capped
1613 St. Roche 3Bb3	50.8	32.6		TSP	Capped
1613 St. Roche 3Bc1	46.5	30.5		TSP	Capped
1613 St. Roche 3Bc2	50.2	34.9	33.7	TSP	Capped
1613 St. Roche 3Bc3	48.5	35.7		TSP	Capped
1613 St. Roche 3Bd1	48.9	25.0		TSP	Capped
1613 St. Roche 3Bd2	47.3	22.7	24.4	TSP	Capped
1613 St. Roche 3Bd3	49.6	25.5		TSP	Capped
Average	47.3	28.6			Change 18.6%
std	2.5	4.1			
min	43.1	22.7			
max	50.8	35.7			
range	7.7	13.0			
1613 St. Roche 4Ba1	43.0	39.9		CONTROL	Capped
1613 St. Roche 4Ba2	41.9	39.1	38.7	CONTROL	Capped

Table 5.5 - continued

1613 St. Roche 4Ba3	41.2	37.3		CONTROL	Capped
1613 St. Roche 4Bb1	42.4	37.8		CONTROL	Capped
1613 St. Roche 4Bb2	43.3	38.2	37.1	CONTROL	Capped
1613 St. Roche 4Bb3	43.0	35.2		CONTROL	Capped
1613 St. Roche 4Bc1	44.1	38.6		CONTROL	Capped
1613 St. Roche 4Bc2	40.7	45.7	43.5	CONTROL	Capped
1613 St. Roche 4Bc3	42.4	46.3		CONTROL	Capped
1613 St. Roche 4Bd1	44.9	48.3		CONTROL	Capped
1613 St. Roche 4Bd2	44.5	47.7	48.1	CONTROL	Capped
1613 St. Roche 4Bd3	44.7	48.5		CONTROL	Capped
Average	43.0	41.9			Change 1.1%
std	1.3	4.8			
min	40.7	35.2			
max	44.9	48.5			
range	4.2	13.3			

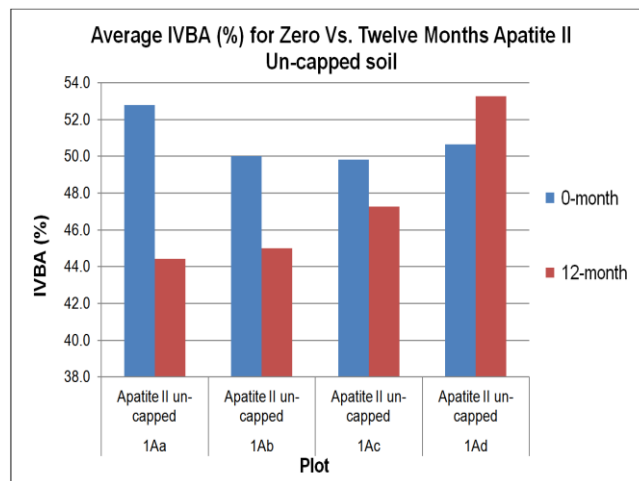


Figure 5.1 Comparison of average IVBA (%) between zero and twelve months apatite II un-capped 1613 St. Roche soil.

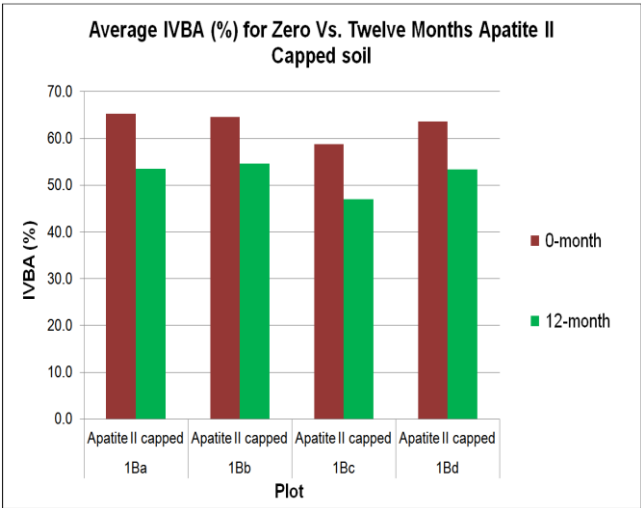


Figure 5.2 Comparison of average IVBA (%) between zero and twelve months apatite II capped 1613 St. Roche soil.

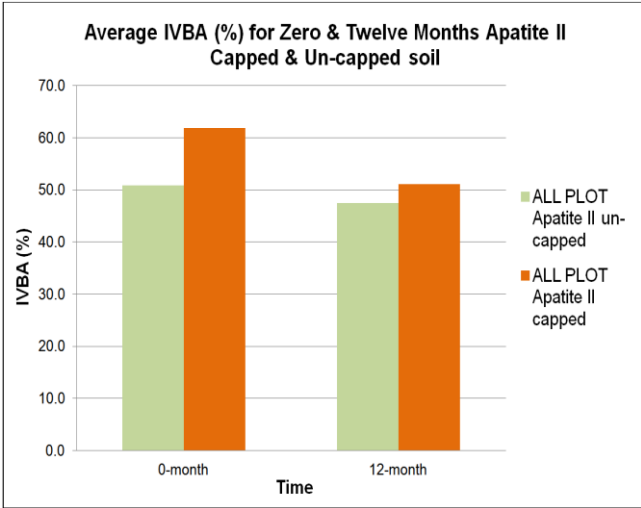


Figure 5.3 Comparison of average IVBA (%) between zero and twelve months apatite II capped and un-capped 1613 St. Roche soil.

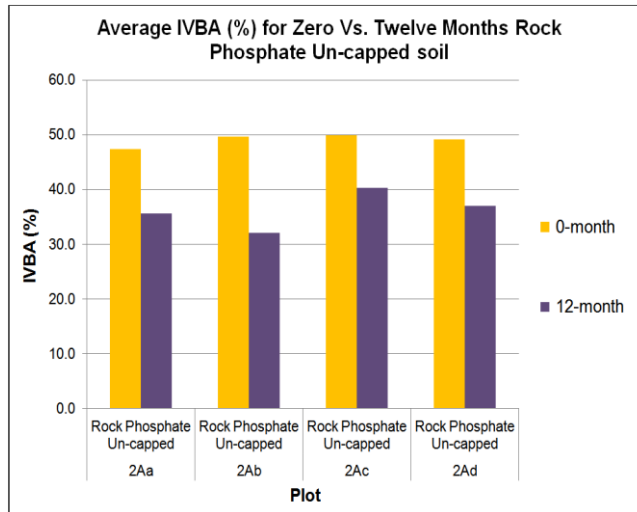


Figure 5.4 Comparison of average IVBA (%) between zero and twelve months rock phosphate un-capped 1613 St. Roche soil.

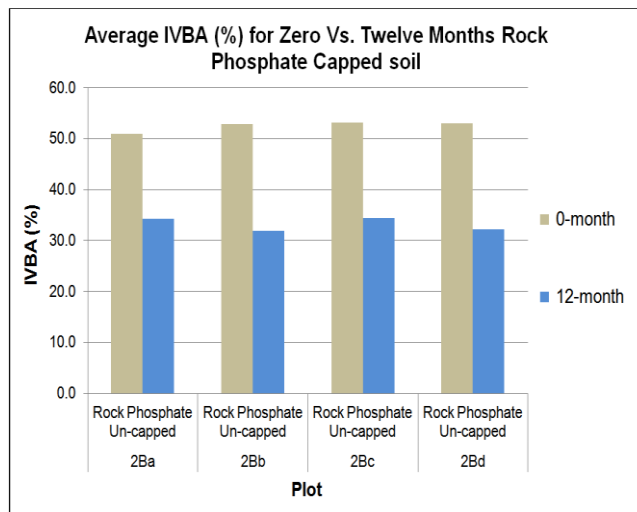


Figure 5.5 Comparison of average IVBA (%) between zero and twelve months rock phosphate capped 1613 St. Roche soil.

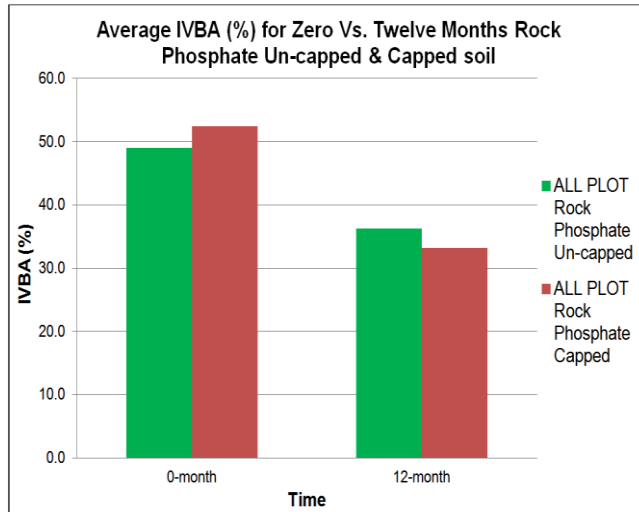


Figure 5.6 Comparison of average IVBA (%) between zero and twelve months rock phosphate capped and un-capped 1613 St. Roche soil.

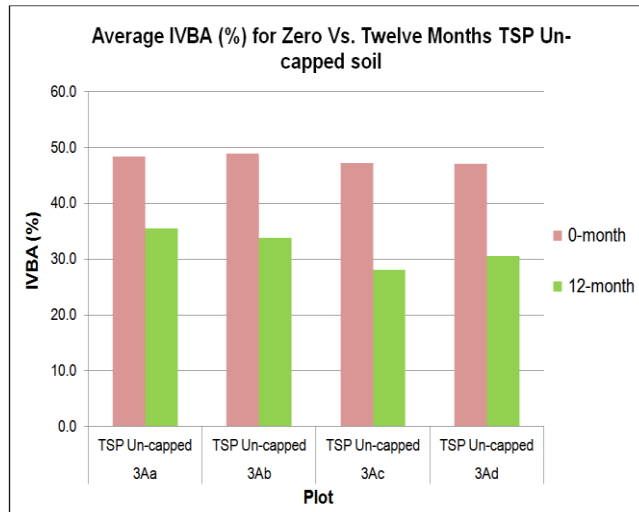


Figure 5.7 Comparison of average IVBA (%) between zero and twelve months TSP un-capped 1613 St. Roche soil.

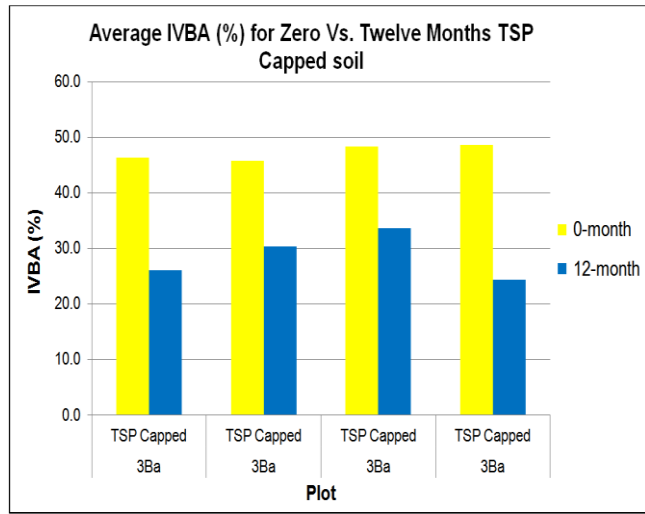


Figure 5.8 Comparison of average IVBA (%) between zero and twelve months TSP capped 1613 St. Roche soil.

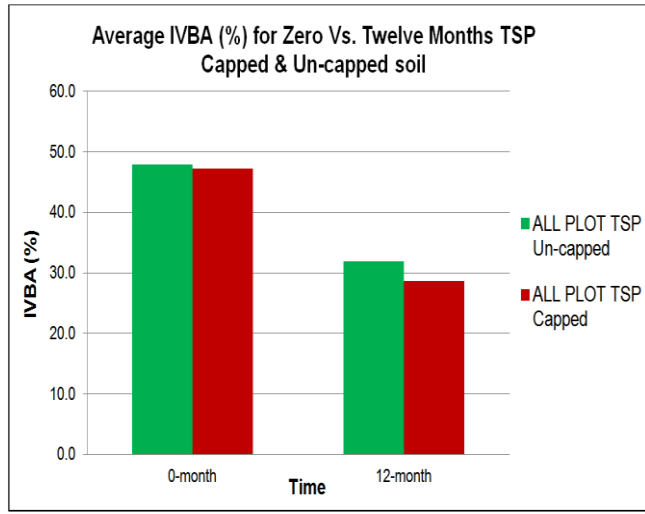


Figure 5.9 Comparison of average IVBA (%) between zero and twelve months TSP capped and un-capped 1613 St. Roche soil.

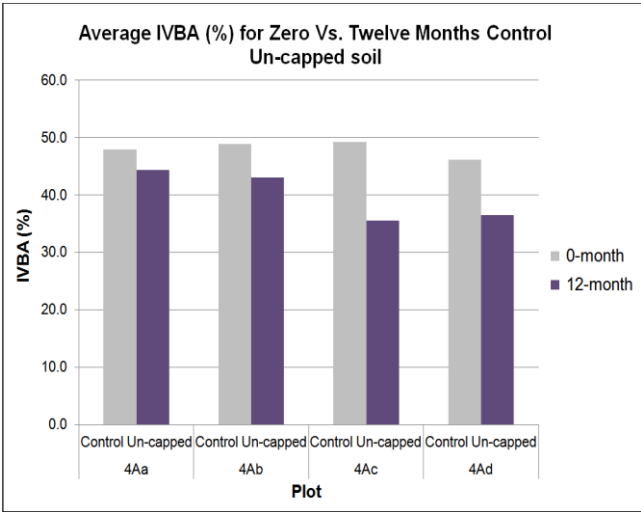


Figure 5.10 Comparison of average IVBA (%) between zero and twelve months control un-capped 1613 St. Roche soil.

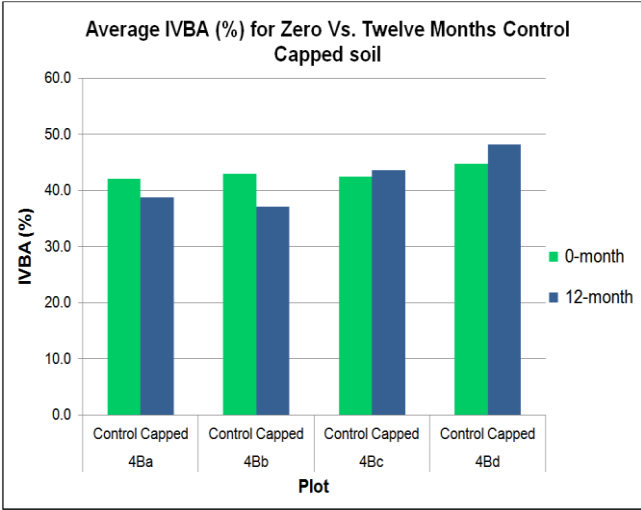


Figure 5.11 Comparison of average IVBA (%) between zero and twelve months control capped 1613 St. Roche soil.

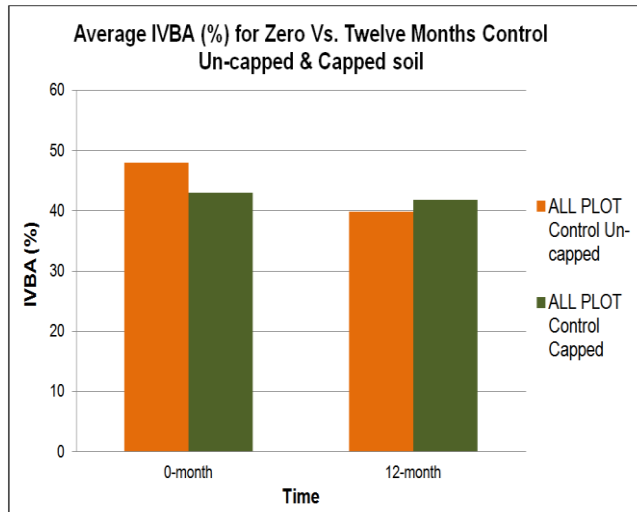


Figure 5.12 Comparison of average IVBA (%) between zero and twelve months control capped and un-capped 1613 St. Roche soil.

5.1.1.3 Soil pH, Loss On Ignition (LOI), and Moisture content

Soil characteristics (pH, organic matter content by Loss on Ignition (LOI), and Moisture content) were measured for the three different sites. The purpose of determining the pH of the soil was to assess whether the acidity of the soil would favor the Pb and phosphorous reaction, and whether the soil needed be acidified by adding iron sulfate (if the soil was highly alkaline).

The organic matter content of the soil was estimated by the LOI method it is known that Pb can bind to the clay humus complex and this binding might vary between sites depending on the organic matter content of the soils. Also, the percentage of moisture in the soil was calculated to provide some indication of the soil moisture conditions at the start of the field trials. All results are listed below:

Table 5.6 Average LOI, Average pH at both t = 0 and t = 12 Months and Average Moisture Content Data per Plot for Uncapped Soils for 1613 St. Roche Ave. Site.

Plot	n	Average LOI (%)	Average pH at time = 0 months	Average pH at time = 12 months	Average Moisture content (%)
1A (Apatite II)	4	15.16	7.12	7.85	7.41
2A (Rock Phosphate)	4	13.21	7.28	7.82	12.60
3A (Triple Super Phosphate)	4	13.41	7.33	7.86	8.99
4A (Control)	4	10.54	7.34	7.85	5.68

Table 5.7 Average LOI, Average pH at both t = 0 and t = 12 Months and Average Moisture Content Data per Plot for Capped Soils for 1613 St. Roche Ave. Site.

Plot	n	Average LOI (%)	Average pH at t = 0 months	Average pH at time = 12 months	Average Moisture content (%)
1B (Apatite II)	4	12.18	7.12	6.94	10.58
2B (Rock Phosphate)	4	10.35	7.30	6.76	10.01
3B (Triple Super Phosphate)	4	11.51	7.17	6.79	10.17
4B (Control)	4	14.08	7.22	6.61	10.89

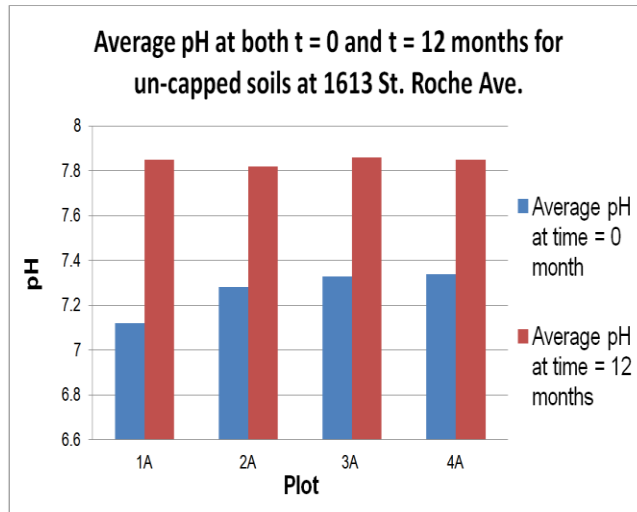


Figure 5.13 Average pH at both t = 0 and t = 12 months for un-capped soils at 1613 St. Roche Ave. site.

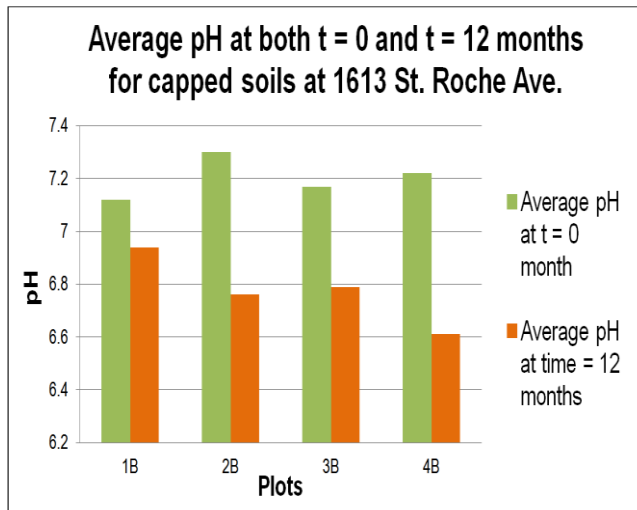


Figure 5.14 Average pH at both t = 0 and t = 12 months for capped soils at 1613 St. Roche Ave. site.

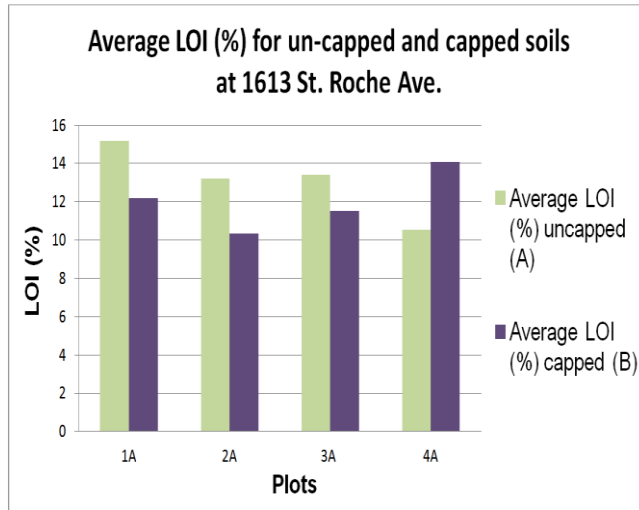


Figure 5.15 Average LOI (%) for un-capped and capped soils at 1613 St. Roche Ave. site.

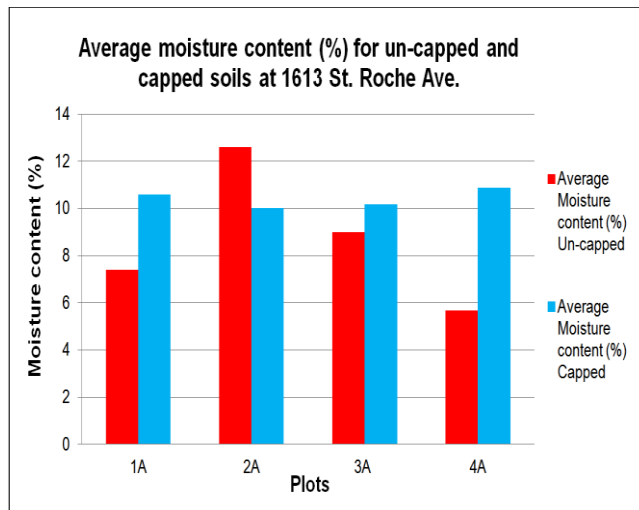


Figure 5.16 Average moisture content (%) for un-capped and capped soils at 1613 St. Roche Ave. site.

The results of the average pH, LOI, and moisture content for 1613 St. Roche Ave. site are set out in figures 5.1 - 5.4. The pH at both time $t = 0$ and $t =$

12 months for capped soils range from 6.6 to 7.3 and un-capped soils from 7.1 to 7.85, the pH of these soils is close to neutral.

The average LOI percent for the capped and un-capped soils at zero months is shown in figure 5.3. The LOI percent ranges between 10 and 15, and shows relatively small variation between the four plots indicating a degree of homogeneity in soil OM content.

The average moisture content for the capped and un-capped soils at zero months is shown in figure 5.4. The moisture content in soil ranges between 5.5 and 12.5 percent. The variability across the different plots is a reflection of water retention by the soil, the soil matrix and variability in precipitation in the sub-tropical climate.

Table 5.8 Average LOI, Average pH at both t = 0 and t = 12 Months and Average Moisture Content Data per Plot for Uncapped Soils for 1818 Dumaine St. Site.

Plot	n	Average LOI (%)	Average pH at time = 0 months	Average pH at time = 12 months	Average Moisture content (%)
1A (Hydroxyapatite)	4	12.85	7.52	7.89	36.20
2A (Phosphorous Pentoxide)	4	10.73	7.44	7.55	31.68
3A (Apatite II)	4	14.82	7.58	7.22	35.98
4A (Control)	4	9.40	7.37	7.21	22.56

Table 5.9 Average LOI, Average pH at both t = 0 and t = 12 Months and Average Moisture Content Data per Plot for Capped Soils for 1818 Dumaine St. Site.

Plot	n	Average LOI (%)	Average pH at time = 0 months	Average pH at time = 12 months	Average Moisture content (%)
1B (Hydroxyapatite)	4	10.35	7.64	7.85	29.25
2B (Phosphorous Pentoxide)	4	26.07	7.55	7.85	27.34
3B (Apatite II)	4	8.18	7.50	7.84	20.69
4B (Control)	4	12.17	7.55	7.90	20.13

The results of the average pH, LOI, and moisture content for 1818 Dumaine St. site are presented in figures 5.5 - 5.8. The pH at both t = 0 and t = 12 months for Un-capped soils ranges from 7.37 to 7.58 and 7.21 to 7.89, and the capped soils pH ranges from 7.50 to 7.64 at zero month and 7.84 to 7.90 respectively, suggesting all the soils were marginally basic.

The average LOI percent for the capped and un-capped soils at zero months is shown in figure 5.7. The LOI percent ranges between 8.18 and 26.07, the latter value was anomalous and a more realistic value for soil OM content was approximately 10%. This was similar to the soil OM content measure at the St. Roch site.

The average moisture content percent for the capped and un-capped soils at zero months is shown in figure 5.8. The moisture content in soil ranges between 20.13 and 36.20 percent. In general, the small change variability across different

plots is due to the unequal amount of water content in each sample. The soil moisture content at this site was far higher than that measured at the 1613 St Roch Site. However, this can be accounted for by differences in the times of installation the degree of precipitation over the intervening period. Nevertheless, the Pb conversion process of interest is mediated through the soil pore water and it is obvious that the soil moisture content can easily facilitate the process (the soils in this area are rarely dry for long periods of time).

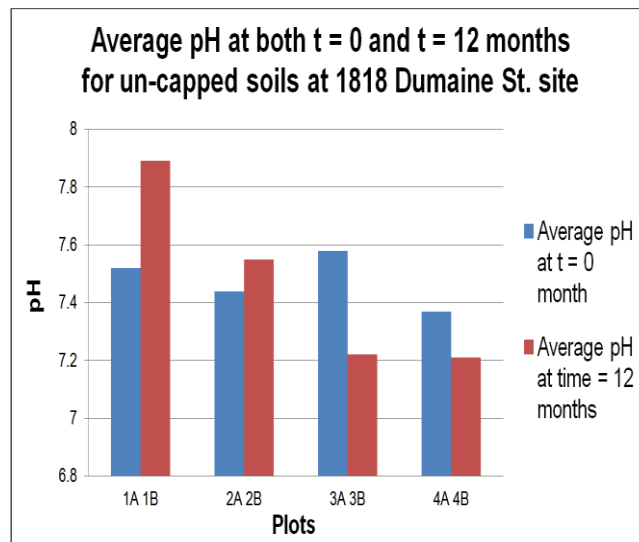


Figure 5.17 Average pH at both t = 0 and t = 12 months for un-capped soils at 1818 Dumaine St. site.

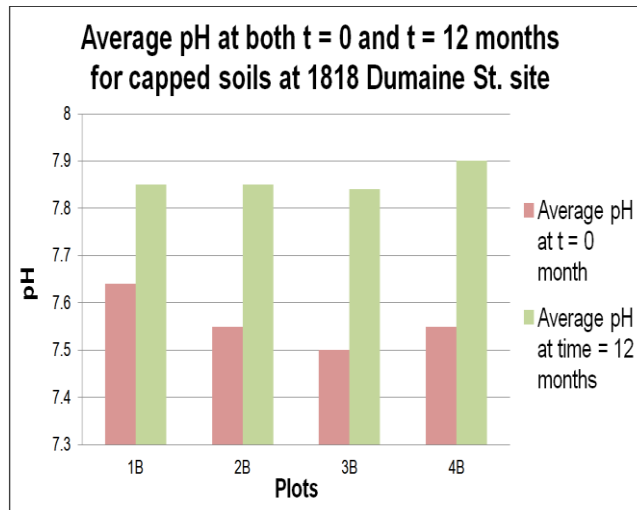


Figure 5.18 Average pH at both t = 0 and t = 12 months for capped soils at 1818 Dumaine St. site.

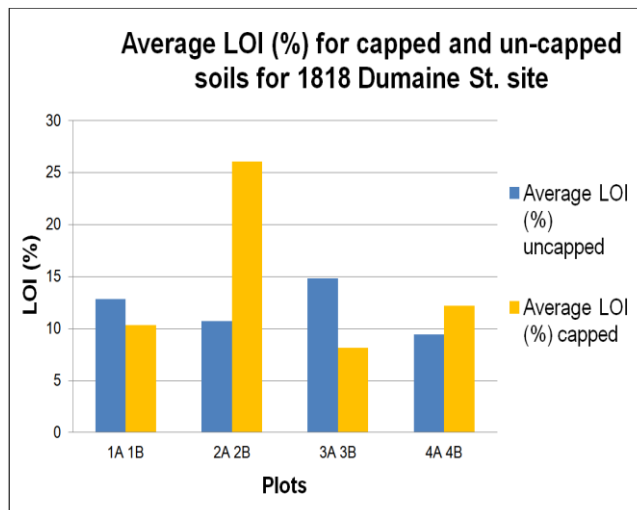


Figure 5.19 Average LOI (%) for capped and un-capped soils for 1818 Dumaine St. site.

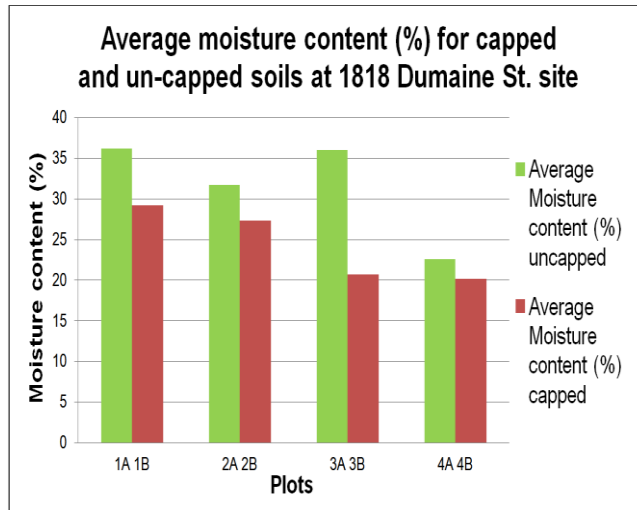


Figure 5.20 Average moisture content (%) for capped and un-capped soils at 1818 Dumaine St. site.

Table 5.10 Average LOI, Average pH at both t = 0 and t = 12 Months and Average Moisture Content Data per Plot for Capped Soils for 2224 N.Prieur St. Site.

Plot	n	Average LOI (%)	Average pH at time = 0 months	Average pH at t = 12 months	Average Moisture content (%)
1A (Control)	4	7.45	7.52	7.59	20.25
2A (Bone Char)	4	9.30	7.40	7.56	18.60
3A (Apatite II)	4	14.77	7.36	7.50	28.61
4A (Bone Meal)	4	10.97	7.31	7.46	19.99

Table 5.11 Average LOI, Average pH at both t = 0 and t = 12 Months and Average Moisture Content Data per Plot for Uncapped Soils for 2224 N.Prieur St. Site.

Plot	n	Average LOI (%)	Average pH at time = 0 months	Average pH at t = 12 months	Average Moisture content (%)
1B (Control)	4	9.61	7.25	7.60	19.42
2B (Bone Char)	4	8.50	7.41	7.57	18.86
3B (Apatite II)	4	13.59	7.39	7.52	16.51
4B (Bone Meal)	4	12.99	7.42	7.36	19.75

The results of the average pH, LOI, and soil moisture content for 2224 N. Prieur site are presented in figures 5.9 - 5.12. The pH at both t = 0 and t = 12 months for un-capped soils ranges from 7.25 to 7.42 at zero month and 7.36 to 7.60 at twelve months, whereas for capped soils, pH ranges from 7.31 to 7.52 at zero month and 7.46 to 7.59 respectively, the soil at this site was slightly alkaline and remained so over the course of the experiment. The average LOI percent for the capped and un-capped soils at zero months is shown in figure 5.11. The LOI percent ranges between 7.45 and 14.77 and shows a small random variation between the four plots due to the soil heterogeneity.

The average percentage of moisture content for the capped and un-capped soils at zero months is shown in figure 5.12. The moisture content in soil ranged between 16.51 to 28.61 percent. In general, small variability across the different

plots is likely due to the unequal amount of water retention since the last precipitation event.

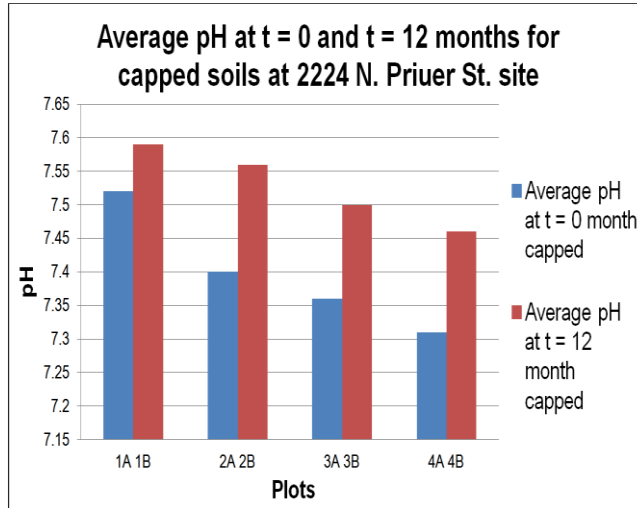


Figure 5.21 Average pH at t = 0 and t = 12 months for capped soils at 2224 N. Prieur St. site.

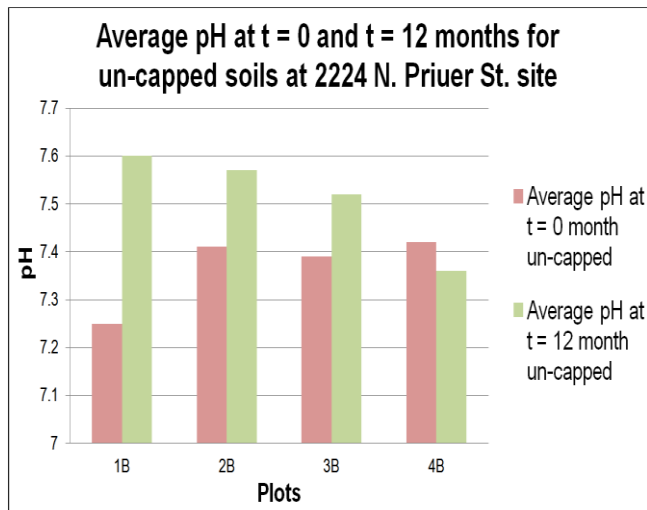


Figure 5.22 Average pH at t = 0 and t = 12 months for un-capped soils at 2224 N. Prieur St. site.

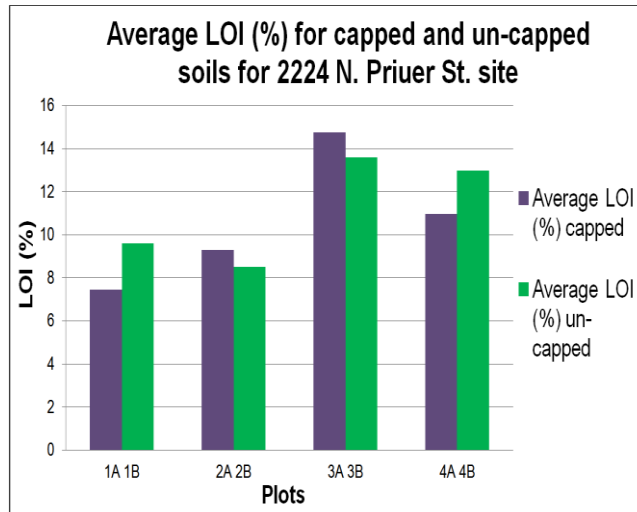


Figure 5.23 Average LOI (%) for capped and un-capped soils for 2224 N. Prieur St. site.

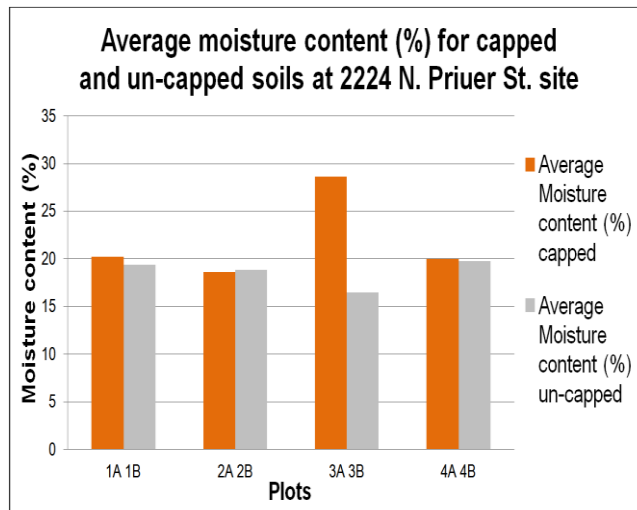


Figure 5.24 Average moisture content (%) for capped and un-capped soils at 2224 N. Prieur St. site.

5.1.1.4 Extended X-ray Absorption Fine Structure Spectroscopy (EXAFS)

The results from the EXAFS test with un-capped plots soil samples are presented in table 5.16. Due to budgetary constraints, EXAFS analysis was only performed on samples from the uncapped plots. For the soils at 1613 St. Roche at zero months, it appears that Pb was present in the pre-treated soils in mainly five different forms. Namely: (i) the Pb-carbonate mineral forms Hydrocerussite (basic Pb-carbonate) and Cerussite (PbCO_3), (ii) a Pb-phosphate phase, (iii) organically bound Pb, (iv) plumboferrite, and (v) mineral bound Pb.

Lead-carbonate forms are typically associated with old Pb-bearing paint, Pb-phosphate is likely the result of P originally present in the soil combining with contaminant Pb, and the organically bound Pb is Pb that has entered the soil solution and become bound to organic matter complexes, Plumboferrite is an Fe- and Mn-Pb phase and this association may represent the post dissolution of original Pb contamination preference of Pb poor soil Fe- and Mn-oxides, the mineral bound Pb is less easily explained as this phase represents Pb that is strongly bound in the matrix (by ionic substitution in the lattice structure) of various soil minerals.

This association is not easily explained. Samples collected from soils treated with apatite II (1A plot), rock phosphate (2A plot), and TSP (3A plot) at twelve months showed different mineral associations. At 12 months irrespective of the type of phosphate addition with which the soil was amended, three Pb

forms were dominant. These were: (i) an apatite sorbed phase, (ii) chloropyromorphite, and (iii) the plumboferrite phase.

The minimal change over 12 months in the percentage of plumboferrite in the soil suggests this phase did not change over the trial, the loss of the Pb-carbonate and to some extent the organic bound phases suggest the repartitioning of the Pb in these phases to new associations with soil phosphorus (from the phosphate amendments) either as a sorbed phase or as a newly formed Pb-PCI mineral phase (chloropyromorphite).

Interestingly the Pb-P phase identified at time zero is absent at 12 months, and it was anticipated that such phase would be stable in the soil. Changes in the amount of Pb defined as mineral bound is not readily explicable at this time.

EXAFS results for soil Pb speciation at the 1818 Dumaine St. site are set out in Table 5.16. At zero months, the Pb-phase content of the soil was dissimilar to that in the soil at 1613 St. Roch St. site. At the start of the trial in two of the plots Pb-carbonate was recorded and in the third Pb-oxide (litharge and plattnerite) was identified. The Pb in the soils at the start of the trial was also bound to P, organic material and Fe/Mn-phases. There was no mineral bound Pb identified at this site at any time.

A Pb phase identified as leadhillite (sulfate carbonate hydroxide mineral) was also present in the soil at time zero. This phase is akin to the Pb-sulfate Anglesite which is a not uncommon pigment in Pb-bearing paints. The major

change at 12 months here was the loss of leadhillite as a Pb phase, and as in the case of the 1613 St. Roch site, the loss of the Pb-P phase. At 12 months new Pb phases in the form of apatite sorbed Pb and chloropyromorphite appeared in the soil.

The Pb-phases at time zero and at time 12 months at the 2224 Prieur site were more difficult to interpret. Lead-carbonates were present at time zero, but on a percentage basis were at greater levels at the 12 month sampling. It is understood that Pb-carbonate is fairly soluble so an increase in Pb-carbonate over time is unexpected and was not particularly evident at the other two sites. Lead-oxide phases were identified at both time points, although the Pb-monoxide (identified here as litharge) was dominant.

The major changes in this soil as was the case at the other two sites, was loss of a Pb-P phase at 12 months and the appearance of an apatite sorbed phase and a chloropyromorphite phase at 12 months. The Pb-sulfate phase identified as leadhillite was also initially present in the soil at elevated levels but at 12 months was present at much lower levels. Organically bound Pb was much less important at this site compared to the other two, but as in the case of the other two sites a plumboferrite phase was substantially present at both time zero and time 12 months.

In summary, the EXAFS data revealed a consistent pattern of a loss of a Pb-P phase that was initially present in all the soils, and a replacement by an

apatite sorbed Pb phase and a chloropyromorphite phase. It appearance of the latter two phases was not unanticipated given the addition of phosphate products to the soil. However, it was expected that the emergence of apatite sorbed Pb and chloropyromorphite would be at the expense of relatively soluble Pb-carbonate compounds rather than accompanying the loss of a Pb-P phase present originally in the soil.

Table 5.12 Weighted Speciation Distribution Percent EXAFS Data for St. Roche, Dumaine St., and N. Prieur St. Soils at Time Zero and Twelve Months.

Sample Name	Weighted Speciation Distribution (%)											χ^2	
	Hydrocerussite	Cerussite	Organic Bound Pb	Leadhillite	Pb-Apatite Sorb	Pb ₃ (PO ₄) ₂	Chloropyromorphite	Plumbogummit	Plumboferriite	Litharge	Plattnerite		Mineral Bound Pb
Solubility Product (K _{sp})	$7.2 \times 10^{-17.6}$	$10^{-12.8}$				1×10^{-54}	$10^{-84.4}$	$10^{-69.3}$	$1 \times 10^{-112.6}$	$1 \times 10^{-12.9}$	$1 \times 10^{-49.6}$		
1613 Time = 0 month 1A	13	5	24			9		4	20	2	3	20	0.0002
1613 Time = 0 month 2A	14	3	18			11		5	23	4	3	20	0.0001
1613 Time = 0 month 3A	12	4	21			10		4	25		4	19	0.0002
1613 Time = 12 Months 1A	8		10		11		31	3	25	7	5		0.0002
1613 Time = 12 Months 2A	6		20		13		18	5	25	5	4	4	0.0002
1613 Time = 12 Months 3A	8		7		17		22	4	28	3	5	6	0.0005
1818 Time = 0 month 1A			13	26		12		9	15	12	12		0.0011
1818 Time = 0 month 2A	8		28	19		10		9	20	2	5		0.0002
1818 Time = 0 month 3A	12	5	16	20		11		3	27		5		0.0004
1818 Time = 12 Months 1A			18		24	2	18	4	13	11	8	3	0.0017
1818 Time = 12 Months 2A	12		19	8	12		15	7	21		5		0.0006
1818 Time = 12 Months 3A	10		16		13		27		30		4		0.0003
2224 Time = 0 month 2B	9		12	32		11		2	20	5	4	5	0.0003
2224 Time = 0 month 3B	3		8	38		7		3	23		5	12	0.0003
2224 Time = 0 month 4B	9		11	30		9		6	25	5	4		0.0002
2224 Time = 12 Months 2B	13	4		3	7		34	3	31		5		0.0003
2224 Time = 12 Months 3B	12		7	3	9	1	26	8	25	2	6		0.0004
2224 Time = 12 Months 4B	7	1	33	10	11		11	4	12	7	3	1	0.0007

5.1.1.5 Water phosphorous content data (Lysimeters) by Induced Coupled Plasma Mass Spectroscopy (ICP-MS)

Pore water was tested at the three sites with 1-, 2-, 3-, 4-, 5-, 6-, and 12 months for its phosphorous content by ICP-MS. The aim of this test is to evaluate the potential for down-profile transport of phosphorous that has entered the soil solution from phosphate amendments. All results are presented in the tables 5.17 through 5.19 and figures 5.13 through 5.27 below:

Table 5.13 Phosphorous Water Content at 1-, 2-, 3-, 4-, 5-, 6- and 12- Months at 1613 St. Roche Ave. Site.

1613 St Roche Ave. Lysimeter Data								
	Total Phosphorous (µg/L)							
Month	1	2	3	4	5	6	12	Average
Plot								
1A (Apatite II)	26	18	5	1	3	12	15	11
2A (Roch Phosphate)	21	8	20	18	23	72	167	47
3A (TSP)	16	13	58	4	37	23	9	22.85
4A (Control)	8	18	12	7	19	30	10	14.87

The results from the 1A plot treated with Apatite II indicates the decrease in phosphorous released in the first five months started from the highest concentration of 26 µg/L to 3 µg/L with a slight increase in the six and twelve month samples to 15 µg/L. For the Rock Phosphate amendment at plot 2A, an increase in the phosphorous content trend was determined to be the highest concentration of 167 µg/L.

Also, TSP min plot 3A had a variation of phosphorous release with the highest P concentration 58 µg/L at 3 months and the lowest, 4 µg/L at 4 months. The 4A control plot showed the highest P release of 30 µg/L at 6 months and the lowest P concentration with 7 µg/L at 4 months. Apatite II was found to release relatively less P over the twelve months than rock phosphate and TSP amendments.

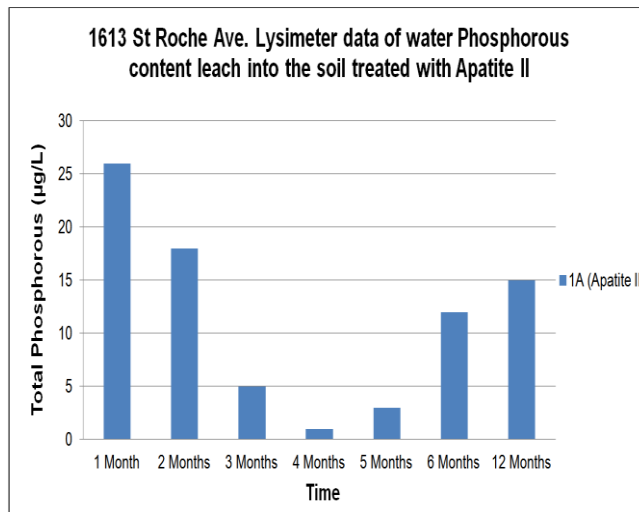


Figure 5.25 Lysimeter data of water Phosphorous content leach into the soil treated with Apatite II at 1613 St Roche Ave. site.

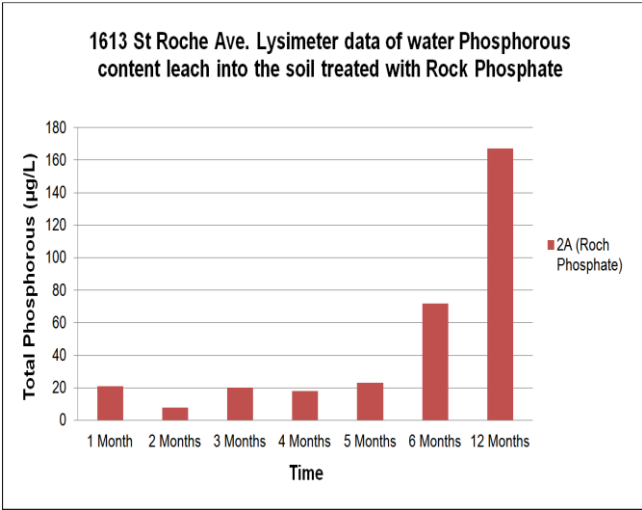


Figure 5.26 Lysimeter data of water Phosphorous content leach into the soil treated with Roch Phosphate at 1613 St Roche Ave. site.

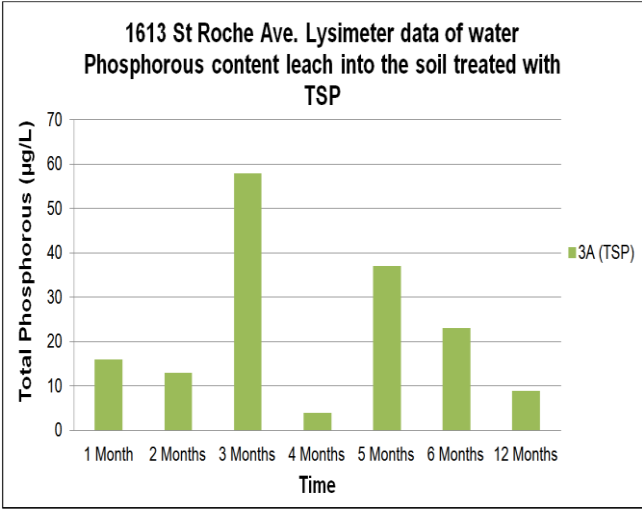


Figure 5.27 Lysimeter data of water Phosphorous content leach into the soil treated with TSP at 1613 St Roche Ave. site.

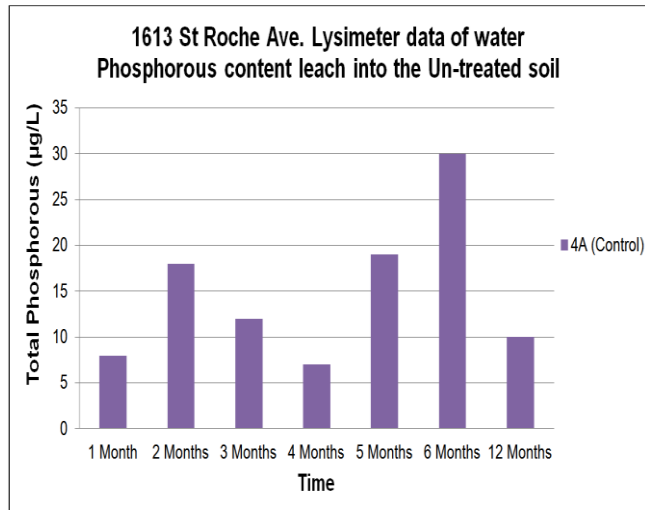


Figure 5.28 Lysimeter data of water Phosphorous content leach into the Un-treated soil at 1613 St Roche Ave. site.

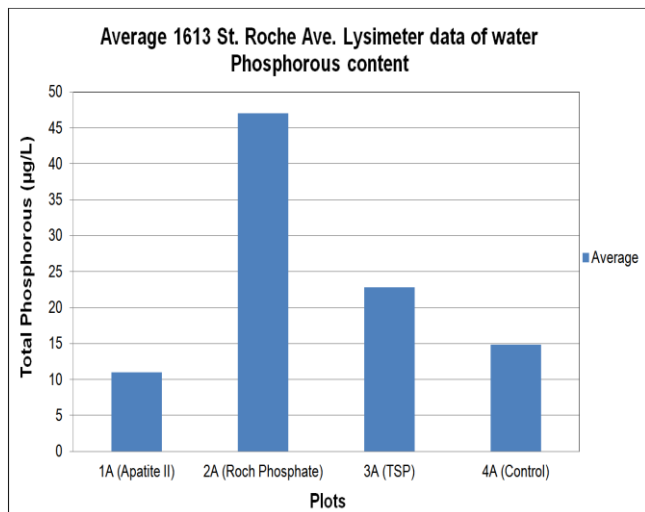


Figure 5.29 A twelve months average Lysimeter data of water Phosphorous content leach into the soil at 1613 St. Roche Ave. site.

Table 5.14 Phosphorous Water Content at 1-, 2-, 3-, 4-, 5-, 6- and 12- Months at 1818 Dumaine St. Site.

1818 Dumaine St. Lysimeter Data								
Month Plot	Total Phosphorous ($\mu\text{g/L}$)							Average
	1	2	3	4	5	6	12	
1A (Hydroxyapatite)	12	19	18	15	11	17	21	16
2A (Phosphorous Pentoxide)	13	14	14	10	13	10	10	12
3A (Apatite II)	27	13	6	14	8	9	6	11.85
4A (Control)	27	13	17	24	35	34	6	22.3

The phosphorous water content results from the 1A plot treated with Hydroxyapatite indicate a slight increase in phosphorous release during the twelve months, which started from a low concentration of 12 $\mu\text{g/L}$ to 21 $\mu\text{g/L}$ and an average of 16 $\mu\text{g/L}$. For the Phosphorous Pentoxide amendment at plot 2A, the phosphorous content trend was determined to be relatively straight with an average of 12 $\mu\text{g/L}$. The Apatite II, at plot 3A, had a variation of phosphorous release with the highest P concentration being 27 $\mu\text{g/L}$ during the first month and the lowest being 6 $\mu\text{g/L}$ at three and twelve months. The lowest total average was 11.85 $\mu\text{g/L}$ among all the amendments.

The 4A control plot showed the highest P release of 35 $\mu\text{g/L}$ at five months and the lowest P concentration, 6 $\mu\text{g/L}$, was at twelve months with a total average P concentration of 22.3 $\mu\text{g/L}$. Apatite II was determined to release relatively less P over the twelve months than the Hydroxyapatite and Phosphorous Pentoxide amendments.

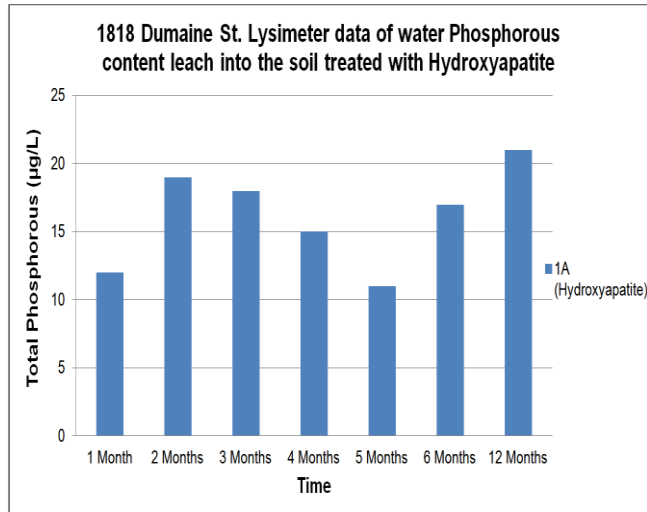


Figure 5.30 Lysimeter data of water Phosphorous content leach into the soil treated with Hydroxyapatite at 1818 Dumaine St. site.

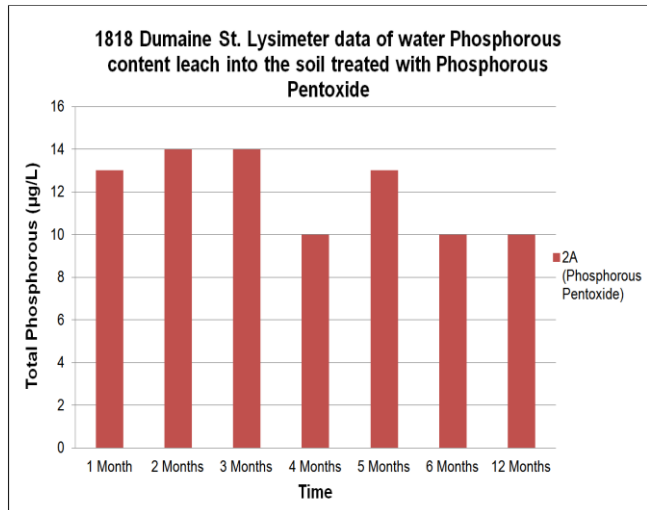


Figure 5.31 Lysimeter data of water Phosphorous content leach into the soil treated with Phosphorous Pentoxide at 1818 Dumaine St. site.

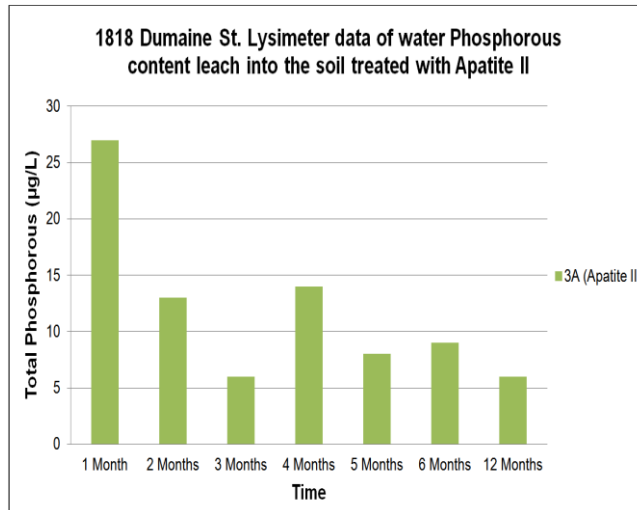


Figure 5.32 Lysimeter data of water Phosphorous content leach into the soil treated with Apatite II at 1818 Dumaine St. site.

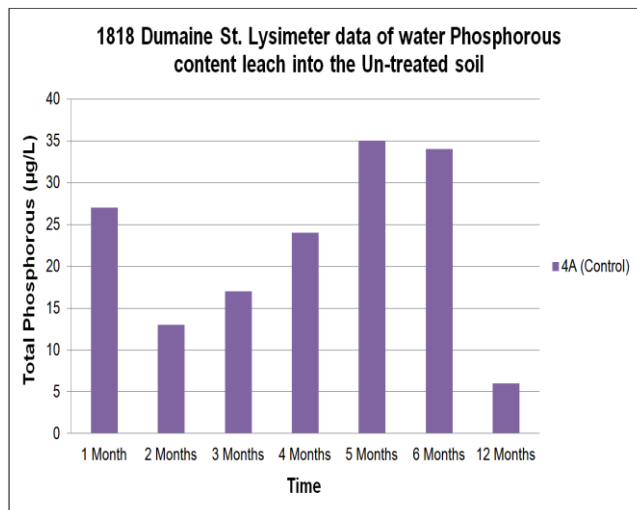


Figure 5.33 Lysimeter data of water Phosphorous content leach into the Un-treated soil at 1818 Dumaine St. site.

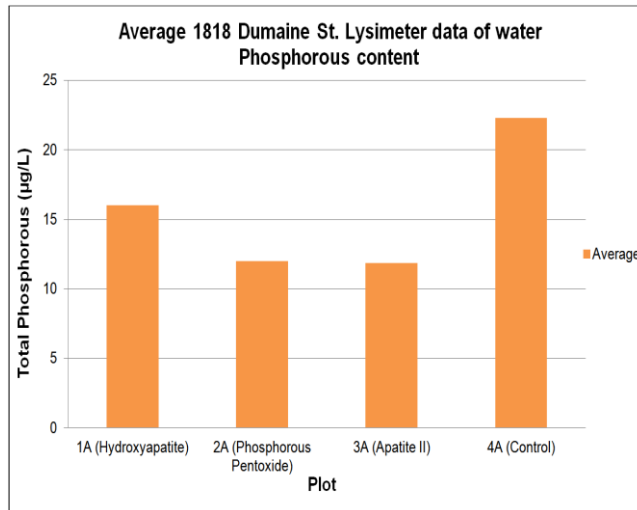


Figure 5.34 A twelve months average Lysimeter data of water Phosphorous content leach into the soil at 1818 Dumaine St. site.

Table 5.15 Phosphorous Water Content at 1-, 2-, 3-, 4-, 5-, and 6- Months at 2224 N. Prieur St. Site.

2224 N. Prieur St. Lysimeter Data							
Month Plot	Total Phosphorous (µg/L)						Average
	1	2	3	4	5	6	
1B (Control)	12	11	17	18	9	Missing	13.4
2B (Bone Char)	10	15	9	9	17	15	12
3B (Apatite II)	12	12	8	Insufficie- -nt	10	Missing	10.5
4B (Bone Meal)	25	12	21	Insufficie- -nt	Insuffic- -ient	13	19

The phosphorous water content results from the 1B un-treated plot indicate a slight increase in phosphorous release during the four months, which started at concentrations of 12 µg/L to 18 µg/L with an average of 13.4 µg/L. For

the Bone Char amendment at plot 2B, the phosphorous water content was determined to be less variable with an average of 12 $\mu\text{g/L}$. The Apatite II at plot 3B had a variation in the phosphorous release, with the highest P concentrations at 12 $\mu\text{g/L}$ during the first and second months and the lowest at 8 $\mu\text{g/L}$ during the third month, with the lowest total average of 10.5 $\mu\text{g/L}$ among all the amendments.

The 4B Bone Meal treated plot showed the highest P release of 25 $\mu\text{g/L}$ during the first month and the lowest P concentration of 12 $\mu\text{g/L}$ during the second month, with a total average of P concentration of 19 $\mu\text{g/L}$. Apatite II was determined to release relatively less P over the six months than Bone Char and Bone Meal amendments. Unfortunately, the Lysimeters were broken during the sixth month of the experiment and there was missing data from the six-month trial for the 2224 N. Prieur St. site due to a storm that occurred on the August 29, 2012. There was an insufficient quantity of water found during the fourth and fifth months for plots 3B and 4B.

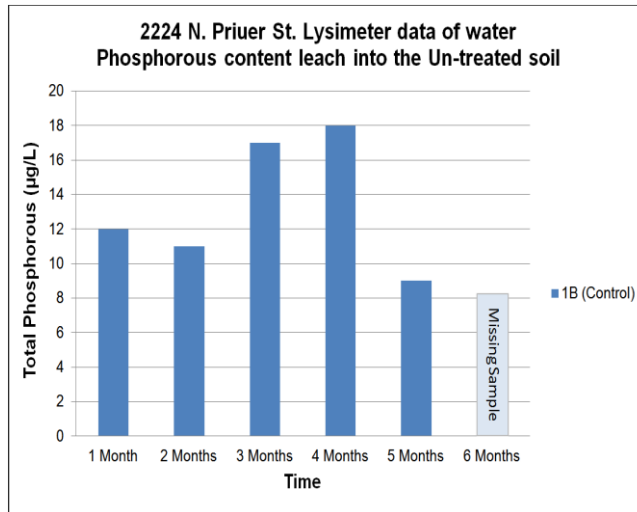


Figure 5.35 Lysimeter data of water Phosphorous content leach into the Un-treated soil at 2224 N. Priuer St. site.

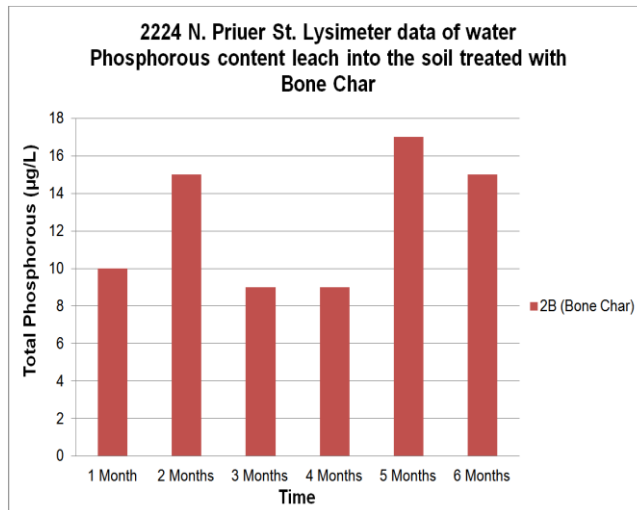


Figure 5.36 Lysimeter data of water Phosphorous content leach into the soil treated with Bone Char at 2224 N. Priuer St. site.

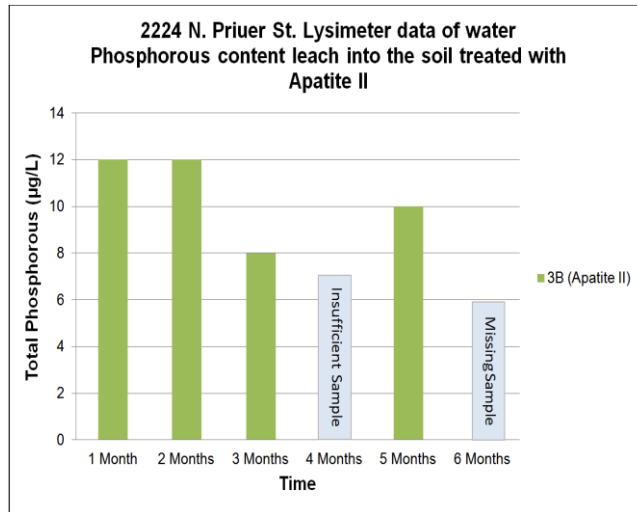


Figure 5.37 Lysimeter data of water Phosphorous content leach into the soil treated with Apatite II at 2224 N. Priuer St. site.

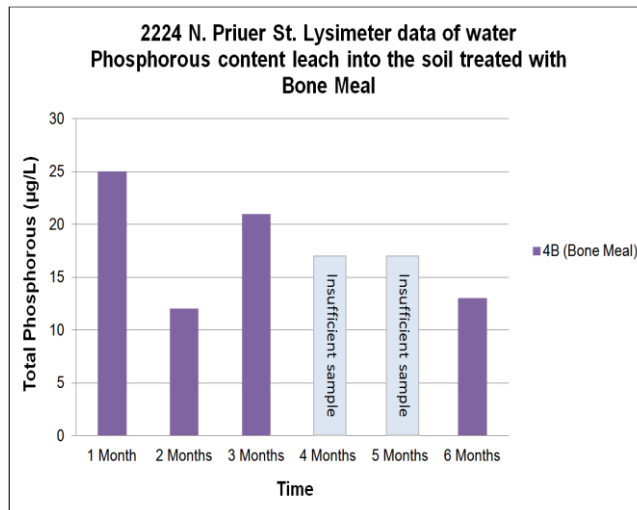


Figure 5.38 Lysimeter data of water Phosphorous content leach into the soil treated with Bone Meal at 2224 N. Priuer St. site.

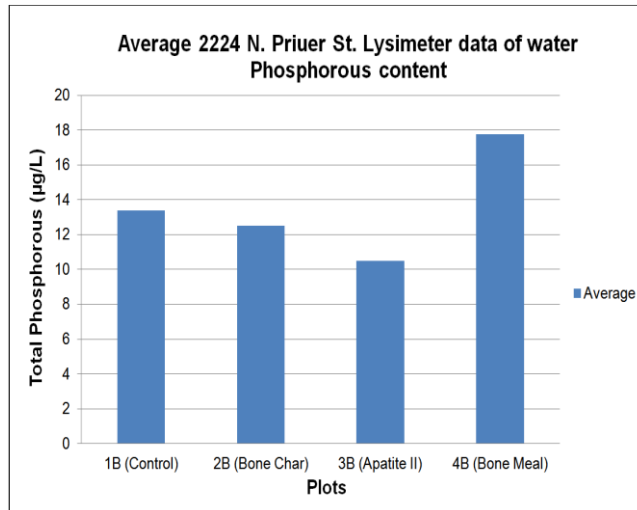


Figure 5.39 A twelve months average Lysimeter data of water Phosphorous content leach into the soil at 2224 N. Prieur St. site.

5.1.1.7 Scanning Electron Microscope (SEM) Analysis

5.1.1.7.1 Zero Month Soil Samples: Individual Particle Analysis (IPA)

Uncapped Soil samples were examined at the three sites to determine the presence of morphology and composition of Pb or pre- existence of pyromorphite before any amendments were added. Pb was expected to have two possible sources: Pb in paint or Pb in gasoline. In this study, we describe our microscopy findings on a plot-by-plot basis.

5.1.1.7.1.1 1613 St. Roche plots (1A, 2A, 3A, 4A)

Lead was found associated with P in all a, b, c, and d quadrants. As noticed, the Pb was present as a surface layer (or cryptocrystalline particles), and was associated with P and Zn, Fe, and Mn (Appendix B Figures B.1, B.6, B.7 & B.10). Lead was also observed as aggregate hexagonal particles, which is a

distinguishing feature for Cerussite (Appendix B Figure B.4). Other metals were found in Pb with P, such as Cr and Ti (Appendix B Figure B.7 & B.9).

Calcium was also associated with PbP phases because of the calcium associate with phosphate that present in soil. Barium was observed in the 2A and 4A plots with the Pb in soil taking the most likely form of Barium sulfate (Appendix B Figure B.13, B.16 & B. 38). Lead was found associated with P in very small rounded particles in the soil (Appendix B Figure B.19) or sorbed into CaP particles (Appendix B Figure B.24 & B. 25). The difference in the ratio of Pb to P in a particle was determined based on the spectra peaks length (Appendix B Figure B.26, B.27 & B. 28).

5.1.1.7.2 Summary of results obtained from IPA analysis of Pb in the soils sampled at zero months at 1613 St. Roche Ave.

The most obvious outcome of the investigating of Pb-bearing particles collected at zero months, was the discrete form of Pb associated with P either in amorphous or cryptocrystalline on surface phases or below surface precipitation, which is hard to determine because of instrument limitations.

5.1.1.7.3 Twelve Months Soil Samples: Individual Particle Analysis (IPA)

5.1.1.7.1.2 1613 St. Roche Ave. plots (1A, 2A, 3A, 4A)

In these plots, Lead was associated with P in all a, b, c, and d quadrants. Obviously, Pb presented as a surface layer (Appendix C Figures C.1 & C.6) or cryptocrystalline particles (Appendix C Figures C.2, C.3 & C.5), and was

associated with P and Zn, Fe, and Mn (Appendix C Figures C.14, C.16, & C.28). Lead was also observed as small tabular particles with Cr and Ti accumulated on a surface of Si, Al, and Ca particles in the rock phosphate treated 2A plot (Appendix C Figure C.13 & C.17). The TSP amendment was found in the soil with Pb sorbed onto the surface (Appendix C Figure C.18). Also, Barium, possibly as a Barium sulfate constituent, presented in 4A (control) plot with Pb in the soil (Appendix C Figure C.32, C.33). Plot 1A was treated with apatite II and the Pb was associated with P on the surface of the amendment (sorbed or cryptocrystalline phases) (Appendix C Figure C.1 & C.5).

5.1.1.7.4 Summary of results obtained from IPA analysis of Pb in the soils sampled at twelve months at 1613 St. Roche Ave.

The PbP particles found at twelve months were the discrete form of Pb associated with P either in amorphous or cryptocrystalline form on surface phases or below surface precipitation, which is hard to determine because of instrument limitations. The difference between the zero and twelve month samples were the PbP particles had more residence time in soil and showed poorly formed crystalline forms.

5.1.1.7.5 Zero Month Soil Samples: Individual Particle Analysis (IPA)

5.1.1.7.1.3 1818 Dumaine St. plots (1A, 2A, 3A, 4A)

The soils in all plots also contained PbP. A small sized Pb associated with P (<10 µm) particles was found as a surface sorbed phase (Appendix D Figures

D.1 & D.2). Also fish bone particles were presented with low Pb concentrations (Appendix D Figures D.3 & D.8) or high Pb concentration, with larger and denser particles that could be identified by the backscattered electron image (Appendix D Figure D.6). This suggests that Pb precipitates onto the surface or disseminates throughout grains of fish bones. Other forms of CaP with Pb were found in the soils with Si, Al, Zn, and Fe associated with them (Appendix D Figures D.4 & D.5).

Lead paint was observed in the soil either as a hexagonal particle (Appendix D Figures D.17, D.22 & D.29) or an aggregate of dense bright particles (Appendix D Figure D.9). Also, PbP formed in small (<5 µm) elongated particles (Appendix D Figure D.15), tubular shapes (Appendix D Figures D.27a & D.27b), acicular particles attached to the surface of Si and Al particles (Appendix D Figures D.28a & D.28b), and rounded PbP particles found on Si and Al particles (Appendix D Figures D.31a, D.31b & D.31c).

5.1.1.7.6 Summary of results obtained from IPA analysis of Pb in the soils sampled at zero months at 1818 Dumaine St.

The most obvious outcome of investigating the Pb-bearing particles collected at zero months at 1818 Dumaine St. site, was the discrete form of Pb associated with P either in amorphous or cryptocrystalline on surface phases or below surface precipitation, which is challenging to determine because of

instrument limitations. The PbP forms were generally found as tubular, rounded, and acicular forms, which could be an advanced pyromorphite maturation phase.

5.1.1.7.7 Twelve Months Soil Samples: Individual Particle Analysis (IPA)

5.1.1.7.1.4 1818 Dumaine St. plots (1A, 2A, 3A, 4A)

In these soils, plot 1A was treated with Hydroxyapatite and showed Pb associated with P in discrete forms (Appendix E Figures E.1, E.2 & E.7) or cryptocrystalline phase (Appendix E Figure E.8). An aggregate of rounded bright dense particles was recognized by backscattered electron image (Appendix E Figure E.3). The Pb, Mn, and Fe phases were found in the soil (Appendix E Figure E.4). Lead particles were also observed in the twelve-month soils (Appendix E Figure E.5 & E.6).

Plot 2A was treated with Phosphorous Pentoxide and the same results were found in Pb associated with P in discrete forms (Appendix E Figures E.10, E.11 & E.14) or cryptocrystalline phases (Appendix E Figure E.13). For the apatite II treated plot (3A), spherical bright PbP particles were detected and were found formed onto a surface of fish bone (Appendix E Figure E.17). It is suggested that Pb could be sorbed onto the edges of a fish bone (Appendix E Figures E.18a & E.18b). In plot 4A (control), both aggregates of Pb particles (Appendix E Figure E.22) and Pb associated with P presented (Appendix E Figures E.23, E.24 & E.25) after a twelve-month soil residence time.

5.1.1.7.8 Summary of results obtained from IPA analysis of Pb in the soils sampled at twelve month at 1818 Dumaine St.

The twelve-month PbP particles were found as discrete forms of Pb associated with P either in a cryptocrystalline phase or below sub-surface precipitation, which is hard to determine because of instrument limitations. The difference between the zero and twelve month samples were PbP particles had more residence time in the soil and showed a poorly formed crystalline structure and indistinctive features.

5.1.1.7.9 Zero Month Soil Samples: Individual Particle Analysis (IPA)

5.1.1.7.1.5 2224 N. Prieur St. plots (1A, 2A, 3A, 4A)

Soils from all plots were tested for Pb particles. Irregular shapes of Pb particles were found in the soil (Appendix F Figure F.1) and PbP forms dominated in all plots either sorbed or disseminated onto the surface of P particles (Appendix F Figures F.5, F.11, F.15 & F.8) or precipitated as a cryptocrystalline phase (Appendix F Figures F.2 & F.3). Lead was also found to be associated with Mn and Fe (Appendix F Figure F.6). The Pb was observed bound in Si, Al, Ba, and Ca matrix (Appendix F Figures F.23 & F.14).

5.1.1.7.10 Summary of results obtained from IPA analysis of Pb in the soils sampled at zero months at 2224 N.Prieur St.

The results of the of Pb-bearing particles that were collected at zero months at 2224 N.Prieur St. site, were also the discrete and disseminated forms of

Pb associated with P either in amorphous or cryptocrystalline on surface phases or below surface precipitation, which is challenging to determine because of instrument limitations.

5.1.1.7.11 Twelve Months Soil Samples: Individual Particle Analysis (IPA)

5.1.1.7.1.6 2224 N. Prieur St. plots (1A, 2A, 3A, 4A)

In these soils, plot 1B was un-treated, which showed Pb associated with P in discrete forms (Appendix G Figures G.2, G.3 & G.8) or cryptocrystalline phases (Appendix G Figure G.4). Also, Pb associated with Fe and Zn was bound in a Si-Al-Ca matrix (Appendix G Figure G.5). Plot 2B was treated with Bone Char and the same results were found, Pb was associated with P in discrete forms (Appendix G Figures G.10, G.12 & G.13).

For the apatite II treated plot (3B), cryptocrystalline PbP particles were detected and were formed onto a surface of fish bone (Appendix G Figure G.17 & G.21) or sorbed onto the fish bone porosity (Appendix G Figures G.18, G.20 & G.22). In a Bone Meal treated 4B plot, Pb was found associated with P in discrete forms (Appendix G Figure G.25, G.29 & G.30) and Pb associated with Mn and Fe were found present in the samples (Appendix G Figures G.32).

5.1.1.7.12 Summary of results obtained from IPA analysis of Pb in the soils sampled at twelve months at 2224 N.Prieur St.

The twelve months Pb-bearing outcomes were found to be discrete forms of Pb associated with P either in cryptocrystalline phases or below sub-surface

precipitations, which are hard to determine because of instrument limitations. The difference between the zero and twelve month samples are that PbP particles have more residence time in the soil and showed poor crystalline form but mature PbP particles with distinctive features.

Chapter 6

Discussion and Conclusions

6.1 Discussion

The application of *in situ* chemical stabilization of lead (Pb), through the addition of Phosphorous (P) amendments, was examined in residential urban soils as a function of soil chemistry and composition. The field trial was conducted at three sites in the Treme and St. Roch neighborhoods of New Orleans, LA.

The remediation process involved dividing the yard at each site into eight plots where three of them were treated with different phosphate amendments and one plot was untreated as a control (see chapter three). Apatite II, a biogenic phosphate with a nanocrystalline structure (ground fish bone), was added to plot soils at all sites to evaluate the effectiveness compared to other phosphate amendments (i.e., Rock Phosphate, TSP, Hydroxyapatite, Phosphorous Pentoxide, Bone Char, and Bone Meal).

Apatite II has the ability to precipitate metals at nucleation sites and through its ability to sorb Pb ions (Bostick, 2003). The goal of the project was to determine if apatite II has the potential to be developed as a “method of choice” for the low cost method of reducing the Pb-poisoning risk posed by Pb-contaminated soils. The aim of adding phosphate amendments to the Pb contaminated soil is to provide a P source that can combine with Pb to form a sparingly soluble mineral called "pyromorphite". Pyromorphites are part of the

lead phosphate minerals family (e.g. fluoro-pyromorphite k_{sp} of $10^{-71.6}$, hydroxyl-pyromorphite k_{sp} of $10^{-76.8}$, bromo-pyromorphite k_{sp} of $10^{-78.1}$, and chloro-pyromorphite k_{sp} of 10^{-85}) that are highly insoluble and are thus a bio-persistent Pb-phase in the environment (Chen *et al.* 1997b).

Three different sites (1613 St. Roche Ave., 1818 Dumaine St., and 2224 N. Prieur St.) were chosen as targets for the soil remediation. The two possible sources of Pb that likely contaminated these sites were: (i) Pb-based paint historically applied to building structures, and (ii) historically emitted Pb that at one time was present in gasoline and was deposited on urban soil.

The site selection was based on the specific criteria determined for the reconnaissance samples of soil Pb content (See Tables 5.1, 5.2 & 5.3). Soil samples were taken pre- and post- treatment at time zero (prior to any phosphate product addition) and at twelve months. Comparison of the soils at the two time periods involved the examination of the Pb particle size, crystalline form, degree of incorporation of Pb in particle phases, and the presence of other Pb mineral forms.

Samples were analyzed by Extended X-ray Absorption Fine Structure Spectroscopy (EXAFS) to determine the Pb speciation and type of Pb minerals in the soil. Additionally, phosphorous water content was calculated for each plot to estimate the phosphorous release rate for each amendment (Tables 5.17, 5.18 & 5.19). A principal goal of the study was to compare apatite II with other

amendments in terms of low phosphorous release over a twelve months soil residence time. Another goal was to understand the mechanisms of Pb-P binding in different forms that develop in soils.

The experimental design of the study involved dividing yards at each residential site into eight 10' X 10' plots, where four were capped with 6" of Bonnet Carré Spillway clean soil (Mielke *et al.*, 2006). Each plot was divided into four quadrants for sampling purposes and at each site 3 different amendments were mixed into six of the plots, while two remained untouched as controls. Each site was treated with different phosphate amendments, but apatite II was added to the soil at all three sites (See chapter three).

The solubility of Pb in soil relies on the pH of the soil solution that percolates through the soil profile (Cao *et al.* 2008). For instance, the solubility of PbO ($K_{sp} = 7.9 \times 10^{12}$) is higher than PbCO₃ ($K_{sp} = 1.6 \times 10^{-13}$) and PbSO₄ ($K_{sp} = 2 \times 10^{-8}$) for pH less than 5. However, pH > 7 PbSO₄ is more soluble than PbO and PbCO₃ (Cao *et al.* 2008).

Pyromorphite has much lower solubility constant ($K_{sp} = 4 \times 10^{-85}$) than the other Pb forms. Pyromorphite can be considered as the most thermodynamically stable Pb-mineral in soil and is an end member that Pb will form if P and Cl are present in variable forms. In this experiment, apatite II was assessed as an amendment at the three residential yards in order to determine if it could be considered a preferred soil amendment. Adding apatite II to the soil enhances the

buffer capacity of the soil due to the release of Ca in solution, which prevents Pb from easily dissolving in water (Cao *et al.* 2008).

Bostick suggested that apatite II dissolves slowly in water, which means that the P ions will take a relatively long time to react with Pb ions, thus the pyromorphite transformation will take a long time to complete (2008). The pH measurements for 1613 St. Roche Ave. soils were slightly increased between zero to twelve months for uncapped soils (Table 5.11, Figure 5.1), which allowed them to become slightly more alkaline and may have facilitated the pyromorphite precipitation. The capped plots showed a slight decrease in the pH values (Table 5.11, Figure 5.2), which enhanced the dissolution of Pb to form pyromorphite (Laperche *et al.* 1996).

Understanding of the pyromorphite formation through rapid kinetic processes of the dissolution of Pb and P followed by precipitation of Pb-P phases is an important buffering mechanism that relies on the precipitation of a soluble mineral phase, adsorption to clay, and the stable formation by organic matter contact (Davis 1995).

The soil in New Orleans is classified as silt clay, based on the United States of Agriculture (USDA) (1999), however as the site soils were residential yards with an unknown history of potential fertilizer and extraneous top-soil addition it is unrealistic to assign these soils to a specific soil classification. The city has an average annual rainfall of 162.56 cm (64 inches), which results in

frequent levels of high soil moisture content (Weatherbill, 2014) this is due to the humid subtropical climate of the region. The average percent of loss on ignition (LOI) and the average percent of the moisture content for soils at zero months were presented in this study to provide some indication of the possible speed of the Pb transformation process and the likelihood of binding to the organic matter in the soil, soil Pb bioavailability decreases with high organic matter content (>50%) (Brown *et al.* 2003).

Ma *et al.* (1995) concluded that the solubility of Rock Phosphate increases with carbonate compounds. She also reported a reduction of 22-100% of dissolved Pb in thirteen contaminated sites after the rock phosphate addition. Rock phosphate enhances the neutralizing of the soil acidity because of the free calcium carbonate (Miretzky & Fernandez-Cirelli, 2007). That is, it affects the soils buffering capacity. However, rock phosphate decreases the formation of pyromorphite when used in alkaline soils (Laperche *et al.* 2007).

The second study soil at 1818 Dumaine St. was measured for pH at time zero and twelve months for the un-capped plots and showed relatively negligible changes in pH over time (Table 5.12).

Hydroxyapatite was one of the comparative phosphate additions assessed at the 1818 Dumaine site. The effectiveness of Hydroxyapatite to reduce mobility of different forms of Pb such as cerussite, anglesite, and galena in soil has been tested previously (i.e., Miretzky & Fernandez-Cirelli, 2007). It has been suggested

that the pyromorphite form is produced by precipitation or Pb adsorption on Hydroxyapatite lattices (Miretzky & Fernandez-Cirelli, 2007). It might be expected that this would be the method of soil Pb conversion in the hydroxyapatite amended plots in the yard at 1818 Dumaine.

Phosphorous pentoxide which was applied at fertilizer grade, 85% P₂O₅ has been used previously, with some success, to treat different Pb forms such as cerussite (Pb-carbonate), anglesite (Pb-sulfate), lead oxide, and galena (Pb-sulphide) present in smelter contaminated urban soil in Joplin City, MO (Yang & Mosby, 2006). The concern with the excessive use of phosphorous pentoxide is that if applied in a liquid form could potentially leach through the soil profile.

The data for the 2224 N. Prieur St. site showed that the pH at time zero and twelve months for the un-capped plots exhibited negligible change (Table 5.15). For the capped soils, the average LOI was variable among the plots and the moisture content was slightly higher than the un-capped plots. The pH for the soils remained practically the same over time (Table 5.14). Bone meal has a moderate solubility with carbonate content, and a poorly crystalline structure with effective Pb solution immobility (Miretzky & Fernandez-Cirelli, 2007; Hodson *et al.* 2001; Sneddon *et al.* 2006). Also, bone char, which is composed of around 76 wt % Hydroxyapatite, 7.9 wt % of CaCO₃, and 2.3 wt % acid insoluble ash, has succeeded in reducing the bioavailability of Pb in shoots and roots of Chinese cabbage in a study in Changsha, South China (Chen *et al.* 2006).

The characteristics of Pb speciation in the soils for the three sites at zero and twelve months were analyzed by Extended X-ray Absorption Fine Structure Spectroscopy (EXAFS). The purpose of this analysis was to investigate the pyromorphite formation in soils (See chapter four). At 1613 St. Roche Ave., Chloropyromorphite was identified in the post-treatment twelve month samples, with the highest percentage (31%) recorded for the plot treated with apatite II, and there was less apatite sorption in the TSP and rock phosphate treated plots.

The apatite II treated plot at the 2224 N. Prieur site had high chloropyromorphite Pb levels (27%), with less Pb apatite sorption compared to the plots treated with hydroxyapatite and phosphorous pentoxide at the 1818 Dumaine St. site. However, bone char treated soil had the highest chloropyromorphite Pb levels (34%), with the lowest Pb apatite sorption (7%) compared to the apatite II and bone meal at the 2224 N. Prieur St. site. Forms of Pb such as Plumbogummite and Plumboferrite, which have Fe-Mn associated with Pb, were found in all soils. Also, organic matter bound Pb and Pb-carbonates appeared to be converted to more strongly bound fractions such as sulfide components (Cao *et al.*, 2003; Chen *et al.*, 2003).

It has been reported that bound Pb carbonates decreased from about 40% to 10% for Fe-Mn oxides associated fractions, with an increase of approximately 60% for the residual fraction due to the formation of pyromorphite (Cao *et al.*, 2002; Melamed *et al.*, 2003). Care has to be taken here with the definition of a

residual fraction. In classical sequential chemical extraction methods the residual fraction of an element is the last fraction of that element sequentially extracted that is mobilized by a hot, concentrated, acid attack. In this situation, the residual fraction is that fraction bound in the lattice structure of the soil minerals that can only be extracted by total sample dissolution. Scheckel, *et al.* (2003) reported that the more residual Pb would form over time with stable Pb conversions that occur in the field.

Other forms of Pb, such as leadhillite (a Pb-sulfate mineral), plattnerite (Pb-dioxide), litharge (Pb-oxide), and cerussite (PbCO₃) were identified in various plots (Table 5.16). Pb-sulfates, -carbonates, and -oxides, can all be found as old-Pb based pigments, and so the initial presence of these phase might be attributed to old Pb-paint contamination. The variations between time zero and 12-months for all plots was obvious in the Pb apatite sorption and formation of chloropyromorphite data.

One purpose of this study was to evaluate the mobility of dissolved P derived from apatite II dissolution after it had been added to the soil. And, to evaluate how mobile P released from apatite II was compared to P released from the other added phosphates. Calcium phosphate compounds have different solubility products, for instance, the solubility of Fluoroapatite Ca₁₀(PO₄)₆F₂ is 10^{-55.9}, Hydroxyapatite Ca₁₀(PO₄)₆(OH)₂ is 10^{-110.2} is much more soluble than Calcium monohydrogen phosphate CaHPO₄·2H₂O is 10^{-6.6}, and Calcium

dihydrogen phosphate $\text{Ca}(\text{H}_2\text{PO}_4)_2 \cdot \text{H}_2\text{O}$ is $10^{-1.14}$ (Miretzky & Fernandez-Cirelli, 2007).

A concern is that a high solubility of phosphate amendments could cause eutrophication of the groundwater should the translocated P make its way into a surface water body (Cotton-Howells and Capon 1996). Soil pore water was collected by Lysimeters (see chapter four) and data was presented for all the three sites (Table 5.17, Table 5.18 & Table 5.19) and (Figures 5.13 - 5.17, Figures 5.18 - 5.22 & Figures 5.23 - 5.27). Apatite II showed the lowest phosphorous release among three sites, and thus, may be preferred for low phosphorous release over a relatively long period of time. Lysimeters were broken at the 2224 N. Prieur St. site due to Hurricane Isaac, which hit the area on August 28th 2012 (Table 5.19 & Figures 5.25 - 5.26), so soil P content from this site was more limited.

Scanning Electron Microscope (SEM) identified lead particles in soil at both zero and twelve months as a part of the Pb characterization analysis. Samples of raw amendments of Hydroxyapatite and Bone Meal were examined for the surface particle before any Pb change occurred (Appendix A. Figures A 5 - A 8). Also, Apatite II was examined before and after soil treatments (Appendix A. Figures A 1(a), A 1(b), A 1(c) - A 4).

Soil samples from 1613 St. Roche Ave. were tested at zero months. Notably, Pb-P was readily found before any amendments were added to the soils (Appendix B. Figures B 1 - B 3). The presence of Pb-P particles in the soils at

time zero might be due to an ongoing conversion process involving P already present in the soil. Unfortunately, there was no history available for what might have been added to any of the site soils, if a previous occupant of a property on any site had used an NPK fertilizer on the yard soil this might have provided excess P for Pb conversion.

It was obvious that Pb was present in the soil in the form of hexagonal particles, which is a distinguishing feature for Pb carbonate paint pigment (Appendix B. Figures B 4). Also, Pb was associated with P in a sorbed surface phase (Appendix B. Figures B 11 & B 12), a crypto-crystalline phase (Appendix B. Figures B 5), and a Pb associated with Fe-Mn phase (Cao *et al.* 2002) was identified in a few particles (Appendix B. Figures B 6 & B 7).

The post-treatment samples had the particles with similar associations, except they had either higher amounts of Pb sorbed onto the surface of the amendment phosphates or Pb-crystalline forms developed more mature crystals (Appendix C. Figures C 1 - C 33). Soil treated with apatite II exhibited Pb sorption onto the fish bone edges or into the surfaces that were highly porous (Appendix C. Figures C 1 - C 9). It was very difficult to resolve any specific surface features of the particles due to the SEM resolution limitations (if nano-crystals had formed, it was impossible to confirm this as the SEM magnification limitations could not resolve such features).

Small Pb-P particles were found in the rock phosphate treated plot. It seemed that Pb was sorbed onto the surface of the amendment (Appendix C. Figures C 10 - C 12). Lead was also found as an accumulation of acicular particles associated with Cr that was likely an original Pb-paint pigment (Appendix C. Figures C 13).

The TSP amendment showed high Pb amounts that had been sorbed onto the surface as a surface coat or as a crypto-crystalline phase (impossible to determine at the resolution of the SEM) (Appendix C. Figures C 18 - C 25). Control plot soil, that was untreated, contained Pb-P particles identified in the twelve month samples, where there were also Pb associated with BaSO₄ (a common paint pigment) or Mn-Fe oxides in particles (Appendix C. Figures C 26 - C 33).

Soil samples from 1818 Dumaine St. were investigated for Pb at zero months. Notably, Pb P existed before any amendments were added to the (Appendix D. Figures D 1 - D 8). The presence of Pb-P particles in soils at time zero might be due to the P being present previously in the soil. It was obvious that Pb was presented in the soil in irregular particle shapes, which was highly suggestive of Pb-paint particles (Appendix D. Figures D 9). Also, Pb was associated with P in a possibly mature pyromorphite form with elongated (acicular) crystals present suggesting long term crystal growth (Appendix D. Figures D 10 - D 14 & D 15).

Lead hexagonal particles were recognized as a unique feature originating as Pb - carbonate pigment in Pb-based paint (Appendix D. Figures D 17, D 22 & D 29). The most interesting Pb-P particles were found as a tube-like shape with a high Pb content (Appendix D. Figures D 27a - D 27b), small acicular particles accumulated on the surface of CaP (Appendix D. Figures D 28a - D 28b), and rounded particles acting as a point of nucleation, radiating out from the center were accumulated on Si particle (Appendix D. Figures D 31a - D 31c). Some of these morphologies (e.g., the tube-like structures) are identified in the literature as being associated with a specific Pb-mineral type.

The post- treatment samples also had the same associations, except there were greater amounts of Pb absorbed on the surface of the amendments or more mature (larger and better defined) crystals were present (Appendix E. Figures E 1 - E 27). Soil treated with hydroxyapatite, showed a Pb sorption onto the edges or onto the surface pores (Appendix E. Figures E 1 - E 8). It was very difficult to resolve any sub-micron crystal forms on surfaces of the particles due to the imaging resolution limitations. Small surface Pb-P crystals were observed on particles in the soil from the phosphorous pentoxide treated plot.

These features resembled some form of Pb sorbed onto the surface of the amendment and had possibly developed a crypto-crystalline habit or possibly no crystals were formed at all (Appendix E. Figures E 9 - E 16). Lead were found as a group of rounded particles (Appendix E. Figures E 17) or as a sorbed phase onto

the surface associated with micro pores of the apatite II in plot (Appendix E. Figures E 18a & E 18b) or edge sorption effect (Appendix E. Figure E 19). The control plot at this site contained Pb-P particles in the 12month post-amendment samples (Appendix E. Figures E 23 - E 27).

Examination of soil samples at 2224 N. Prieur St. collected at time zero demonstrated the presence of Pb-P particles. As was the case for the other two sites in the pre-treatment soil here Pb-P phases were already present (Appendix F. Figures F 2 - F 8 & F 15). The presence of Pb-P particles in the soil at time zero is suggestive of previous development of Pb-P phases where P was in excess and available for the transformation to occur.

It was obvious that Pb particles were also present in the untreated soil at this site with particle morphology suggestive of a Pb-paint origin (Appendix F. Figure F 1). Also, Pb was associated with P in amorphous pyromorphite stage with high Pb content (Appendix F. Figure F 11). Lead was also observed to be associated with Mn and Fe in the soil (Appendix F. Figures F 6 & F 31).

The post- treatment samples exhibited Pb-particle forms that had been observed at other sites (Appendix G. Figures G 1 - G 32). The plot 1B was an untreated control that showed Pb-P particles (Appendix G. Figures G 1 - G 8). Small surface Pb-P crystal particles were found in the soil from the bone char treated plot. It appeared that Pb was sorbed onto the particle surfaces of the amendment phosphate product (Appendix G. Figures G 9 - G 16). Lead was also found as a

sorbed phase associated with the pores of the apatite II grains (Appendix G. Figures G 18 - G 20) or edge sorption (Appendix G. Figures G 22 - G 24). The 4B plot was treated with Bone Meal and Pb-P element associations were found on the 12-month sample particles as a sorped phase (Appendix G. Figures G 25 - G 32).

The relative bioavailability comparisons and the efforts to reduce the bioaccessibility of the soil Pb through the phosphate amendment efforts were the most important outcomes from this study. These comparisons showed the amount of Pb released from the soils using the in vitro SGF assay at time zero was more than the Pb released at twelve months from the soils to which a phosphate amendment had been applied. The ultimate goal of the field trial being to show that the addition of Apatite II functioned to sequester Pb in a non-bioaccessible form better than other amendments that were applied.

The field trial indicates that the various phosphate products probably have same impact as each other in terms of Pb Pb bioaccessibility reduction. The question of which is the best phosphate to adopt then rest on price point leachability down the soil profile of excess Pb. The lysimeter tests suggested that the apatite II leached most sparingly down the soil profile. Other factor also needs to be taken into account.

Phosphate obtained from mining operations is potentially a problematic source given that peak phosphorous is likely to be reduced by 2030 (Cordell et. al., 2009). Animal bone maybe considered undesirable if pathogenic organisms

are associated with materials. The use of apatite II is essentially a recycling operation making use of a material that would otherwise be discarded.

6.2 Conclusions

6.2.1 Conclusions

This study investigated the use of different soil amendments, which included Apatite II, Rock Phosphate, TSP, Hydroxyapatite, Phosphorous Pentoxide, Bone Char, and Bone Meal, for treated Pb contaminated urban soils at three different sites (1613 St. Roche Ave., 1818 Dumaine St., and 2224 N. Prieur St.).

Lead sources in the baseline soils were thought likely to include leaded gasoline and historic Pb-bearing paint residues that accumulated in the soil due to the deterioration of structure surfaces over time. This is the first study that focuses on Pb immobilization in residential yards, where treatment of these contaminated soils has been investigated. Several conclusions can be drawn from this study:

- The addition of phosphorus (P) in the form of Apatite II resulted in a decrease in the in vitro bioaccessibility of Pb in the trials comparable to Rock Phosphate, TSP, Hydroxyapatite, Phosphorous Pentoxide, Bone Char, and Bone Meal amendments as demonstrated by a simulated gastric fluid (SGF) dissolution assay, which reported on the likely biopersistence of the Pb one year after adding the apatite II to the soil.

- It was concluded that apatite II releases phosphorous into the soil pore water to a lesser degree than any of the other tested phosphate products, potentially indicating that apatite II is a more environmentally friendly phosphate soil addition (from a down-stream eutrophication view-point) than the other tested products.
- For the un-treated control plots, the *in vitro* bioaccessibility of Pb in the test soils were observed to change little when tested one year after the start of the experiment.
- Following the electron microscopy examination, it is postulated that bioaccessibility reduction of Pb in amended soils was controlled by the formation of sparingly soluble pyromorphite, which is a highly insoluble and thermodynamically stable form of Pb that can occur in soils that reduces the Pb bioaccessibility following soil ingestion.
- The addition of apatite II to Pb contaminated soil seems to provide a more feasible solution for reducing Pb toxicity and exposure from contaminated soils in New Orleans than any other amendment. This is extremely important for children who use hand-to-mouth activity, which creates an avenue for contaminated soils to be ingested into the body.

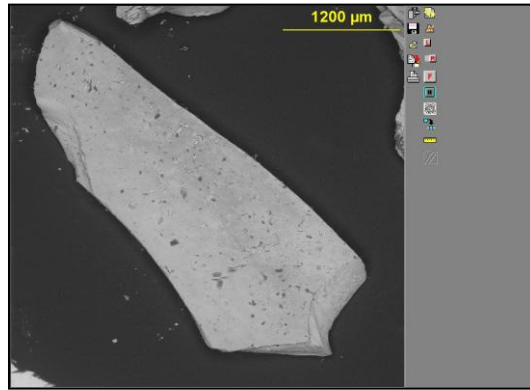
6.2.2 Areas for Future Study

Valuable future work in the specific study of *in situ* chemical stabilization of Pb in urban soils by using phosphate amendments could evolve in several directions. Specifically:

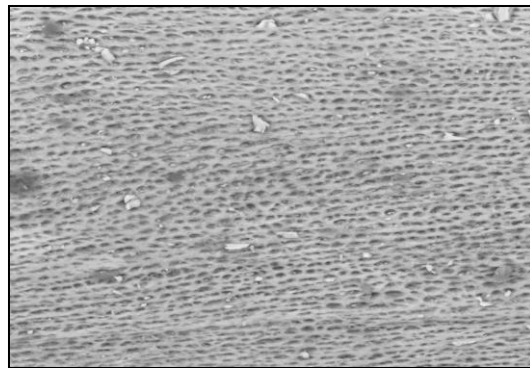
- Extending the treatment process to examine soil Pb changes over longer time periods (extending the residential yard test over another two years). This would provide information on the extended (or not) development of soil Pb into a sparingly soluble phase, and over what extended time this process could occur.
- Pyromorphite conversion phase in soil could be examined using powerful surface analytical techniques such as Transmission Electron Microscopy (TEM). Soil particles examined in the electron microscope at twelve months during the test, presented a surface phenomenon association of Pb and P, which may happen only over longer periods of time with the formation of discrete and disseminated pyromorphite particle forms.

Appendix A

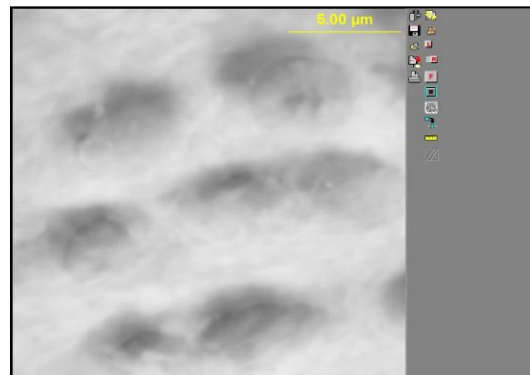
SEM Images and X-Ray Spectra of Amendments



(a)



(b)



(c)

Figure A.1 (a) SEM image shows raw fish bone (Apatite II) (b) SEM image shows surface of raw fish bone (Apatite II) (c) SEM image shows high magnification surface of raw fish bone (Apatite II).

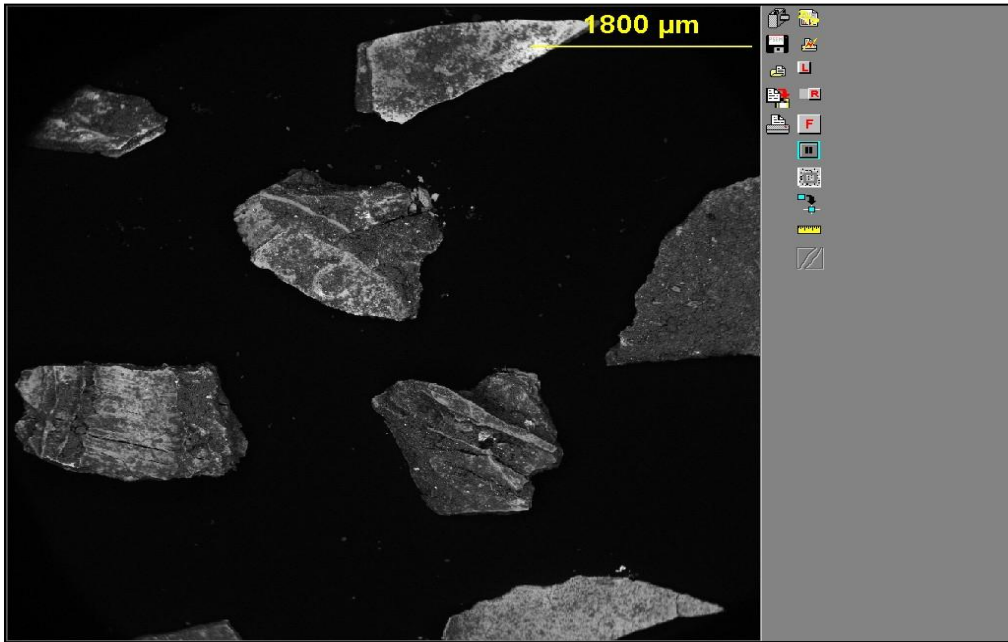


Figure A.2 SEM image shows multiple raw fish bones (Apatite II).

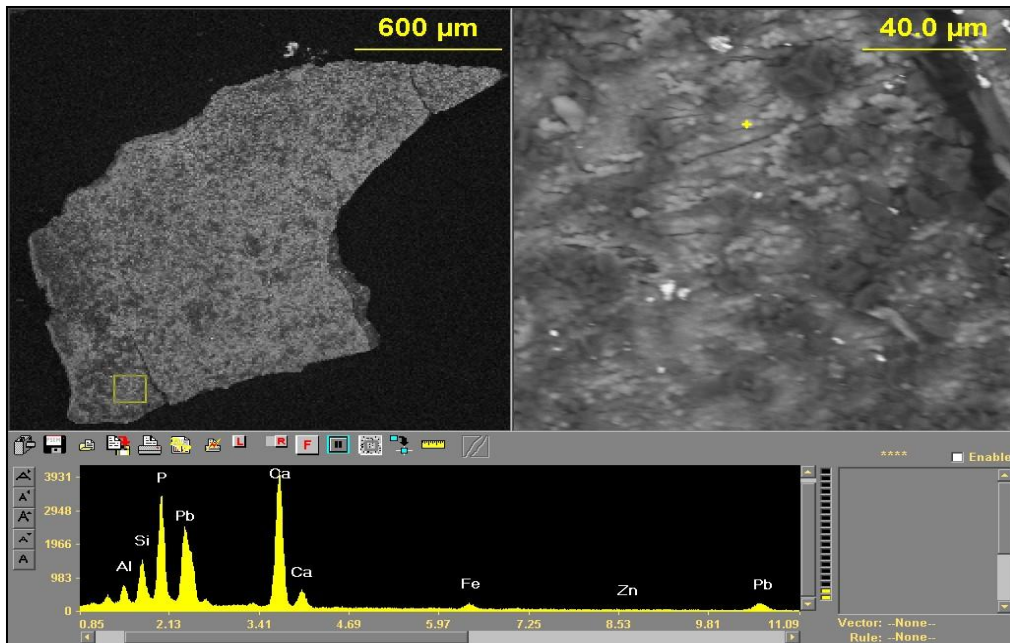


Figure A.3 SEM image shows PbP on the surface of raw fish bones (Apatite II).

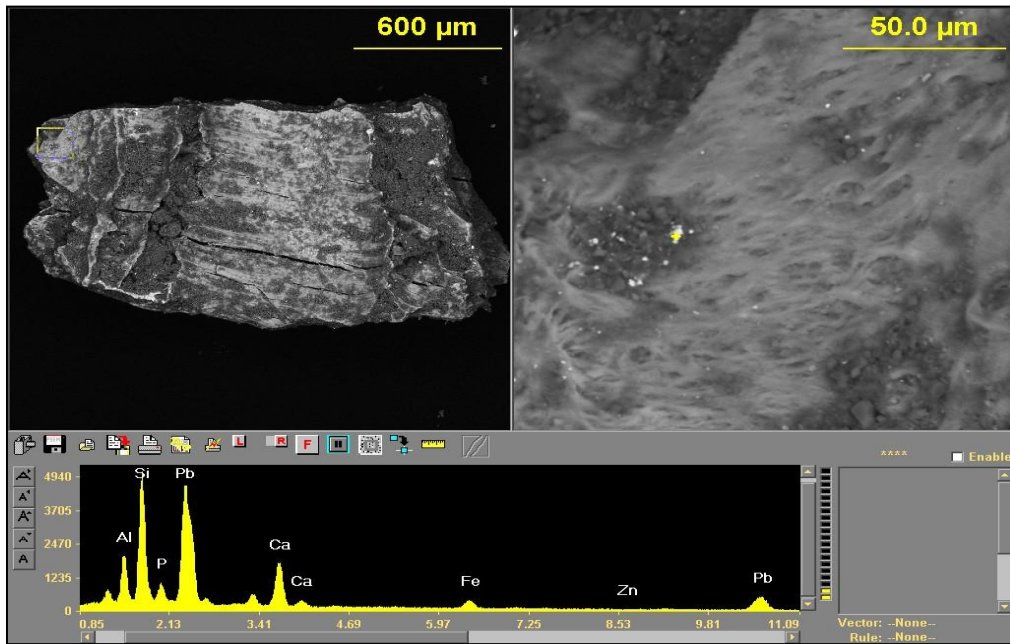


Figure A.4 SEM image shows PbP on the surface of raw fish bones (Apatite II).

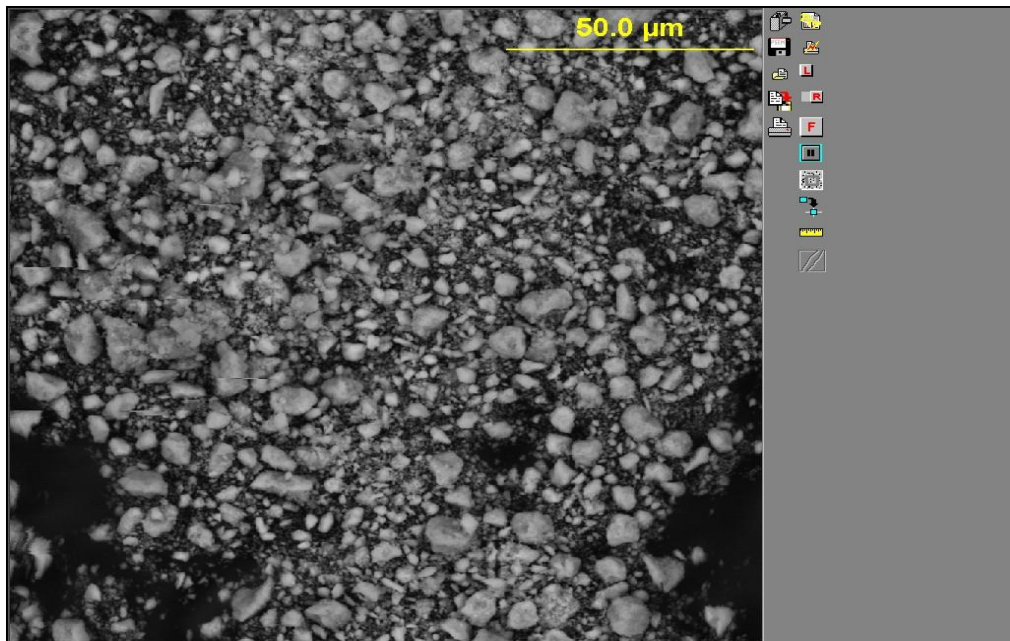


Figure A.5 SEM image shows Hydroxyapatite.

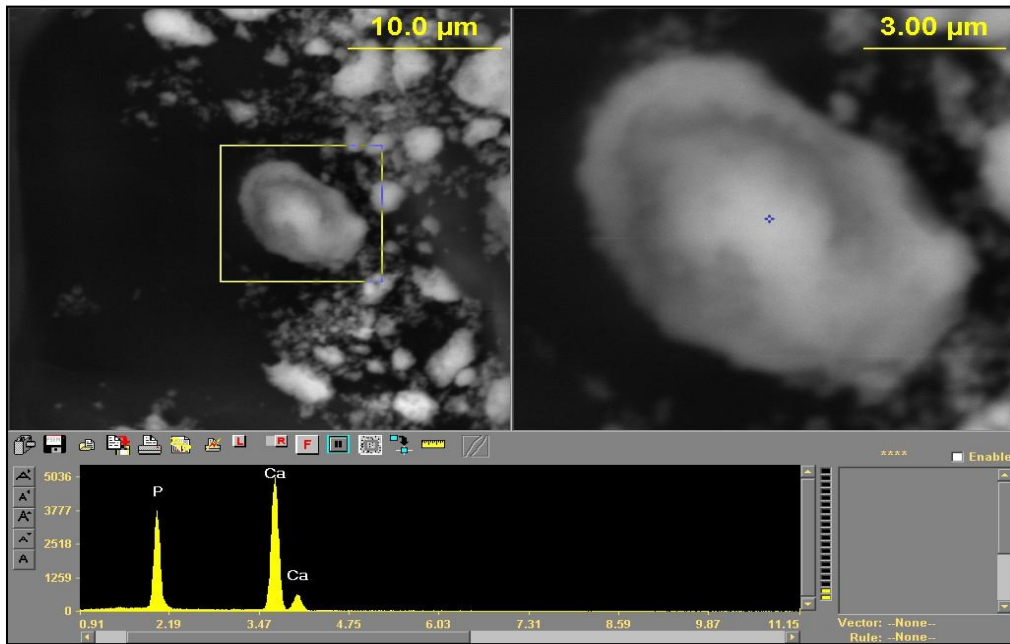


Figure A.6 SEM image shows surface particle of Hydroxyapatite.

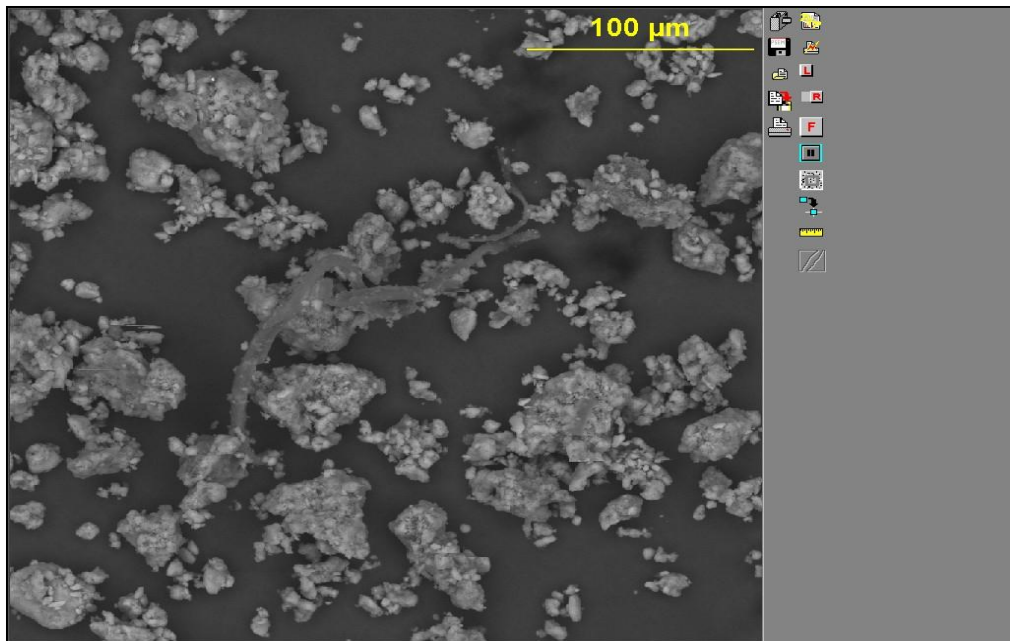


Figure A.7 SEM image shows Bone Meal.

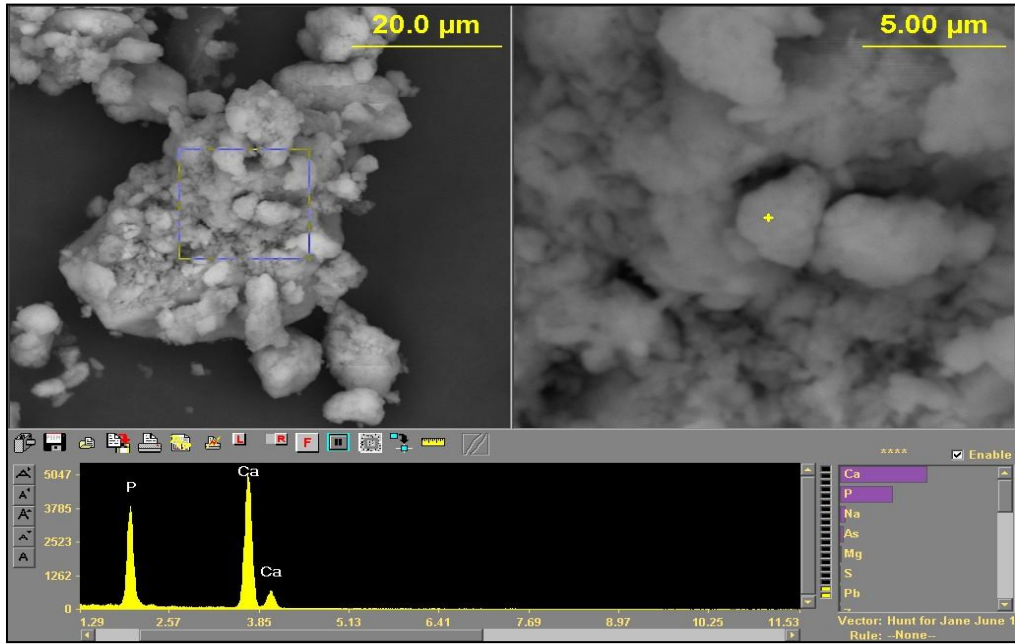


Figure A.8 SEM image shows surface particle of Bone Meal.

Appendix B

SEM Images and X-Ray Spectra of Zero Month 1613 St. Roche Samples

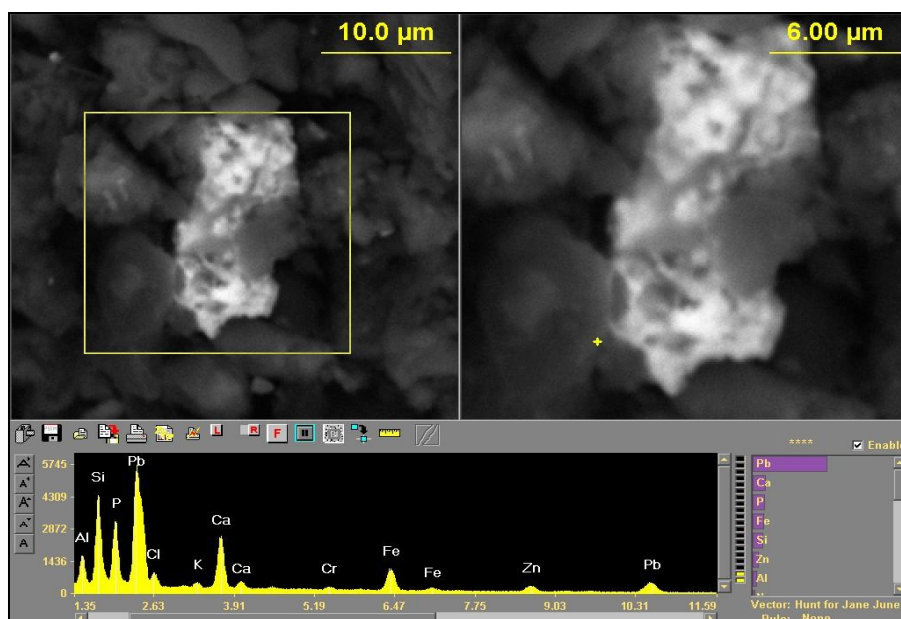


Figure B.1 SEM image shows PbP Fe Cr in Al Ca particle determined in plot 1A
quadrant a.

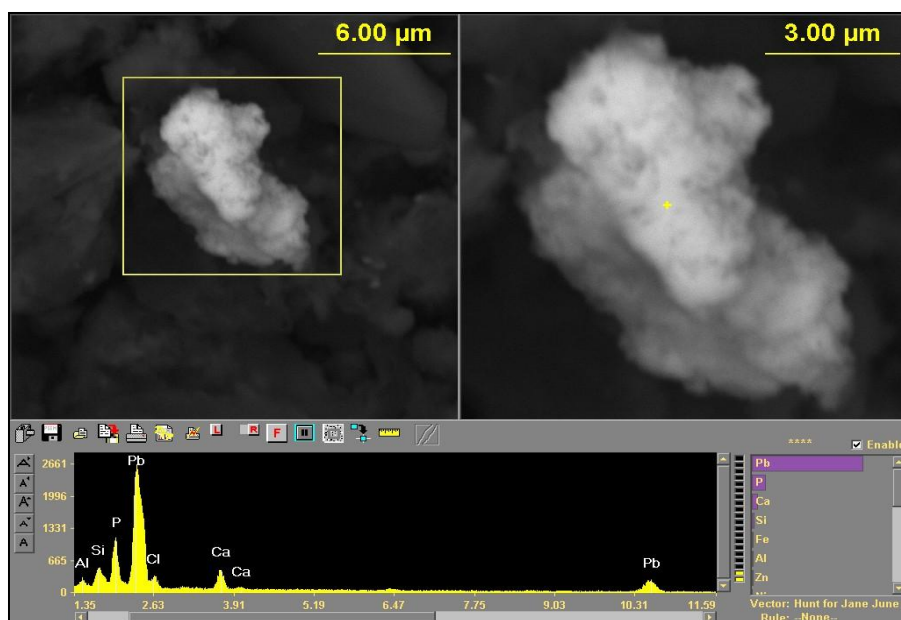


Figure B.2 SEM image shows PbP Fe in Al Ca particle determined in plot 1A
quadrant a.

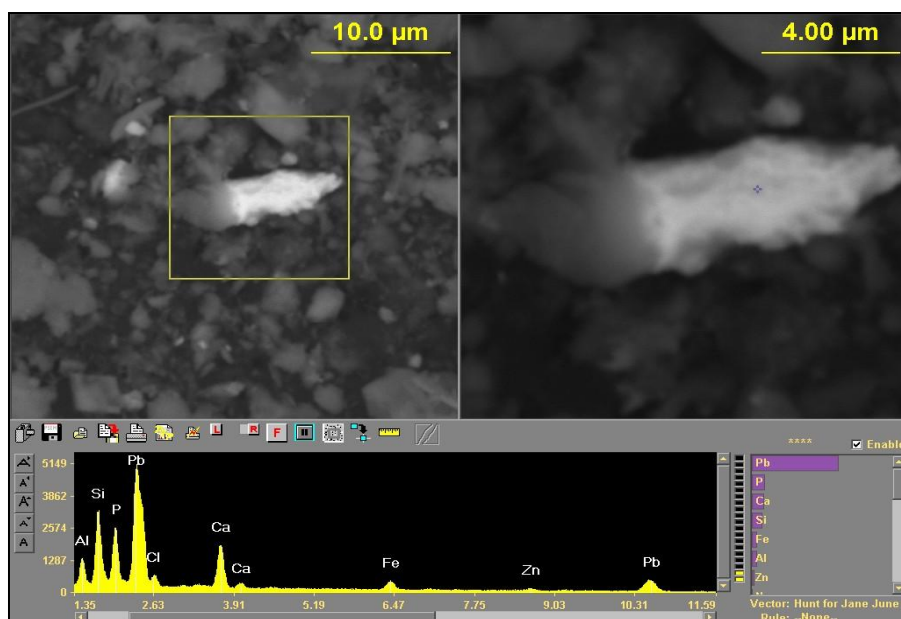


Figure B.3 SEM image shows PbP Fe Zn in Al Si Ca particle determined in plot

1A quadrant b.

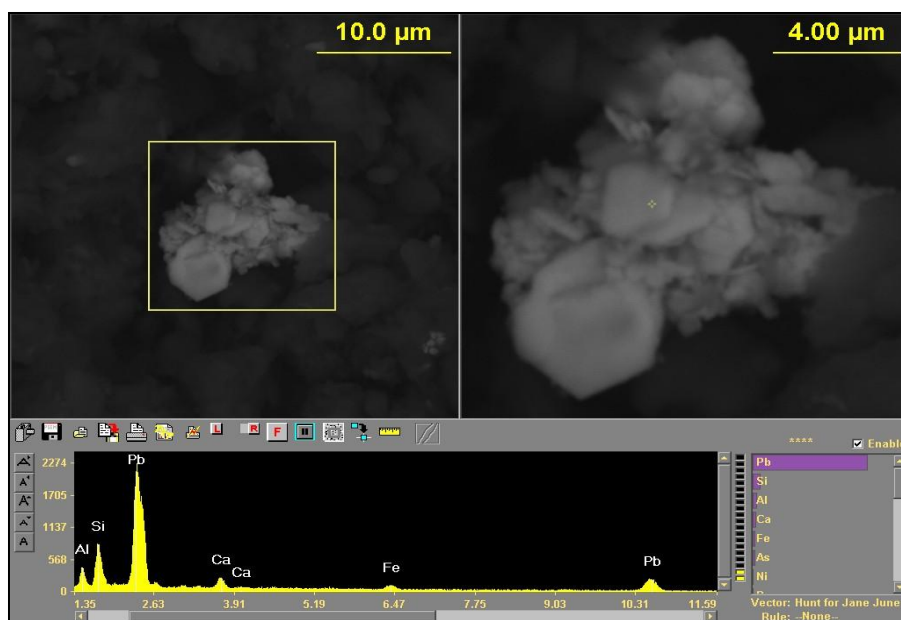


Figure B.4 SEM image shows hexagonal Pb aggregate (Cerussite) determined in

plot 1A quadrant b.

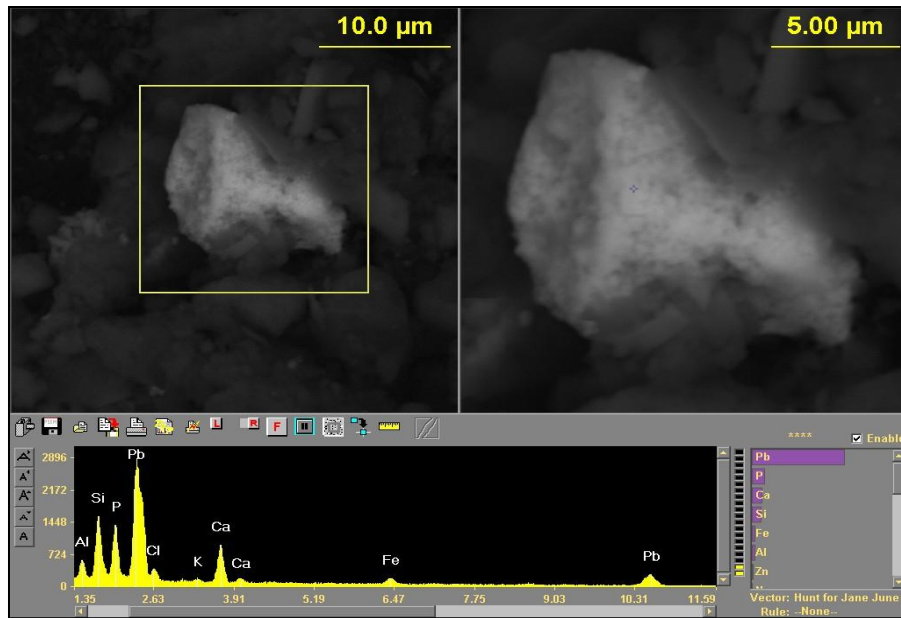


Figure B.5 SEM image shows PbP Cl Fe in Al Si Ca particle determined in plot 1A quadrant b.

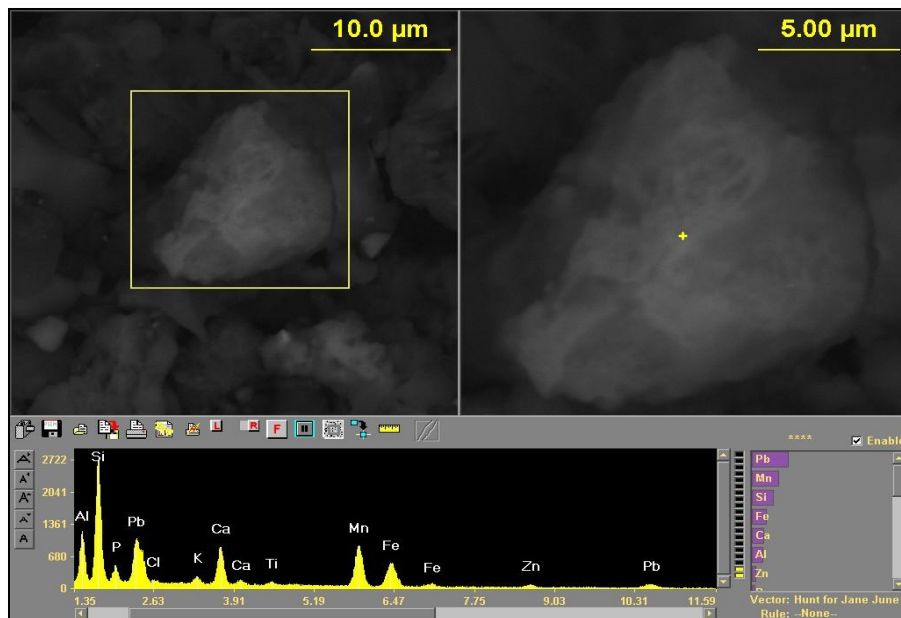


Figure B.6 SEM image shows PbP Mn Fe Zn in Al Si Ca K particle determined in plot 1A quadrant b.

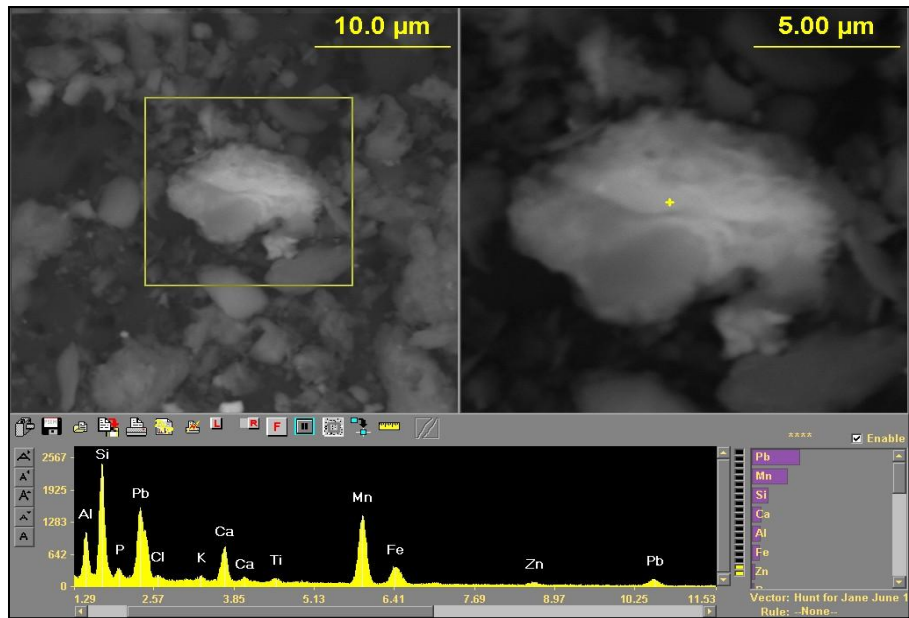


Figure B.7 SEM image shows PbP Mn Fe Zn Ti in Al Si Ca K particle determined in plot 1A quadrant c.

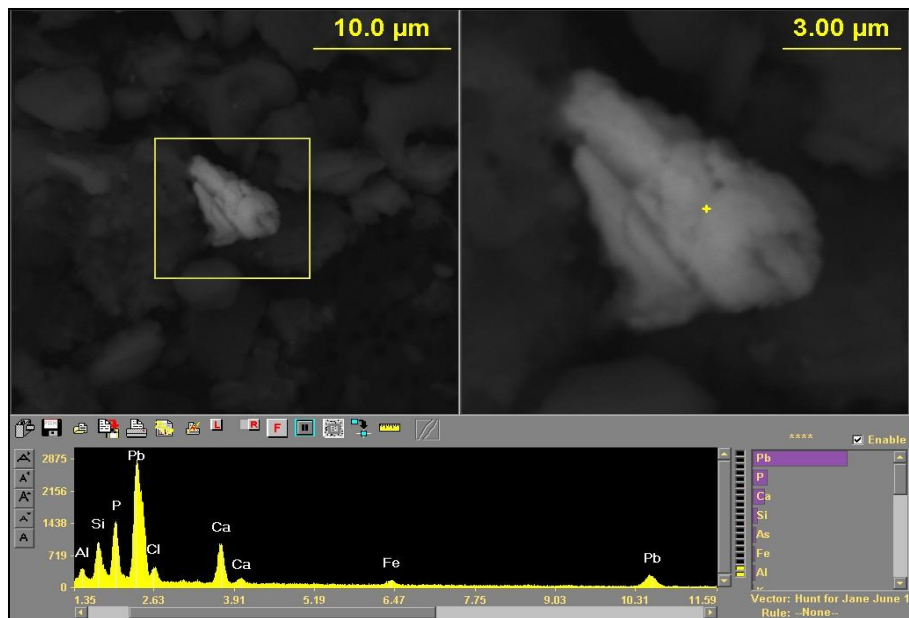


Figure B.8 SEM image shows PbP Fe in Al Si Ca particle determined in plot 1A quadrant c.

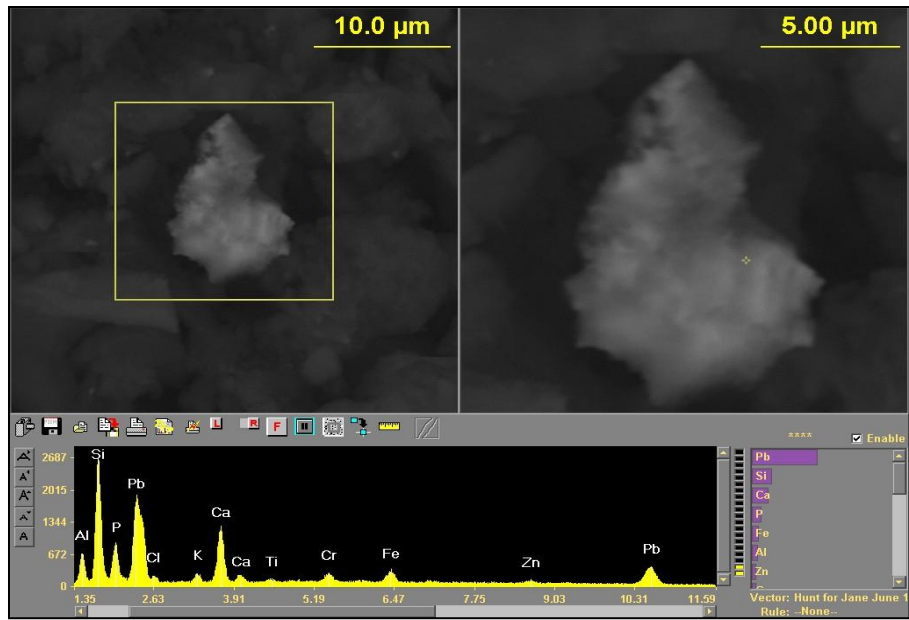


Figure B.9 SEM image shows PbP Fe Cr Zn Ti in Al Si Ca K particle determined in plot 1A quadrant d.

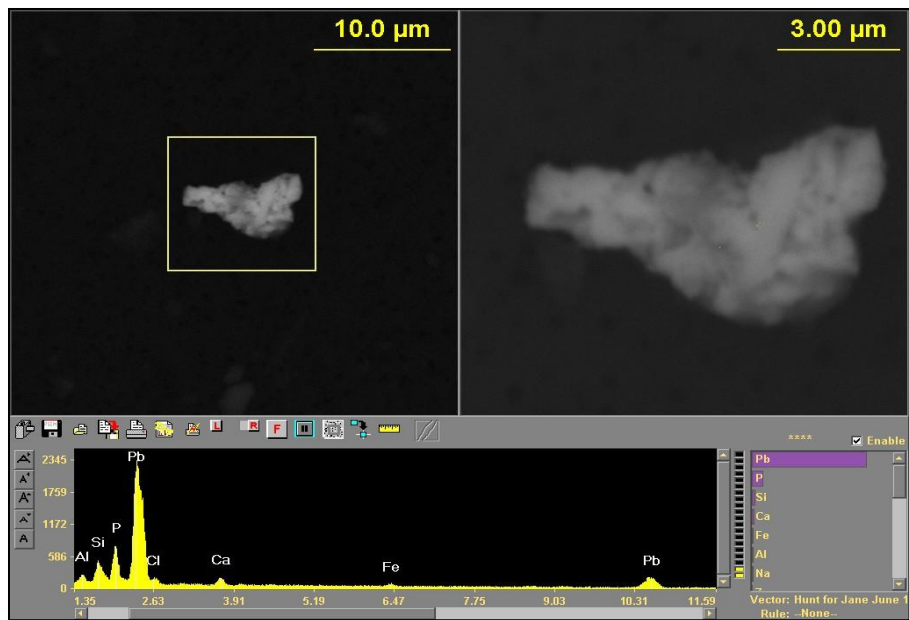


Figure B.10 SEM image shows PbP Fe in Al Si Ca particle determined in plot 1A quadrant d.

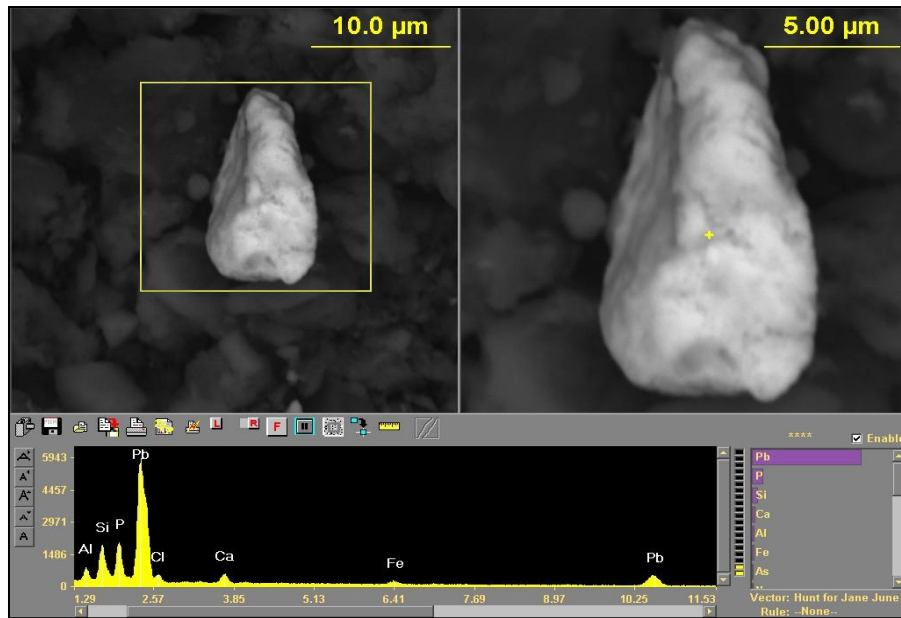


Figure B.11 SEM image shows PbP Cl Fe in Al Si Ca particle determined in plot 2A quadrant a.

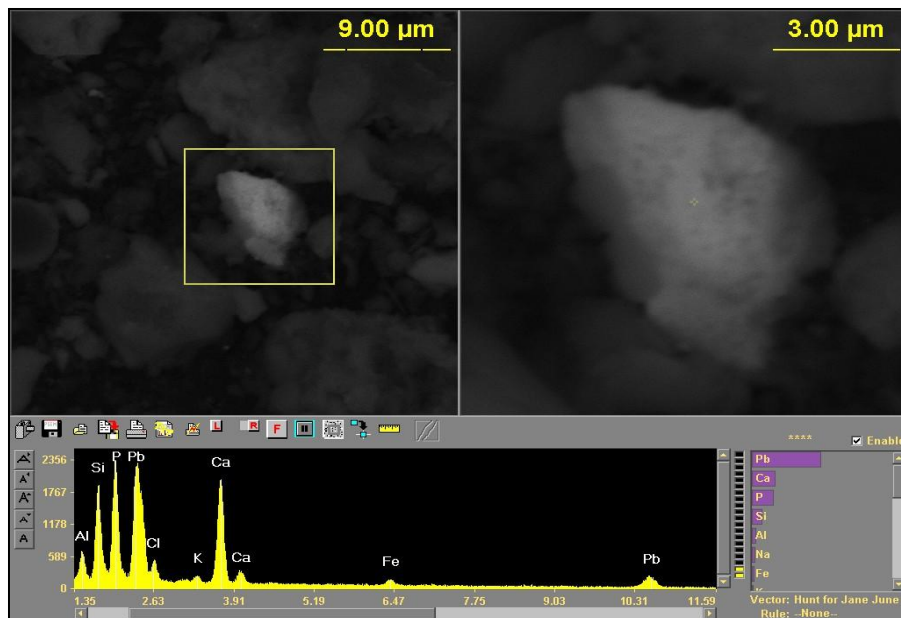
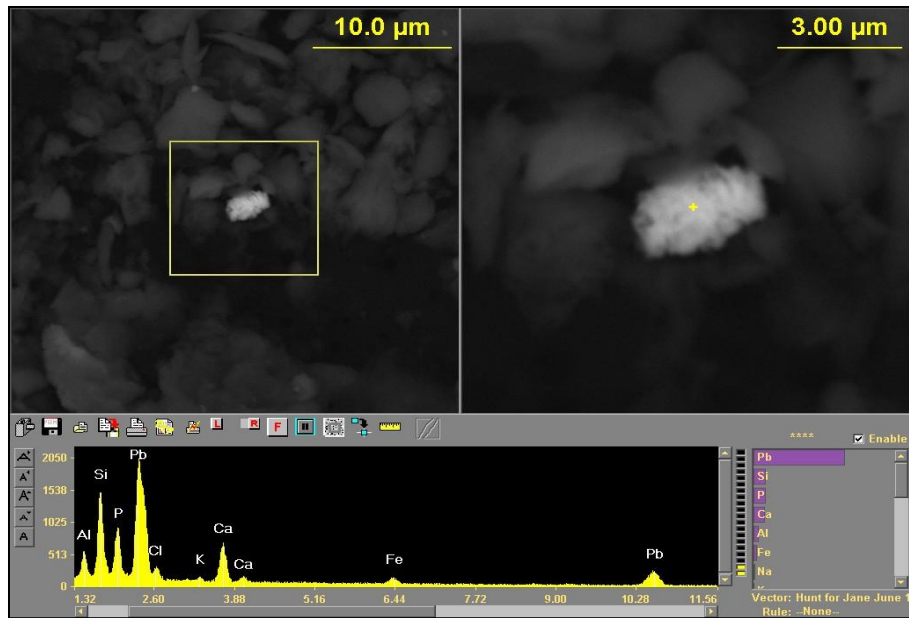
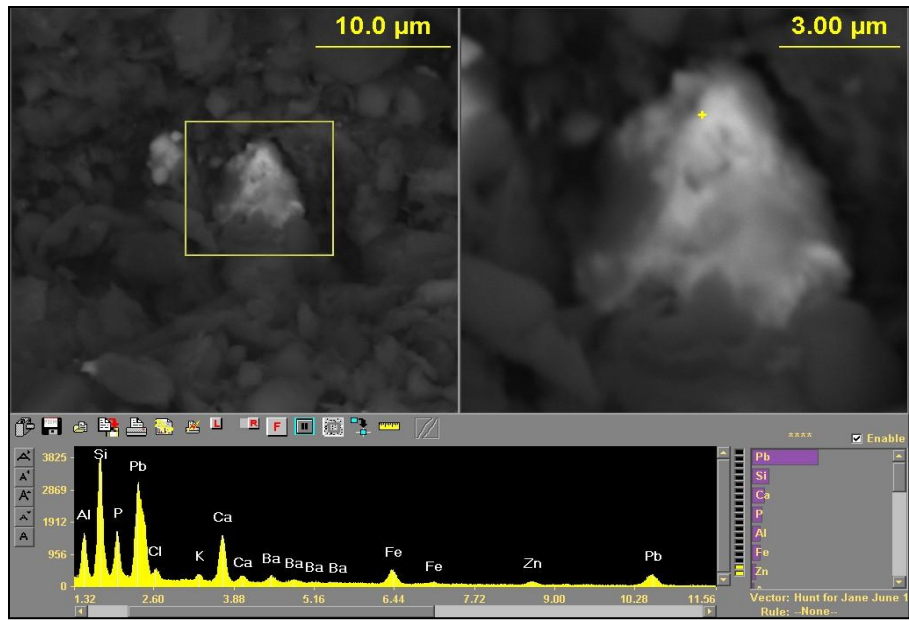


Figure B.12 SEM image shows PbP Cl Fe in Al Si Ca K particle determined in plot 2A quadrant a.



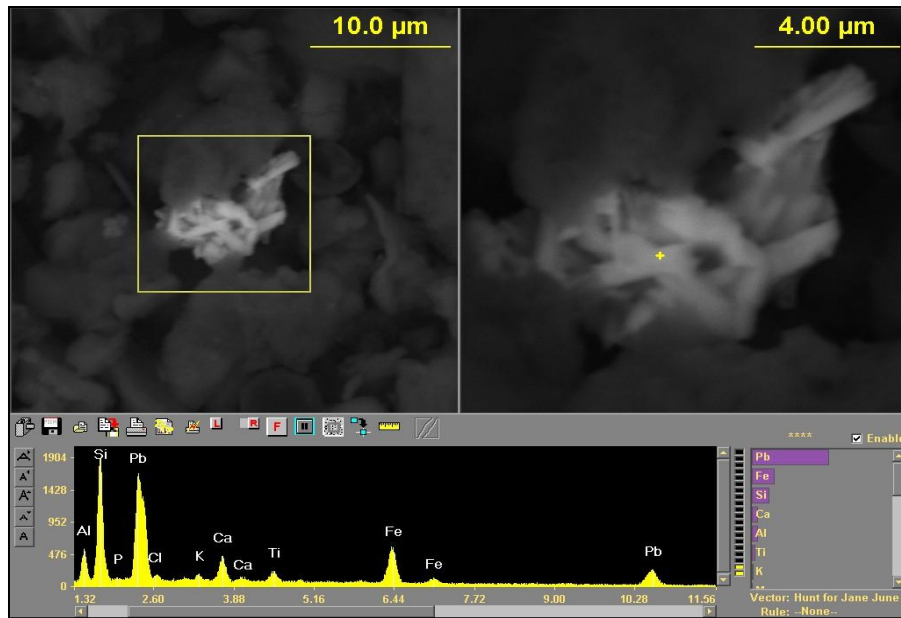


Figure B.15 SEM image shows PbP Cl Fe Ti in Al Si Ca K particle determined in plot 2A quadrant c.

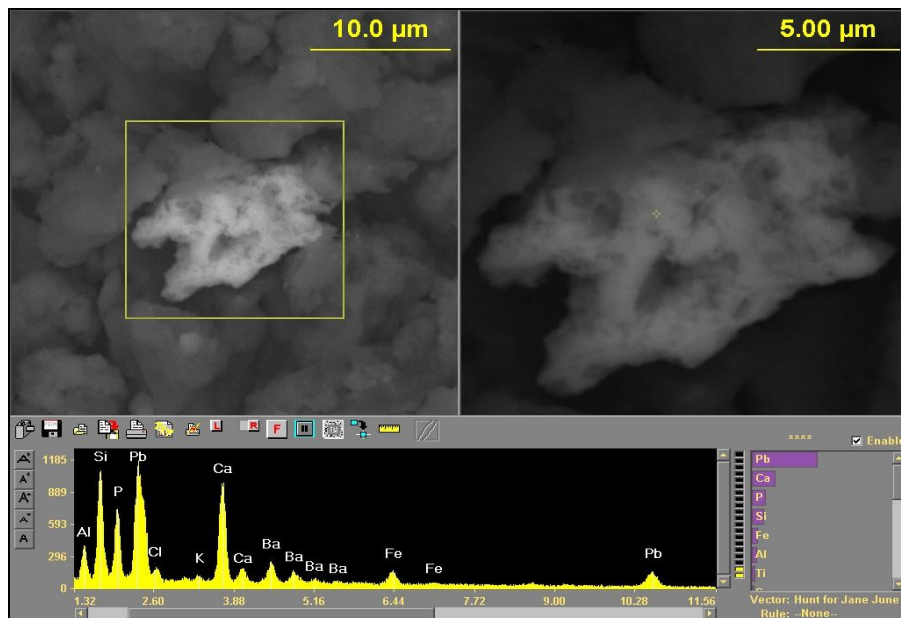


Figure B.16 SEM image shows PbP Cl Fe Ba in Al Si Ca K particle determined in plot 2A quadrant c.

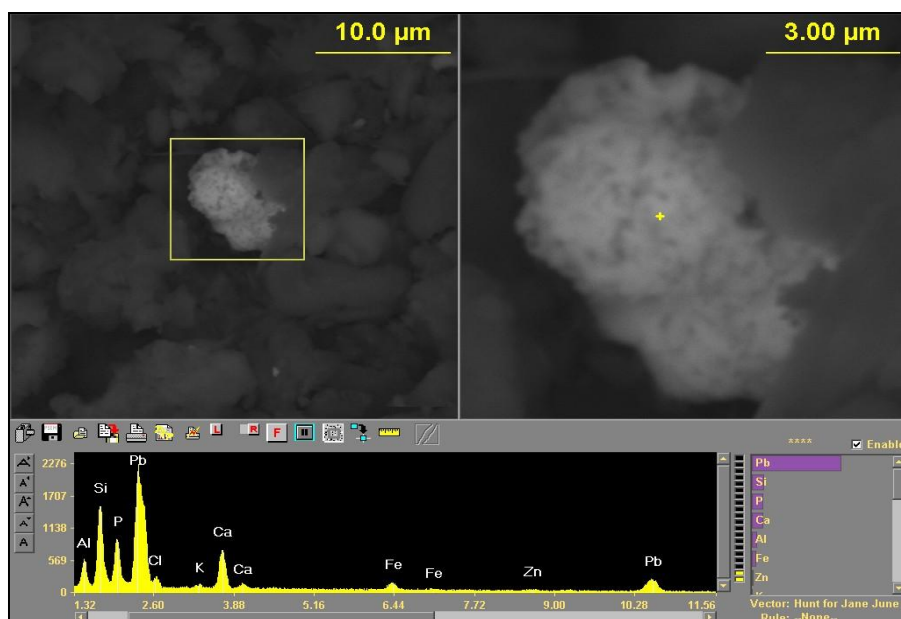


Figure B.17 SEM image shows PbP Cl Fe Zn in Al Si Ca K particle determined in plot 2A quadrant c.

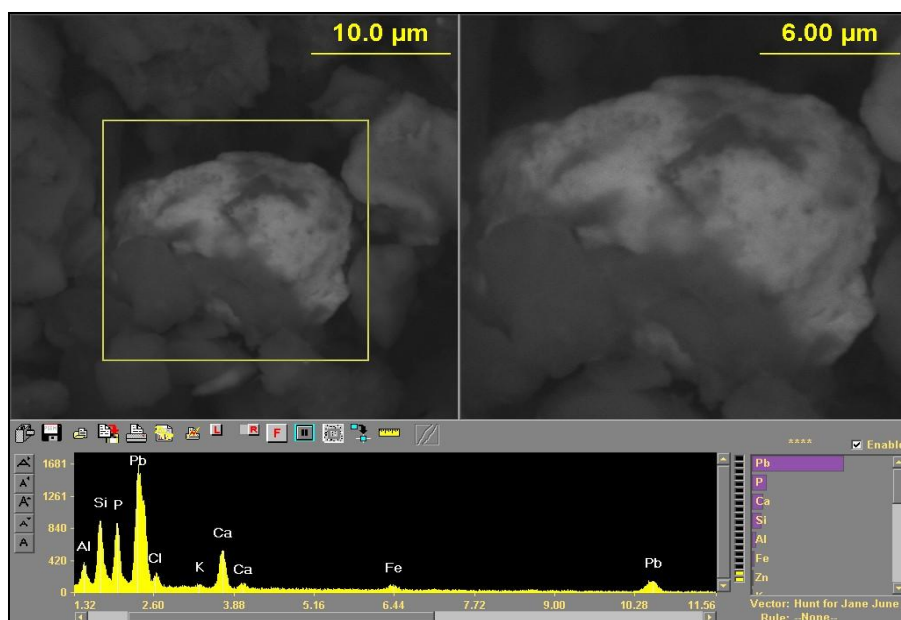


Figure B.18 SEM image shows PbP Cl Fe Zn in Al Si Ca K particle determined in plot 2A quadrant d.

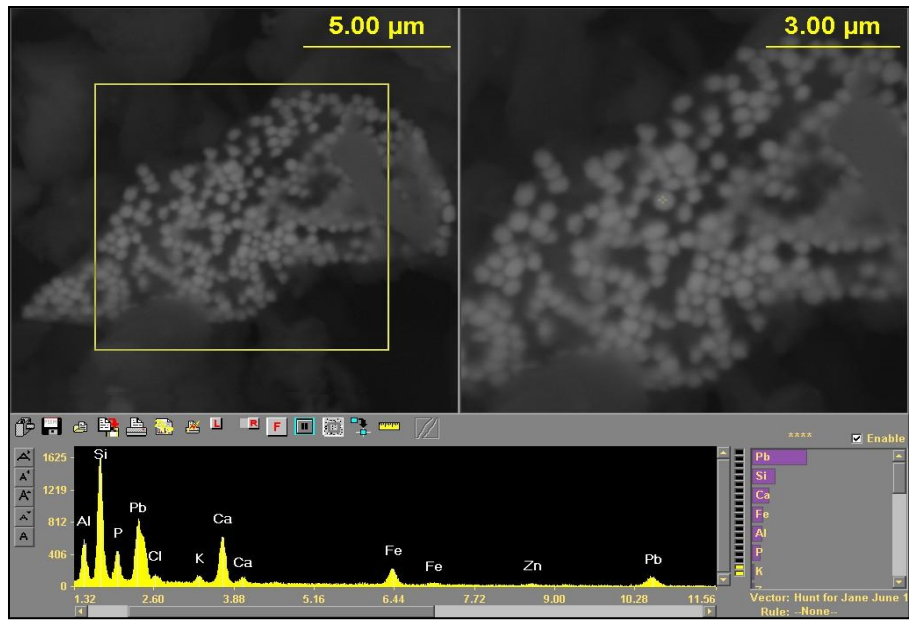


Figure B.19 SEM image shows rounded PbP Cl Fe Zn in Al Si Ca K particle determined in plot 2A quadrant d.

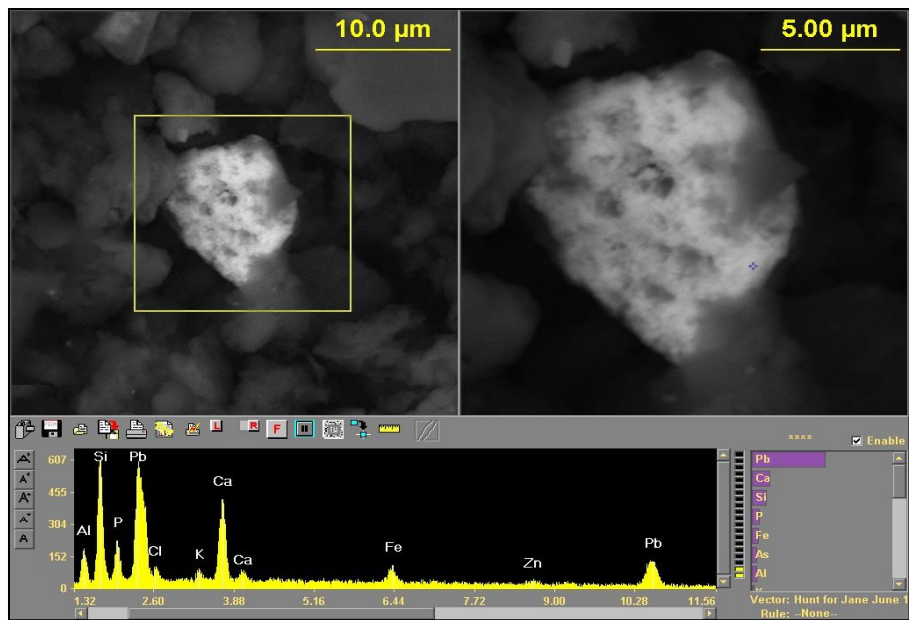


Figure B.20 SEM image shows PbP Cl Fe Zn in Al Si Ca K particle determined in plot 3A quadrant a.

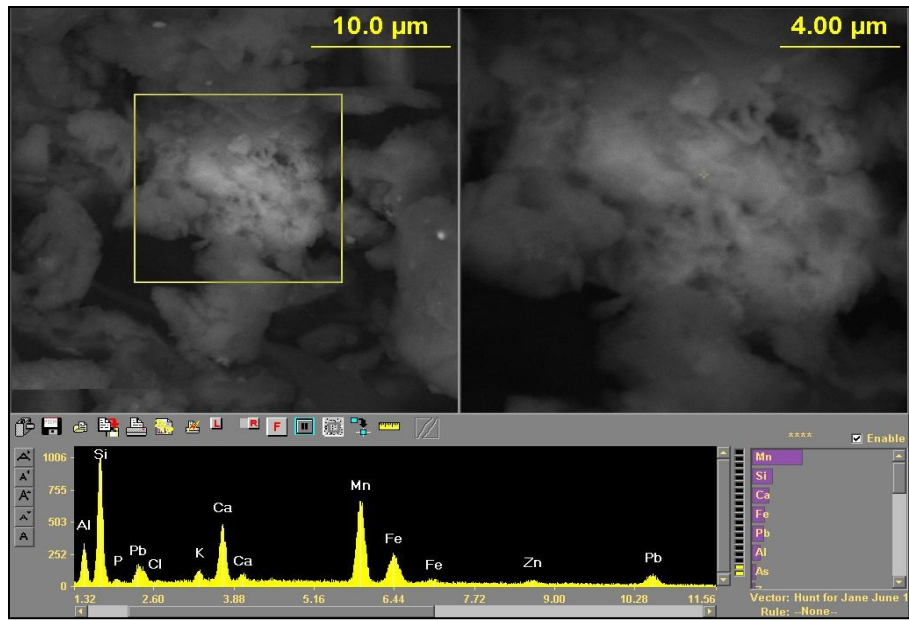


Figure B.21 SEM image shows PbP Cl Mn Fe Zn in Al Si Ca K particle determined in plot 3A quadrant a.

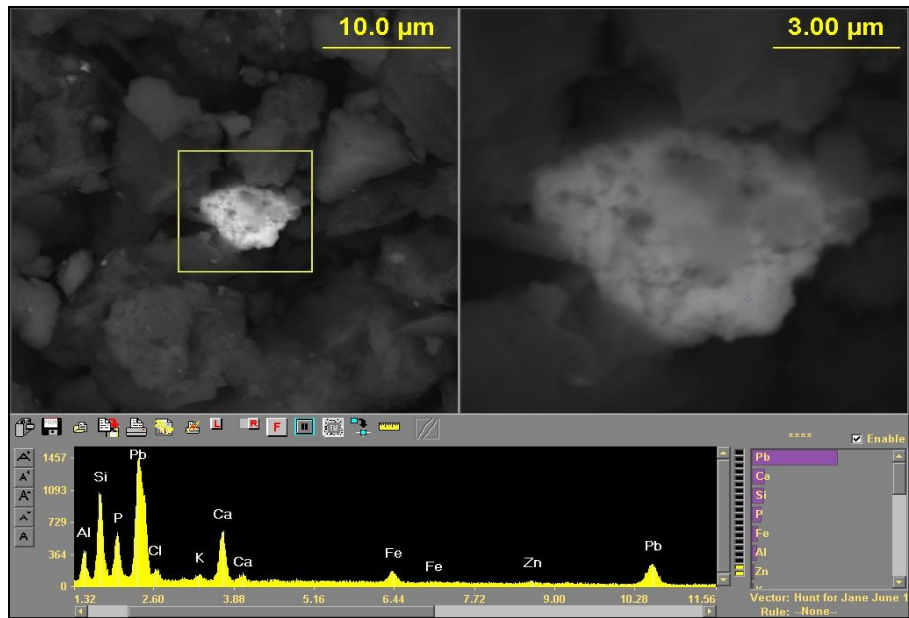


Figure B.22 SEM image shows PbP Cl Fe Zn in Al Si Ca K particle determined in plot 3A quadrant b.

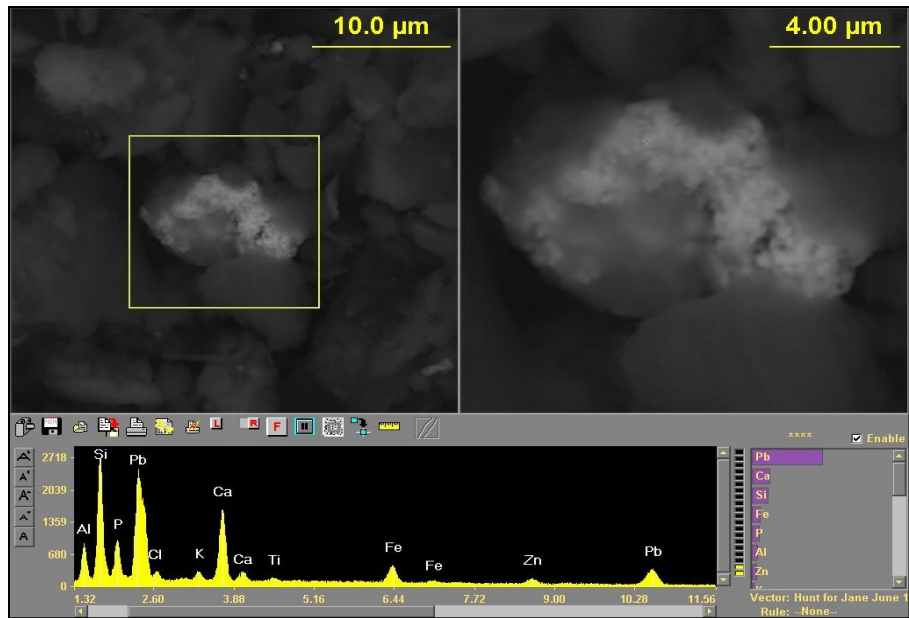


Figure B.23 SEM image shows PbP Cl Fe Zn Ti in Al Si Ca K particle determined in plot 3A quadrant b.

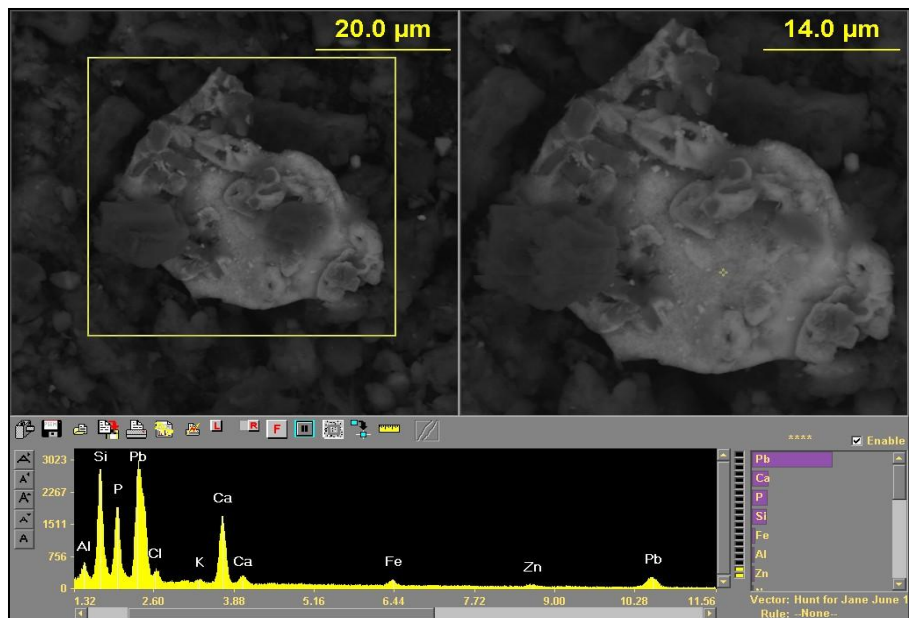


Figure B.24 SEM image shows PbP Cl Fe Zn in Al Si Ca K particle determined in plot 3A quadrant c.

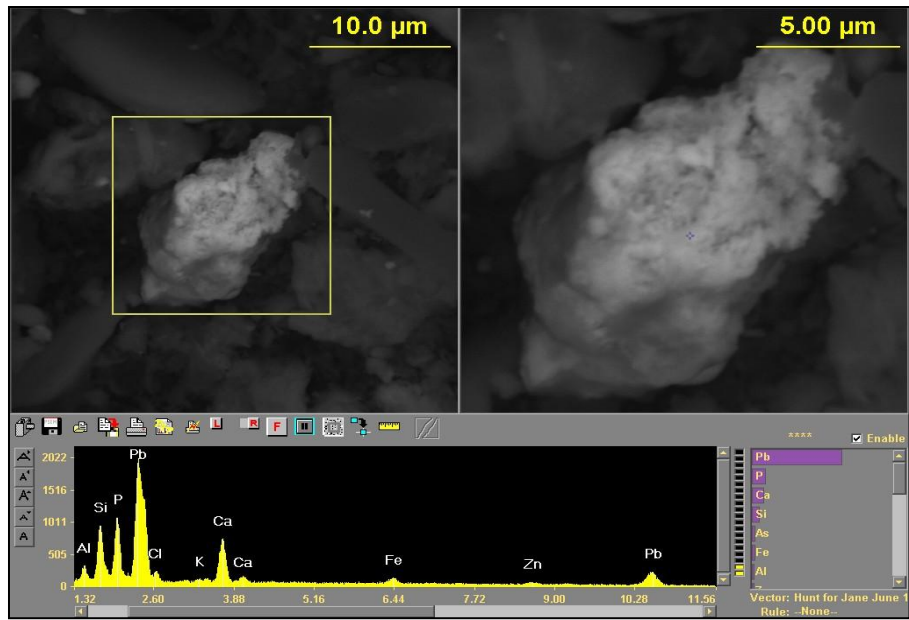


Figure B.25 SEM image shows PbP Cl Fe Zn in Al Si Ca K particle determined in plot 3A quadrant c.

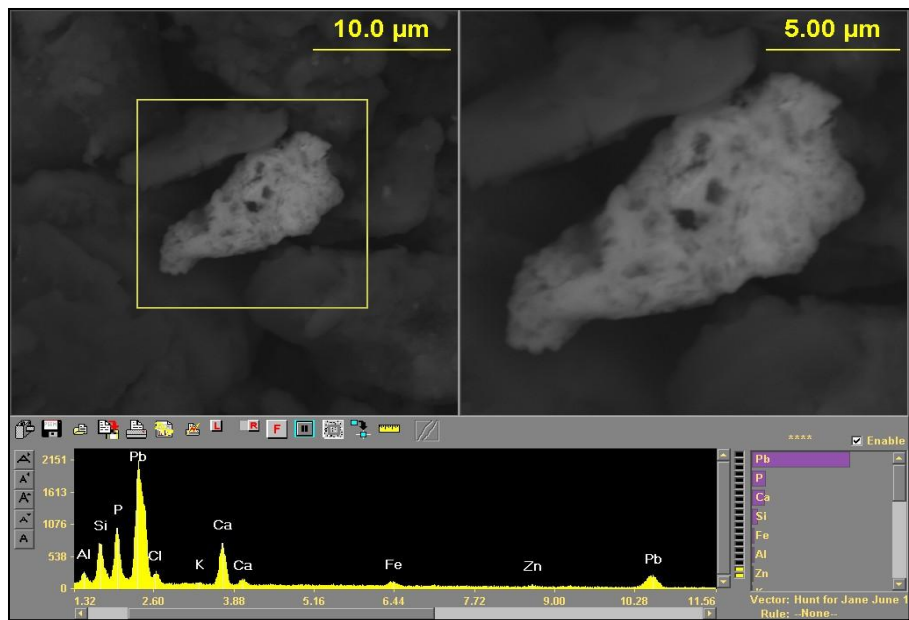


Figure B.26 SEM image shows PbP Cl Fe Zn in Al Si Ca K particle determined in plot 3A quadrant c.

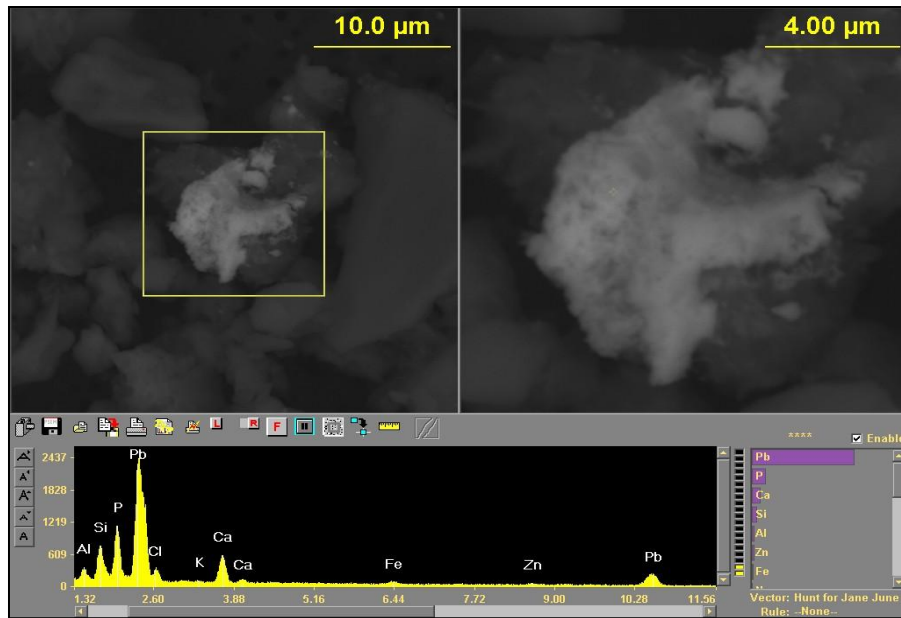


Figure B.27 SEM image shows PbP Cl Fe Zn in Al Si Ca K particle determined in plot 3A quadrant d.

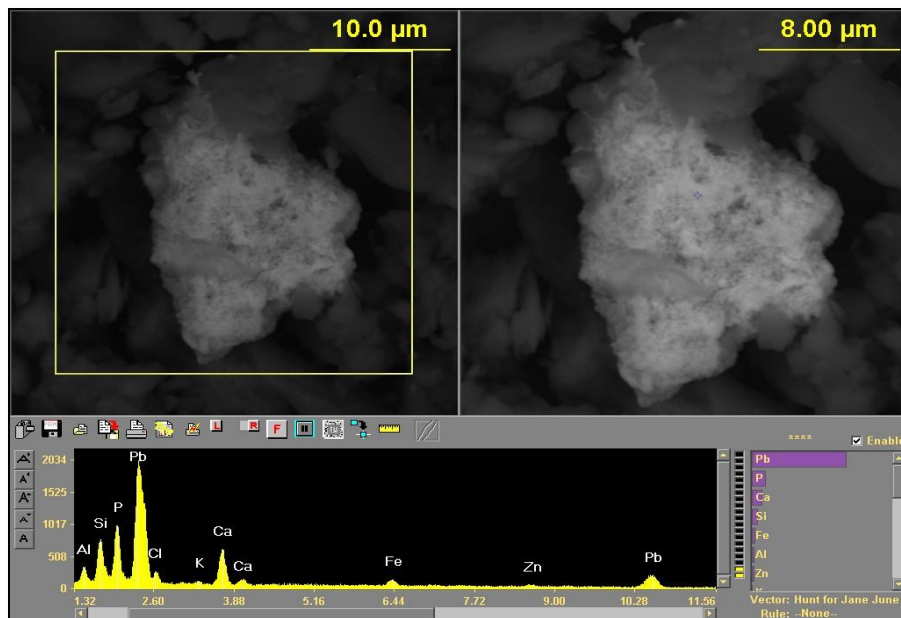


Figure B.28 SEM image shows PbP Cl Fe Zn in Al Si Ca K particle determined in plot 3A quadrant d.

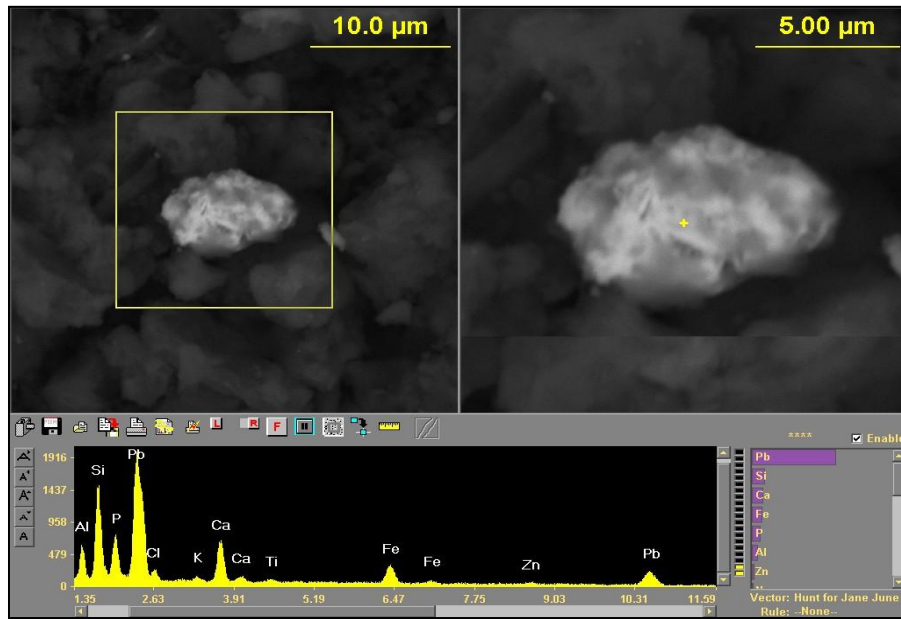


Figure B.29 SEM image shows PbP Cl Fe Ti Zn in Al Si Ca K particle determined in plot 4A quadrant a.

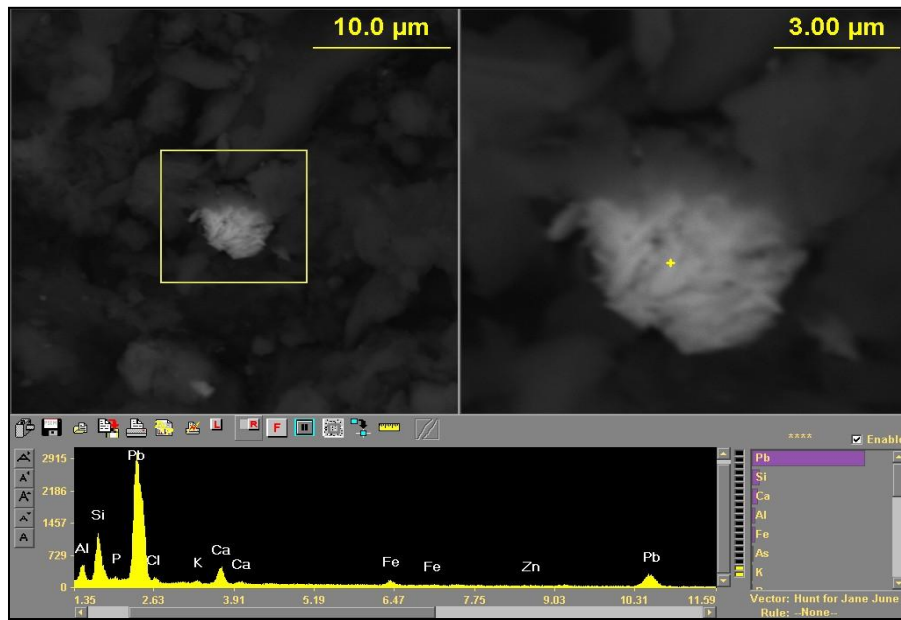


Figure B.30 SEM image shows Pb particle determined in plot 4A quadrant a.

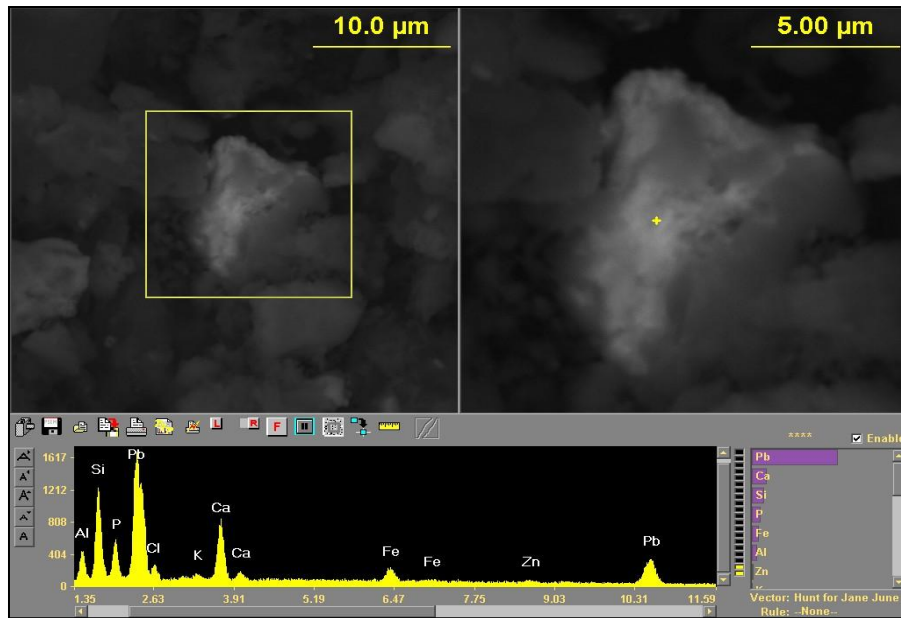


Figure B.31 SEM image shows PbP Cl Fe Zn in Al Si Ca K particle determined in plot 4A quadrant a.

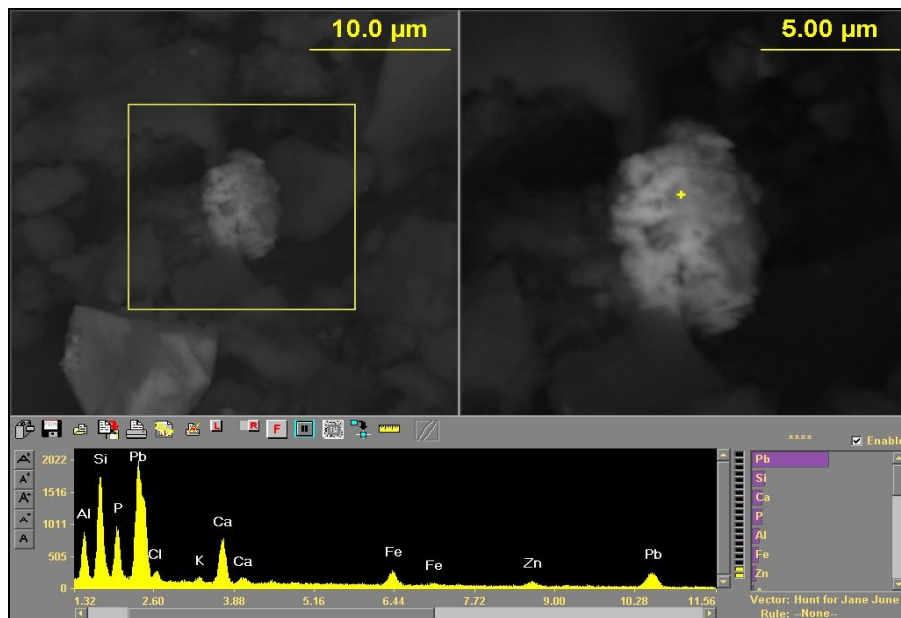


Figure B.32 SEM image shows PbP Cl Fe Zn in Al Si Ca K particle determined in plot 4A quadrant b.

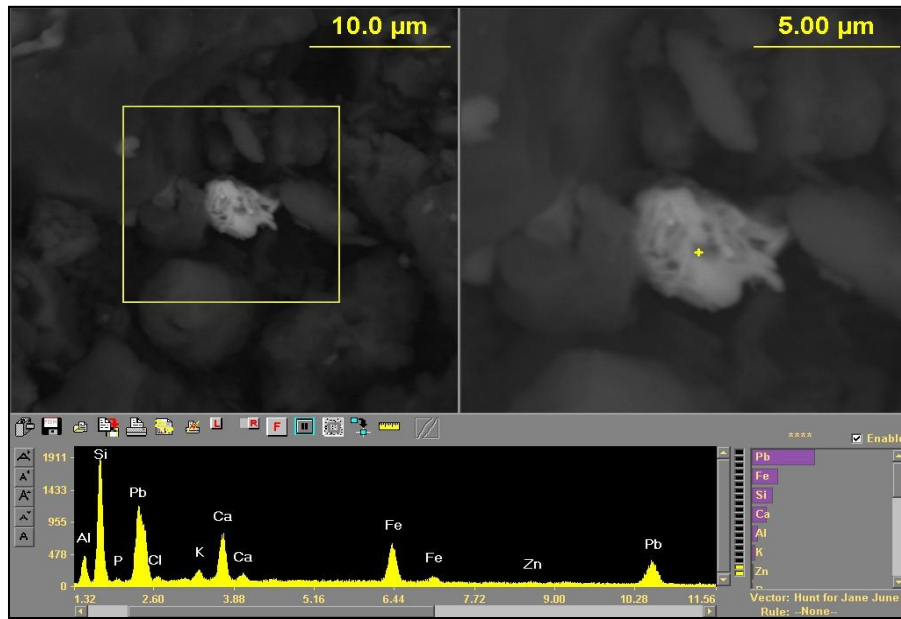


Figure B.33 SEM image shows Pb particle determined in plot 4A quadrant b.

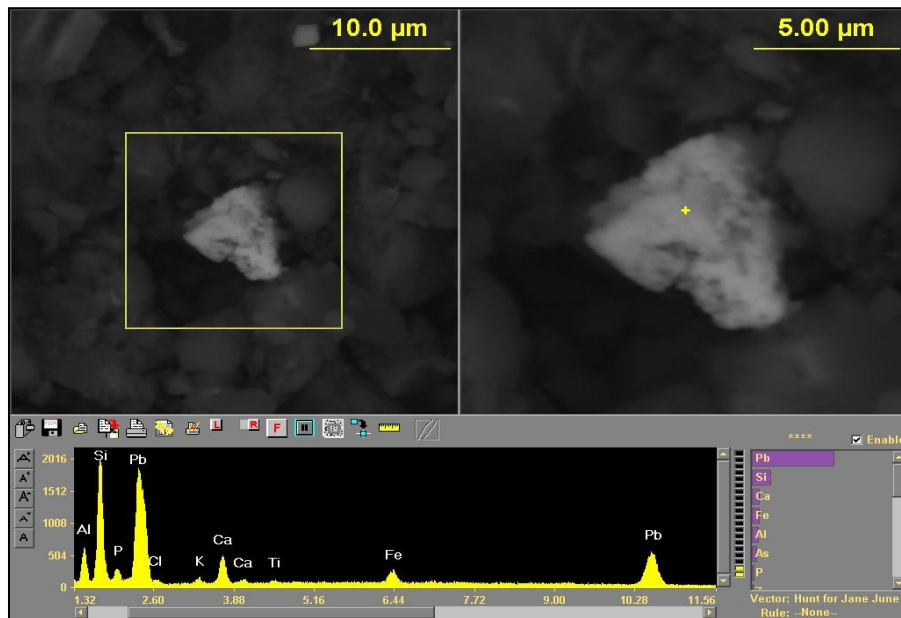


Figure B.34 SEM image shows PbP Cl Fe Ti in Al Si Ca K particle determined in plot 4A quadrant b.

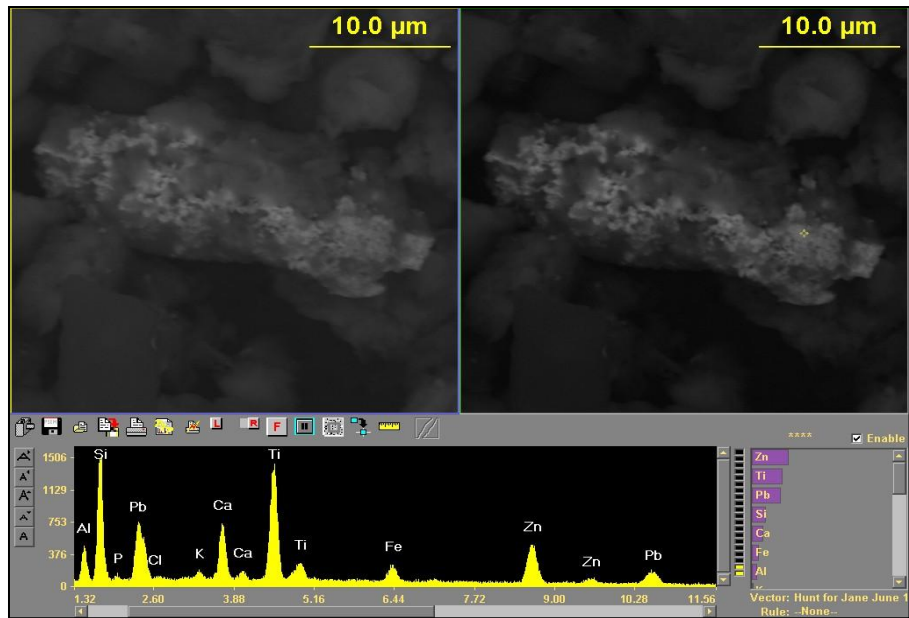


Figure B.35 SEM image shows PbP Cl Fe Ti Zn in Al Si Ca K particle determined in plot 4A quadrant c.

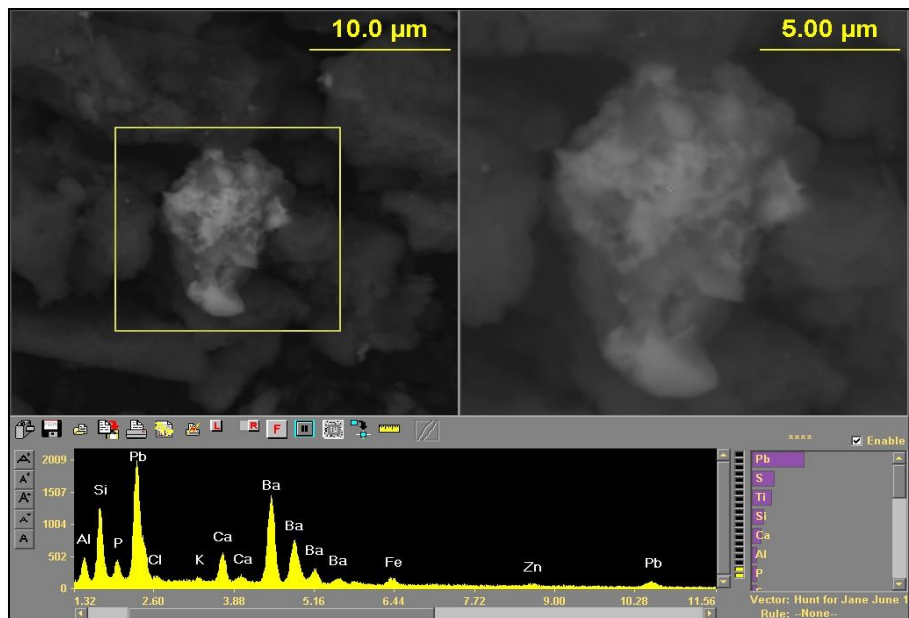


Figure B.36 SEM image shows PbP Cl Fe Ba Zn in Al Si Ca K particle determined in plot 4A quadrant c.

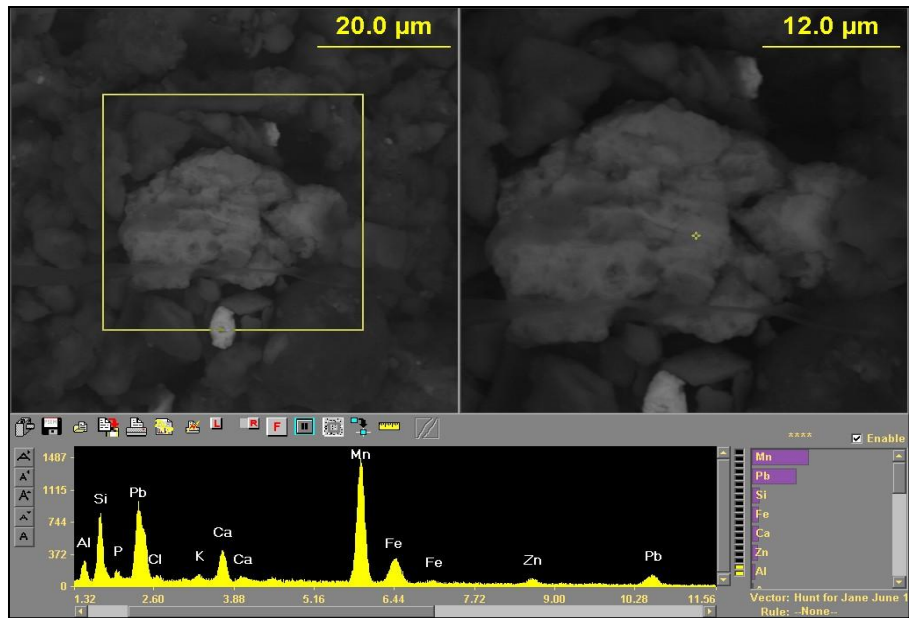


Figure B.37 SEM image shows PbP Cl Mn Fe Zn in Al Si Ca K particle determined in plot 4A quadrant c.

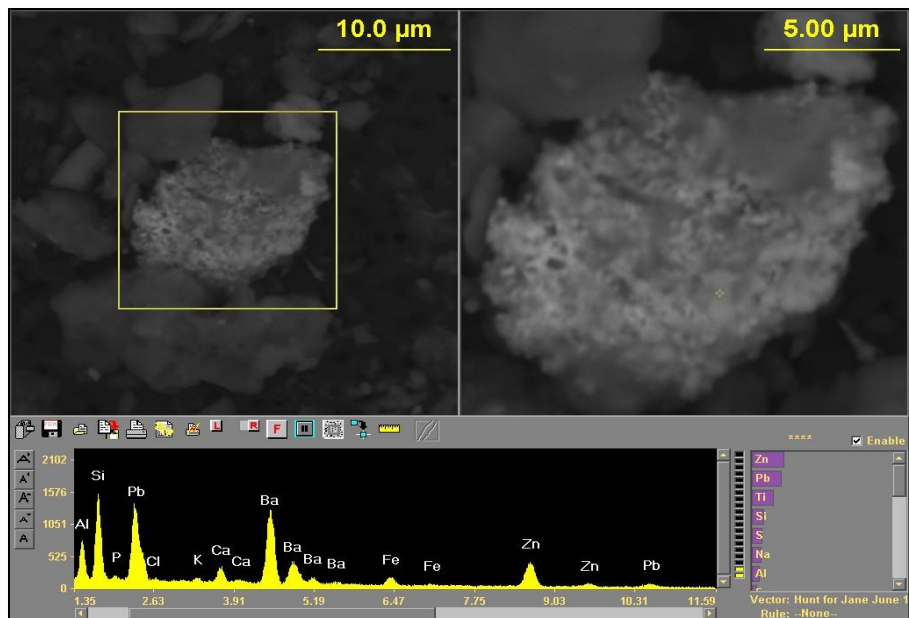


Figure B.38 SEM image shows PbP Cl Ba Fe Zn in Al Si Ca K particle determined in plot 4A quadrant d.

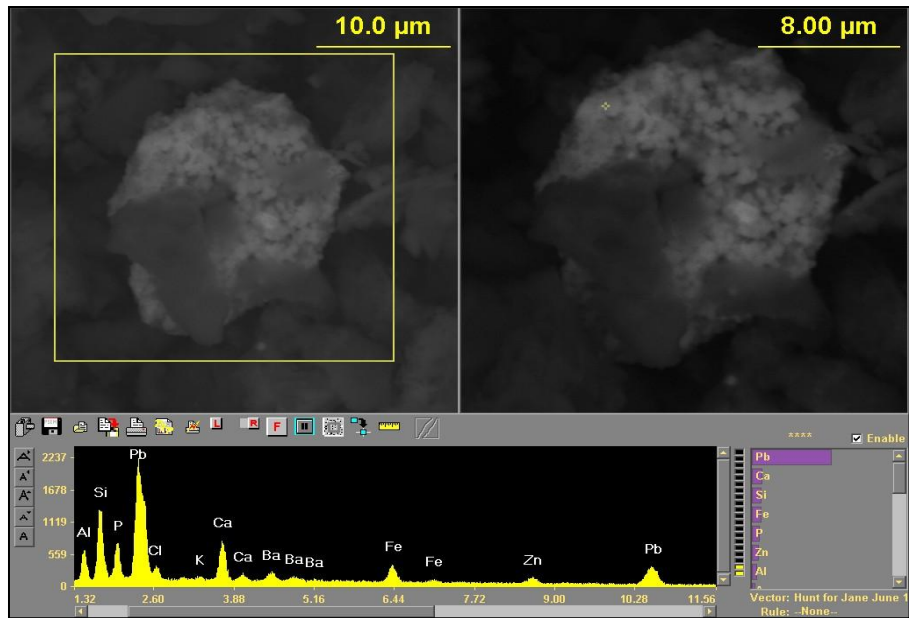


Figure A.39 SEM image shows PbP Cl Ba Fe Zn in Al Si Ca K particle determined in plot 4A quadrant d.

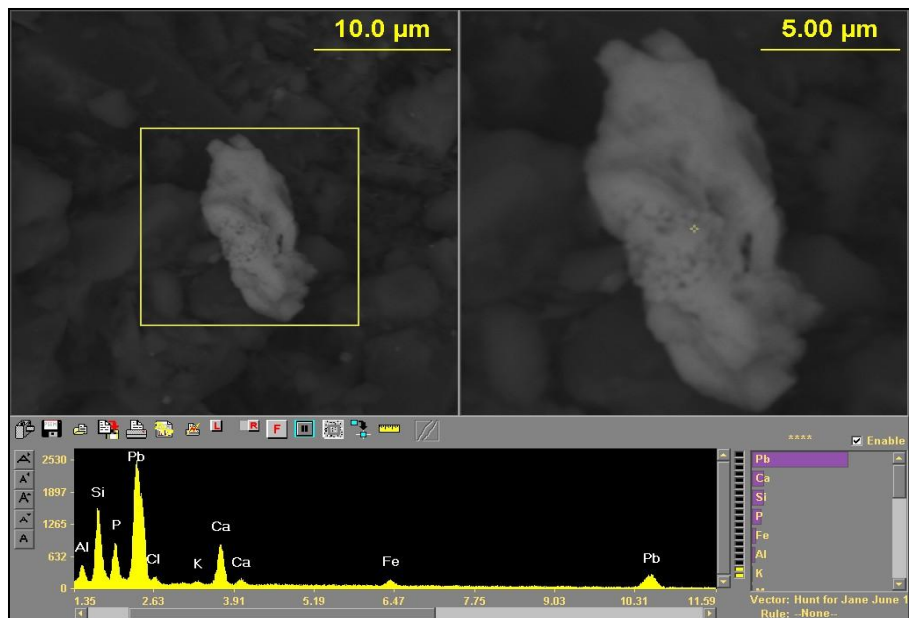


Figure A.40 SEM image shows PbP Cl Fe in Al Si Ca K particle determined in plot 4A quadrant d.

Appendix C

SEM Images and X-Ray Spectra of Twelve Months Post Treatment 1613 St.

Roche Samples

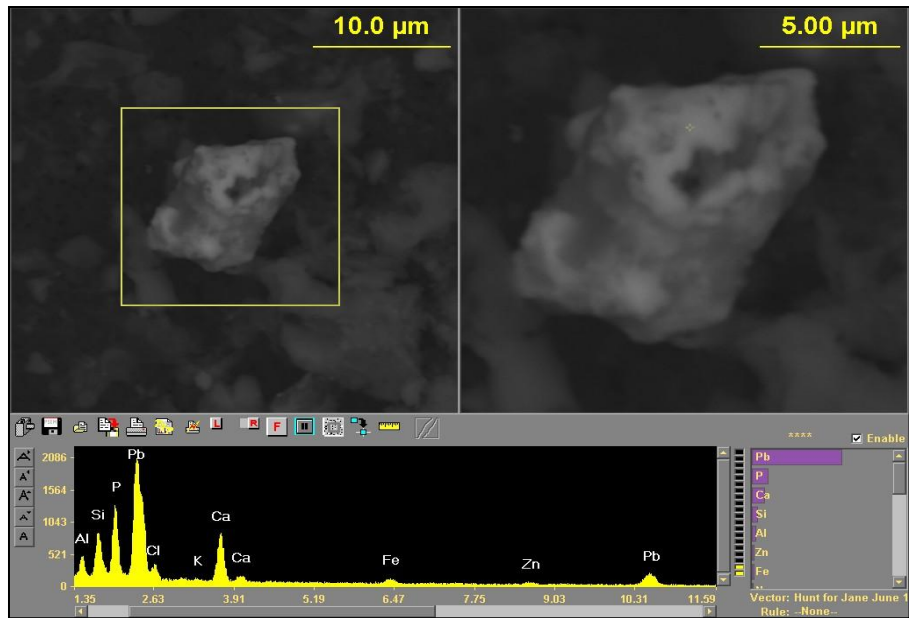


Figure C.1 SEM image shows PbP Fe Zn in Al Ca Si particle determined in plot 1A quadrant a.

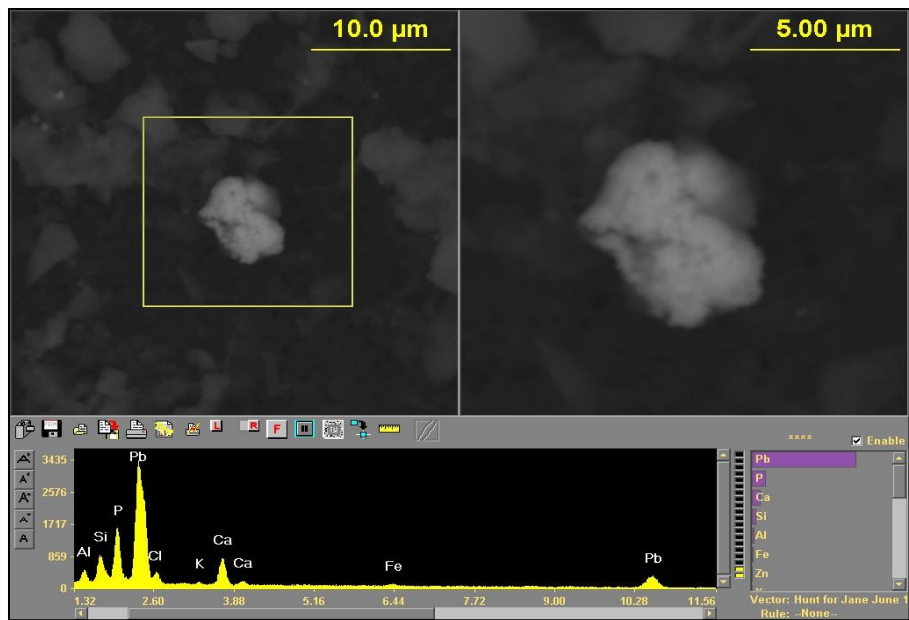


Figure C.2 SEM image shows PbP Fe in Al Ca Si particle determined in plot 1A quadrant a.

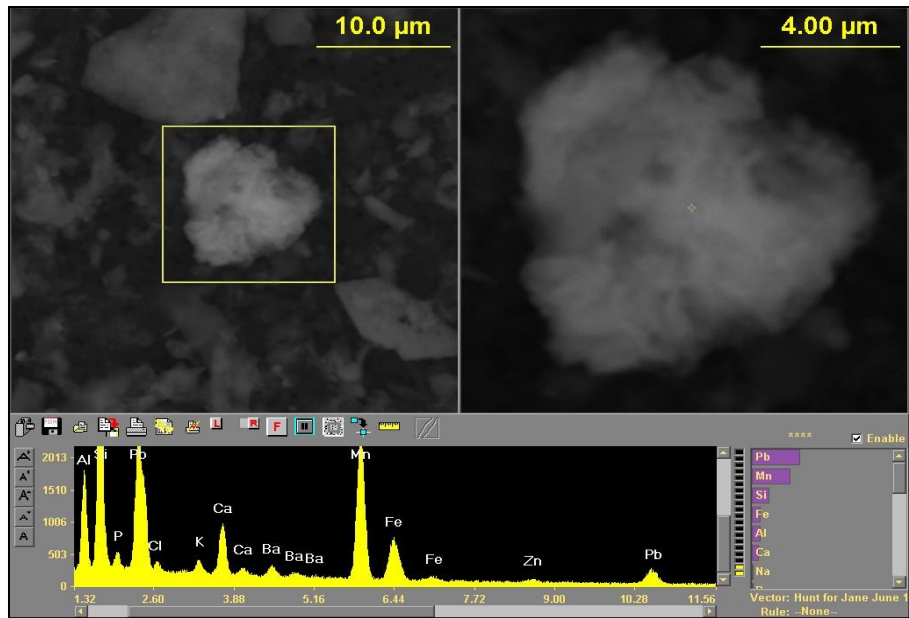


Figure C.3 SEM image shows PbP Mn Fe Zn in Al Ca Si Ba particle determined in plot 1A quadrant b.

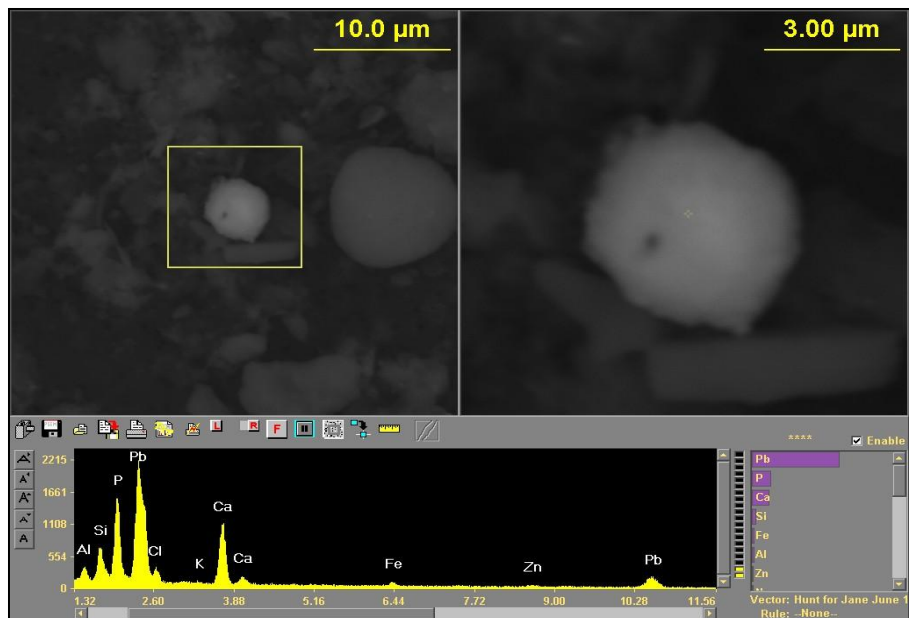


Figure C.4 SEM image shows PbP Fe Zn in Al Ca Si particle determined in plot 1A quadrant b.

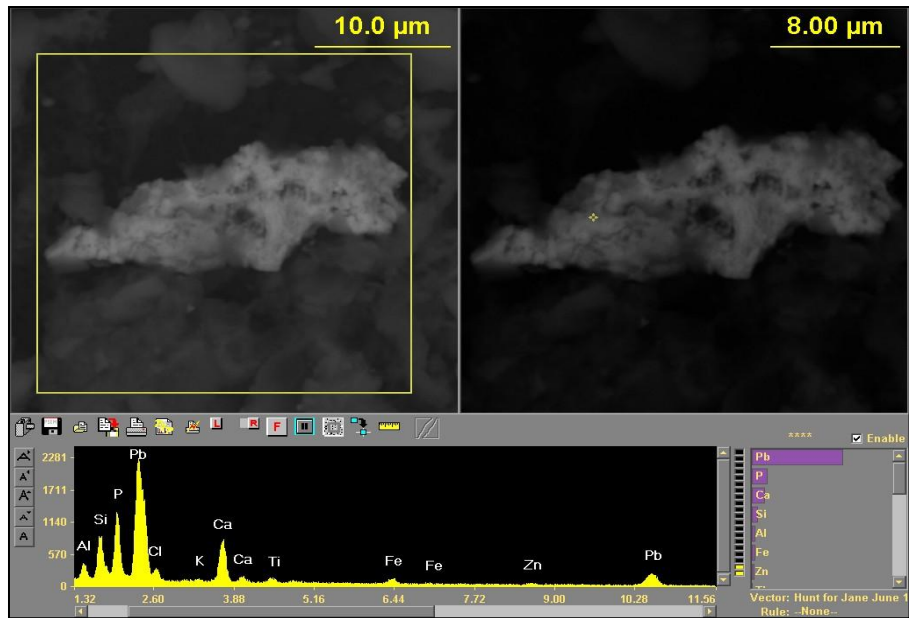


Figure C.5 SEM image shows PbP Fe Zn Ti in Al Ca Si particle determined in plot 1A quadrant c.

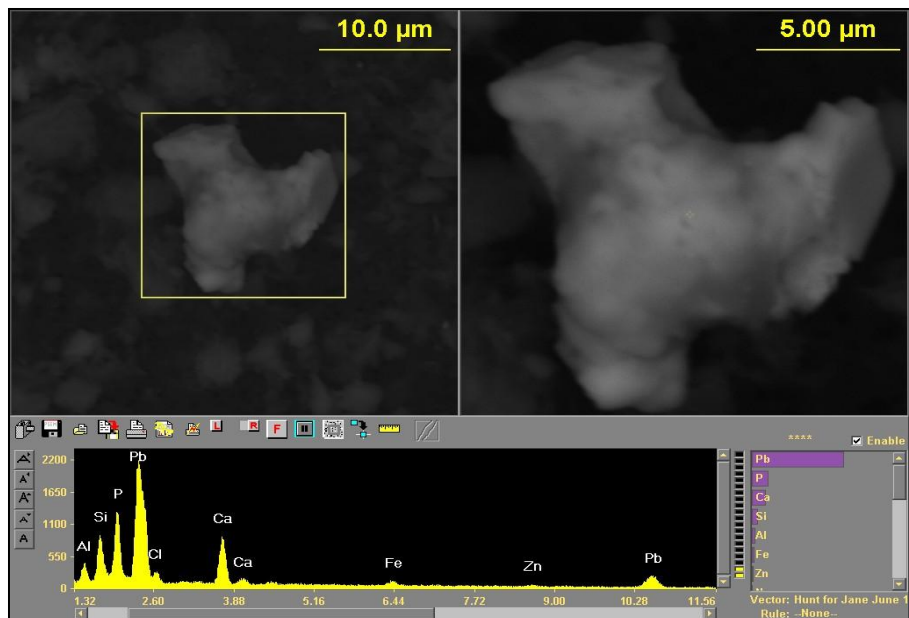


Figure C.6 SEM image shows PbP Fe Zn in Al Ca Si particle determined in plot 1A quadrant c.

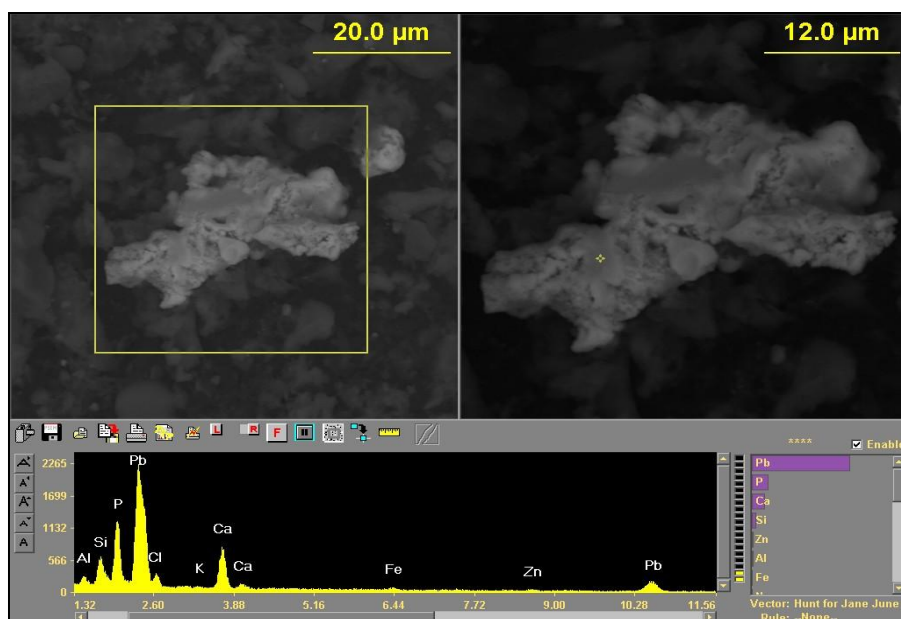


Figure C.7 SEM image shows PbP Fe Zn in Al Ca Si particle determined in plot

1A quadrant c.

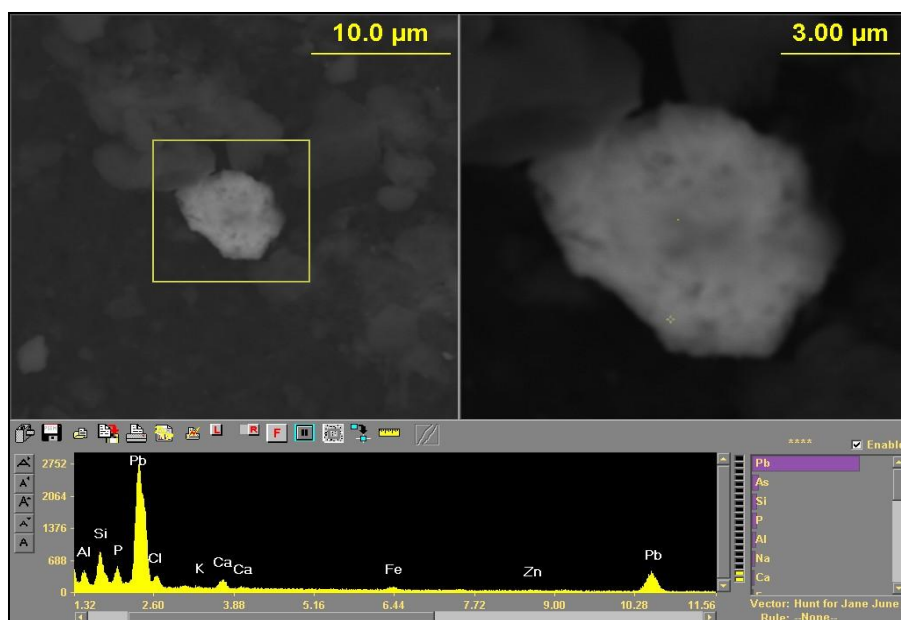


Figure C.8 SEM image shows PbP Fe in Al Ca Si particle determined in plot 1A

quadrant d.

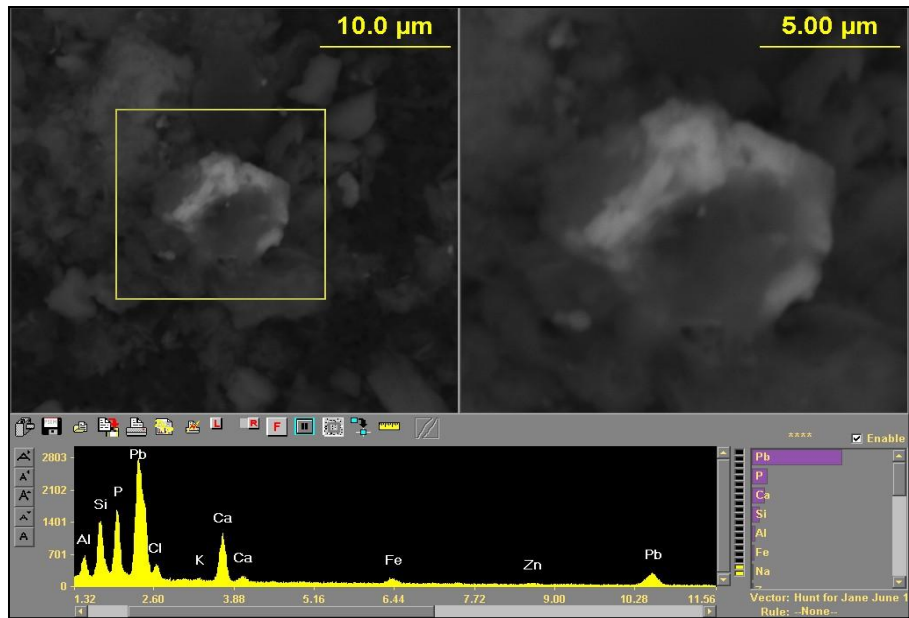


Figure C.9 SEM image shows PbP Fe in Al Ca Si particle determined in plot 1A quadrant d.

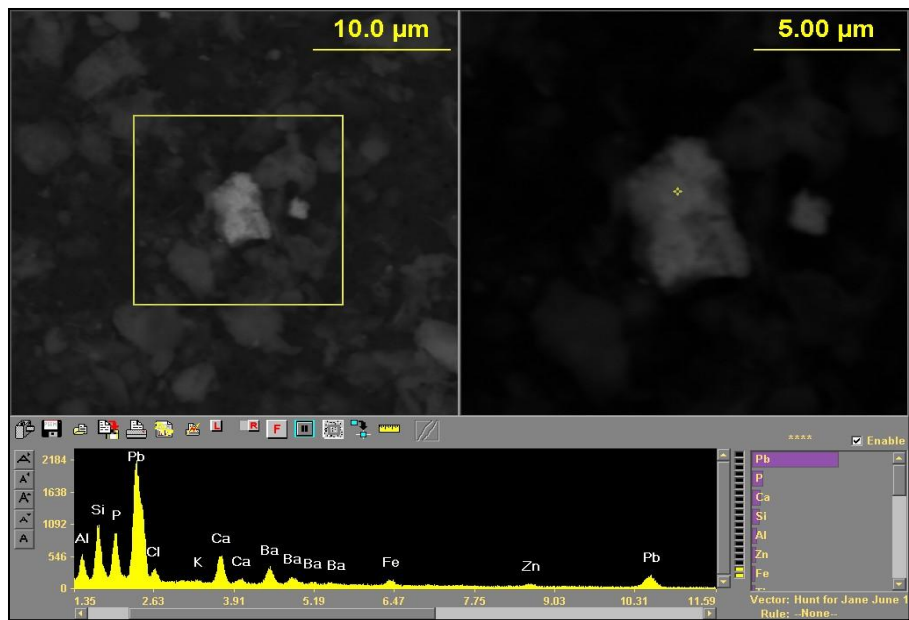


Figure C.10 SEM image shows PbP Fe Ba Zn in Al Ca Si particle determined in plot 2A quadrant a.

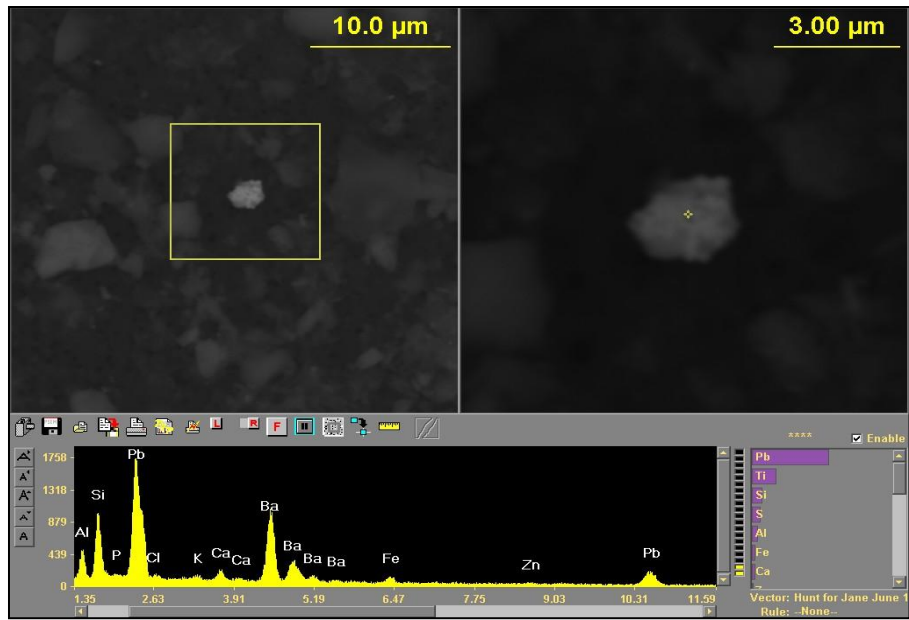


Figure C.11 SEM image shows Pb Fe Ba Zn in Al Ca Si particle determined in plot 2A quadrant a.

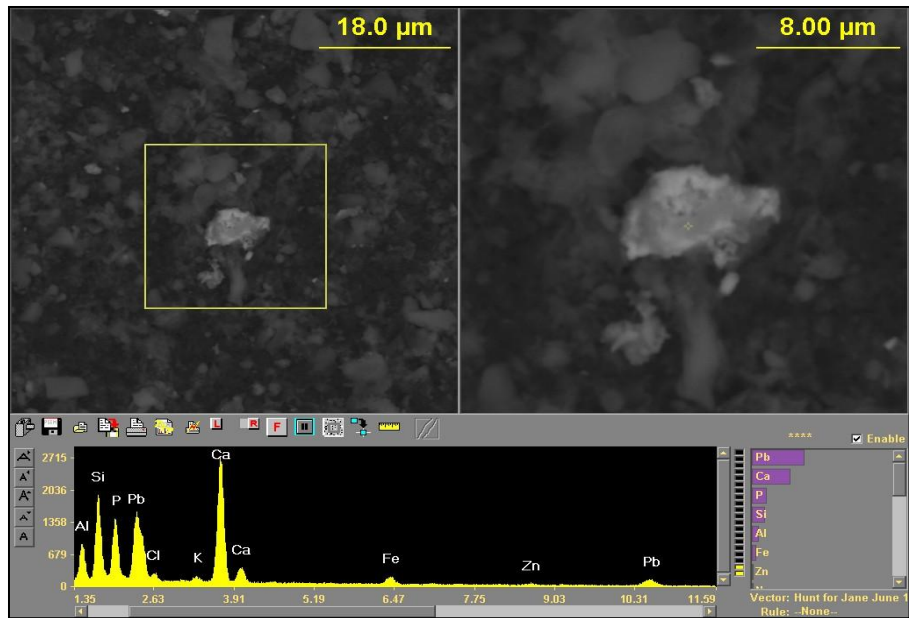


Figure C.12 SEM image shows PbP Fe Zn in Al Ca Si particle determined in plot 2A quadrant b.

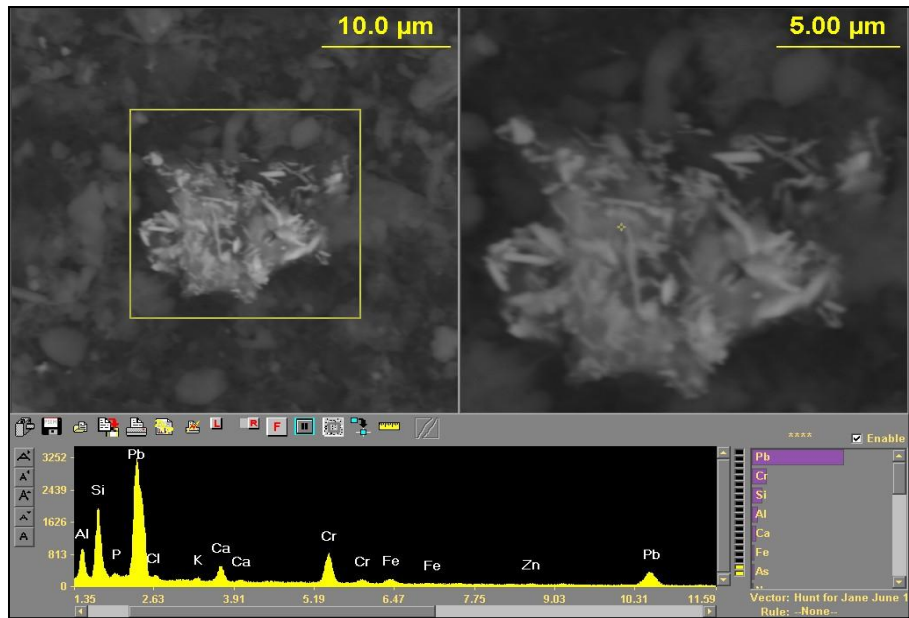


Figure C.13 SEM image shows Pb Cr Fe Zn in Al Ca Si particle determined in plot 2A quadrant b.

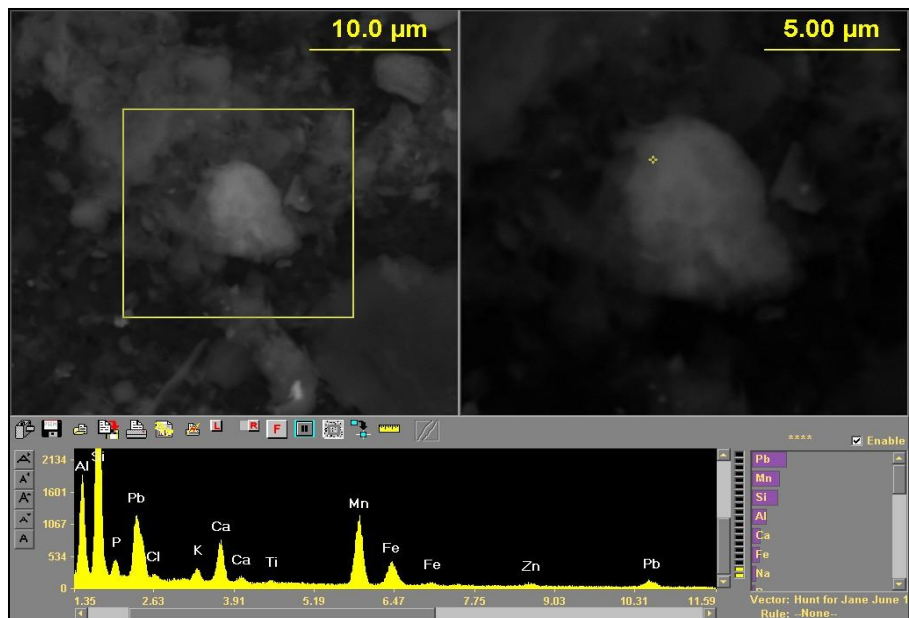


Figure C.14 SEM image shows PbP Mn Fe Zn in Al Ca Si particle determined in plot 2A quadrant c.

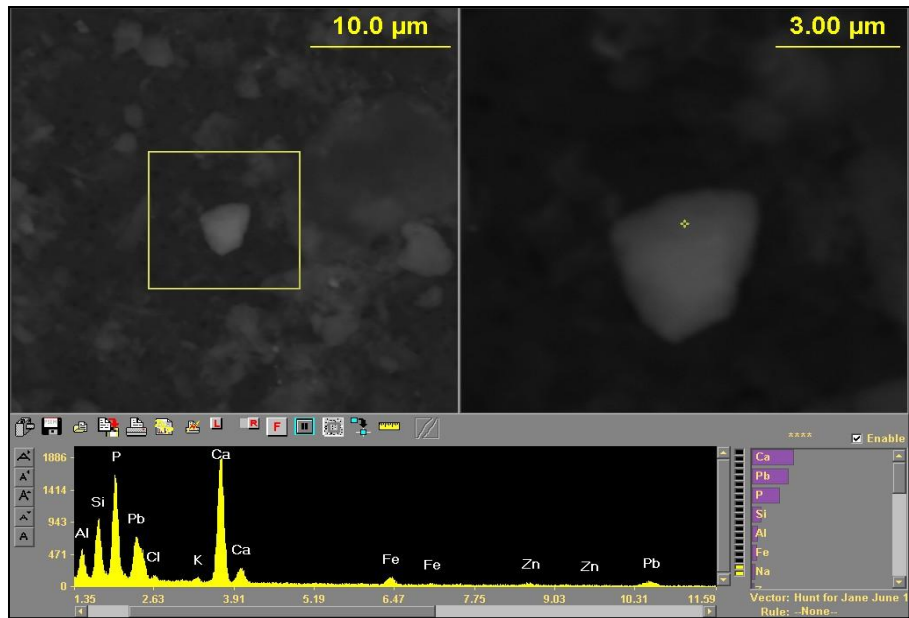


Figure C.15 SEM image shows Pb on CaP particle with Fe Zn Al Ca Si determined in plot 2A quadrant c.

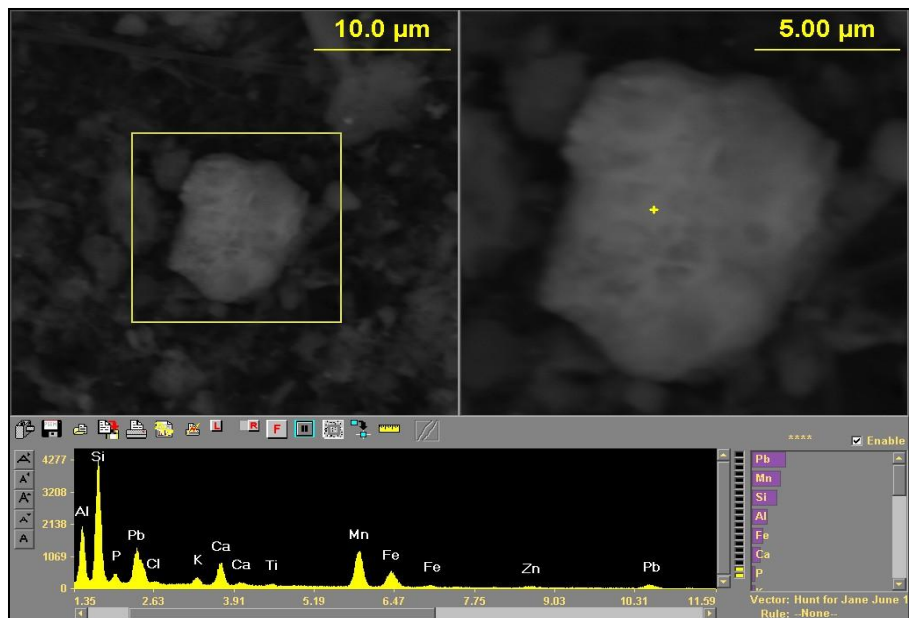


Figure C.16 SEM image shows PbP Mn Fe Zn in Al Ca Si particle determined in plot 2A quadrant d.

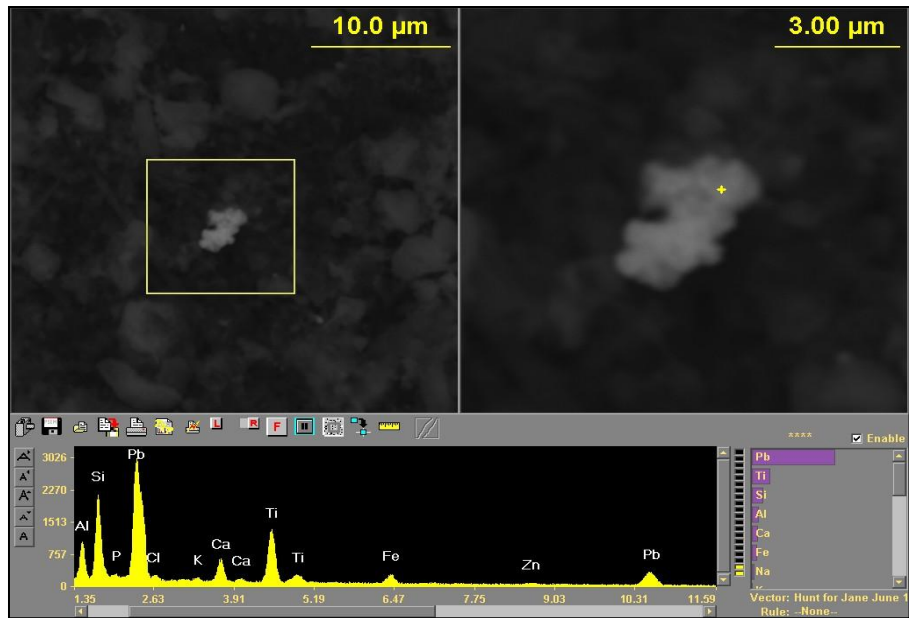


Figure C.17 SEM image shows Pb particle with Ti Fe Zn determined in plot 2A quadrant d.

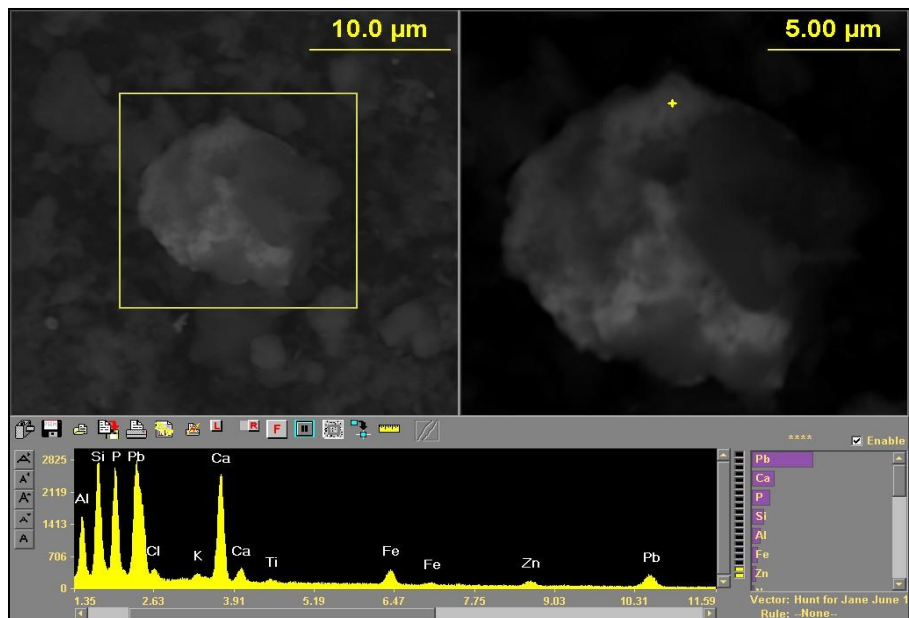


Figure C.18 SEM image shows Pb with CaP particle with Si Al Fe Zn determined in plot 3A quadrant a.

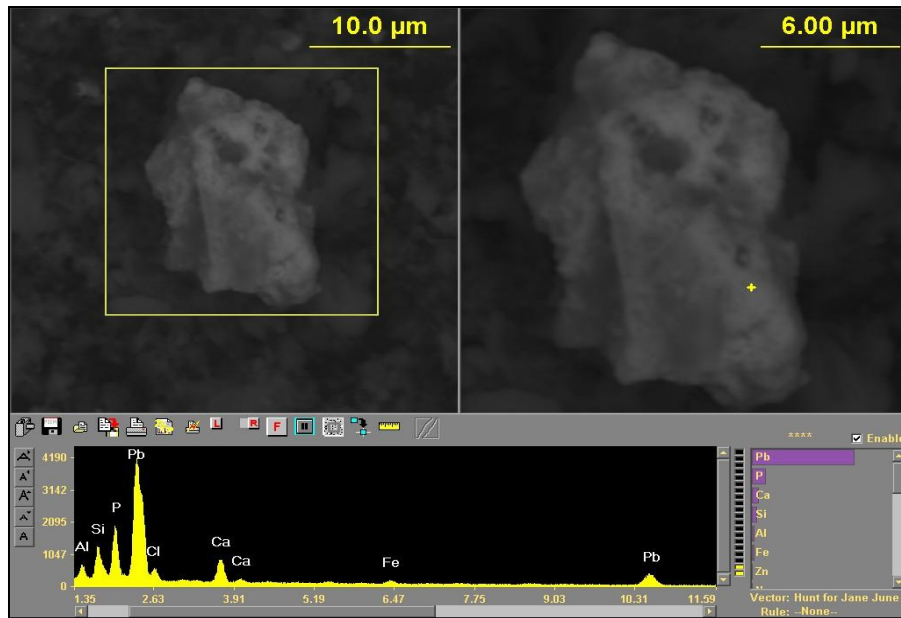


Figure C.19 SEM image shows PbP with Si Al Fe Zn Ca particle determined in plot 3A quadrant a.

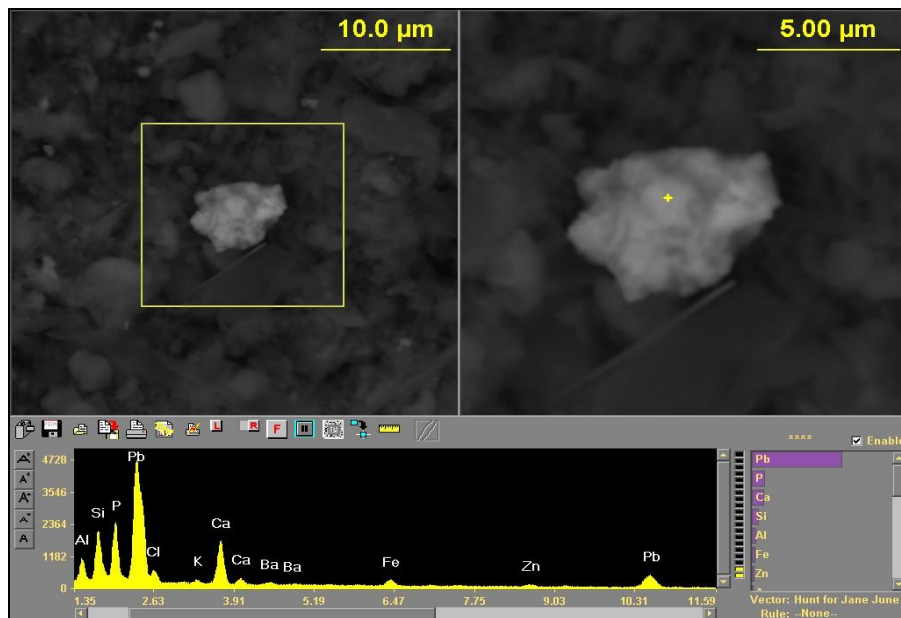


Figure C.20 SEM image shows PbP with Si Al Fe Zn Ca particle determined in plot 3A quadrant b.

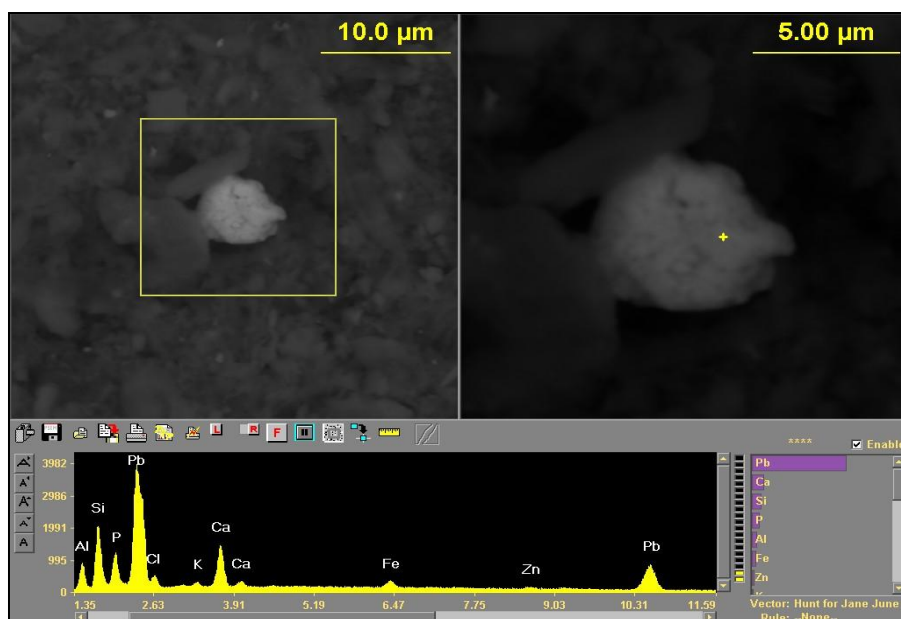


Figure C.21 SEM image shows PbP with Si Al Fe Zn Ca particle determined in plot 3A quadrant b.

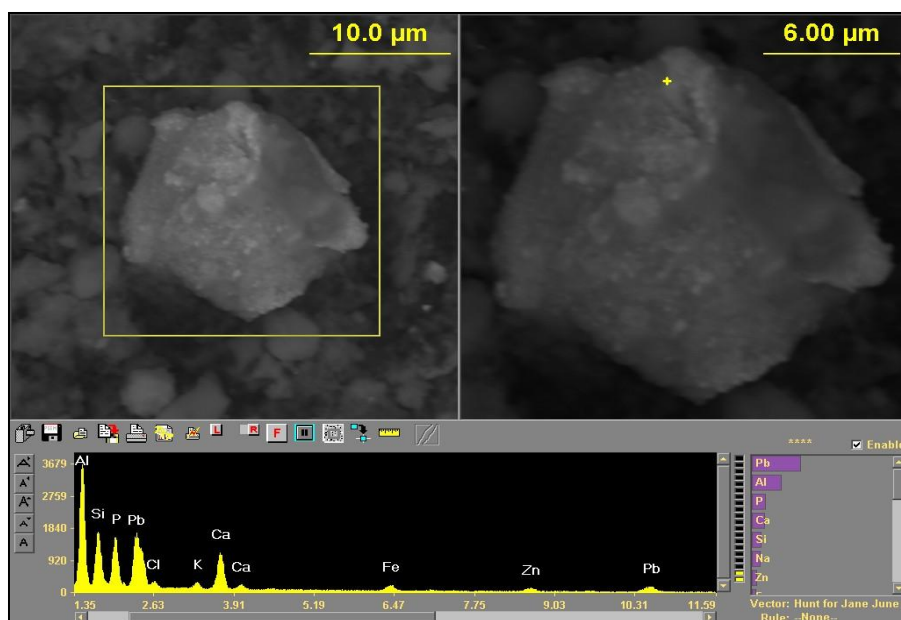


Figure C.22 SEM image shows PbP with Si Al Fe Zn Ca particle determined in plot 3A quadrant c.

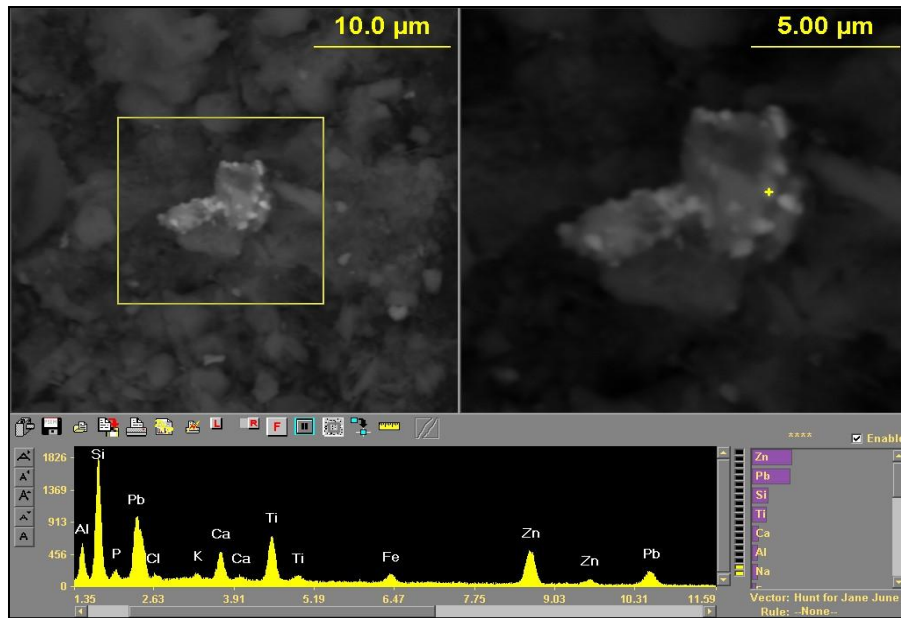


Figure C.23 SEM image shows PbP with Si Al Fe Zn Ti Ca particle determined in plot 3A quadrant c.

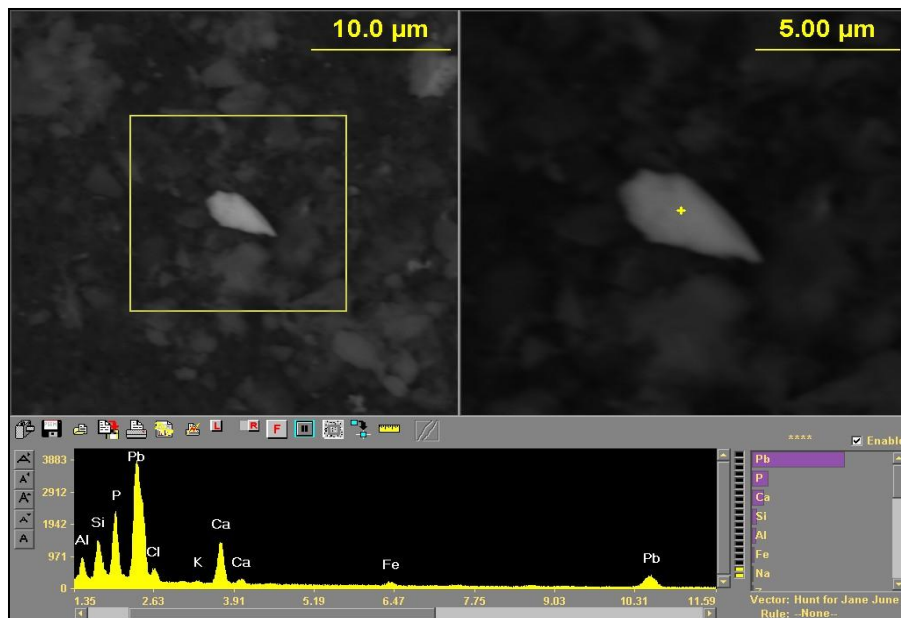


Figure C.24 SEM image shows PbP with Fe Zn in Si Al Ca particle determined in plot 3A quadrant d.

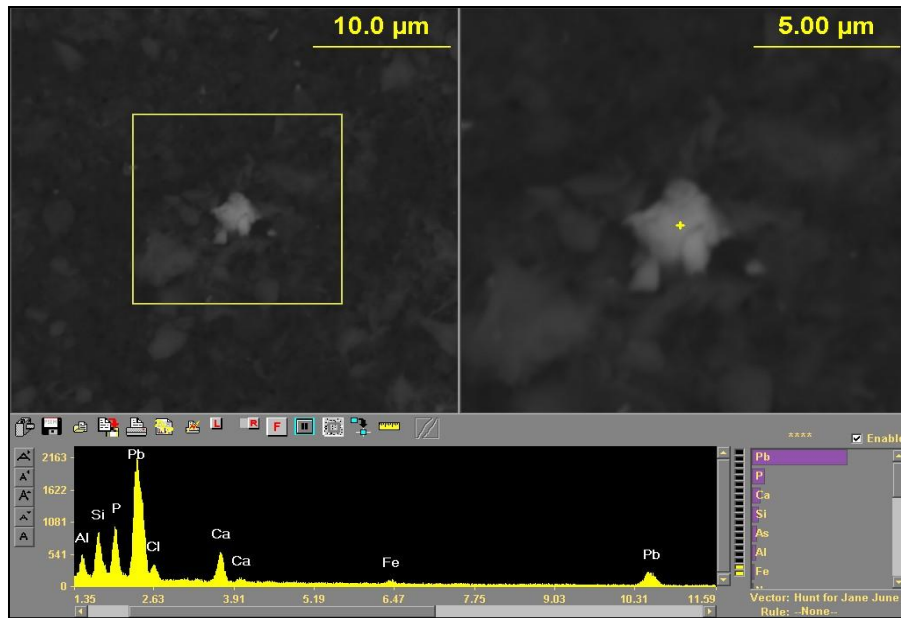


Figure C.25 SEM image shows PbP with Fe in Si Al Ca particle determined in plot 3A quadrant d.

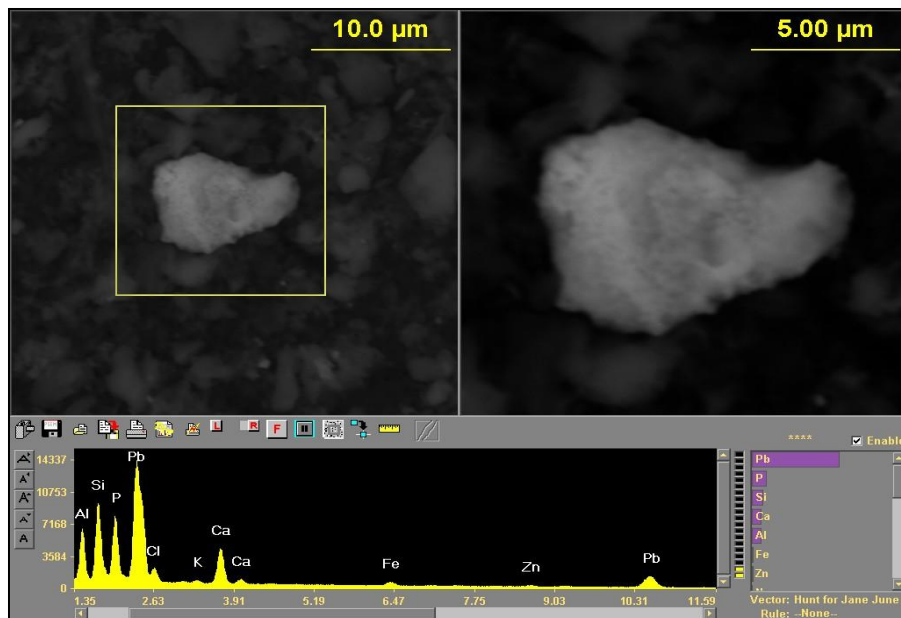


Figure C.26 SEM image shows PbP with Fe Zn in Si Al Ca particle determined in plot 4A quadrant a.

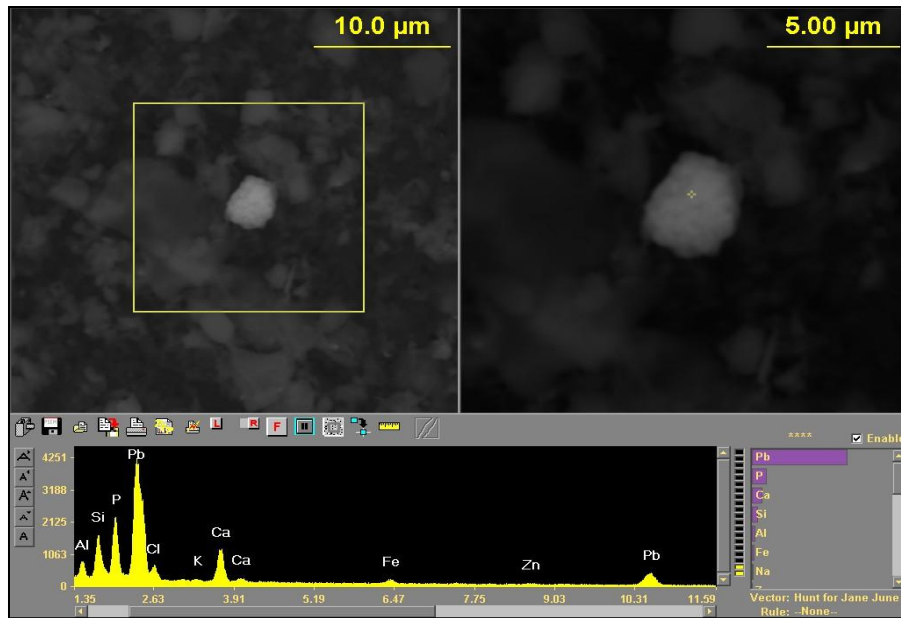


Figure C.27 SEM image shows PbP with Fe in Si Al Ca particle determined in plot 4A quadrant a.

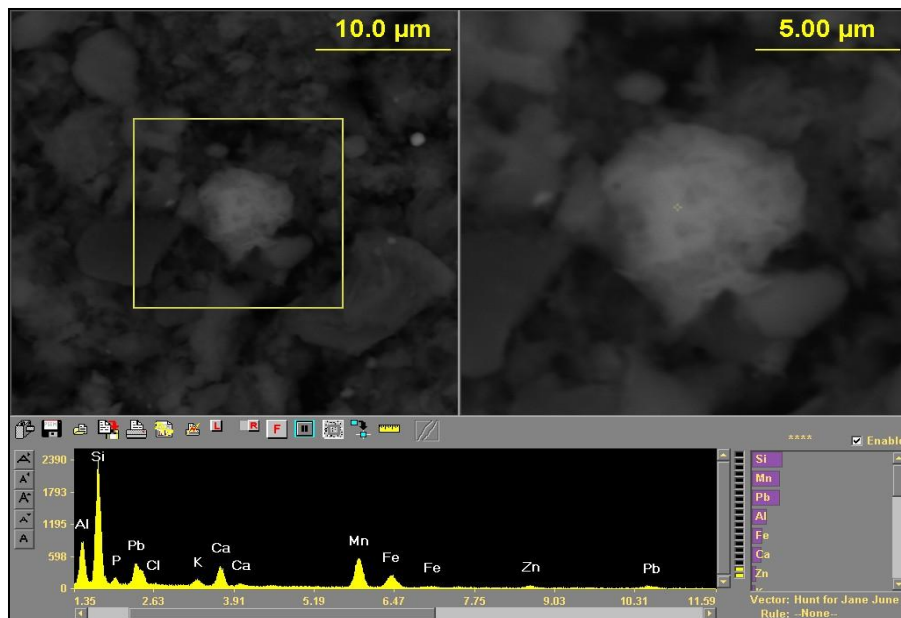


Figure C.28 SEM image shows PbP with Mn Fe Zn in Si Al Ca particle determined in plot 4A quadrant b.

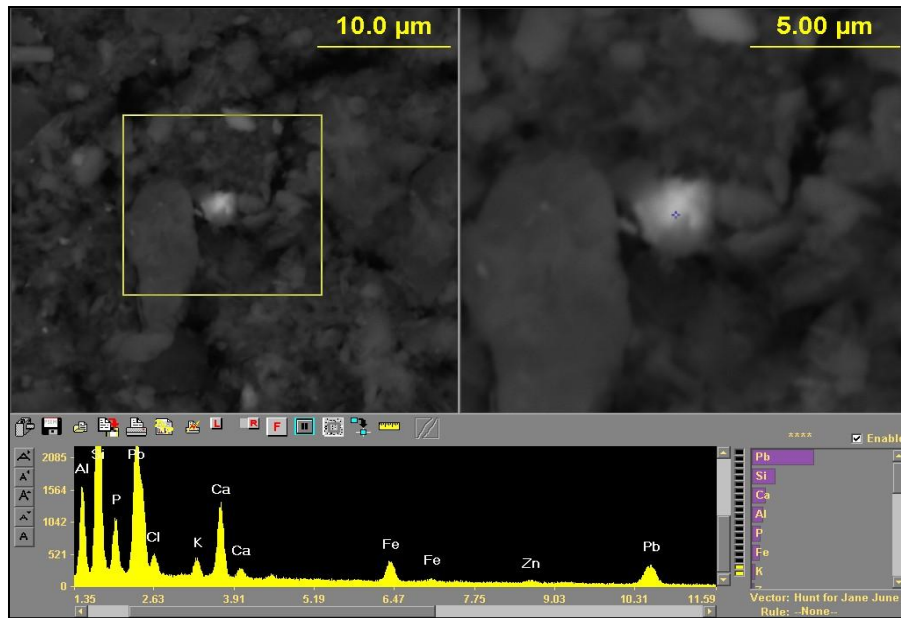


Figure C.29 SEM image shows PbP with Fe Zn in Si Al Ca particle determined in plot 4A quadrant b.

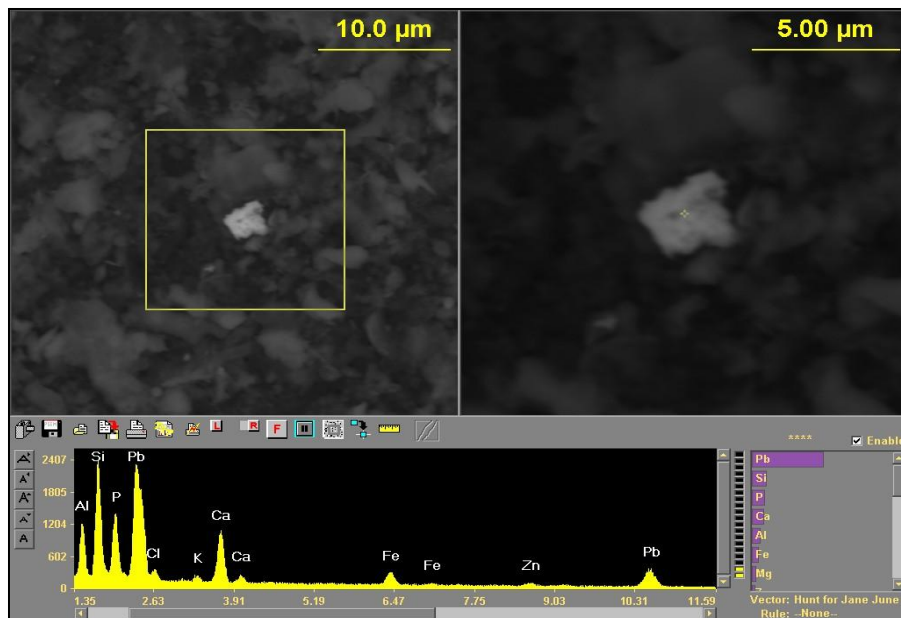


Figure C.30 SEM image shows PbP with Fe Zn in Si Al Ca particle determined in plot 4A quadrant c.

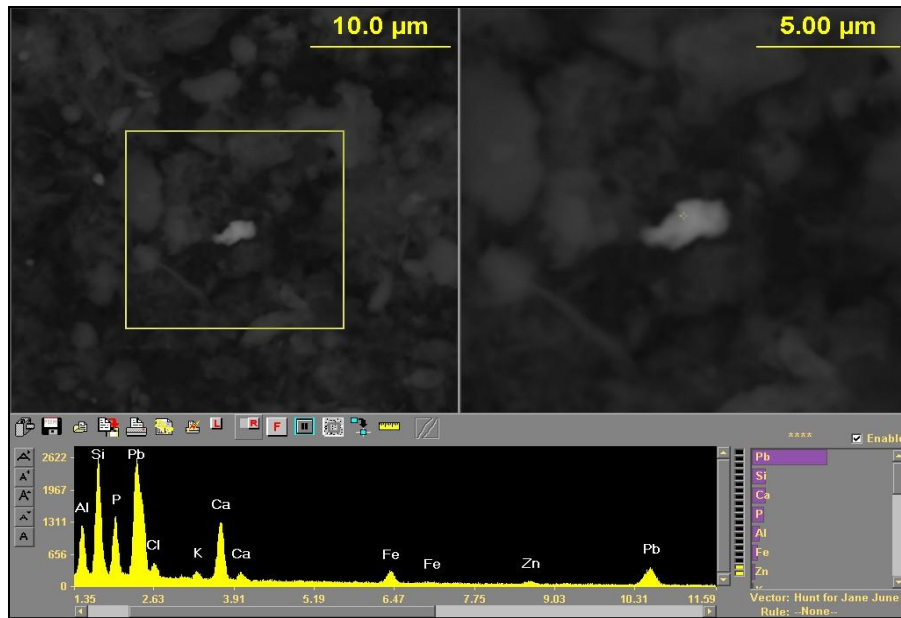


Figure C.31 SEM image shows PbP with Fe Zn in Si Al Ca particle determined in plot 4A quadrant c.

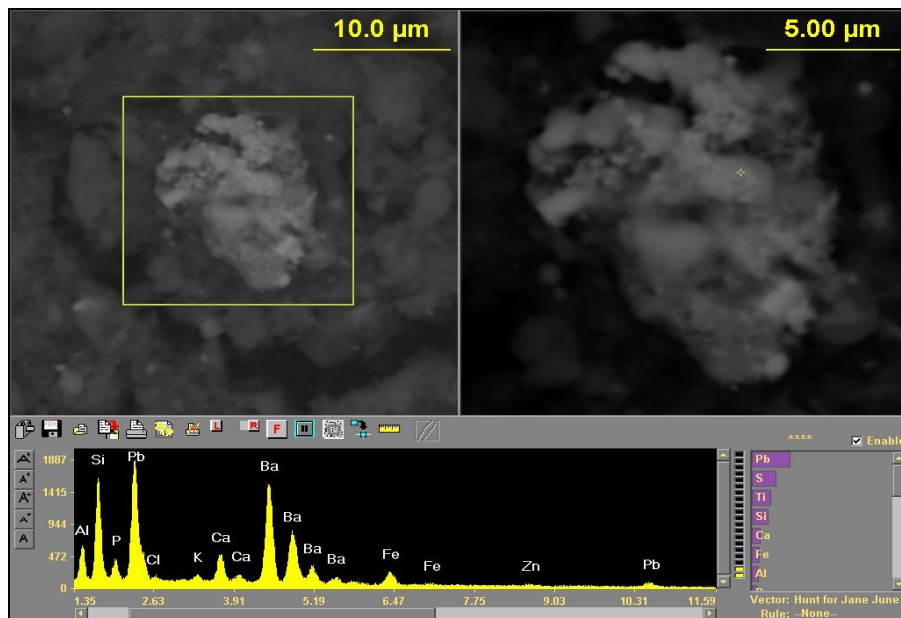


Figure C.32 SEM image shows PbP with Fe Zn Ba in Si Al Ca particle determined in plot 4A quadrant d.

Appendix D

SEM Images and X-Ray Spectra of Zero Months 1818 Dumaine St. Samples

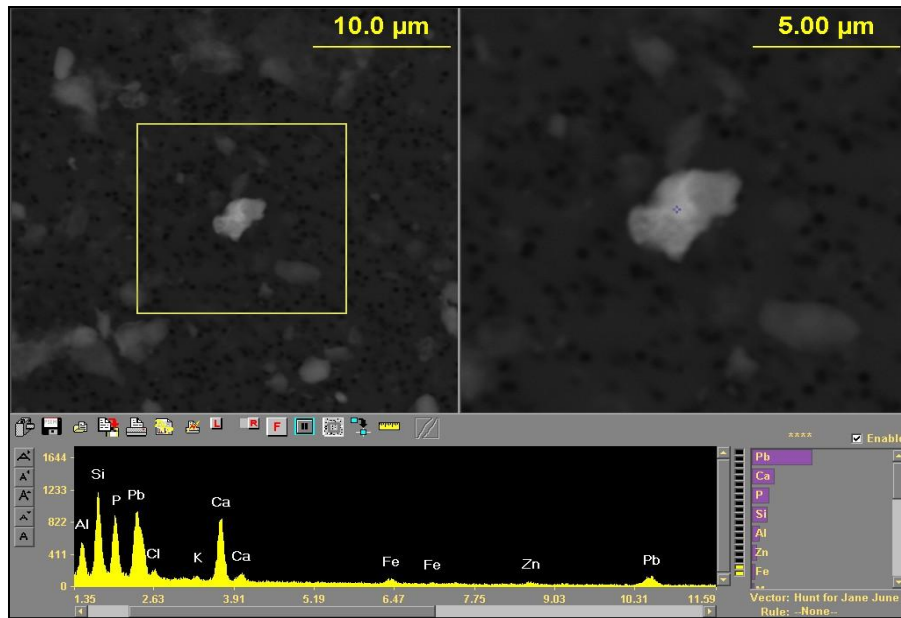


Figure D.1 SEM image shows Pb on CaP with Fe Zn Al Si K particle determined in plot 1A quadrant a.

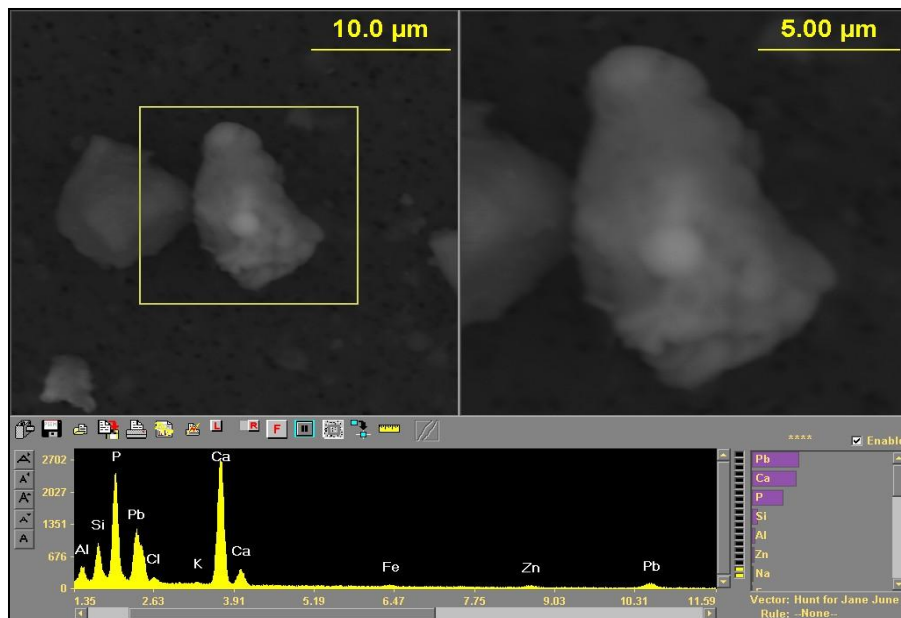


Figure D.2 SEM image shows Pb on CaP with Fe Zn Al Si K particle determined in plot 1A quadrant a.

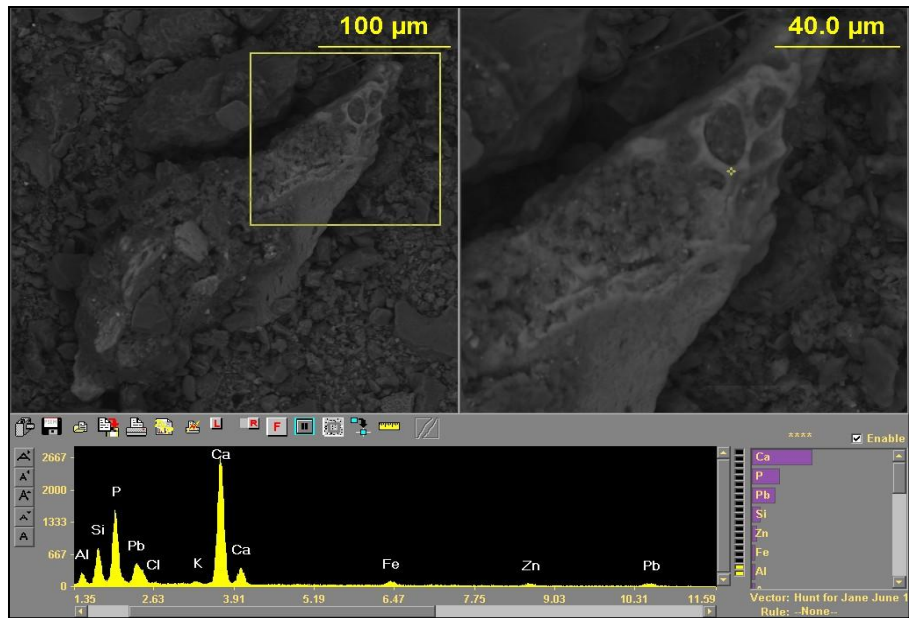


Figure D.3 SEM image shows Pb on CaP particle with Fe Zn Al Si K determined in plot 1A quadrant b.

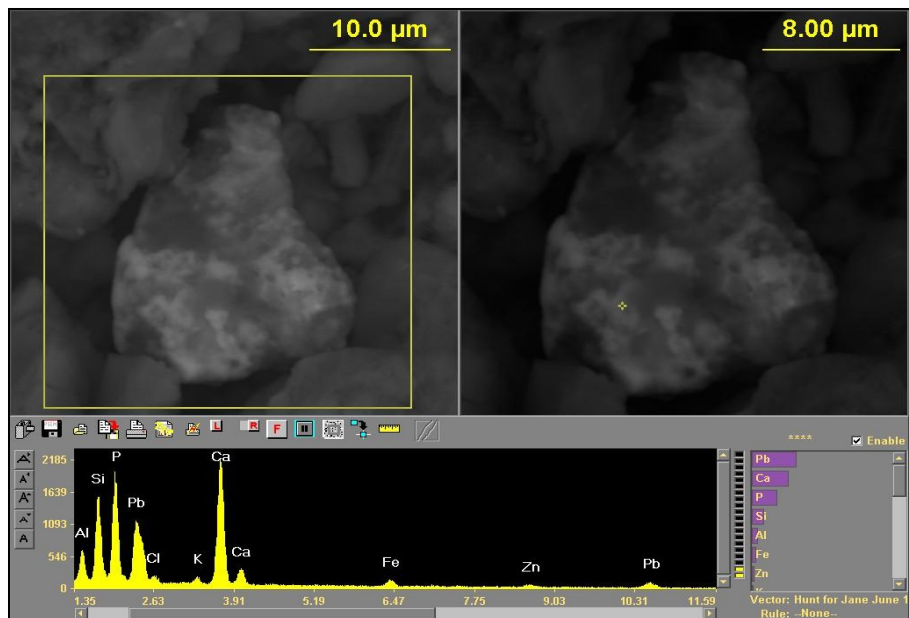


Figure D.4 SEM image shows Pb on CaP particle with Fe Zn Al Si K determined in plot 1A quadrant b.

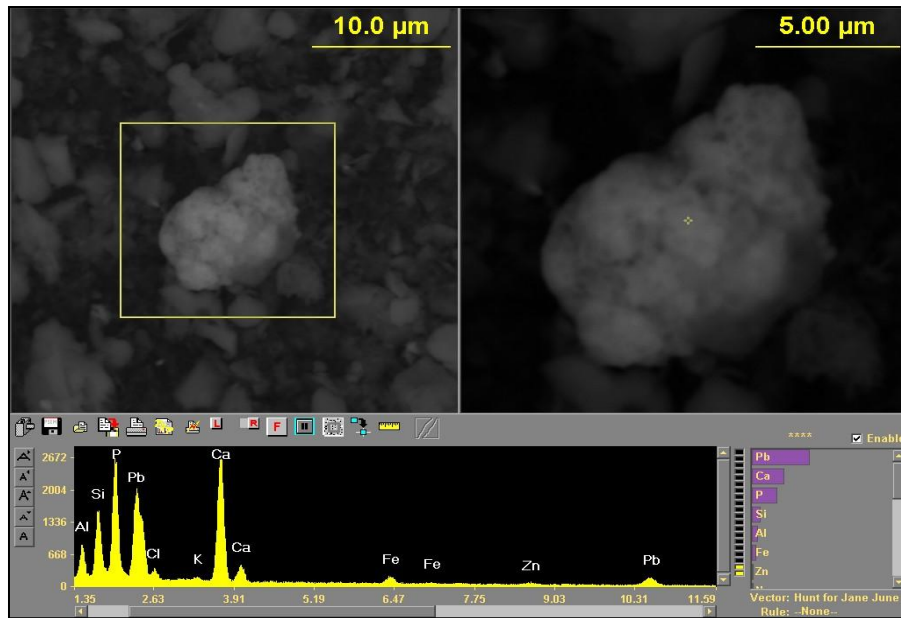


Figure D.5 SEM image shows Pb on CaP particle with Fe Zn Al Si K determined in plot 1A quadrant c.

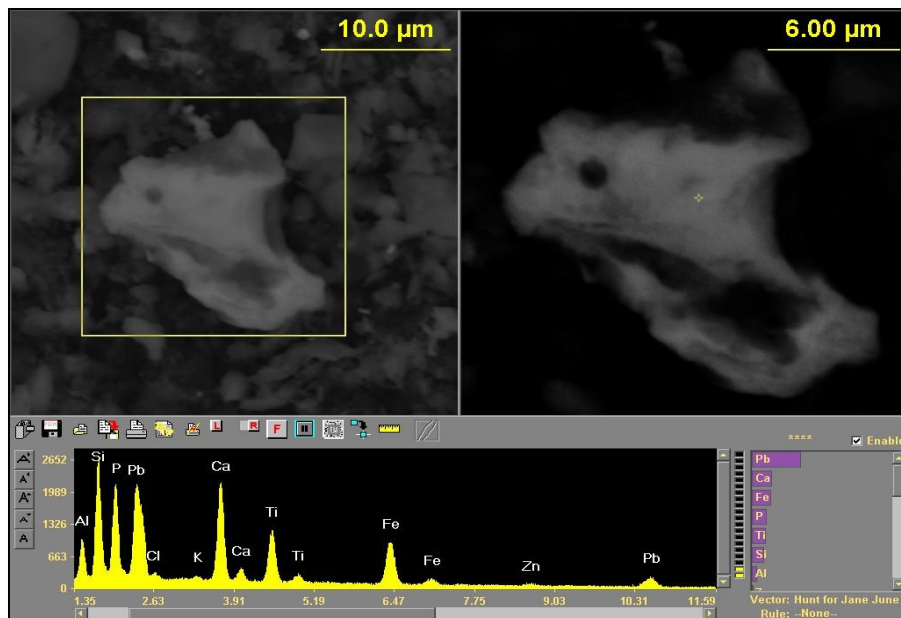


Figure D.6 SEM image shows Pb on CaP particle with Fe Zn Ti Al Si K determined in plot 1A quadrant c.

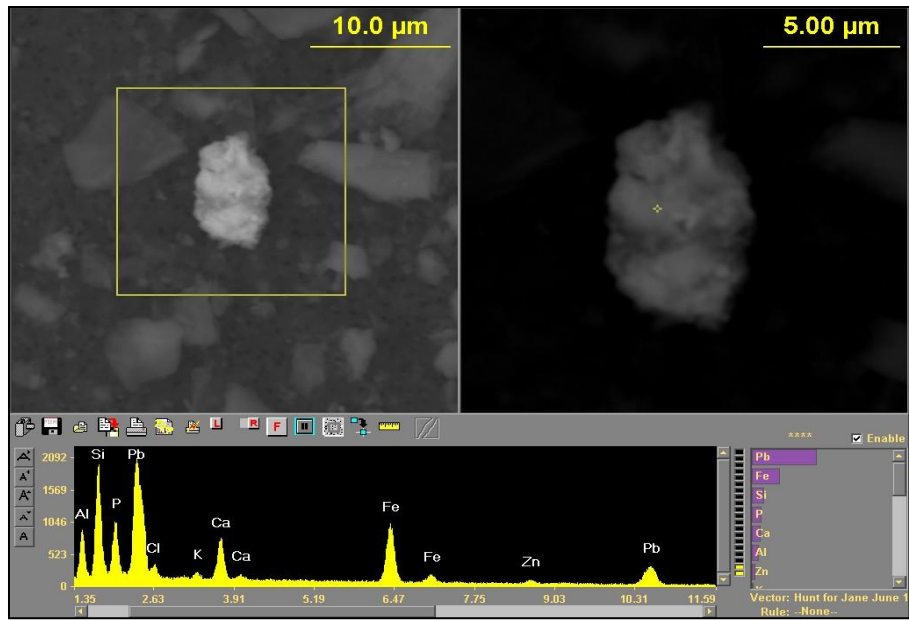


Figure D.7 SEM image shows PbP with Fe Zn in Al Si Ca K particle determined in plot 1A quadrant d.

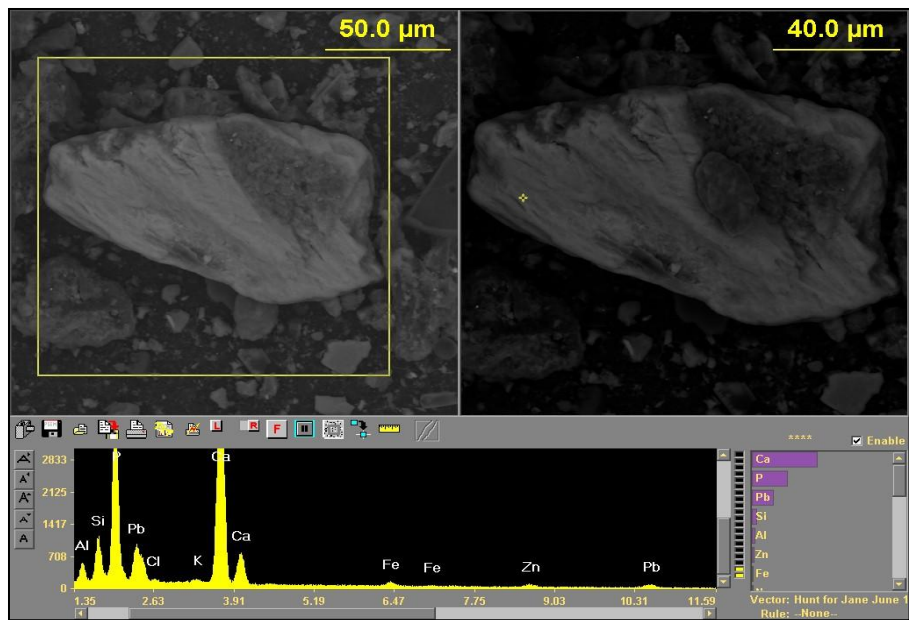


Figure D.8 SEM image shows Pb on CaP particle with Fe Zn Al Si K determined in plot 1A quadrant d.

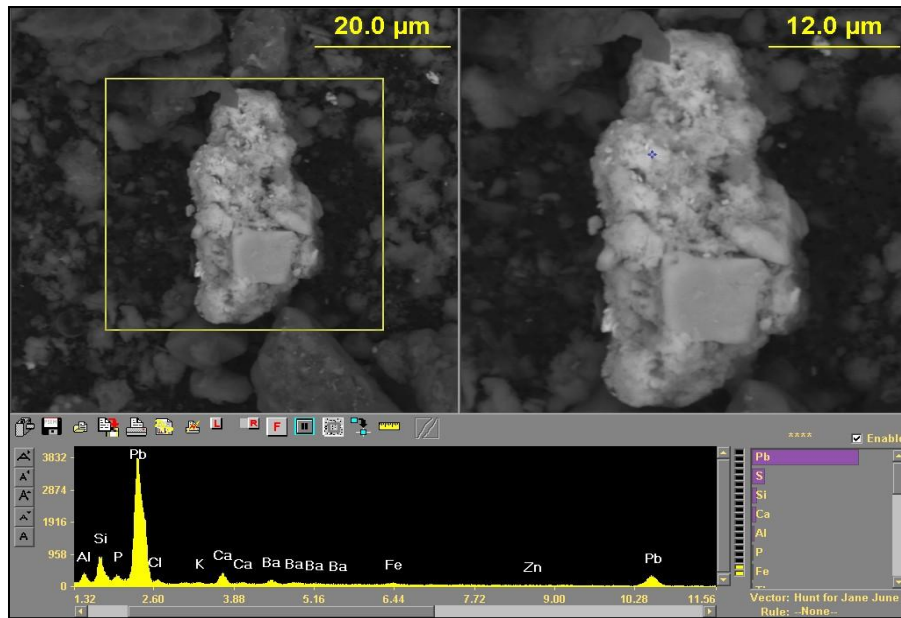


Figure D.9 SEM image shows Pb particle with Fe Ba Al Si Ca determined in plot 2A quadrant a.

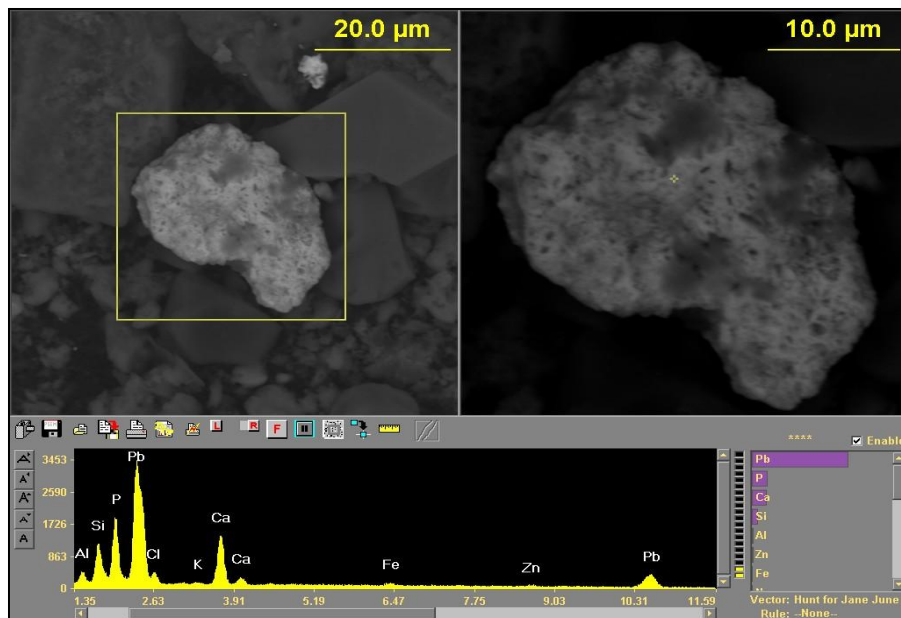


Figure D.10 SEM image shows Pb on CaP particle with Fe Zn Al Si Ca K determined in plot 2A quadrant a.

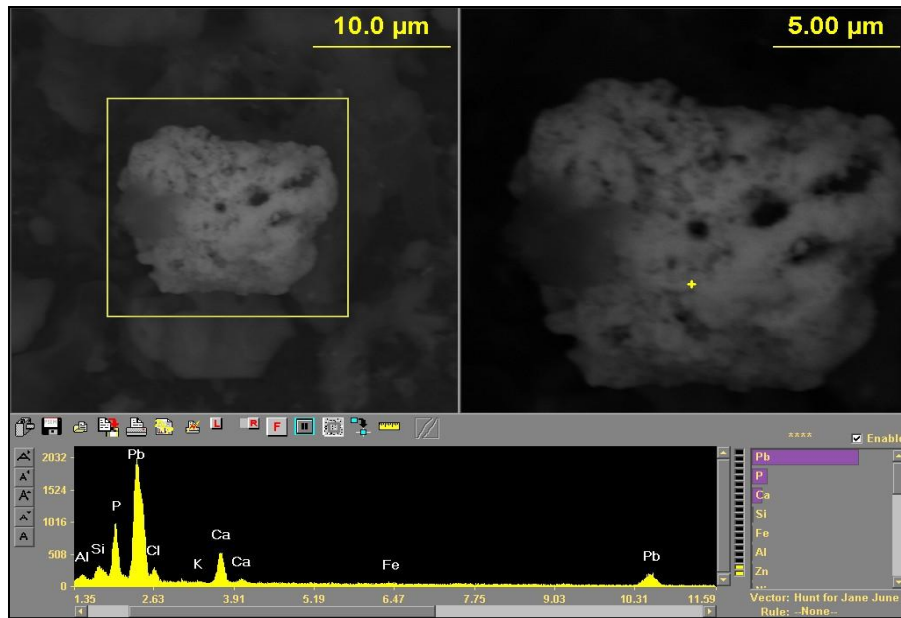


Figure D.11 SEM image shows Pb on CaP particle with Al Si Ca determined in plot 2A quadrant b.

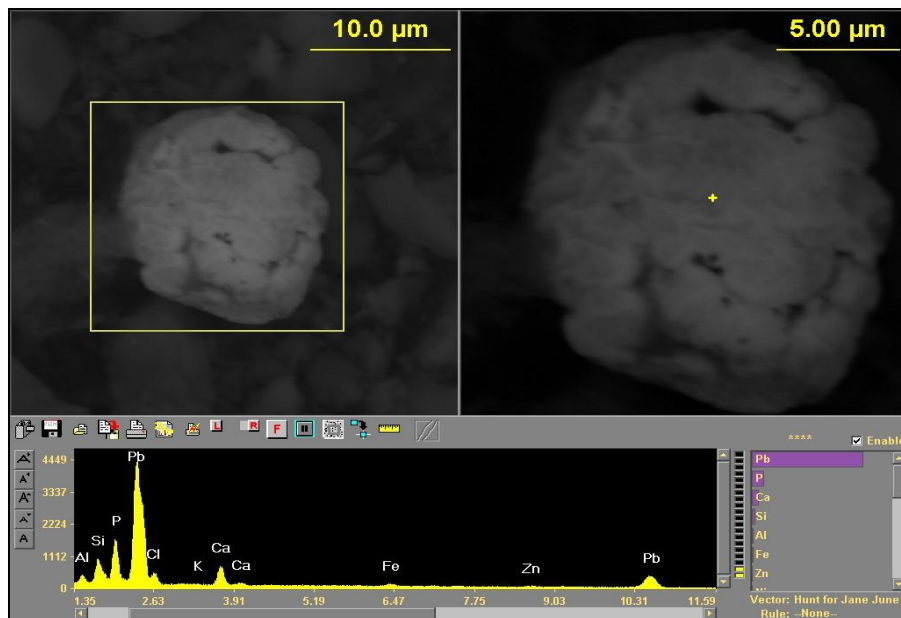


Figure D.12 SEM image shows Pb on CaP particle with Al Si Ca determined in plot 2A quadrant b.

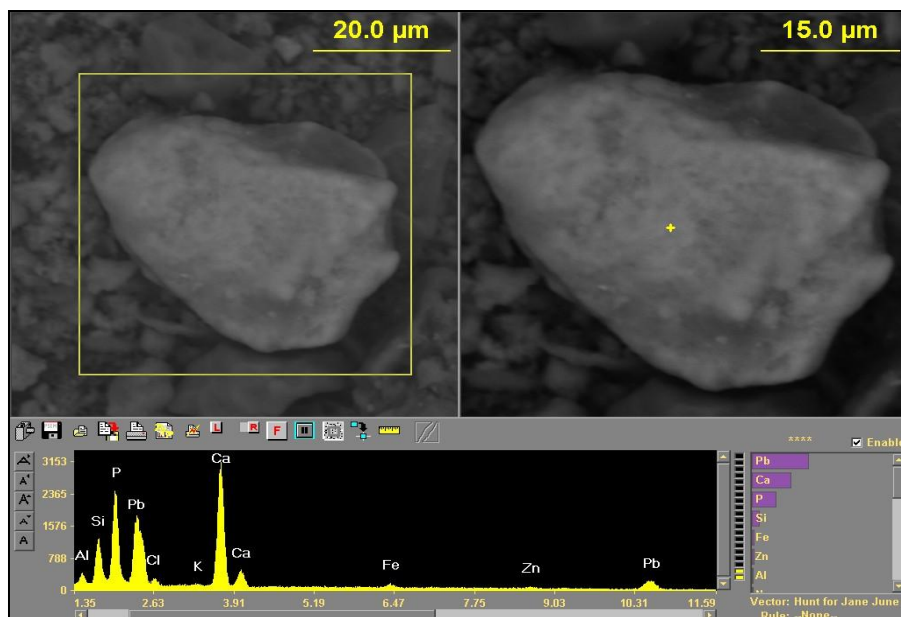


Figure D.13 SEM image shows Pb on CaP particle with Al Si Ca determined in plot 2A quadrant c.

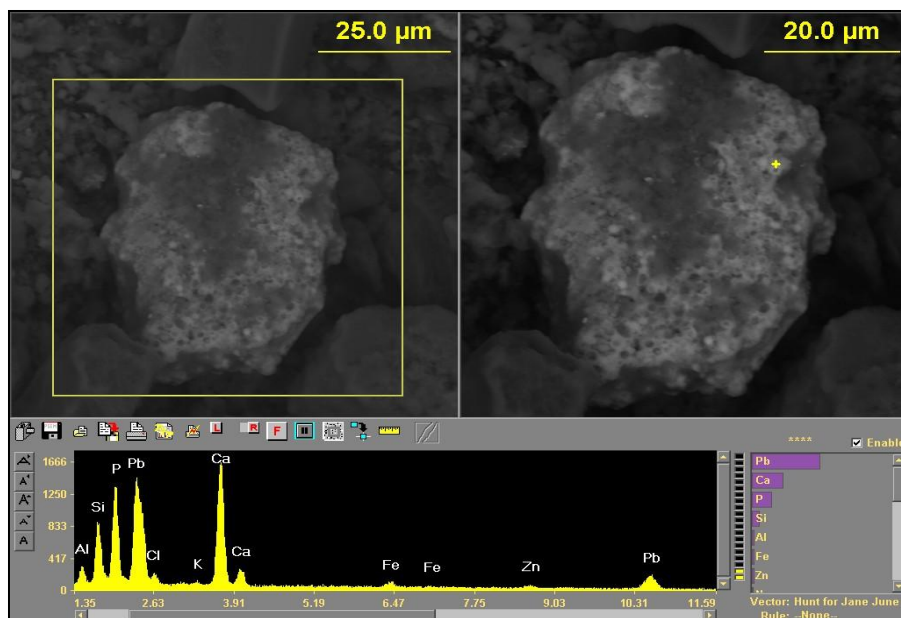


Figure D.14 SEM image shows Pb on CaP particle with Al Si Ca determined in plot 2A quadrant c.

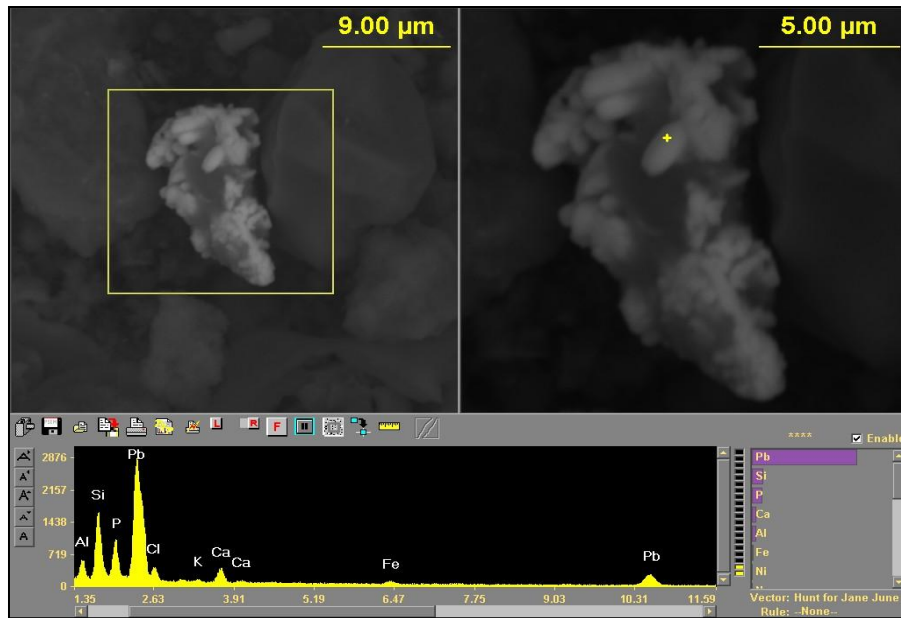


Figure D.15 SEM image shows elongated PbP with Fe on Al Si Ca particle with determined in plot 2A quadrant d.

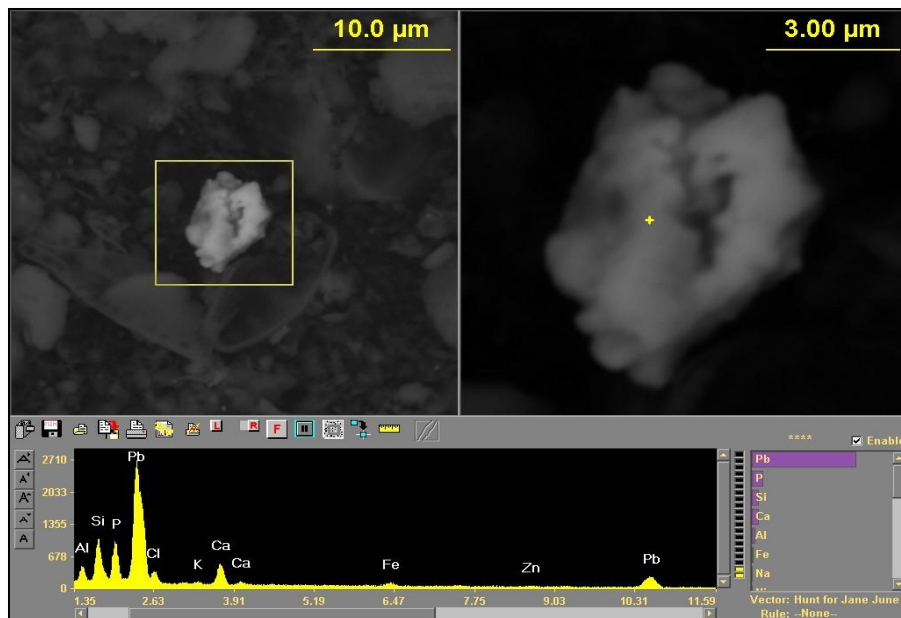


Figure D.16 SEM image shows PbP with Fe Zn on Al Si Ca particle determined in plot 2A quadrant d.

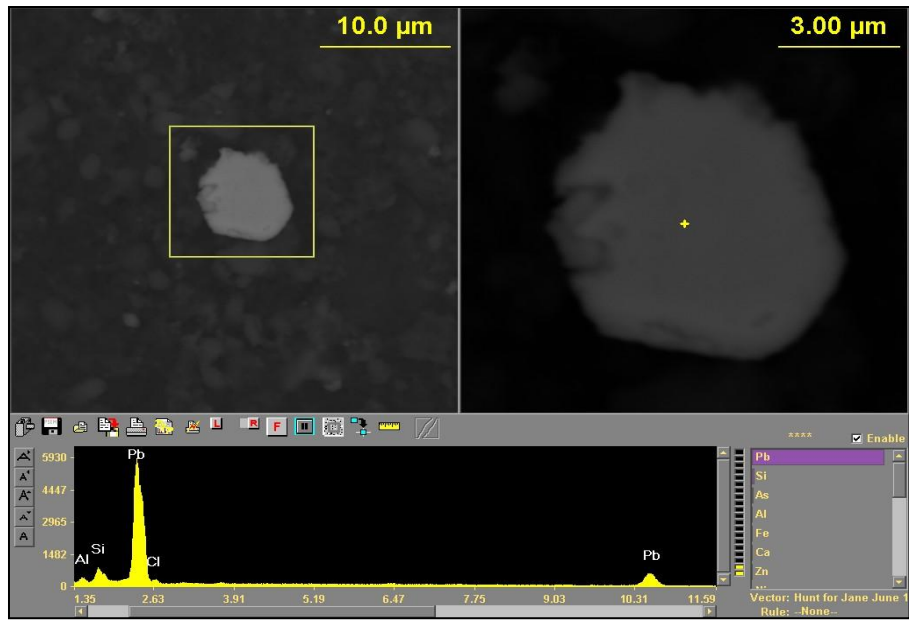


Figure D.17 SEM image shows hexagonal Pb particle determined in plot 3A quadrant a.

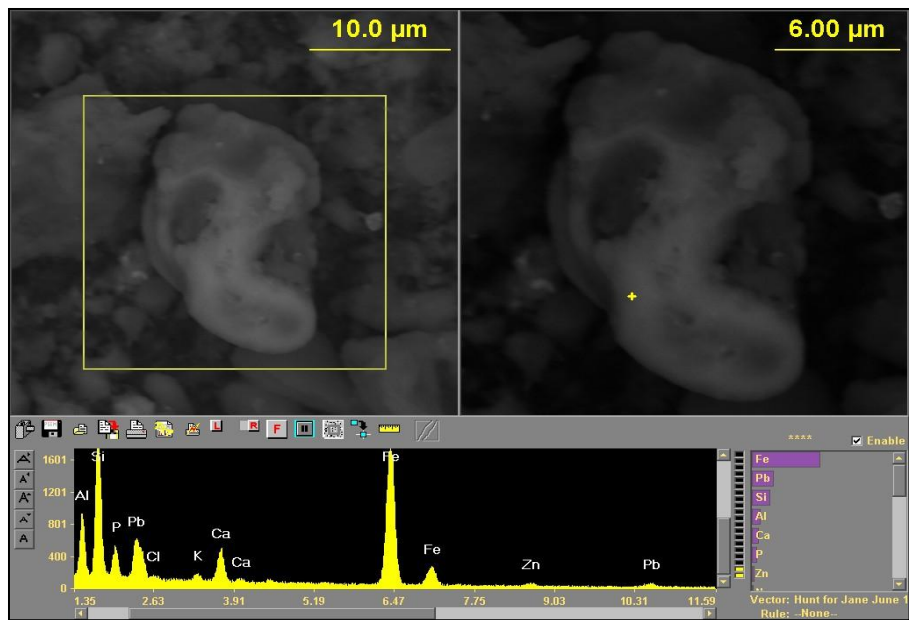


Figure D.18 SEM image shows PbP with Fe Zn on Al Si Ca particle determined in plot 3A quadrant a.

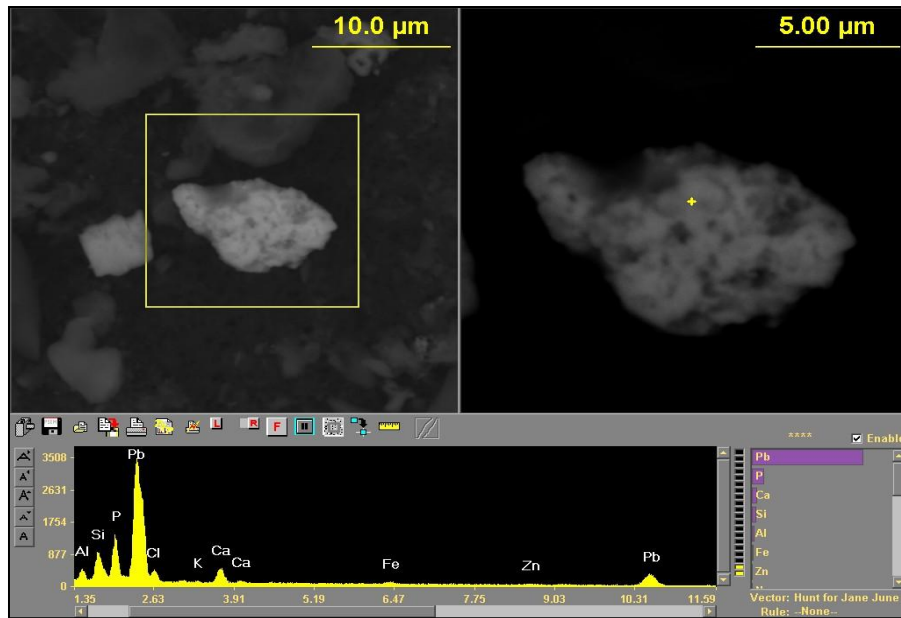


Figure D.19 SEM image shows PbP with Fe on Al Si Ca particle determined in plot 3A quadrant b.

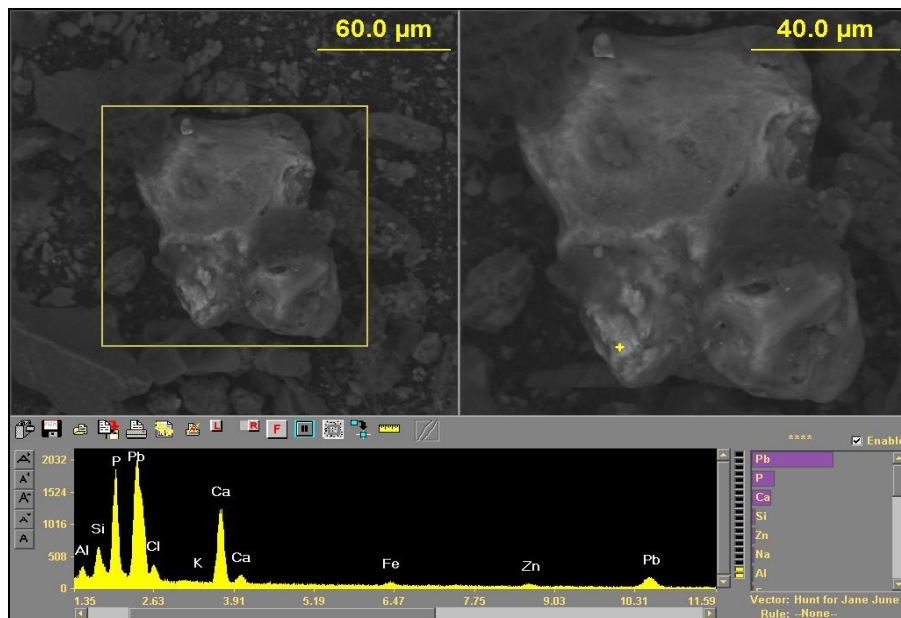


Figure D.20 SEM image shows Pb with CaP with Fe Zn Al Si particle determined in plot 3A quadrant b.

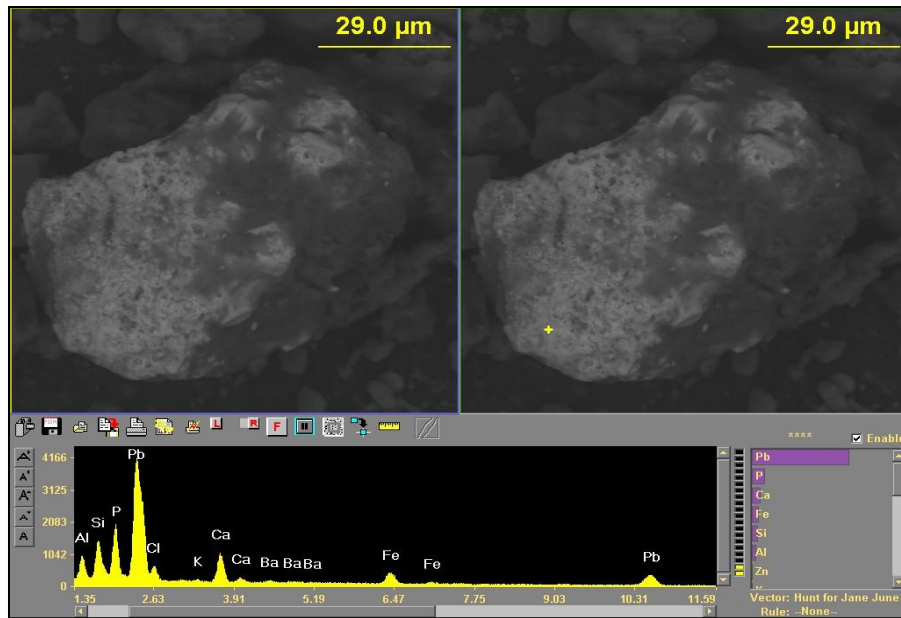


Figure D.21 SEM image shows PbP with Fe on Al Si Ca particle determined in plot 3A quadrant c.

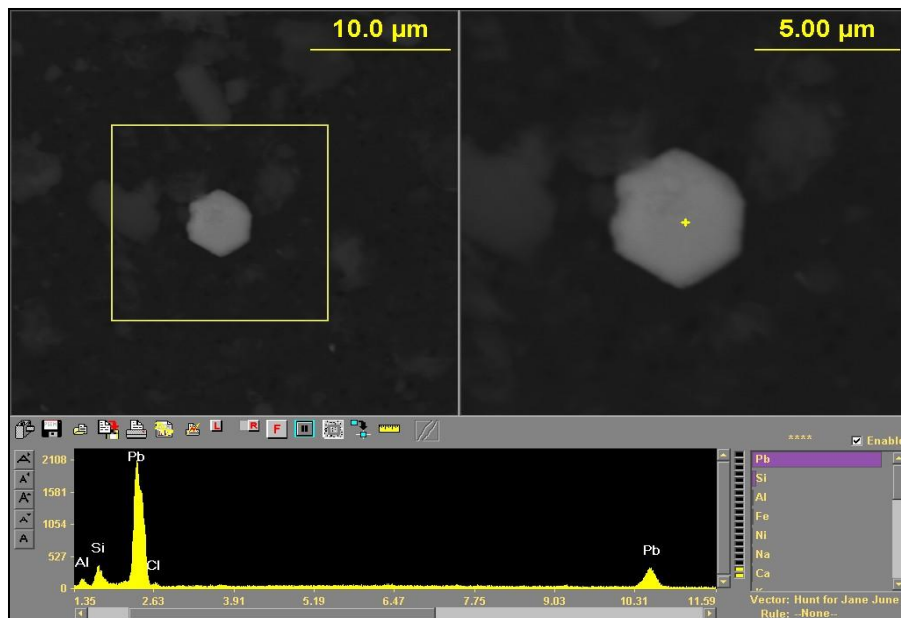


Figure D.22 SEM image shows hexagonal Pb particle determined in plot 3A quadrant c.

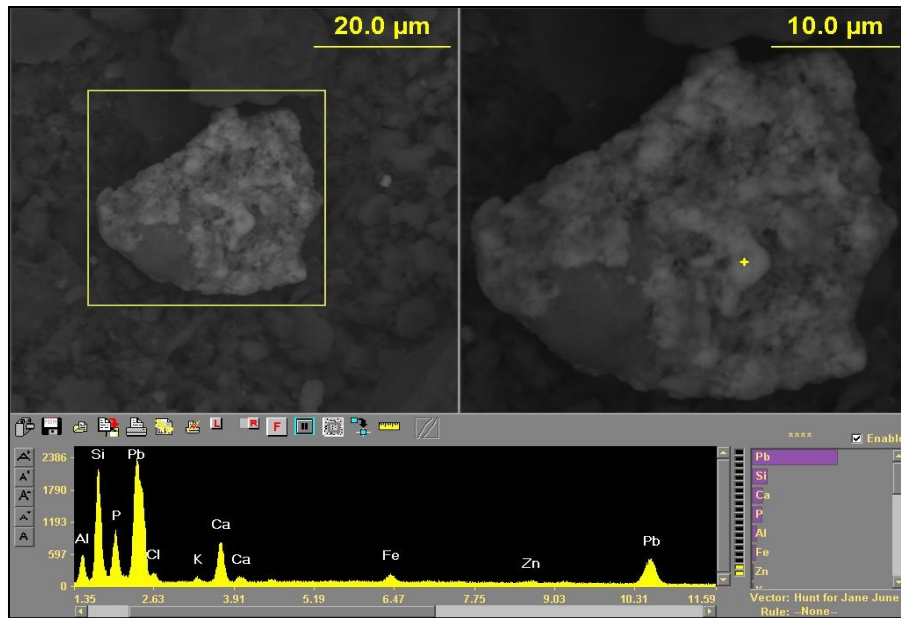


Figure D.23 SEM image shows PbP with Fe on Al Si Ca particle determined in plot 3A quadrant d.

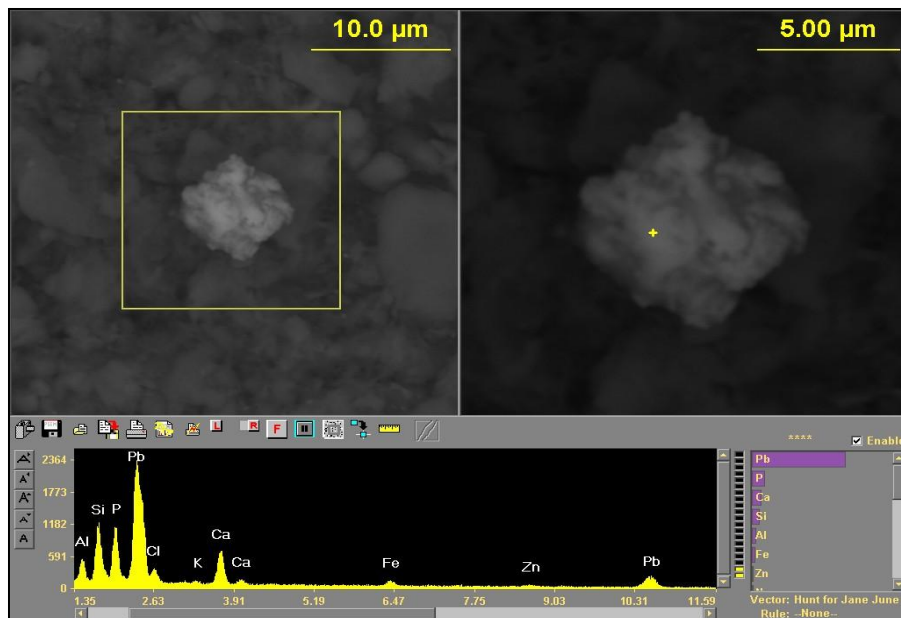


Figure D.24 SEM image shows PbP with Fe on Al Si Ca particle determined in plot 3A quadrant d.

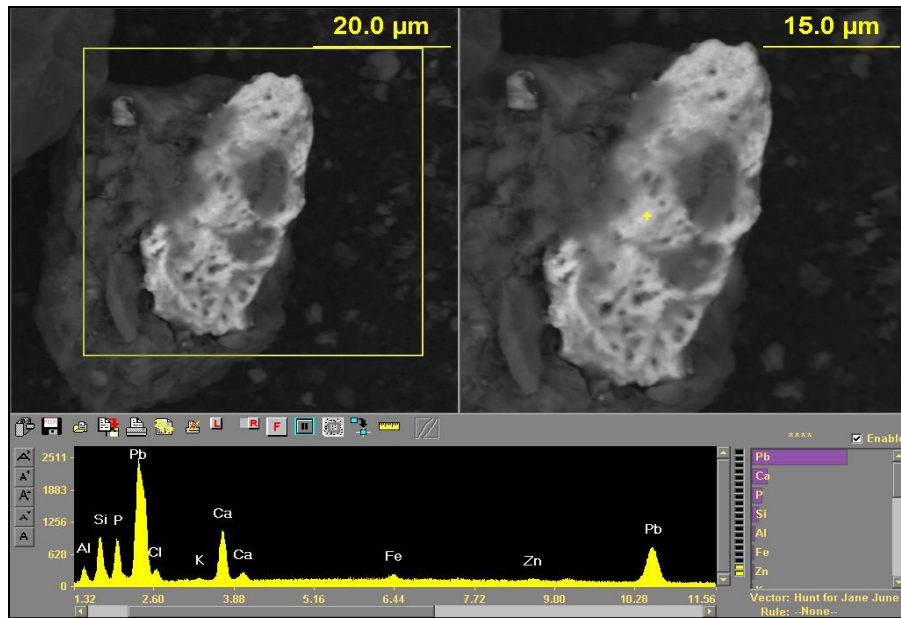


Figure D.25 SEM image shows PbP with Fe on Al Si Ca particle determined in plot 4A quadrant a.

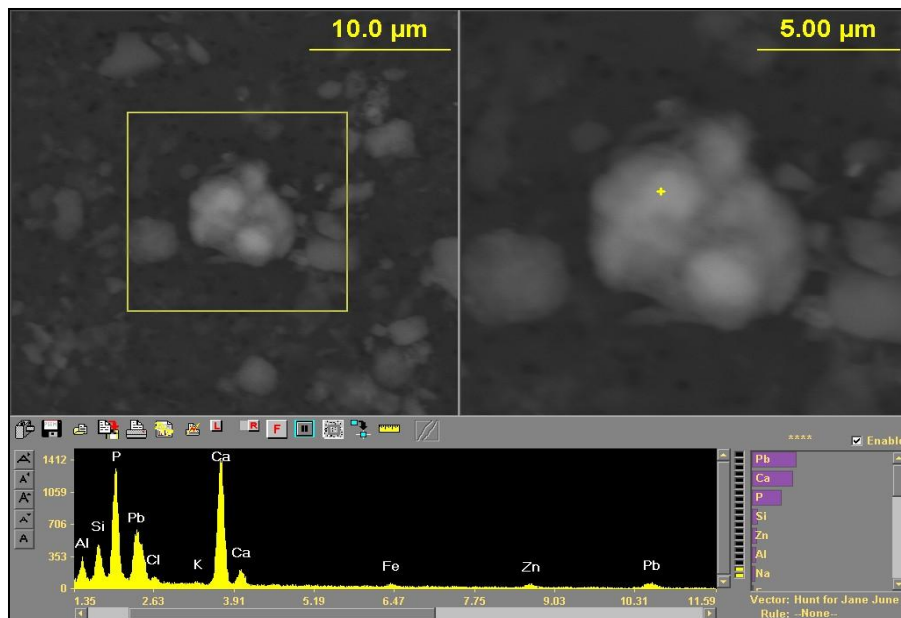
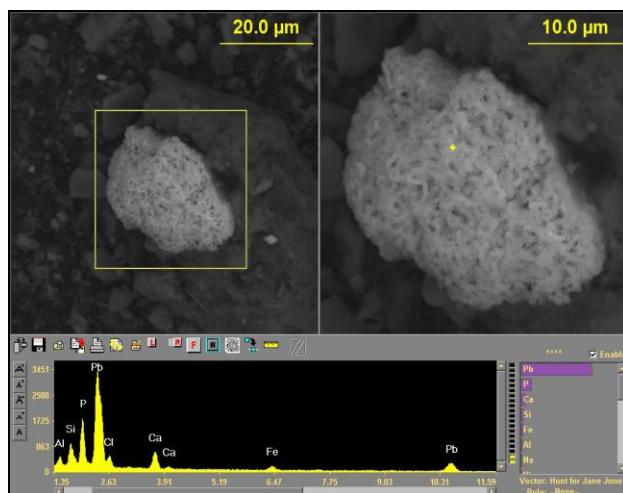
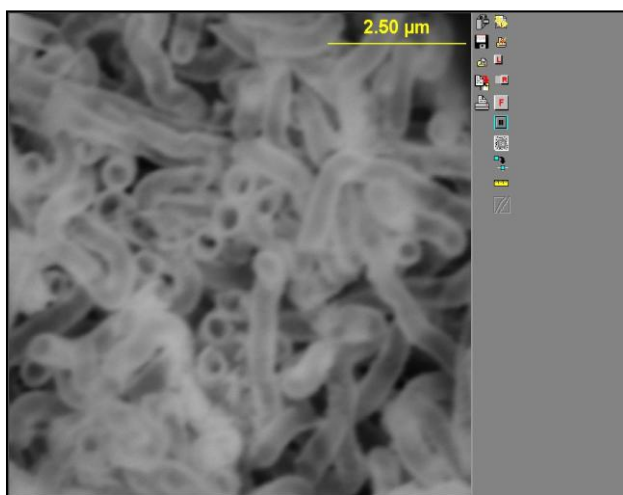


Figure D.26 SEM image shows Pb with CaP with Fe Zn Al Si particle determined in plot 4A quadrant a.

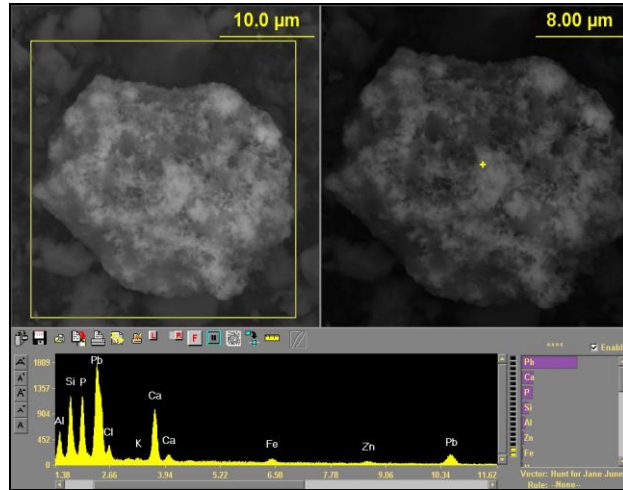


(a)

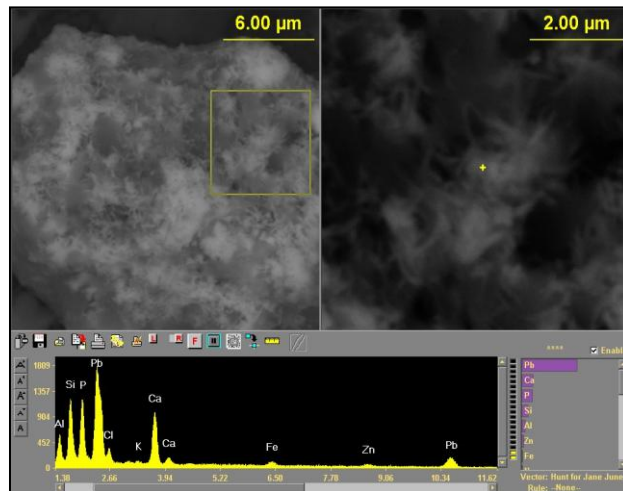


(b)

Figure D.27 (a) SEM image shows tube-like shape of PbP with Fe on Al Si Ca particle determined in plot 4A quadrant b (b) SEM image shows high magnification of tube like shape of PbP with Fe on Al Si Ca particle determined in plot 4A quadrant b.



(a)



(b)

Figure D.28 (a) SEM image shows acicular shape of PbP with Fe on Al Si Ca particle determined in plot 4A quadrant b (b) SEM image shows high magnification of tube like shape of PbP with Fe on Al Si Ca particle determined in plot 4A quadrant b.

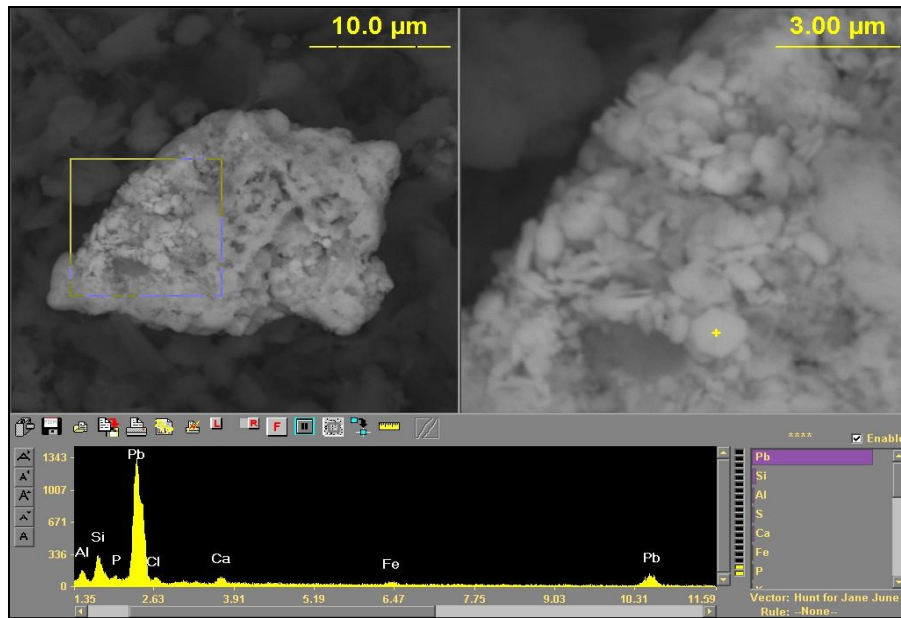


Figure D.29 SEM image shows hexagonal Pb particle determined in plot 4A quadrant c.

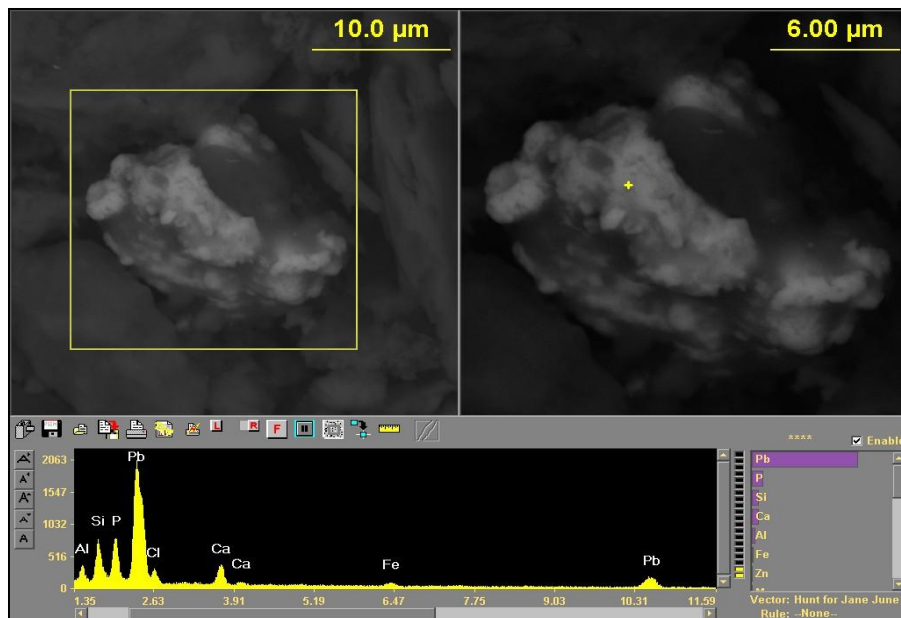
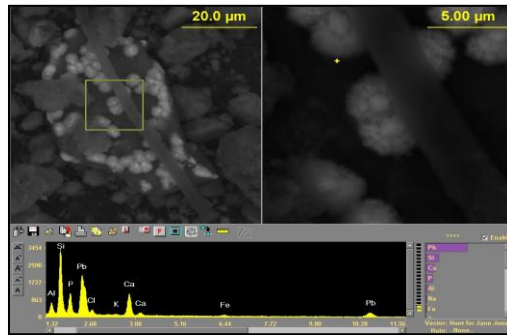
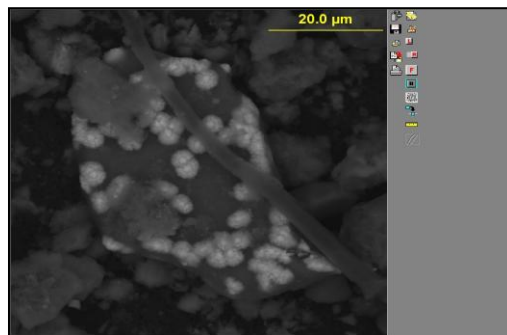


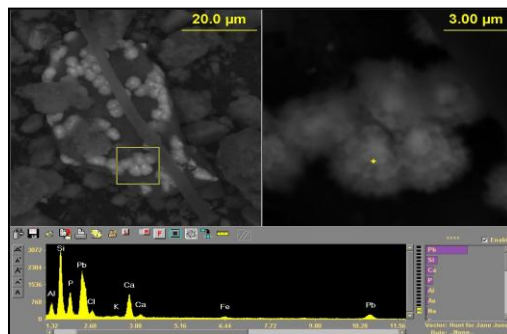
Figure D.30 SEM image shows PbP with Fe on Al Si Ca particle determined in plot 4A quadrant c.



(a)



(b)



(c)

Figure D.31 (a) SEM image shows rounded PbP with Fe on Al Si Ca particle determined in plot 4A quadrant d (b) SEM image shows rounded PbP with Fe on Al Si Ca particle determined in plot 4A quadrant d (c) SEM image shows rounded PbP with Fe on Al Si Ca particle determined in plot 4A quadrant d.

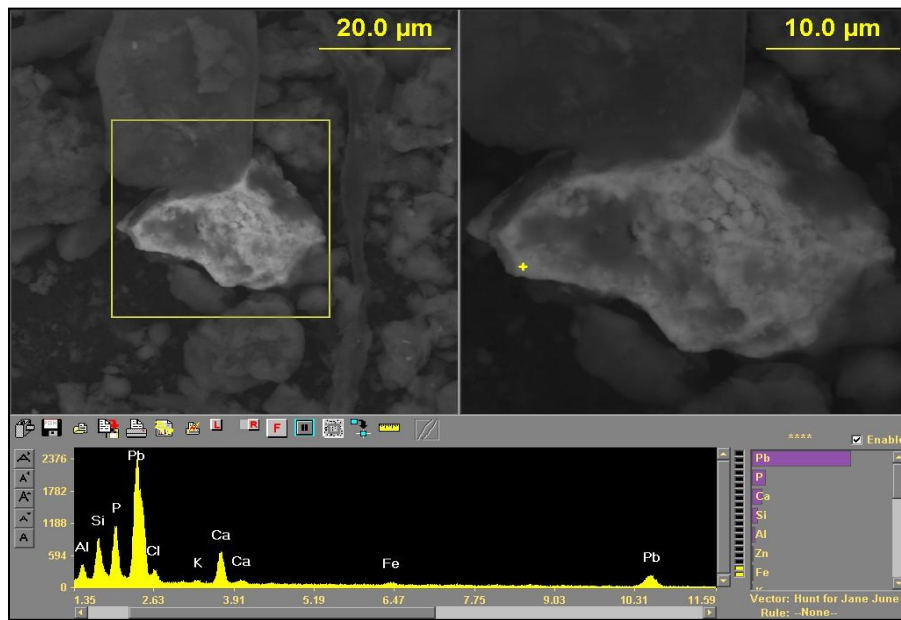


Figure D.32 SEM image shows PbP with Fe on Al Si Ca particle determined in plot 4A quadrant d.

Appendix E

SEM Images and X-Ray Spectra of Twelve Months Post Treatment 1818

Dumaine St. Samples

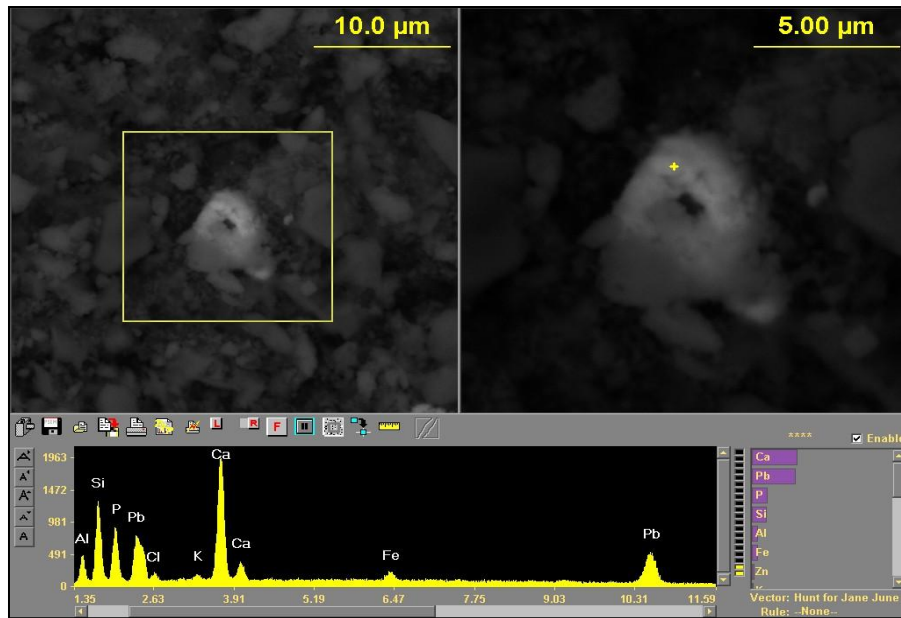


Figure E.1 SEM image shows Pb on CaP with Fe Zn Al Si K particle determined in plot 1A quadrant a.

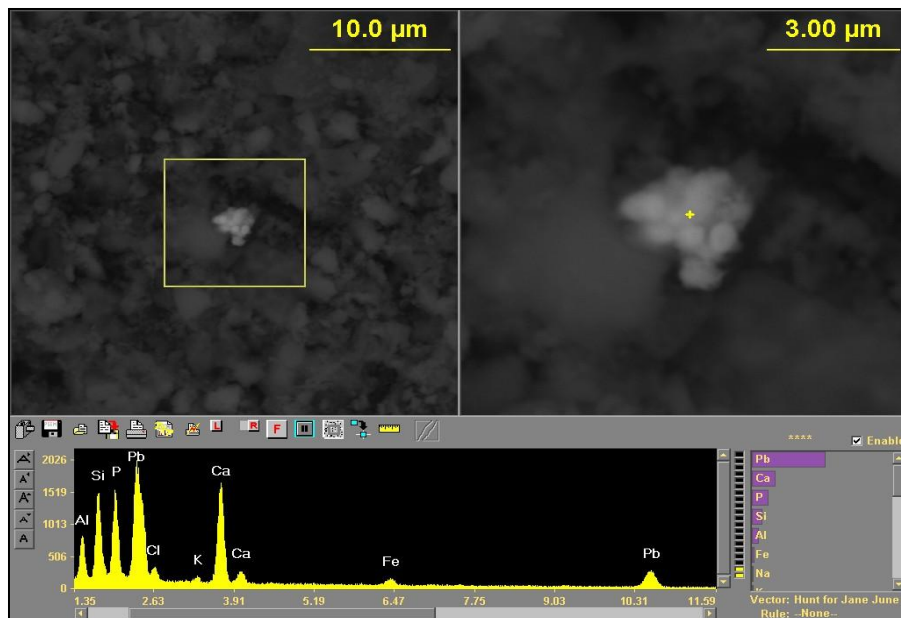


Figure E.2 SEM image shows Pb on CaP with Fe Zn Al Si K particle determined in plot 1A quadrant a.

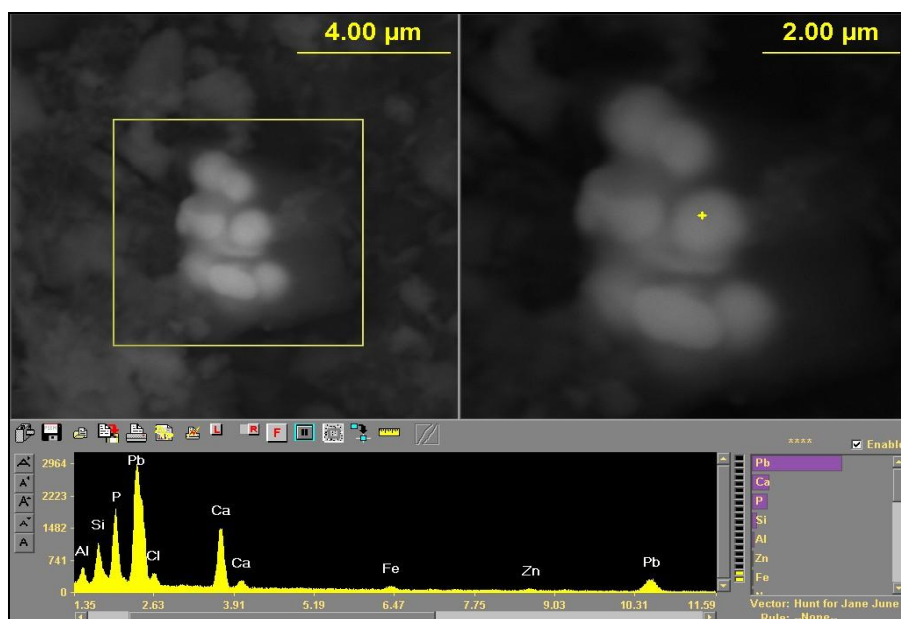


Figure E.3 SEM image shows PbP with Fe Zn on Ca Al Si particle determined in plot 1A quadrant b.

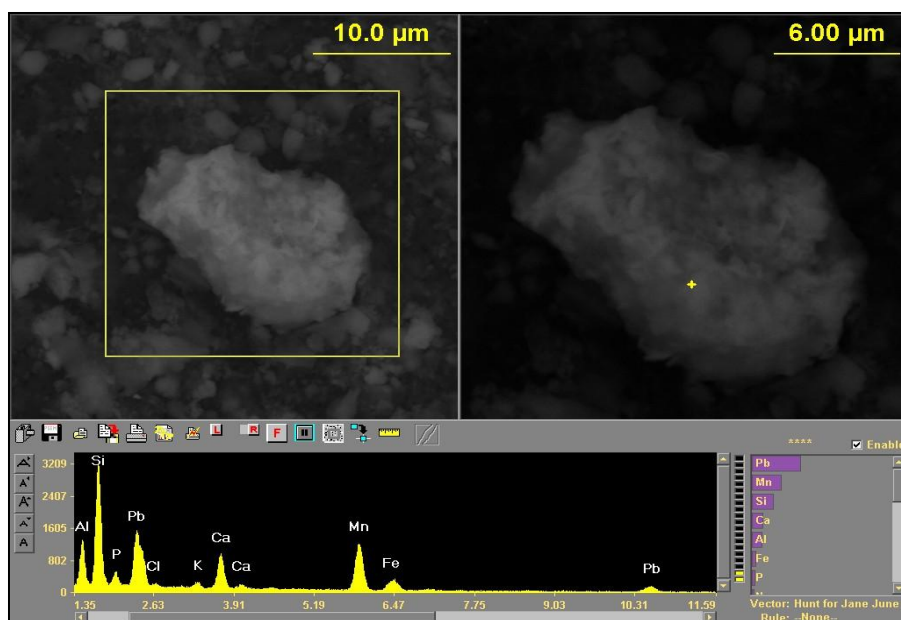


Figure E.4 SEM image shows PbP with Mn Fe on Ca Al Si particle determined in plot 1A quadrant b.

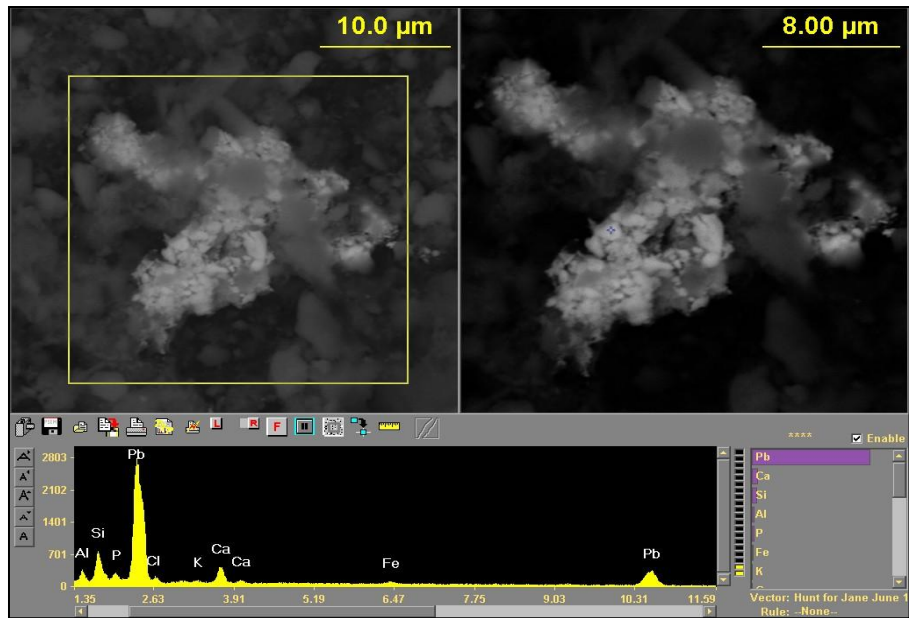


Figure E.5 SEM image shows Pb with Fe on Ca Al Si particle determined in plot

1A quadrant c.

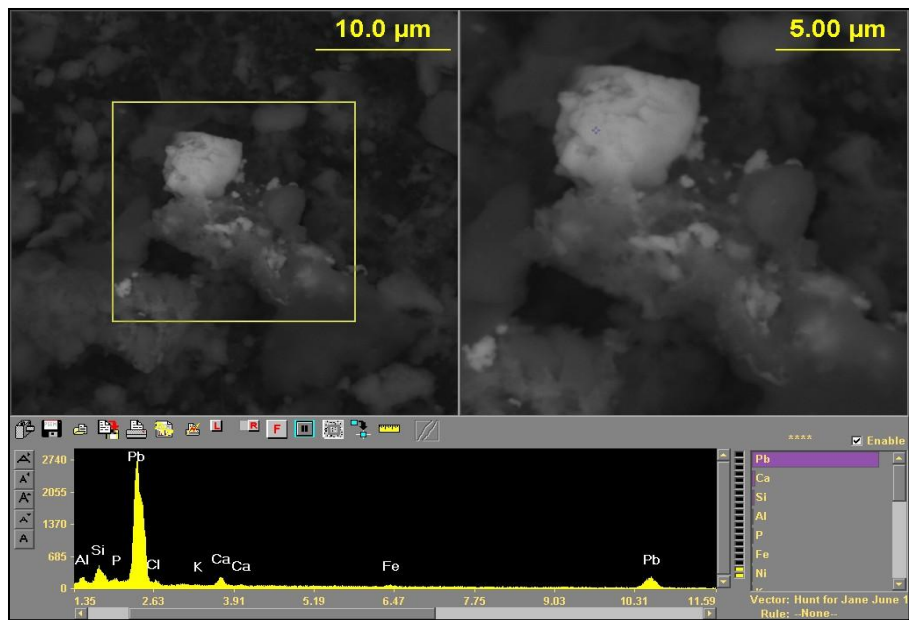


Figure E.6 SEM image shows Pb with Fe on Ca Al Si particle determined in plot

1A quadrant c.

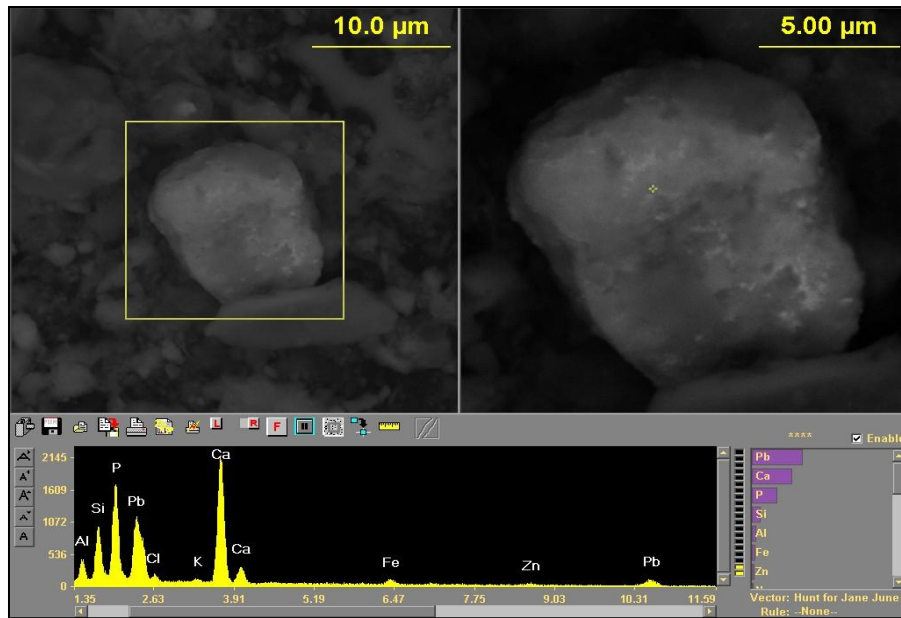


Figure E.7 SEM image shows Pb with CaP and Fe Al Si particle determined in plot 1A quadrant d.

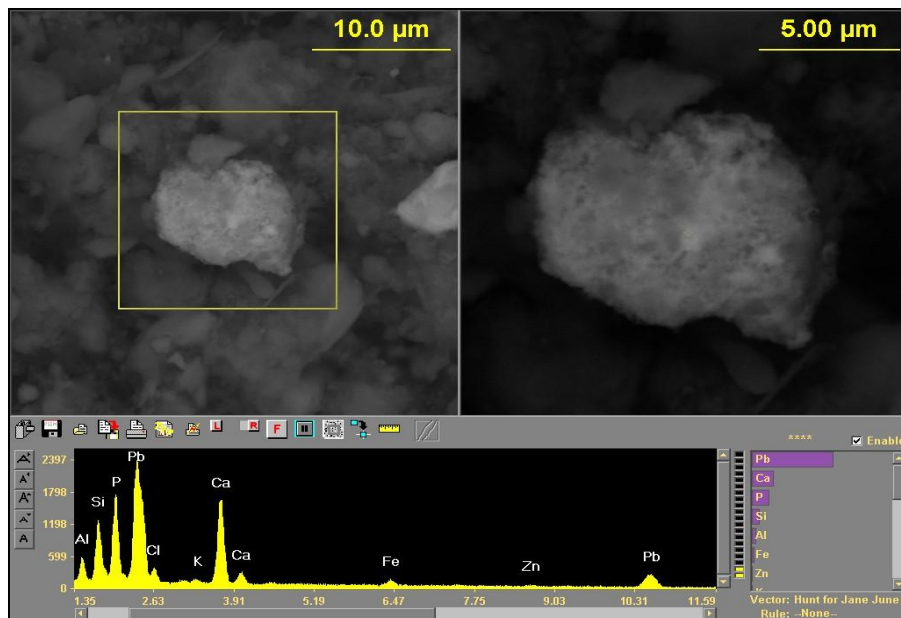


Figure E.8 SEM image shows Pb with CaP and Fe Al Si particle determined in plot 1A quadrant d.

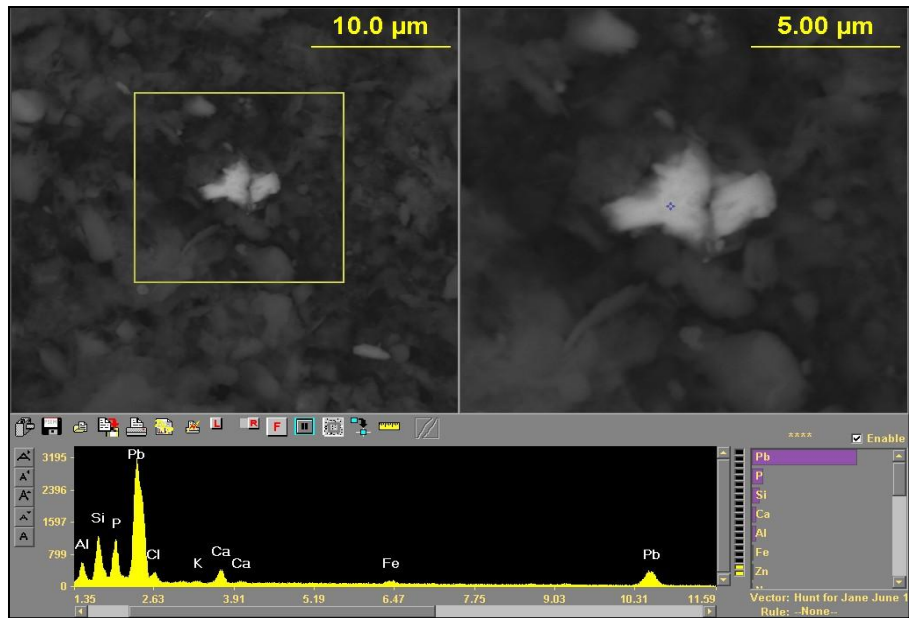


Figure E.9 SEM image shows PbP with Fe on Ca Al Si particle determined in plot 2A quadrant a.

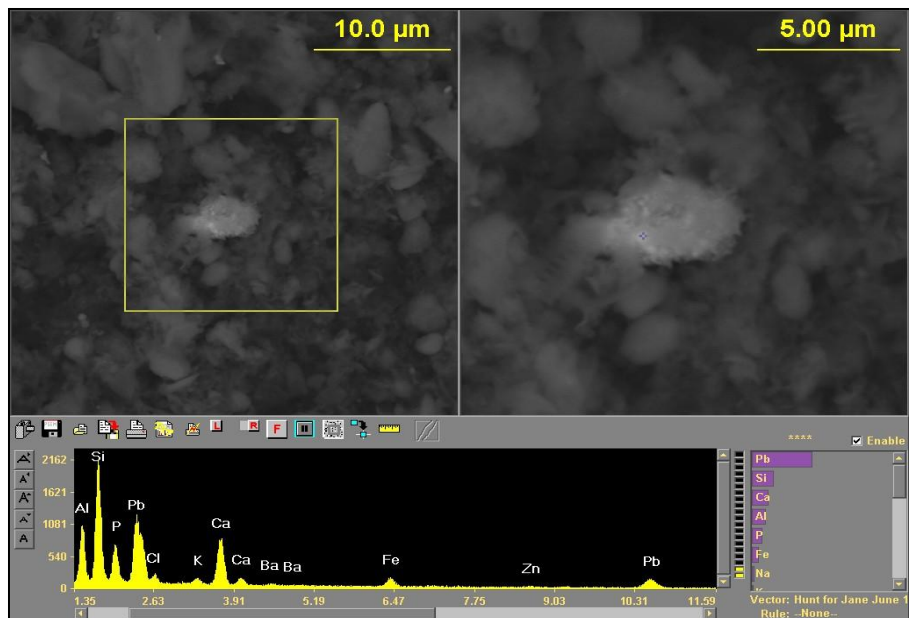


Figure E.10 SEM image shows PbP with Fe on Ca Al Si particle determined in plot 2A quadrant a.

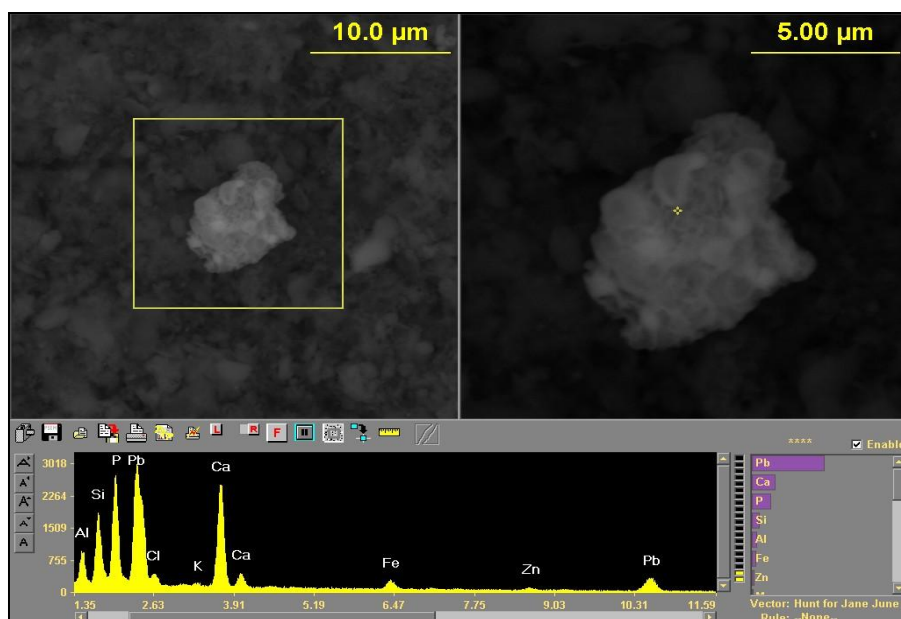


Figure E.11 SEM image shows Pb on CaP with Fe Zn Al Si particle determined in plot 2A quadrant b.

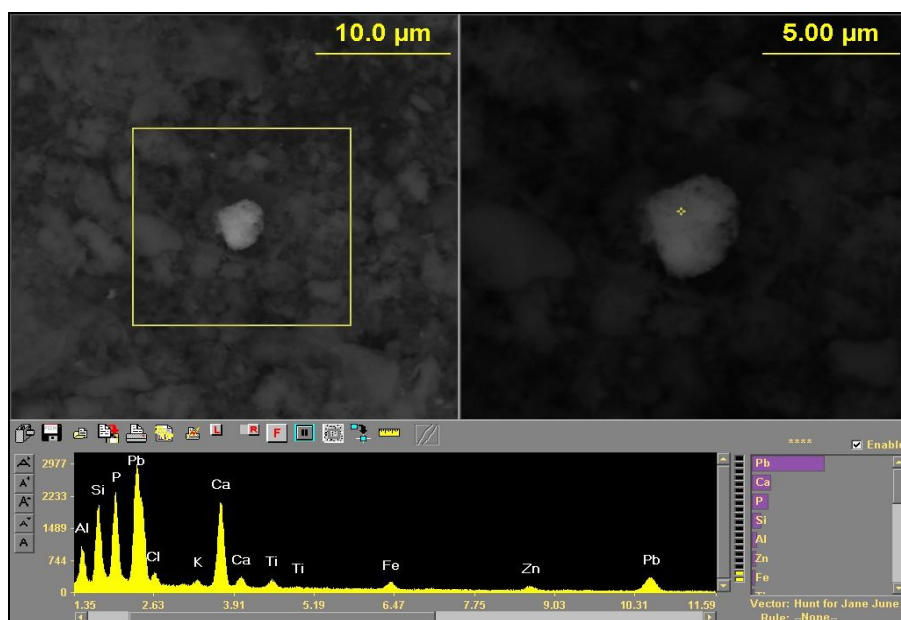


Figure E.12 SEM image shows Pb on CaP with Fe Zn Al Si particle determined in plot 2A quadrant b.

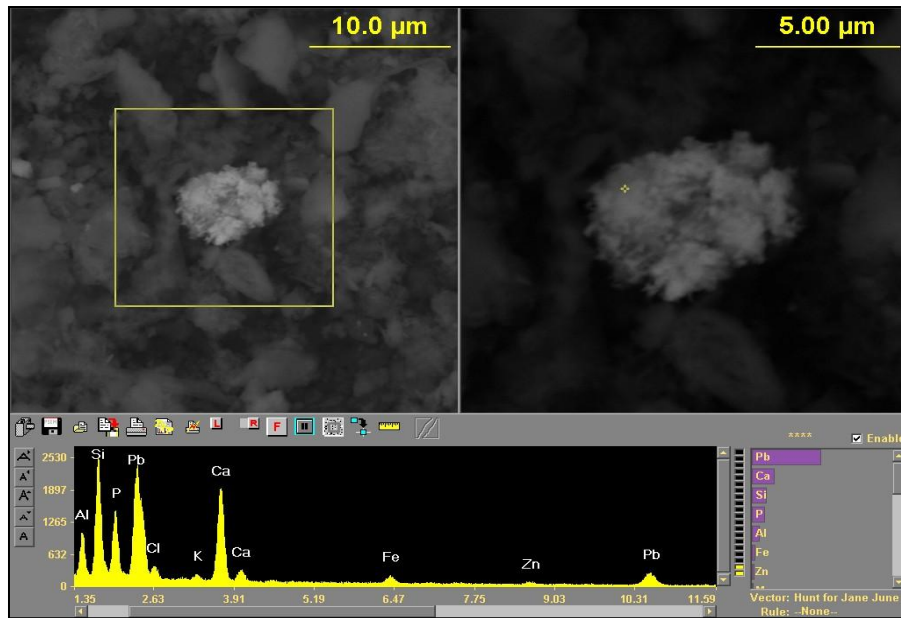


Figure E.13 SEM image shows Pb on CaP with Fe Zn Al Si particle determined in plot 2A quadrant c.

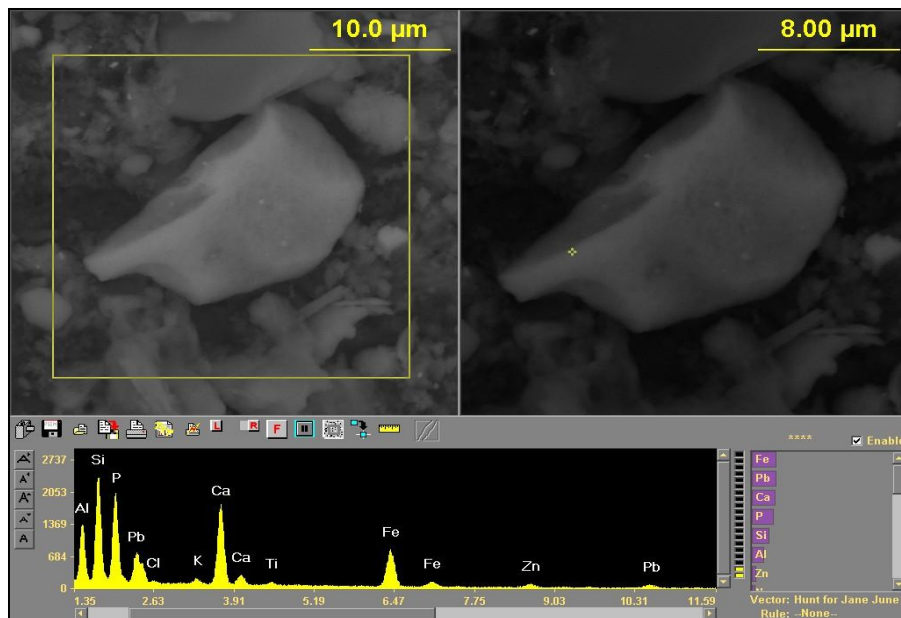


Figure E.14 SEM image shows Pb on CaP with Fe Zn Al Si particle determined in plot 2A quadrant c.

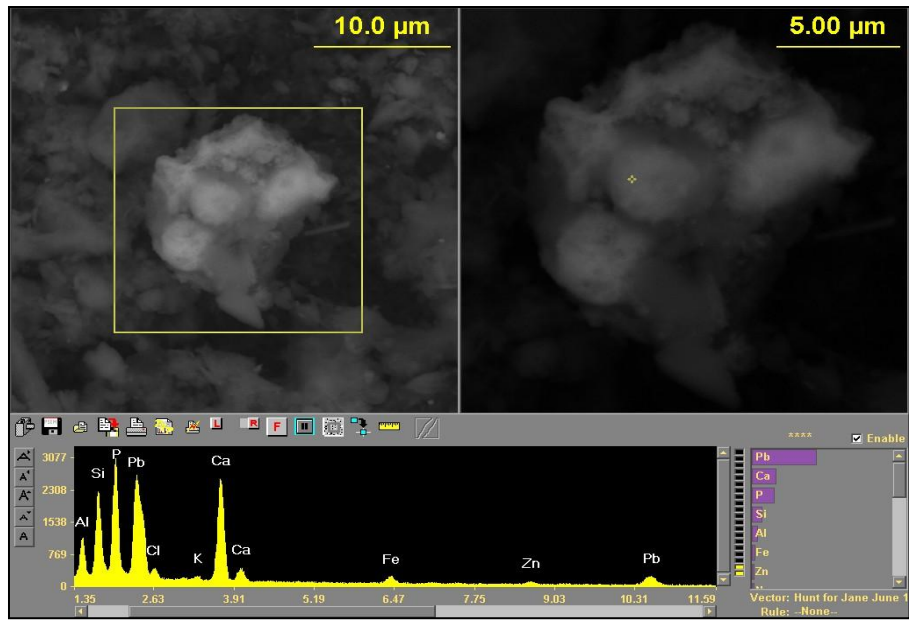


Figure E.15 SEM image shows Pb on CaP with Fe Zn Al Si particle determined in plot 2A quadrant d.

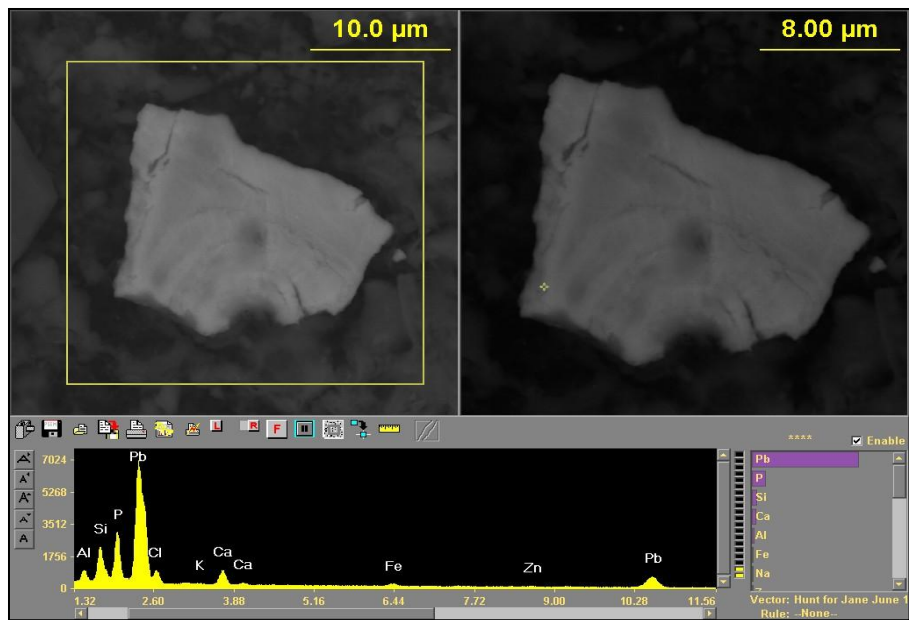
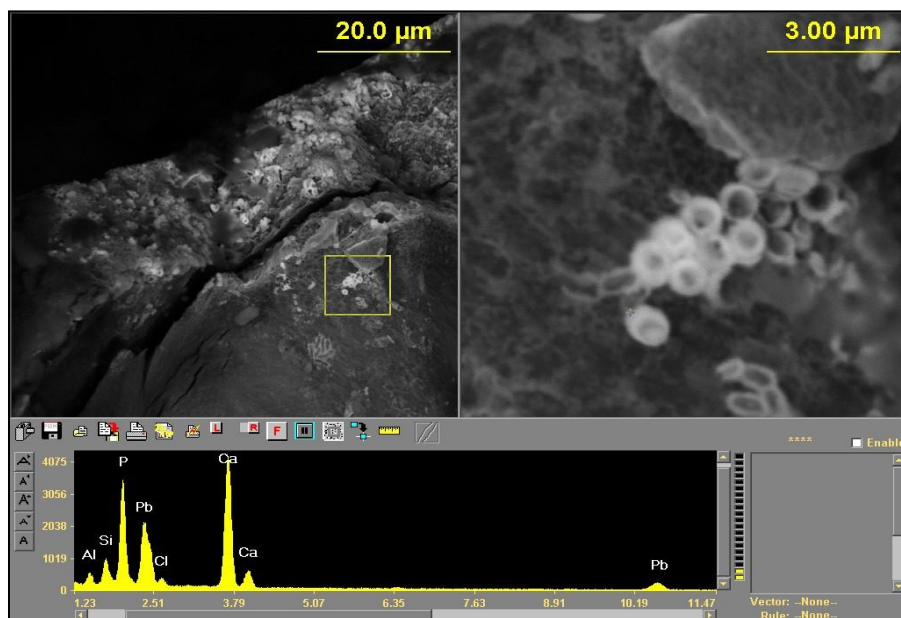
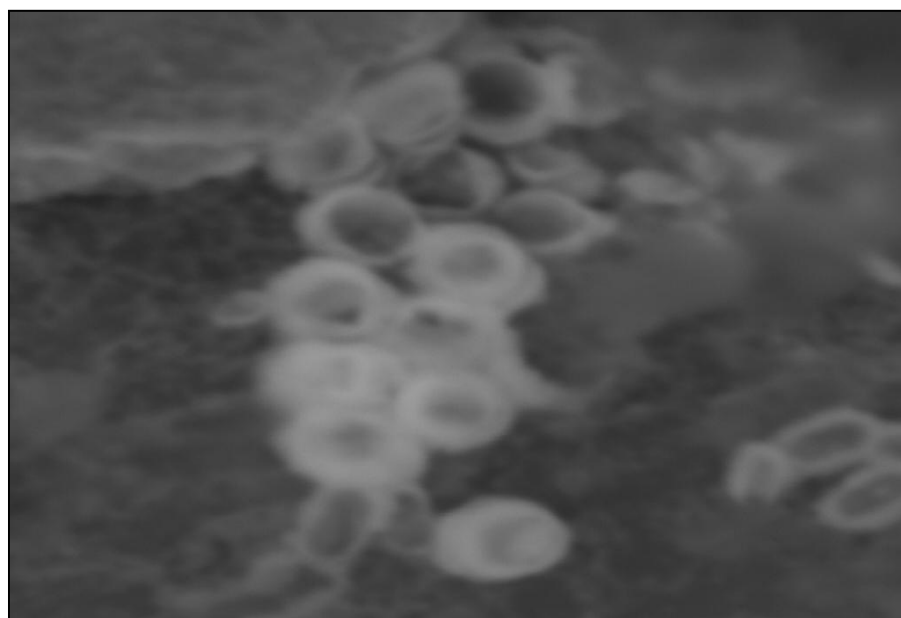


Figure E.16 SEM image shows Pb on CaP with Fe Zn Al Si particle determined in plot 2A quadrant d.

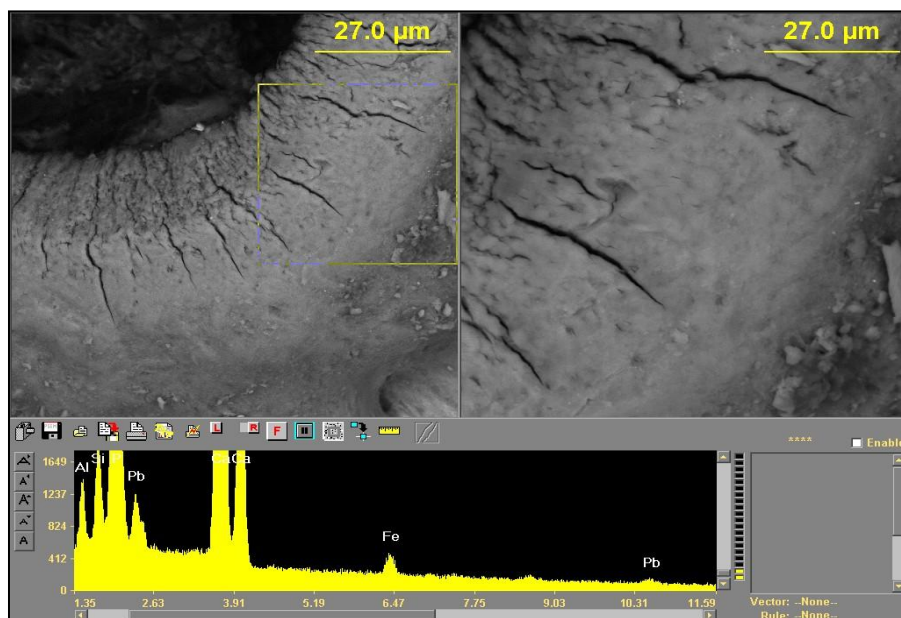


(a)

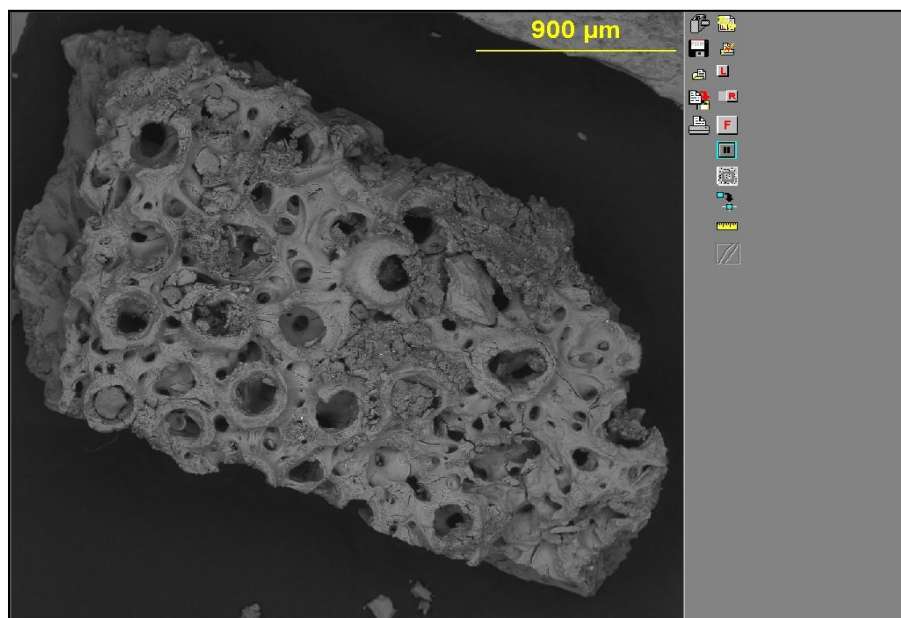


(b)

Figure E.17 (a) SEM image shows Pb sorbed on fish bone determined in plot 3A quadrant a (b) SEM image shows Pb sorbed on fish bone determined in plot 3A quadrant a.



(a)



(b)

Figure E.18 (a) SEM image shows Pb sorbed on fish bone determined in plot 3A quadrant b (b) SEM image shows Pb sorbed on fish bone determined in plot 3A quadrant b.

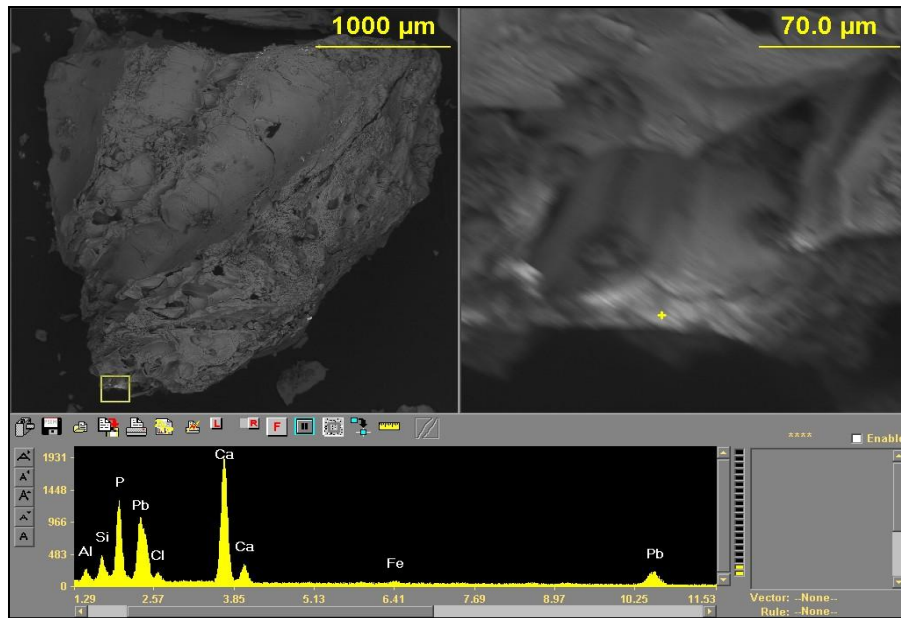


Figure E.19 SEM image shows Pb sorbed on fish bone determined in plot 3A quadrant c.

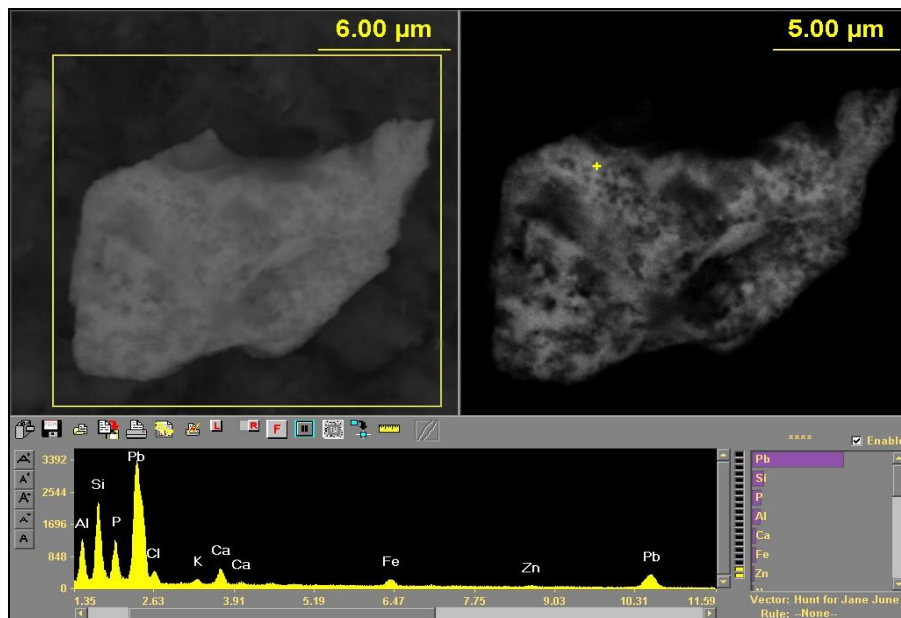


Figure E.20 SEM image shows PbP with Fe Zn in Si Al Ca K particle determined in plot 4A quadrant a.

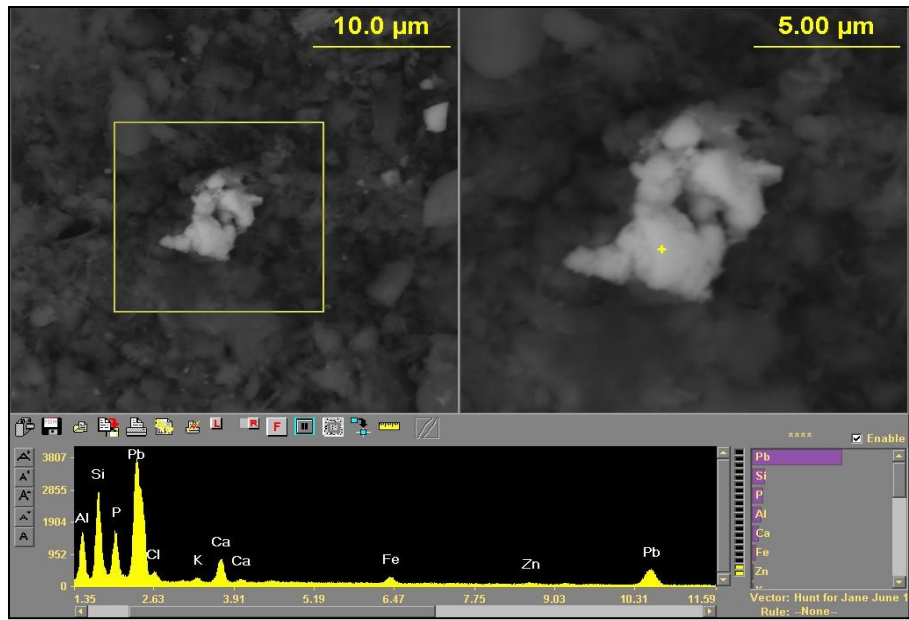


Figure E.21 SEM image shows PbP with Fe Zn in Si Al Ca K particle determined in plot 4A quadrant a.

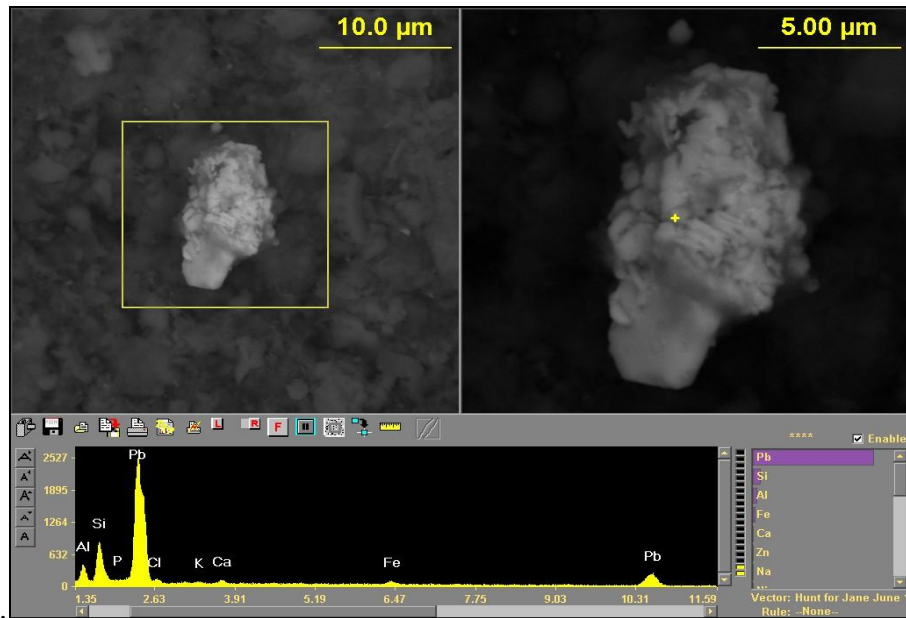


Figure E.22 SEM image shows Pb particle with Fe Si Al Ca K determined in plot 4A quadrant b.

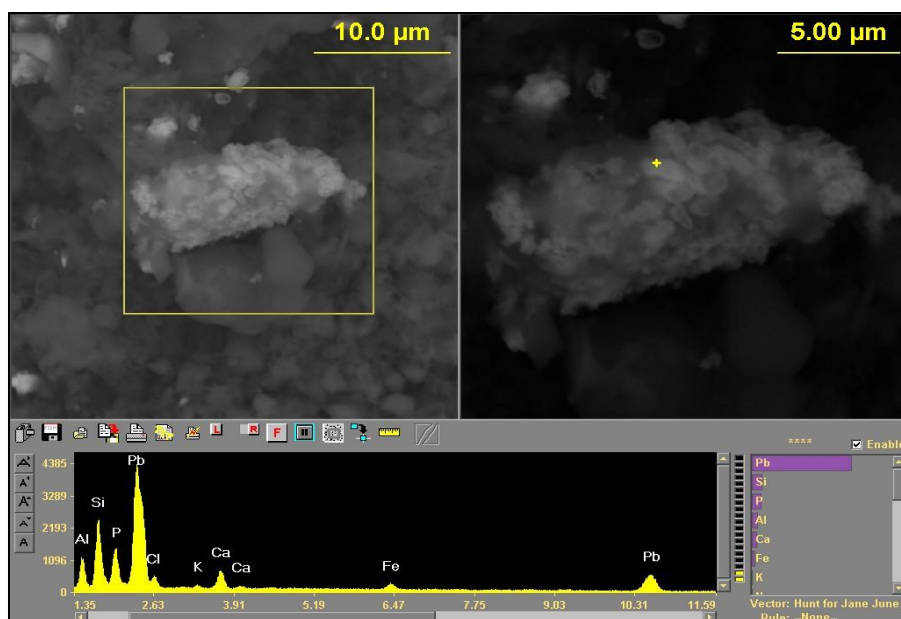


Figure E.23 SEM image shows PbP with Fe in Si Al Ca K particle determined in plot 4A quadrant b.

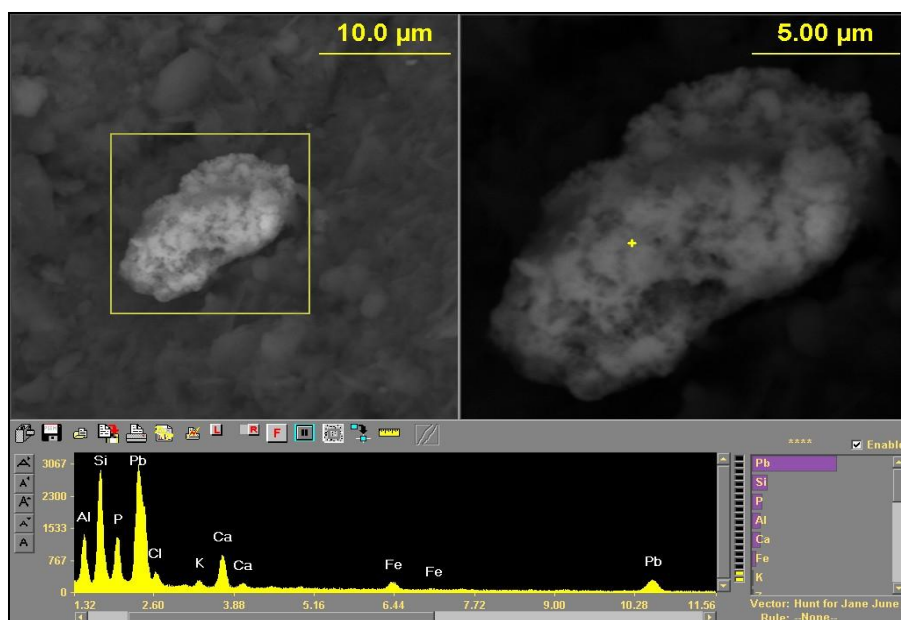


Figure E.24 SEM image shows PbP with Fe in Si Al Ca K particle determined in plot 4A quadrant c.

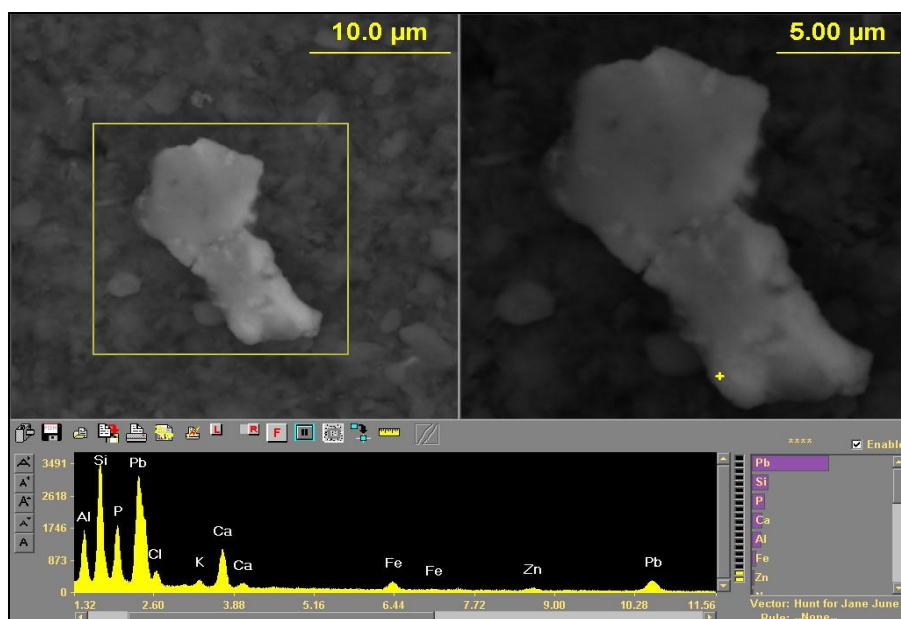


Figure E.25 SEM image shows PbP with Fe in Si Al Ca K particle determined in plot 4A quadrant c.

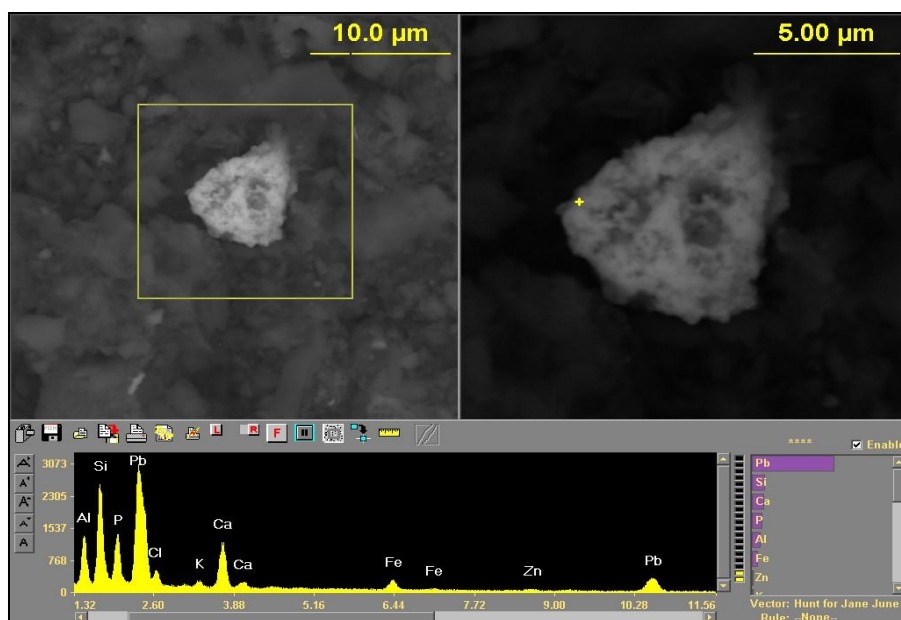


Figure E.26 SEM image shows PbP with Fe Zn in Si Al Ca K particle determined in plot 4A quadrant d.

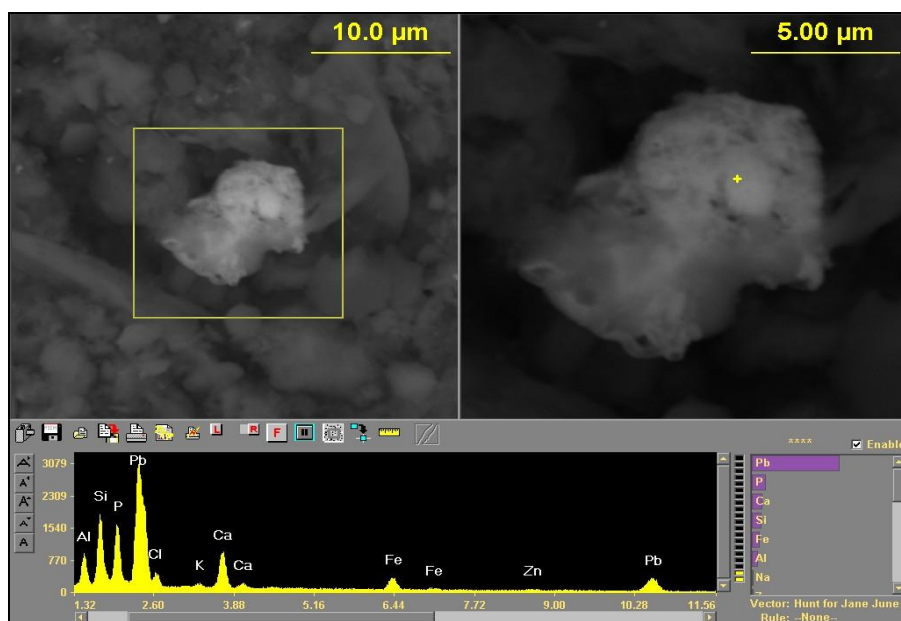


Figure E.27 SEM image shows PbP with Fe Zn in Si Al Ca K particle determined in plot 4A quadrant d.

Appendix F

SEM Images and X-Ray Spectra of Zero Months 2224 N.Prieur St. Samples

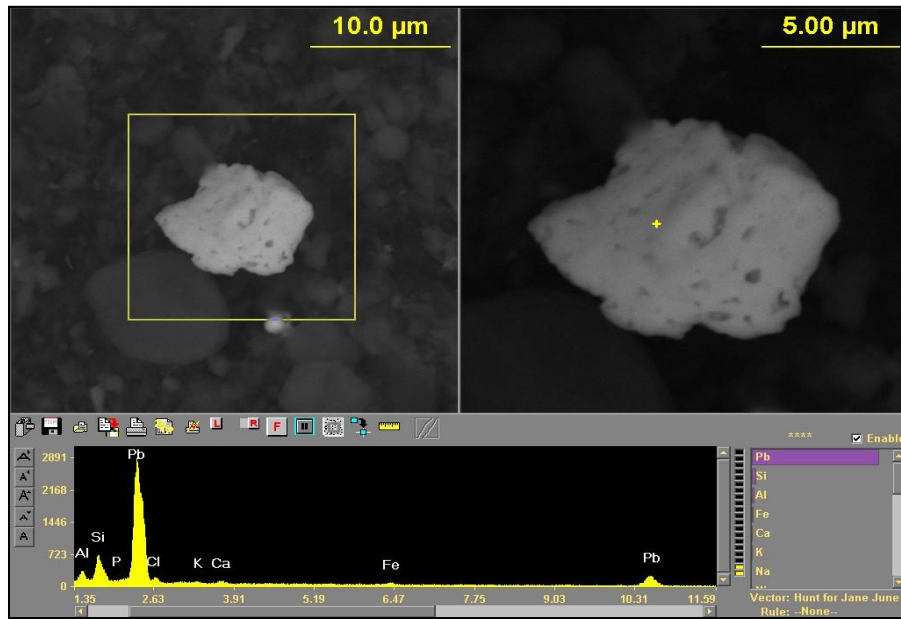


Figure F.1 SEM image shows Pb particle determined in plot 1B quadrant a.

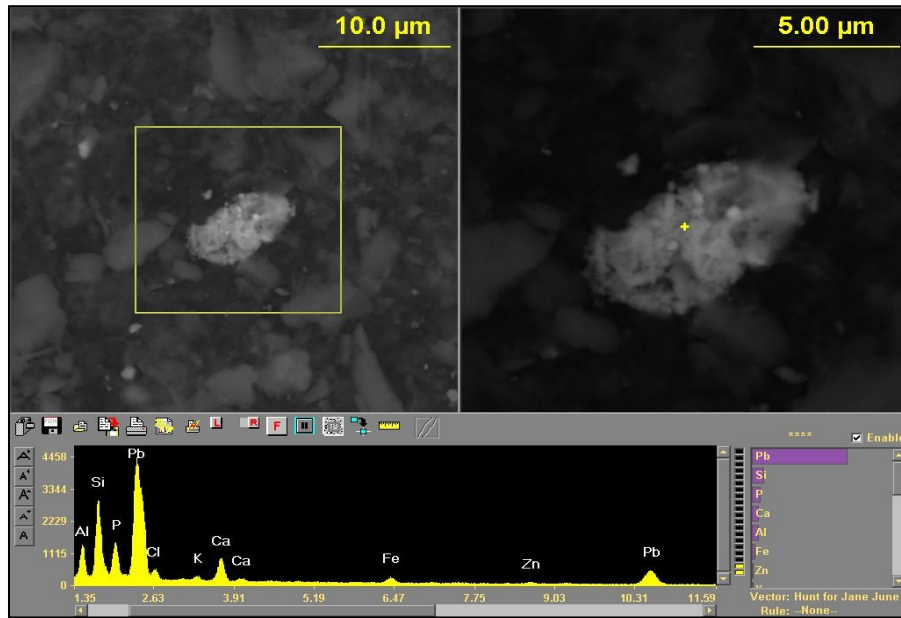


Figure F.2 SEM image shows PbP with Fe Zn in Si Al Ca K particle determined in plot 1B quadrant a.

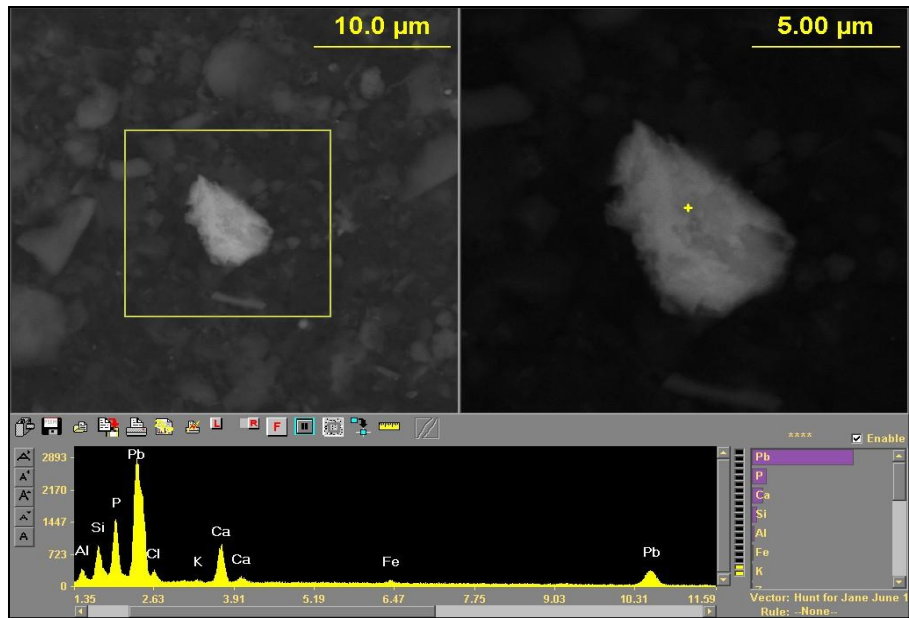


Figure F.3 SEM image shows PbP with Fe Zn in Si Al Ca K particle determined in plot 1B quadrant b.

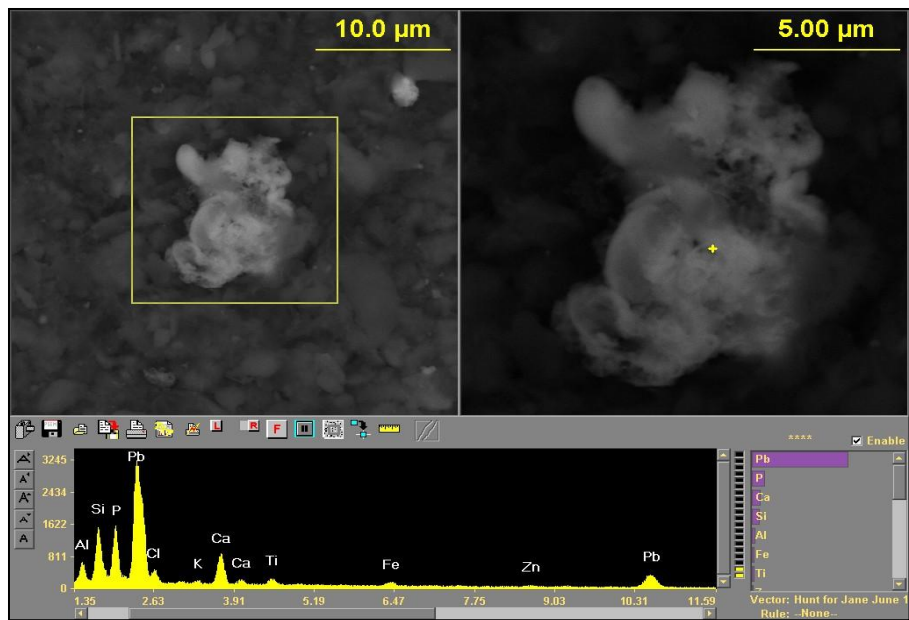


Figure F.4 SEM image shows PbP with Fe Zn in Si Al Ca K particle determined in plot 1B quadrant b.

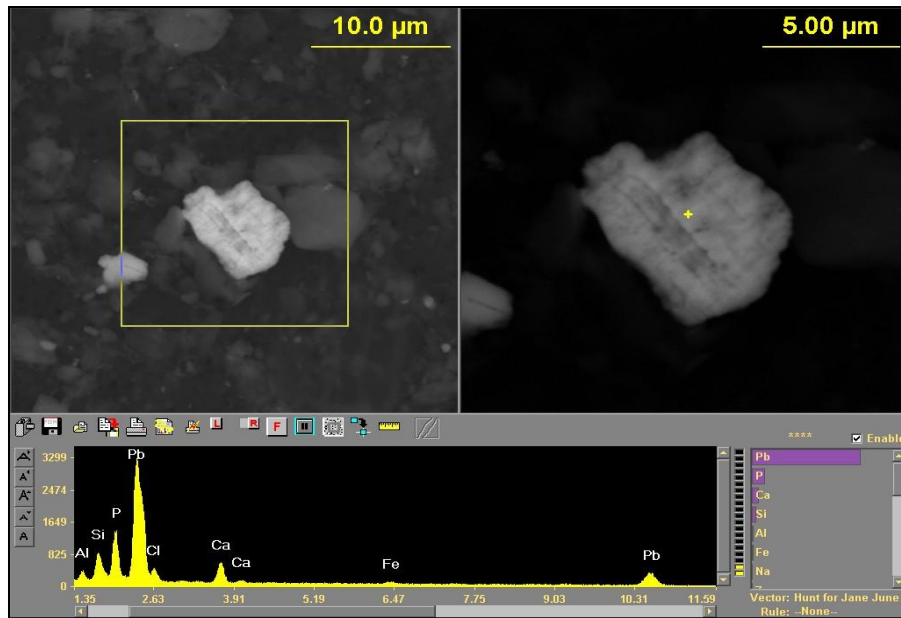


Figure F.5 SEM image shows PbP with Fe Zn in Si Al Ca K particle determined in plot 1B quadrant c.

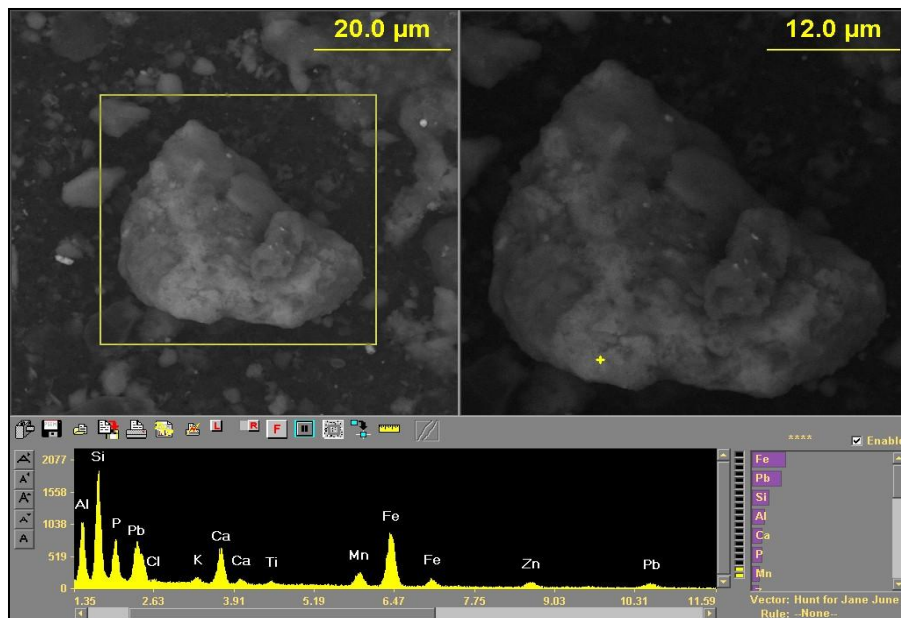


Figure F.6 SEM image shows PbP with Mn Fe Zn in Si Al Ca K particle determined in plot 1B quadrant c.

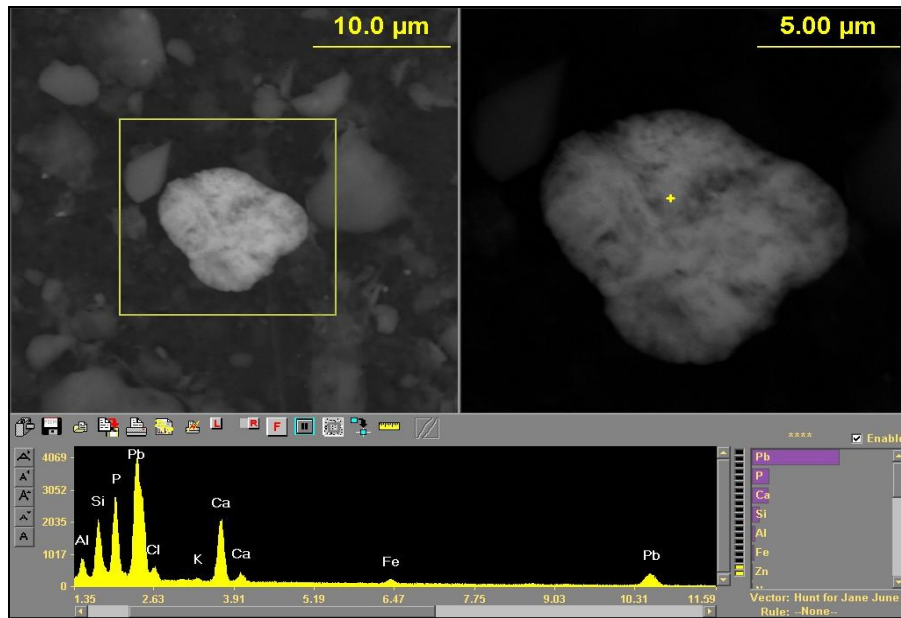


Figure F.7 SEM image shows PbP with Fe in Si Al Ca K particle determined in plot 1B quadrant d.

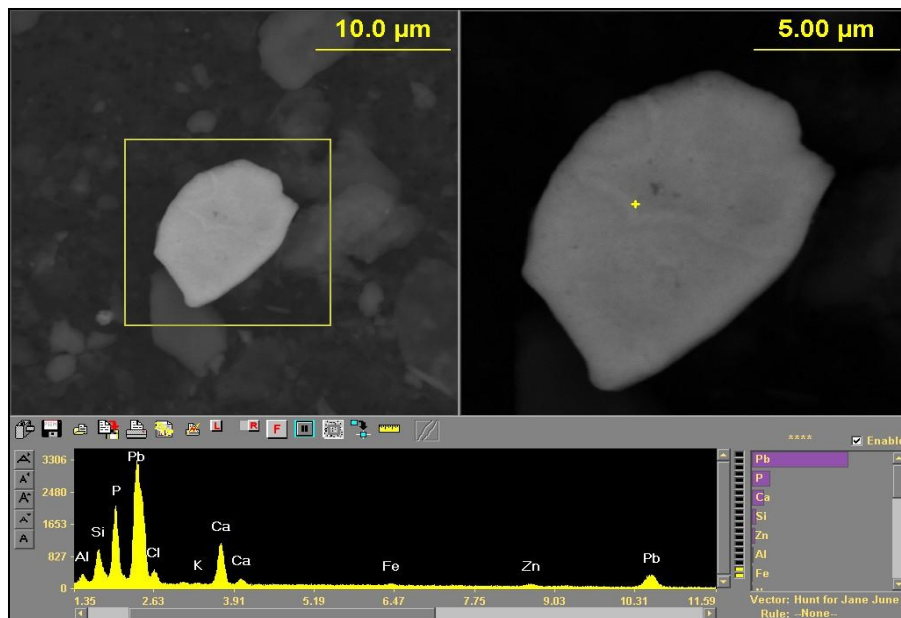


Figure F.8 SEM image shows PbP with Fe in Si Al Ca K particle determined in plot 1B quadrant d.

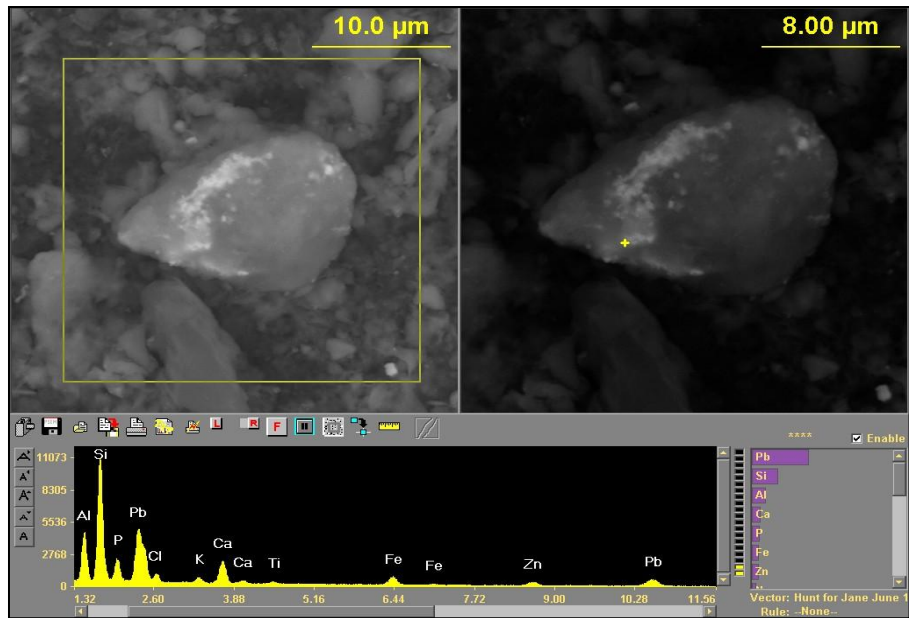


Figure F.9 SEM image shows PbP with Fe Zn in Si Al Ca K particle determined in plot 2B quadrant a.

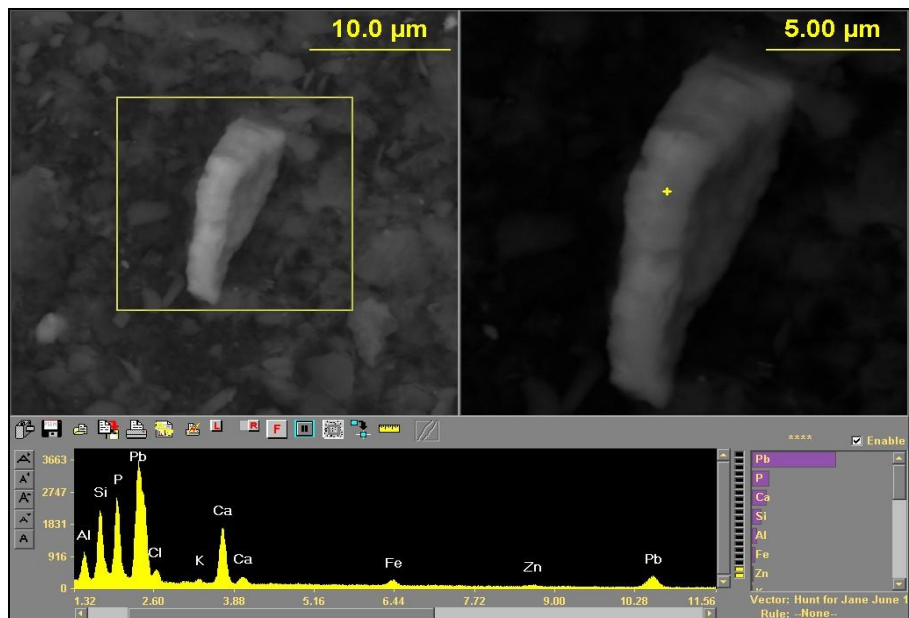


Figure F.10 SEM image shows PbP with Fe Zn in Si Al Ca K particle determined in plot 2B quadrant a.

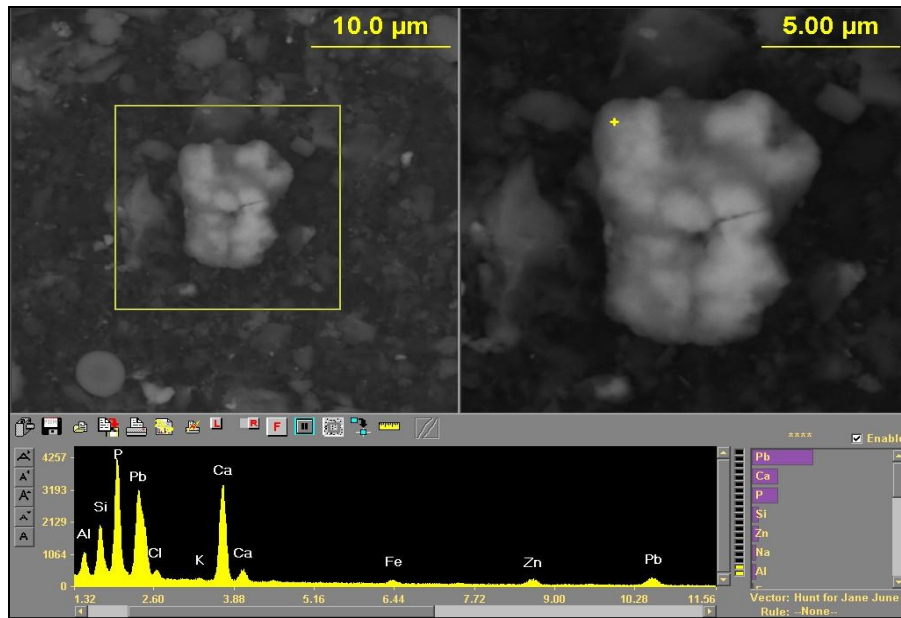


Figure F.11 SEM image shows PbP with Fe Zn in Si Al Ca K particle determined in plot 2B quadrant b.

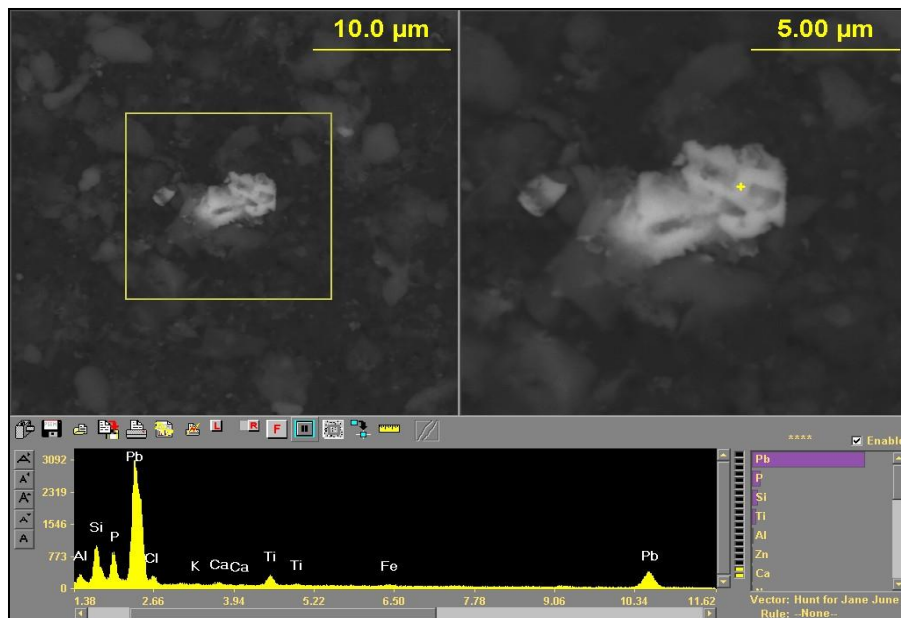


Figure F.12 SEM image shows PbP with Fe Ti in Si Al Ca K particle determined in plot 2B quadrant b.

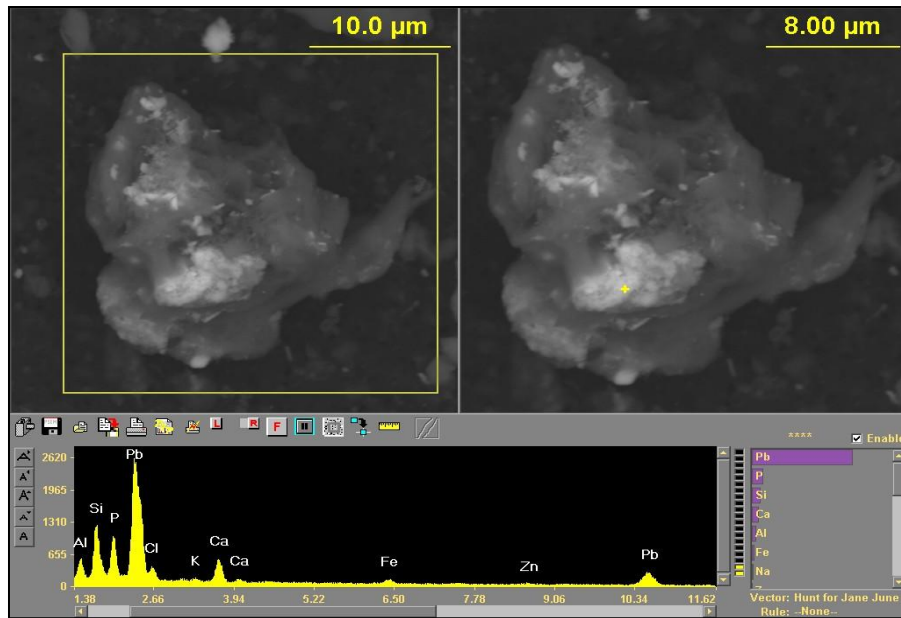


Figure F.13 SEM image shows PbP with Fe in Si Al Ca K particle determined in plot 2B quadrant c.

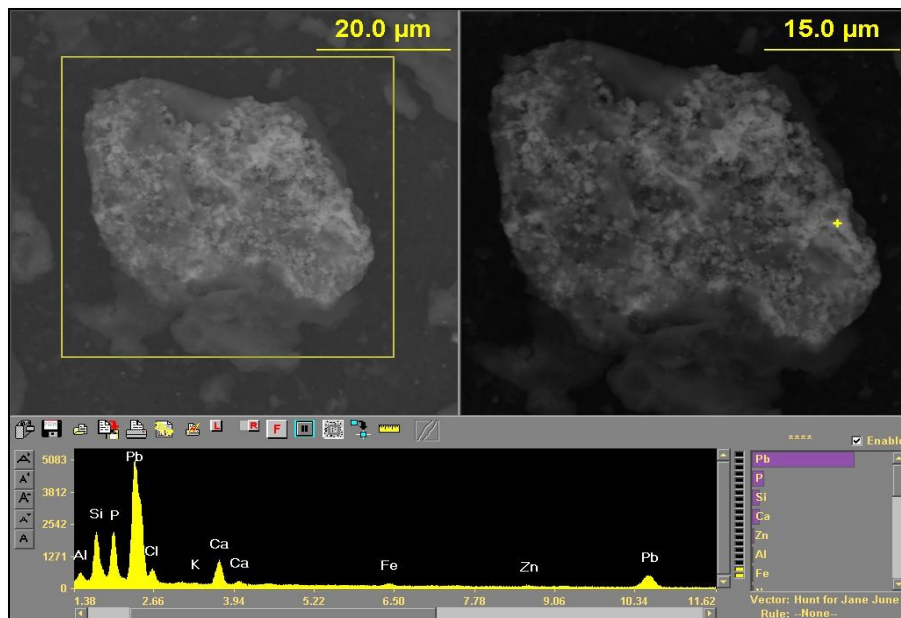


Figure F.14 SEM image shows PbP with Fe in Si Al Ca K particle determined in plot 2B quadrant c.

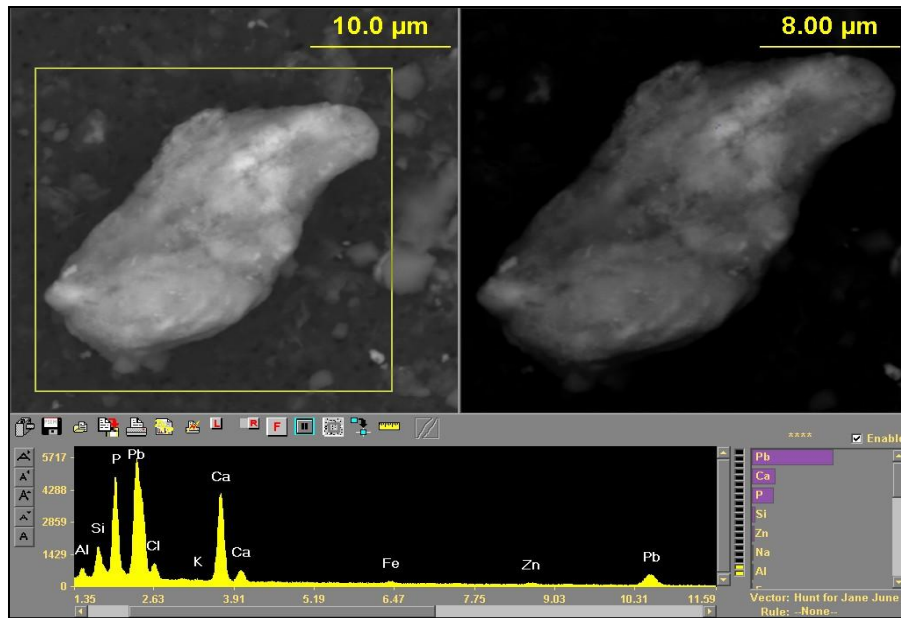


Figure F.15 SEM image shows PbP with Fe Zn in Si Al Ca K particle determined in plot 2B quadrant d.

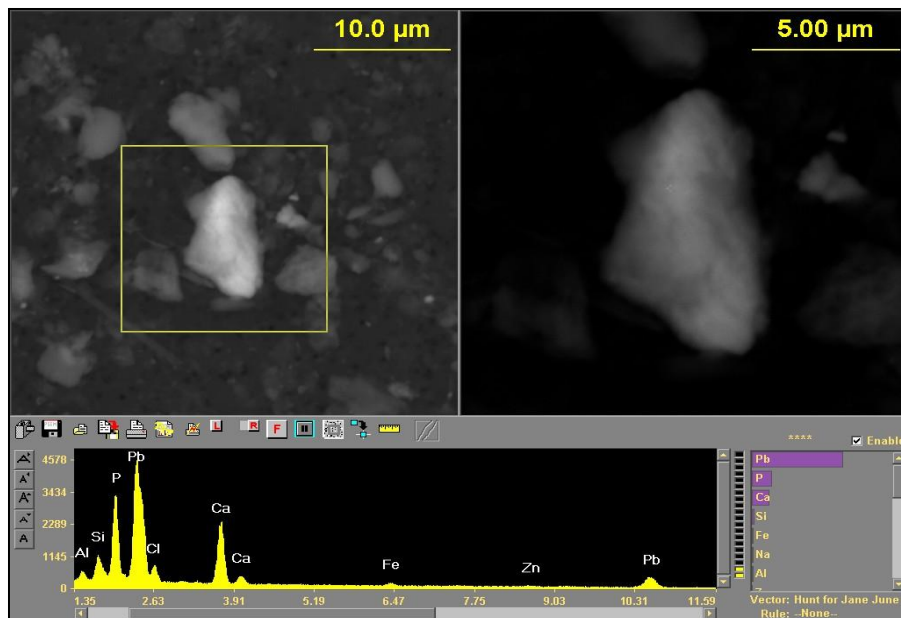


Figure F.16 SEM image shows PbP with Fe in Si Al Ca K particle determined in plot 2B quadrant d.

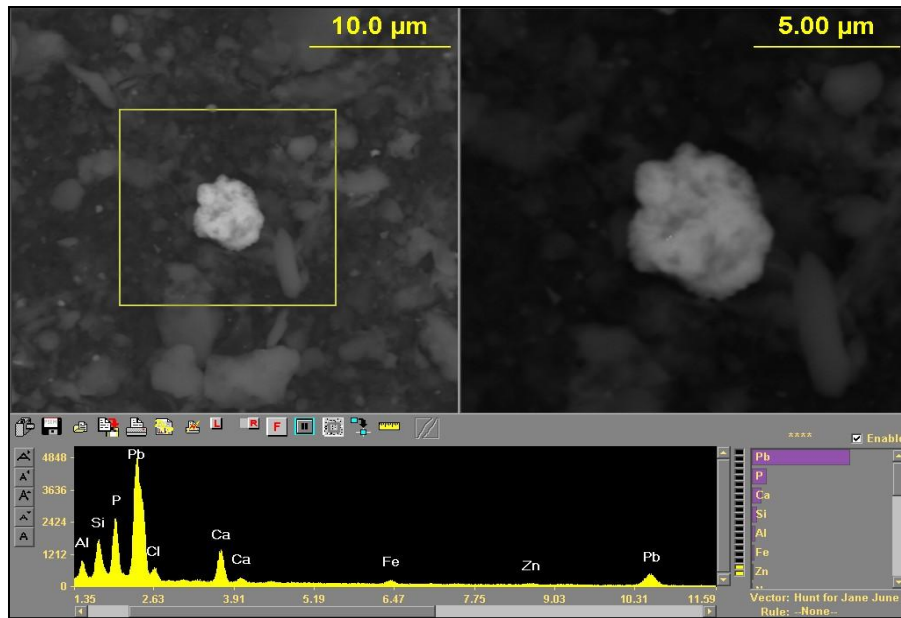


Figure F.17 SEM image shows PbP with Fe Zn in Si Al Ca K particle determined in plot 3B quadrant a.

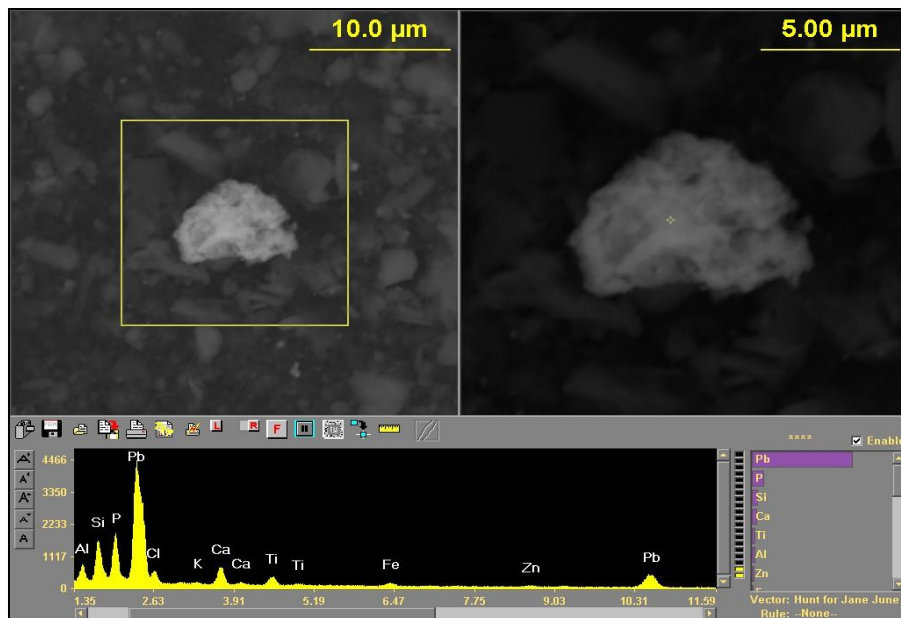


Figure F.18 SEM image shows PbP with Fe Zn Ti in Si Al Ca K particle determined in plot 3B quadrant a.

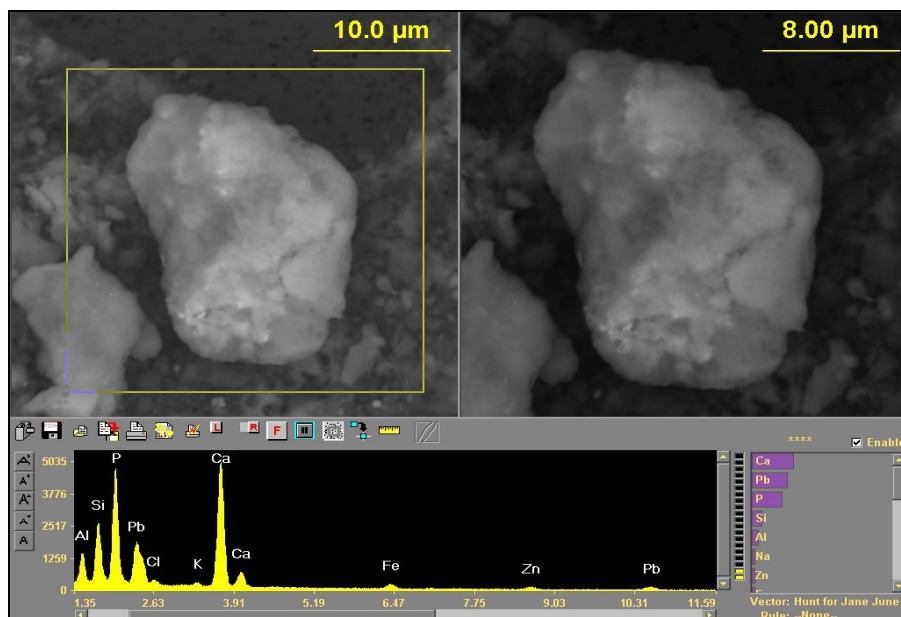


Figure F.19 SEM image shows Pb sorbed on CaP with Fe Zn in Si Al K particle determined in plot 3B quadrant b.

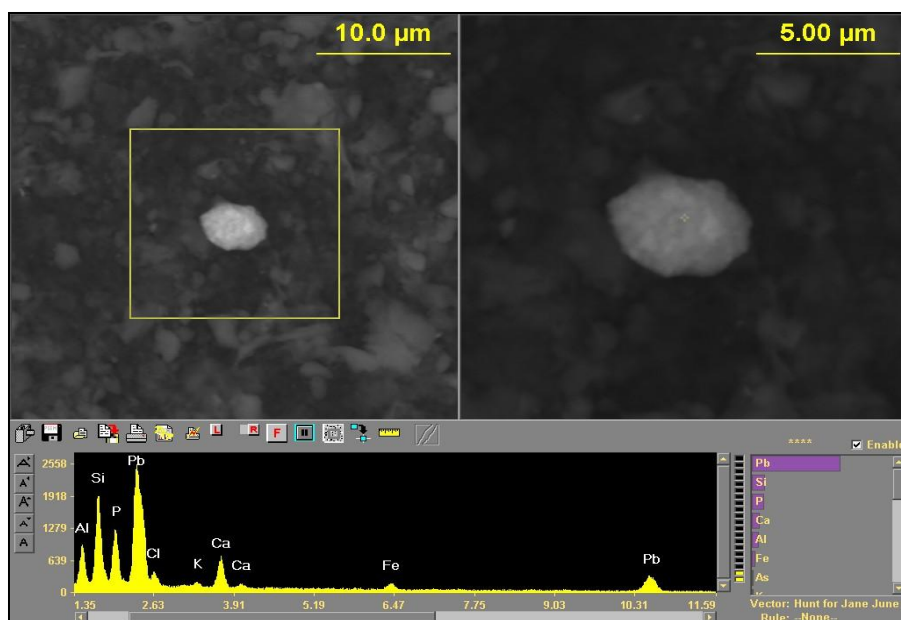


Figure F.20 SEM image shows PbP with Fe in Si Al Ca K particle determined in plot 3B quadrant b.

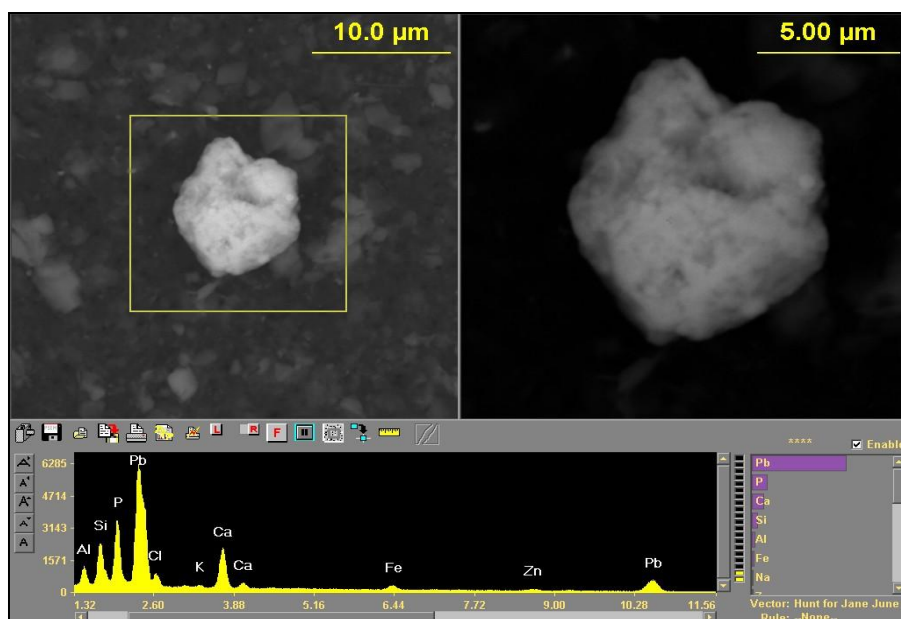


Figure F.21 SEM image shows PbP with Fe in Si Al Ca K particle determined in plot 3B quadrant c.

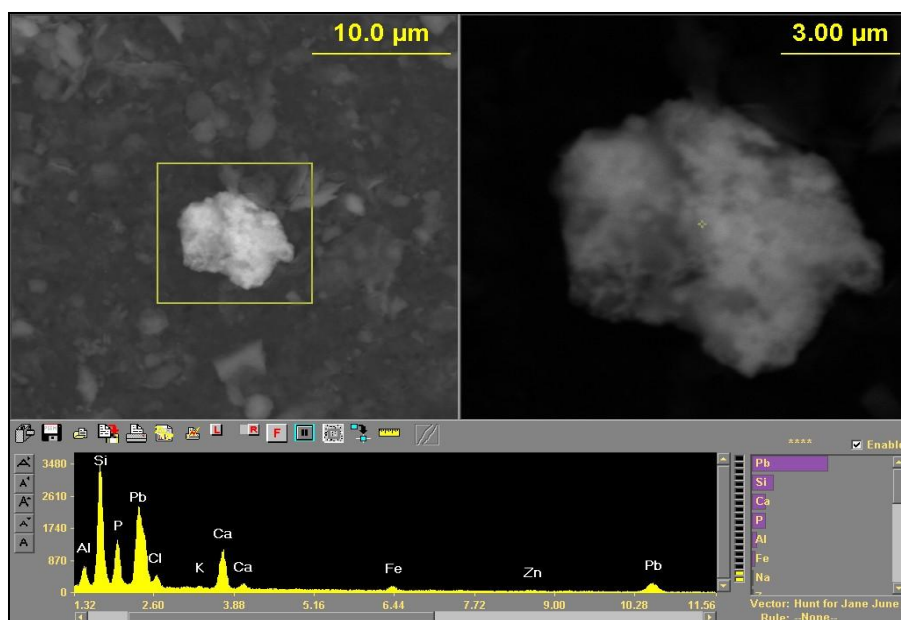


Figure F.22 SEM image shows Pb sorbed on CaP with Fe Zn in Si Al K particle determined in plot 3B quadrant c.

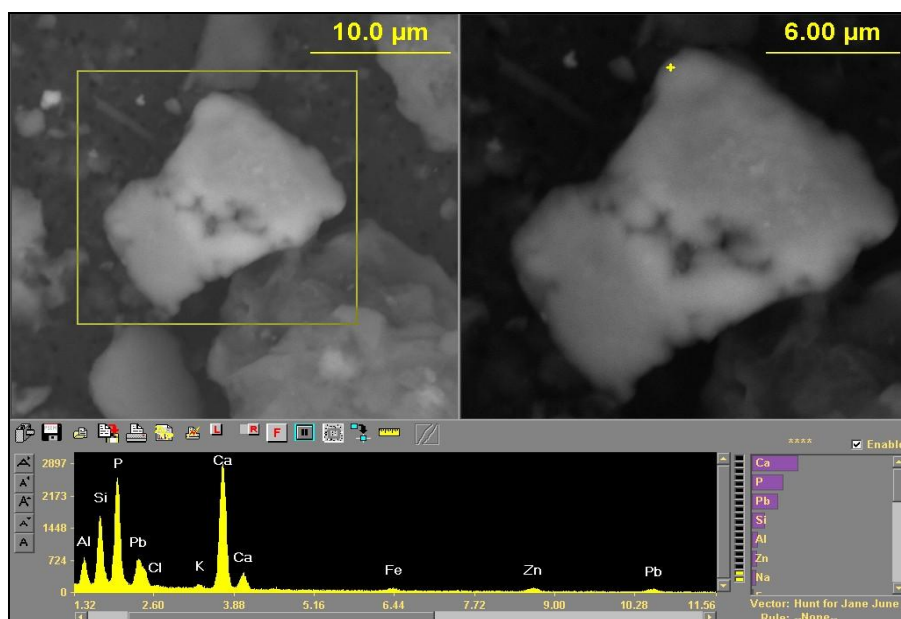


Figure F.23 SEM image shows Pb sorbed on CaP with Fe Zn in Si Al K particle determined in plot 3B quadrant d.

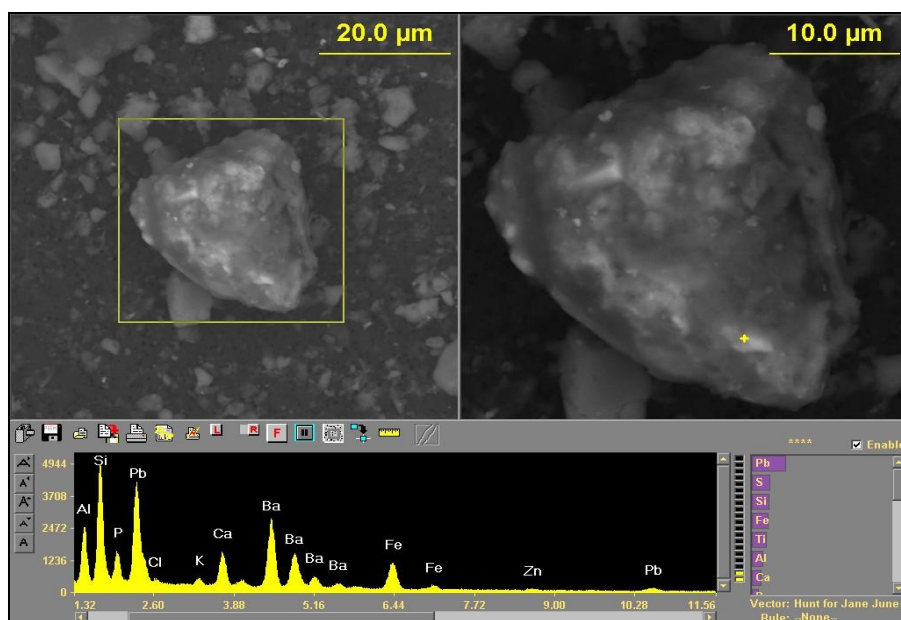


Figure F.24 SEM image shows PbP with Ba Fe Zn in Si Al Ca K particle determined in plot 3B quadrant d.

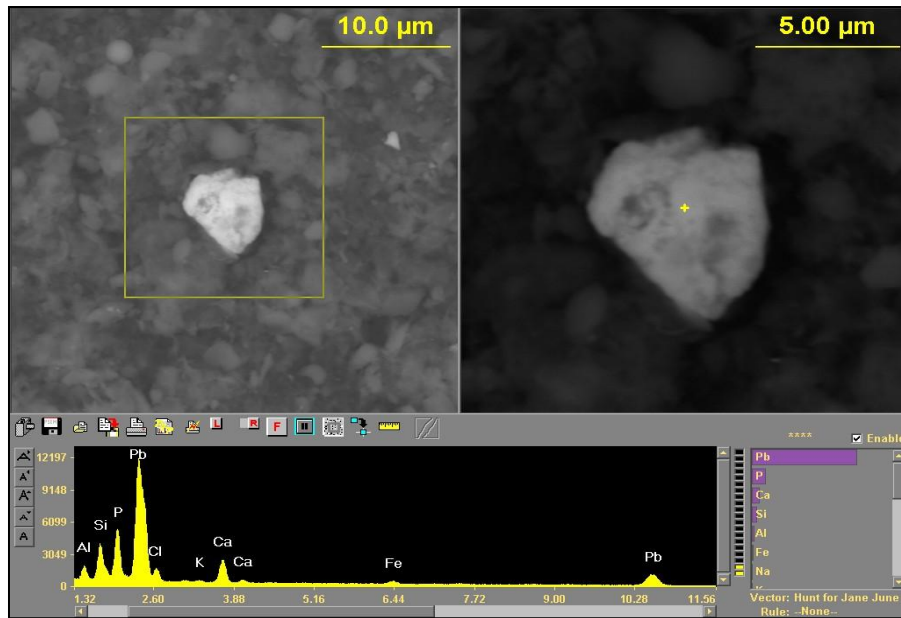


Figure F.25 SEM image shows PbP with Fe in Si Al Ca K particle determined in plot 4B quadrant a.

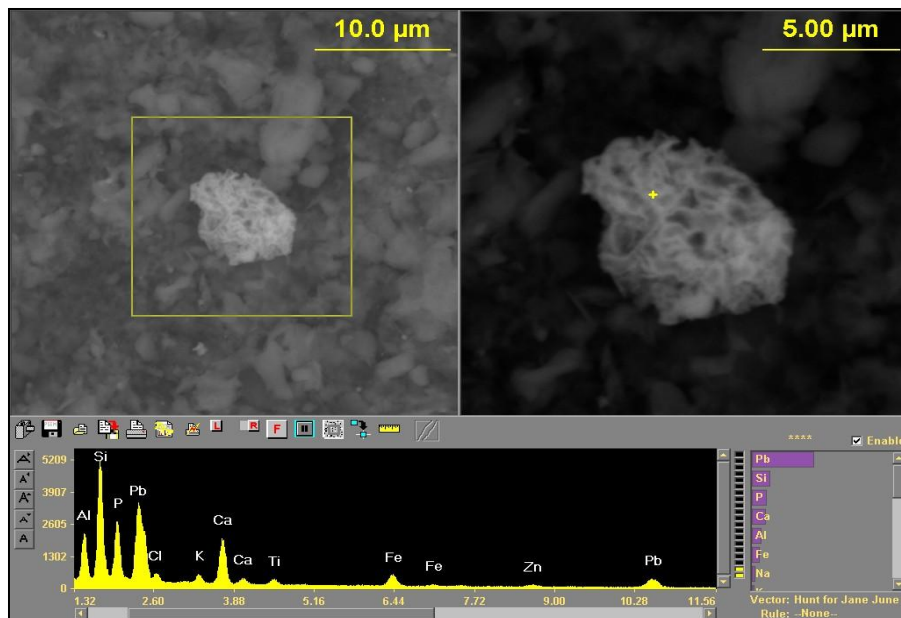


Figure F.26 SEM image shows PbP with Fe in Si Al Ca K particle determined in plot 4B quadrant a.

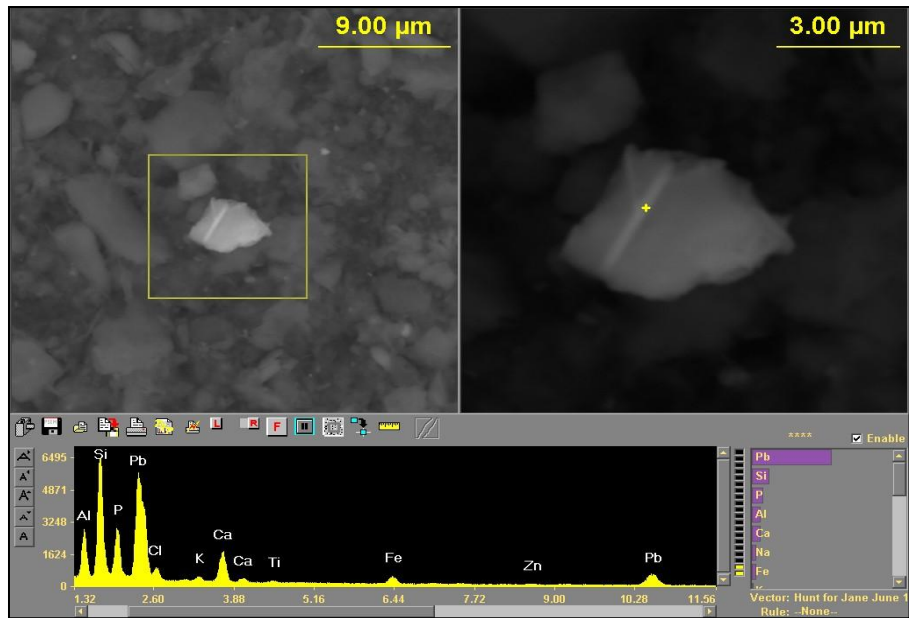


Figure F.27 SEM image shows PbP with Fe in Si Al Ca K particle determined in plot 4B quadrant b.

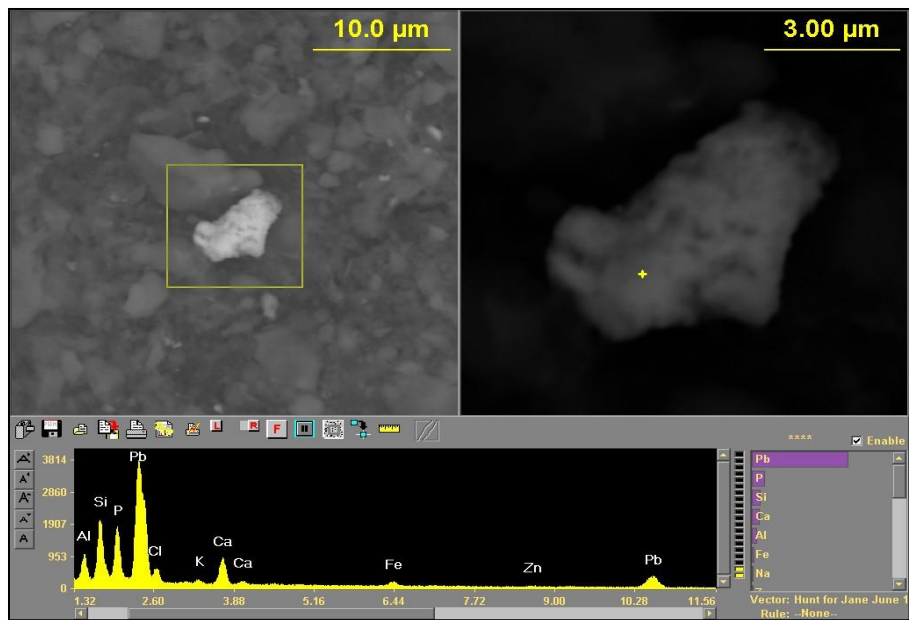


Figure F.28 SEM image shows PbP with Fe in Si Al Ca K particle determined in plot 4B quadrant b.

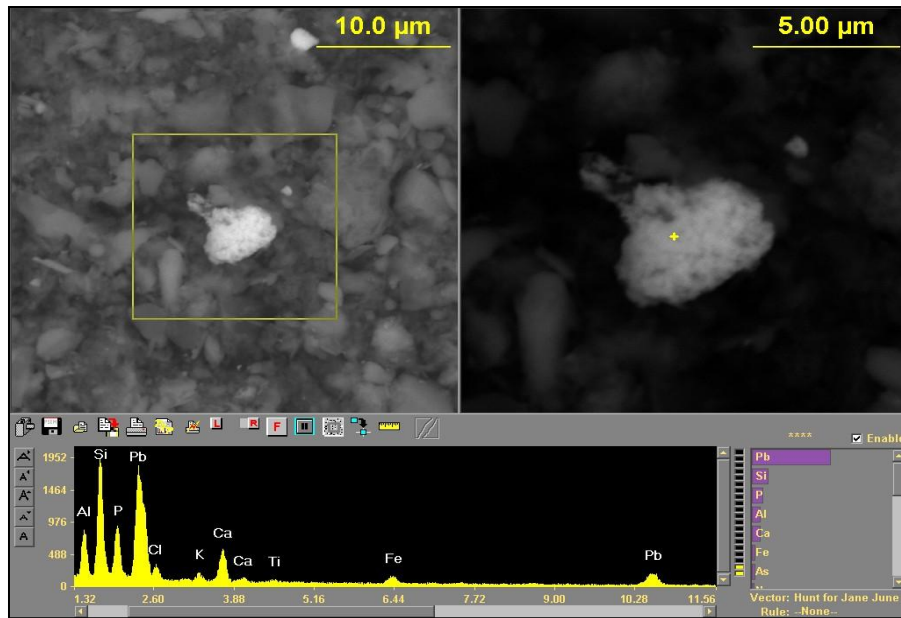


Figure F.29 SEM image shows PbP with Fe in Si Al Ca K particle determined in plot 4B quadrant c.

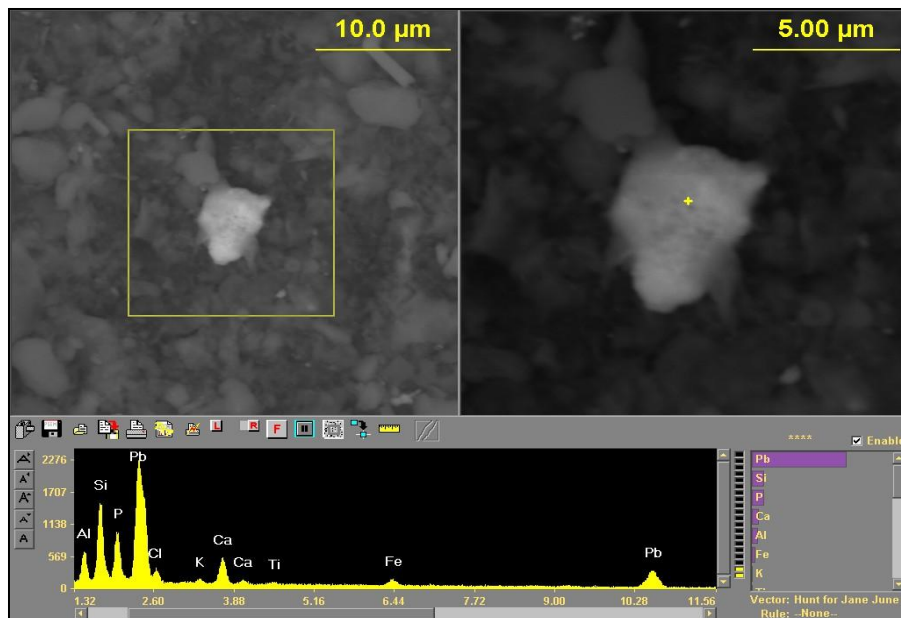


Figure F.30 SEM image shows PbP with Fe in Si Al Ca K particle determined in plot 4B quadrant c.

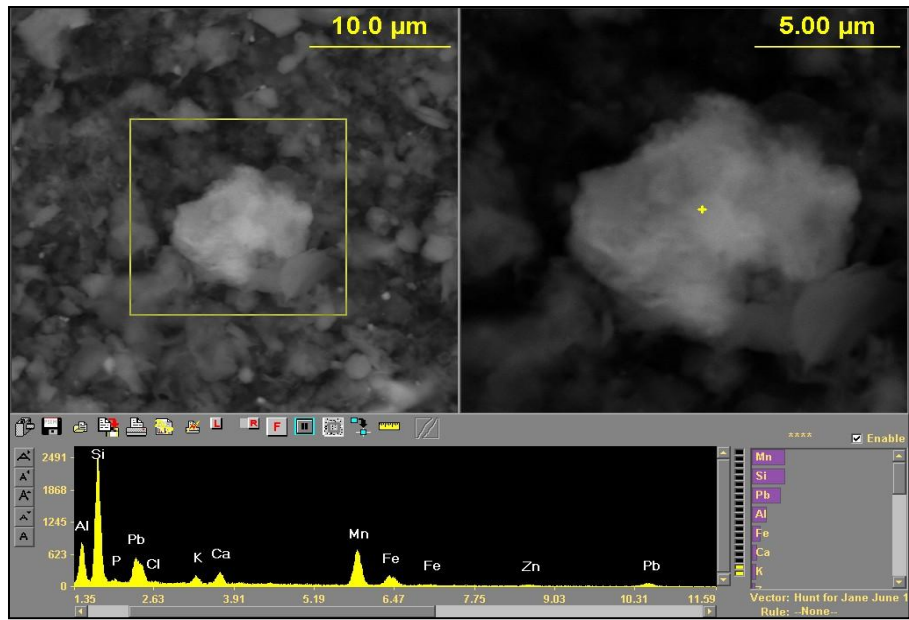


Figure F.31 SEM image shows PbP with Mn Fe Zn in Si Al Ca K particle determined in plot 4B quadrant d.

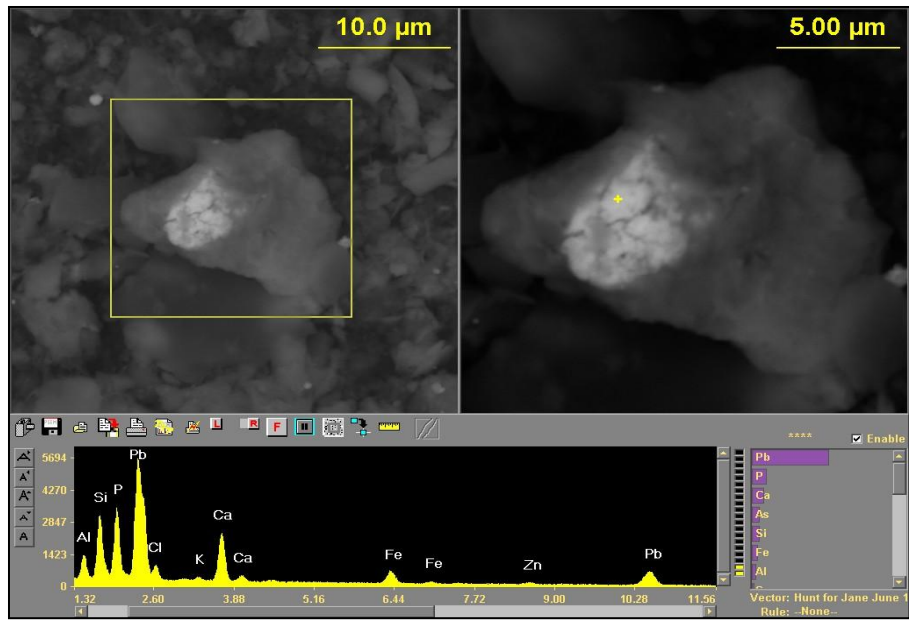


Figure F.32 SEM image shows PbP with Fe in Si Al Ca K particle determined in plot 4B quadrant d.

Appendix G

SEM Images and X-Ray Spectra of Twelve Months Post Treatment 2224 N.Prieur

St. Samples

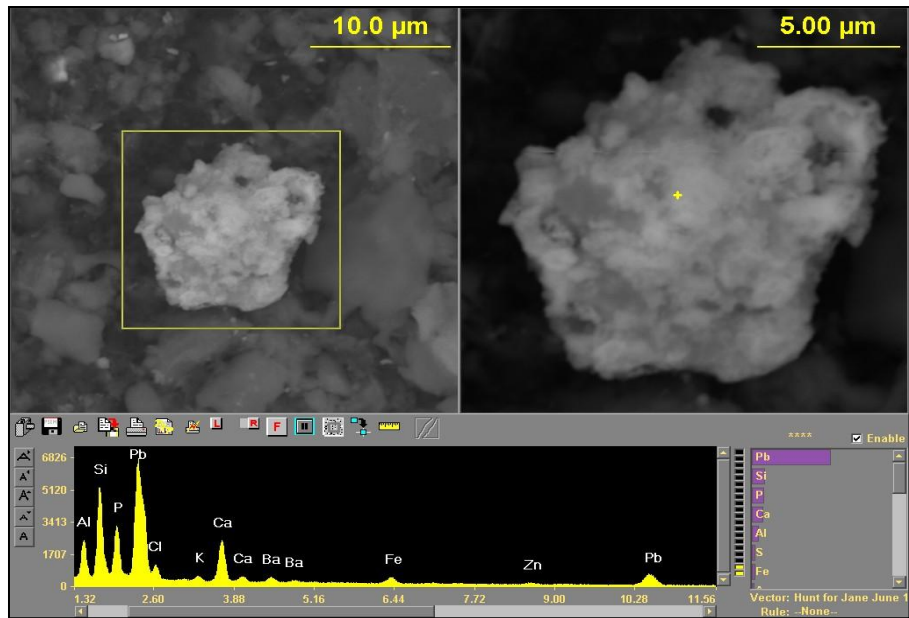


Figure G.1 SEM image shows PbP with Fe Ba Zn in Si Al Ca K particle determined in plot 1B quadrant a.

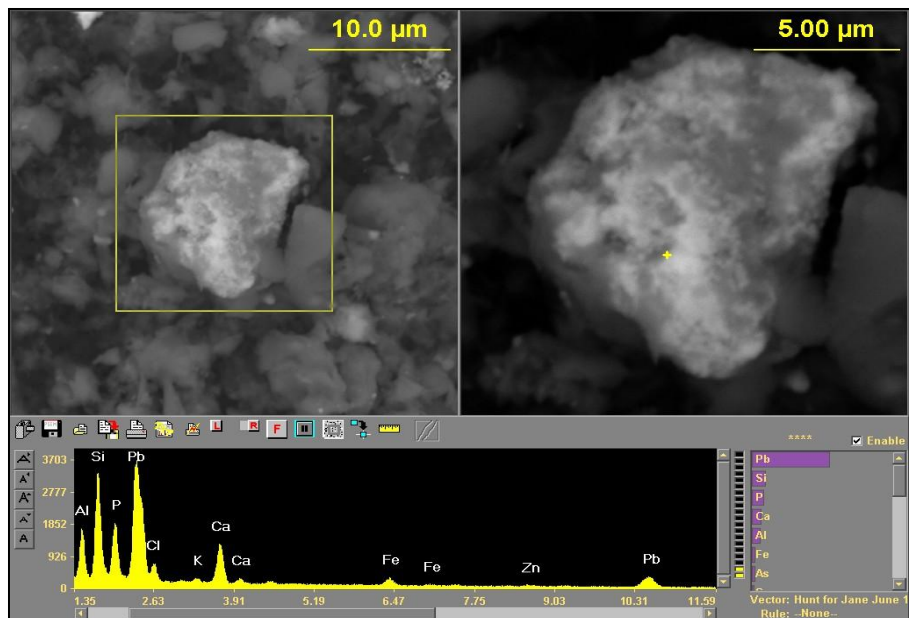


Figure G.2 SEM image shows PbP with Fe in Si Al Ca K particle determined in plot 1B quadrant a.

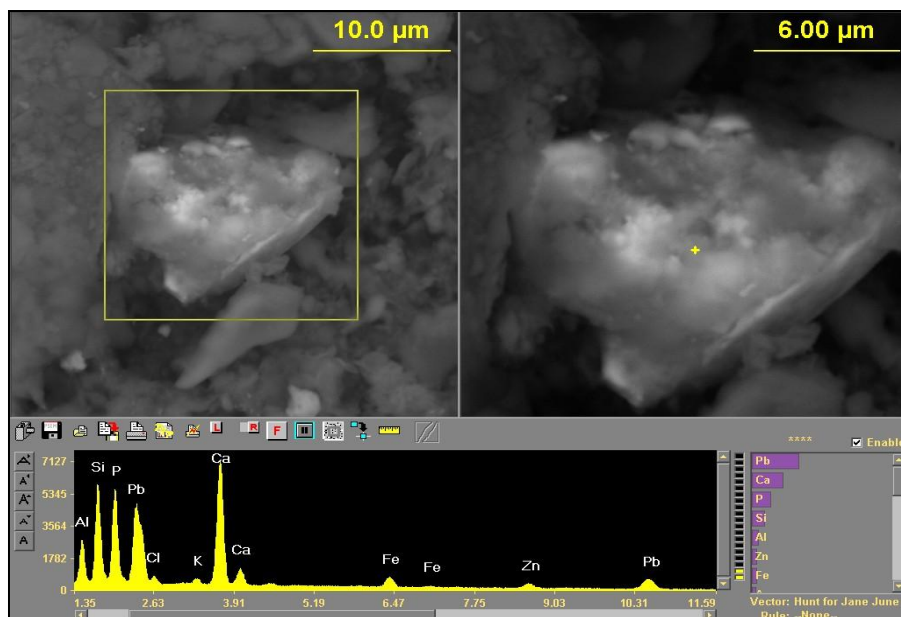


Figure G.3 SEM image shows Pb sorbed on CaP with Fe Zn in Si Al K particle determined in plot 1B quadrant b.

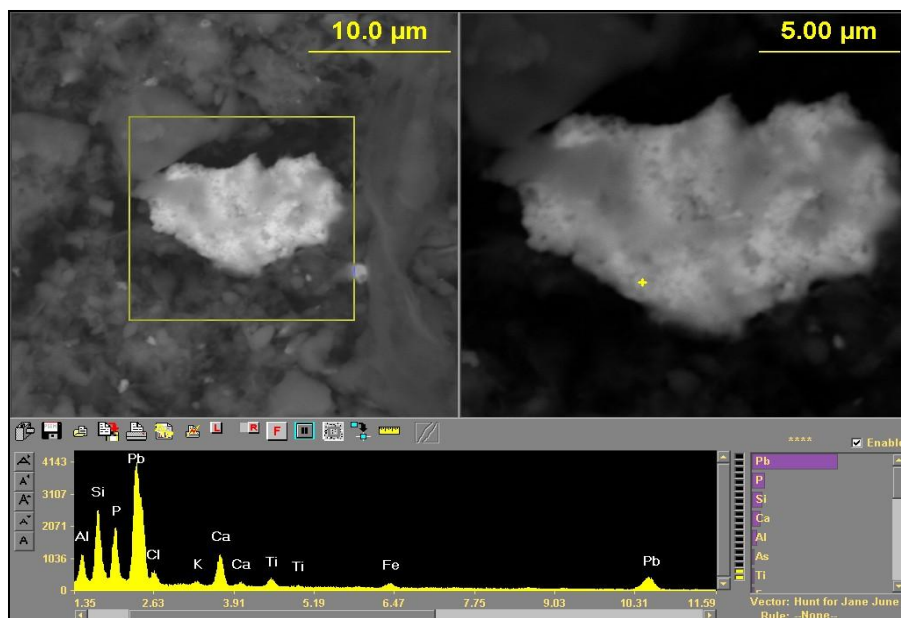


Figure G.4 SEM image shows PbP with Ti Fe in Si Al Ca K particle determined in plot 1B quadrant b.

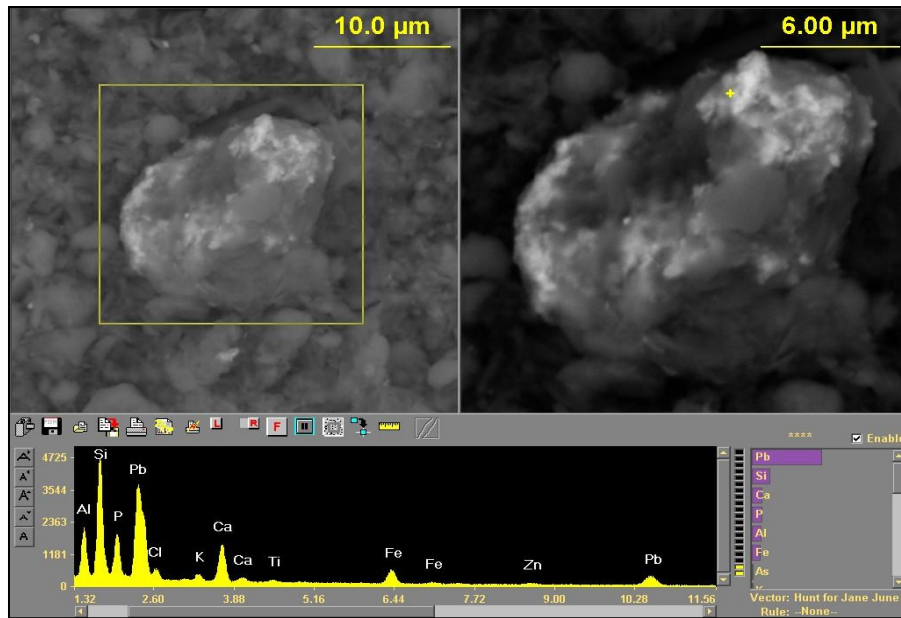


Figure G.5 SEM image shows PbP with Ti Fe in Si Al Ca K particle determined in plot 1B quadrant c.

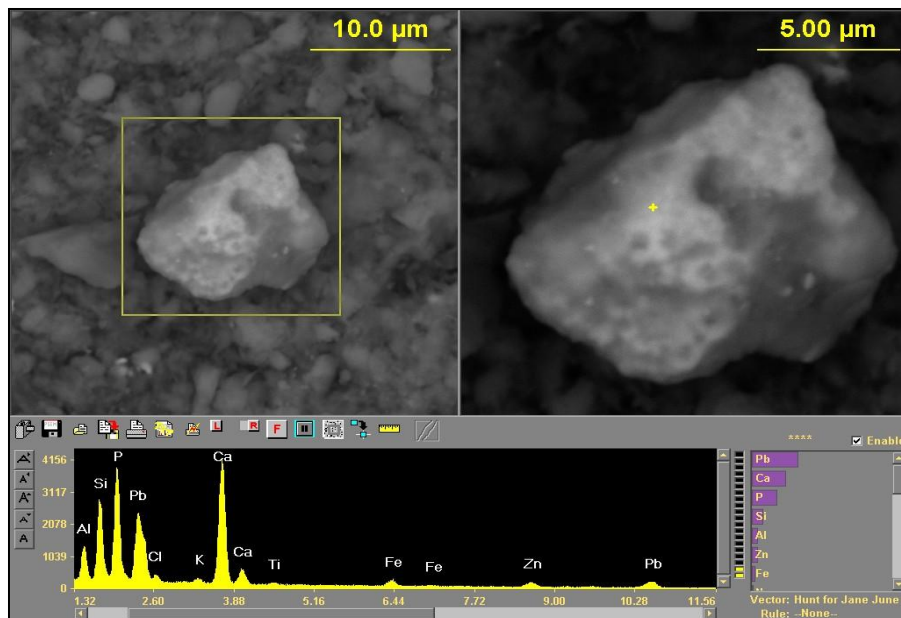


Figure G.6 SEM image shows Pb sorbed on CaP with Fe Zn in Si Al K particle determined in plot 1B quadrant c.

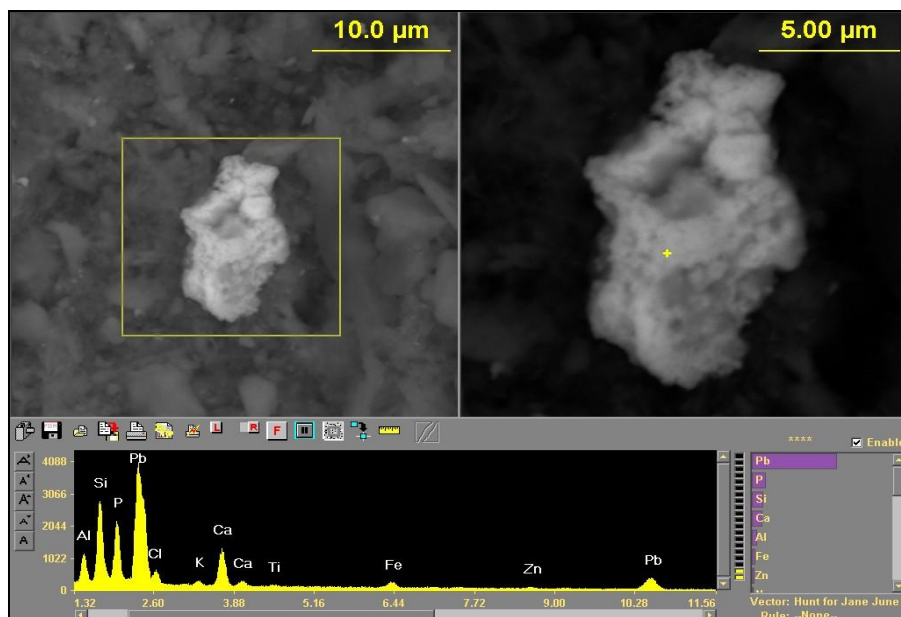


Figure G.7 SEM image shows PbP with Fe in Si Al Ca K particle determined in plot 1B quadrant d.

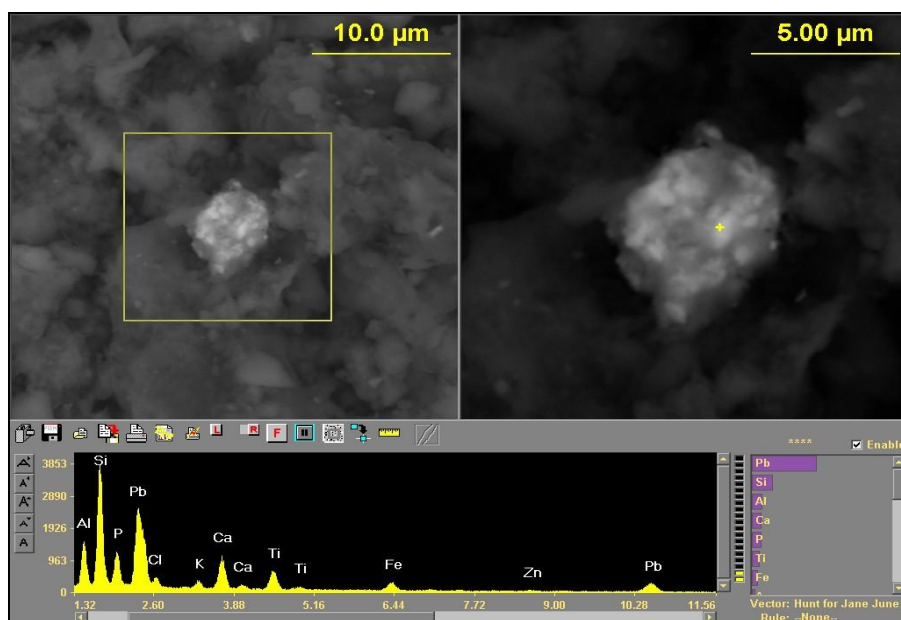


Figure G.8 SEM image shows PbP with Fe in Si Al Ca K particle determined in plot 1B quadrant d.

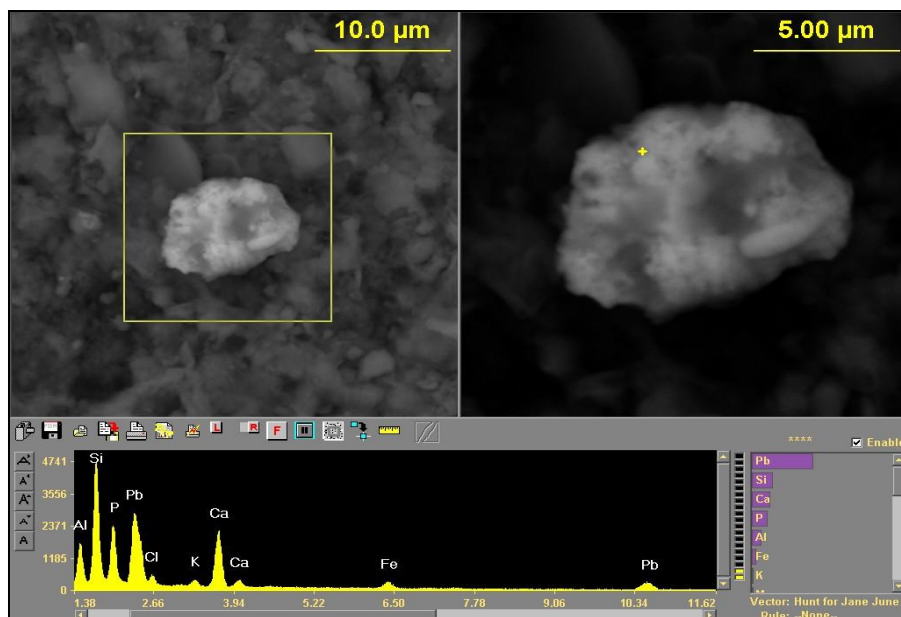


Figure G.9 SEM image shows PbP with Fe in Si Al Ca K particle determined in plot 2B quadrant a.

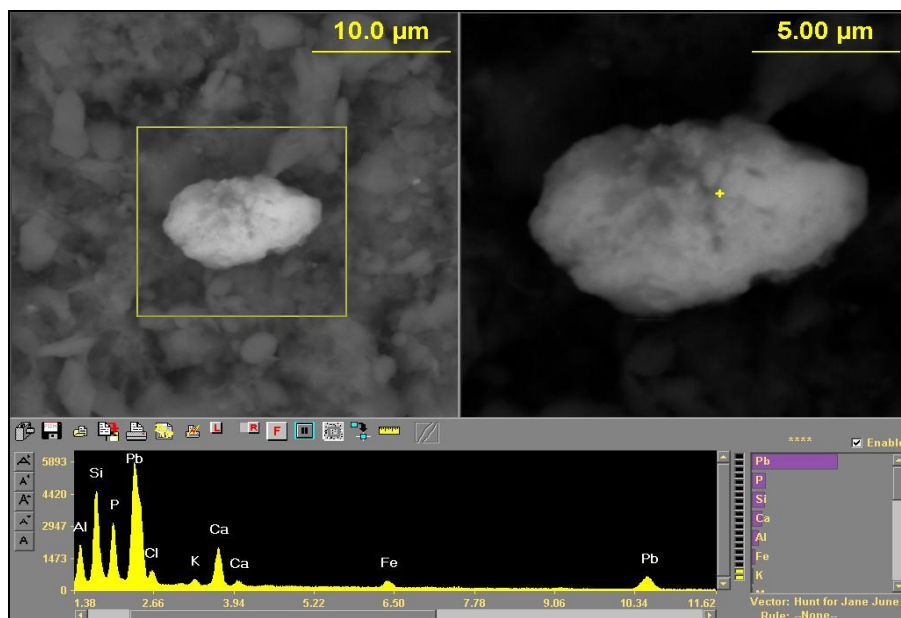


Figure G.10 SEM image shows PbP with Fe in Si Al Ca K particle determined in plot 2B quadrant a.

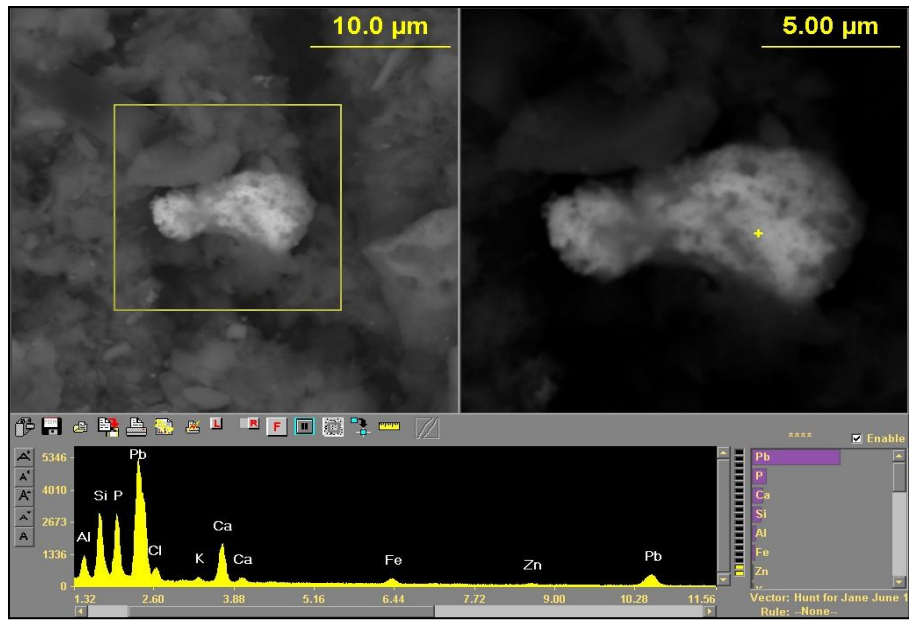


Figure G.11 SEM image shows PbP with Fe Zn in Si Al Ca K particle determined in plot 2B quadrant b.

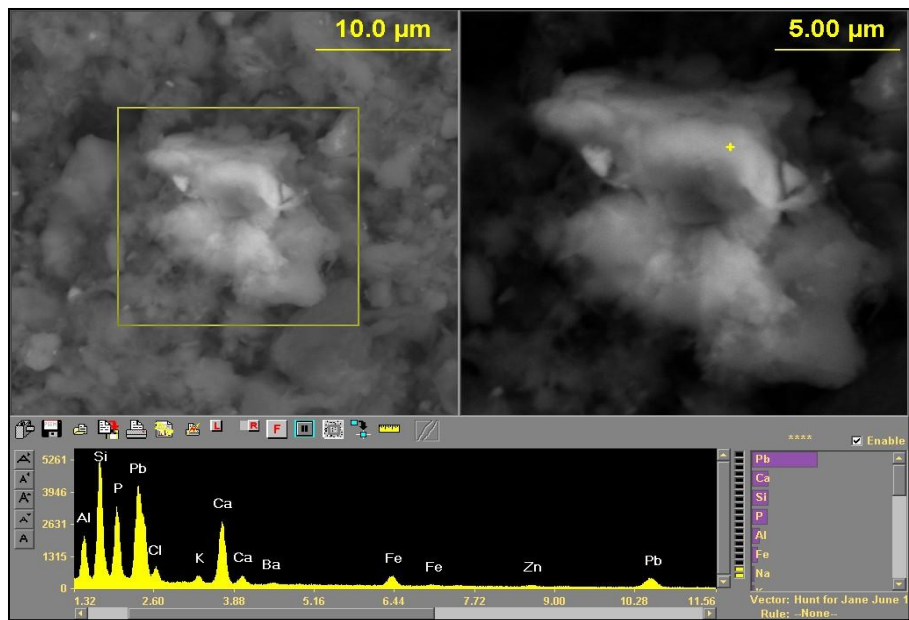


Figure G.12 SEM image shows PbP with Fe Zn in Si Al Ca K particle determined in plot 2B quadrant b.

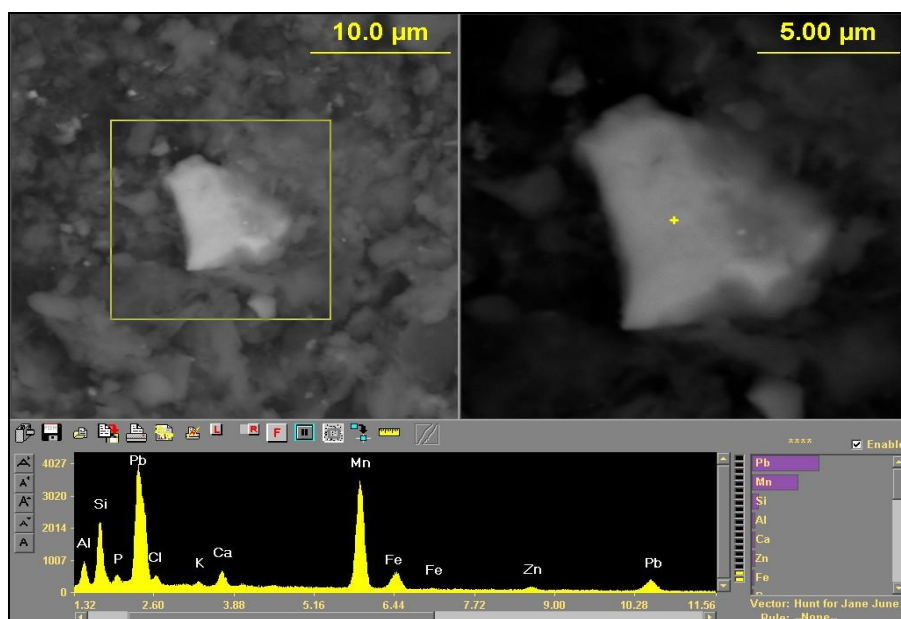


Figure G.13 SEM image shows PbP with Mn Fe Zn in Si Al Ca K particle determined in plot 2B quadrant c.

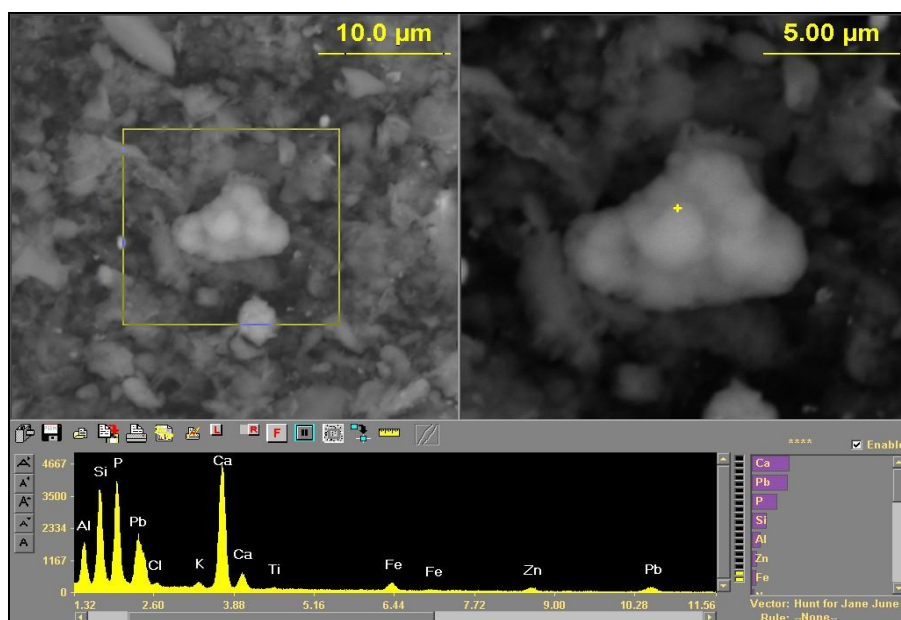


Figure G.14 SEM image shows Pb sorbed on CaP with Fe Zn in Si Al K particle determined in plot 2B quadrant c.

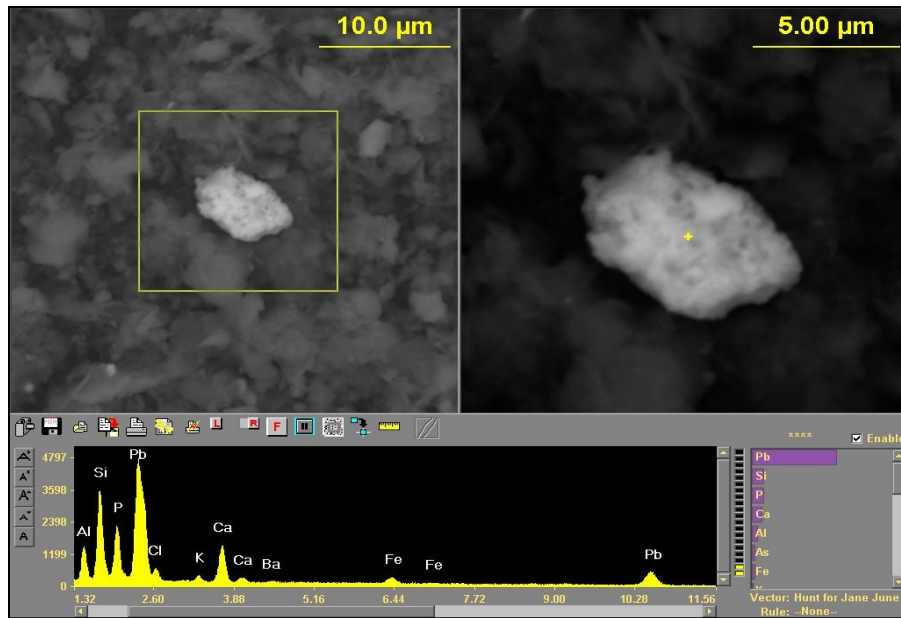


Figure G.15 SEM image shows PbP with Fe Zn in Si Al Ca K particle determined in plot 2B quadrant d.

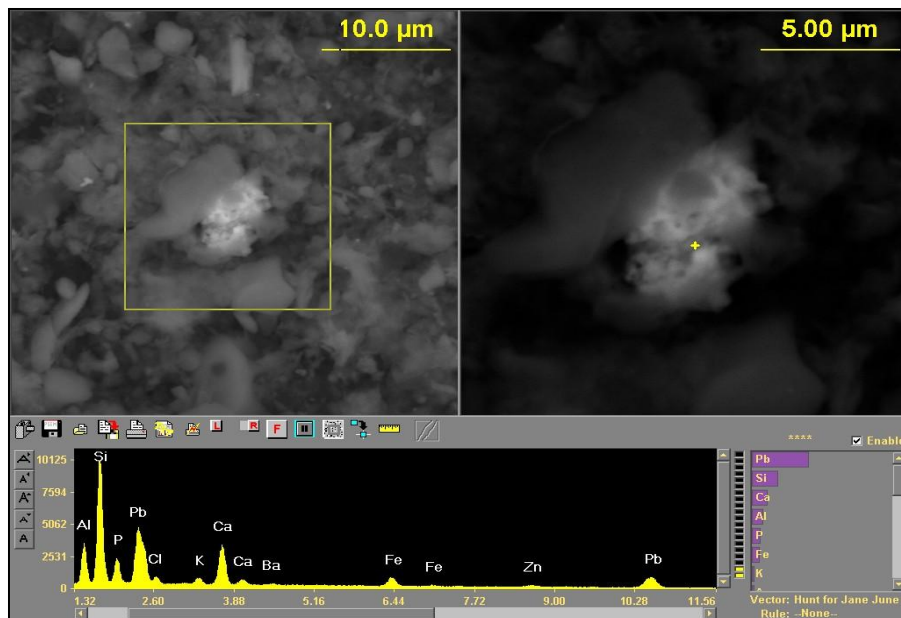


Figure G.16 SEM image shows PbP with Fe Zn in Si Al Ca K particle determined in plot 2B quadrant d.

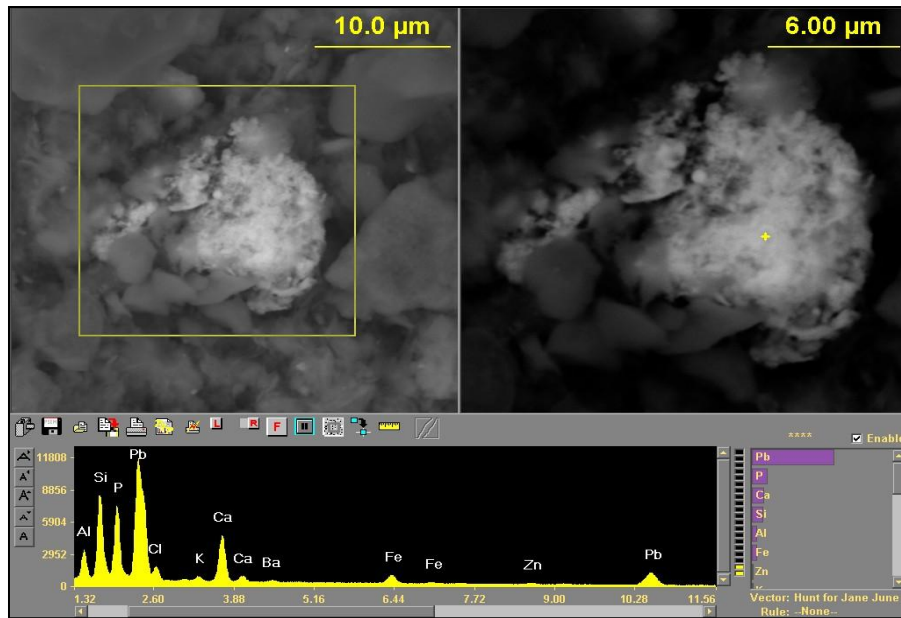


Figure G.17 SEM image shows PbP with Fe Zn in Si Al Ca K particle determined in plot 3B quadrant a.

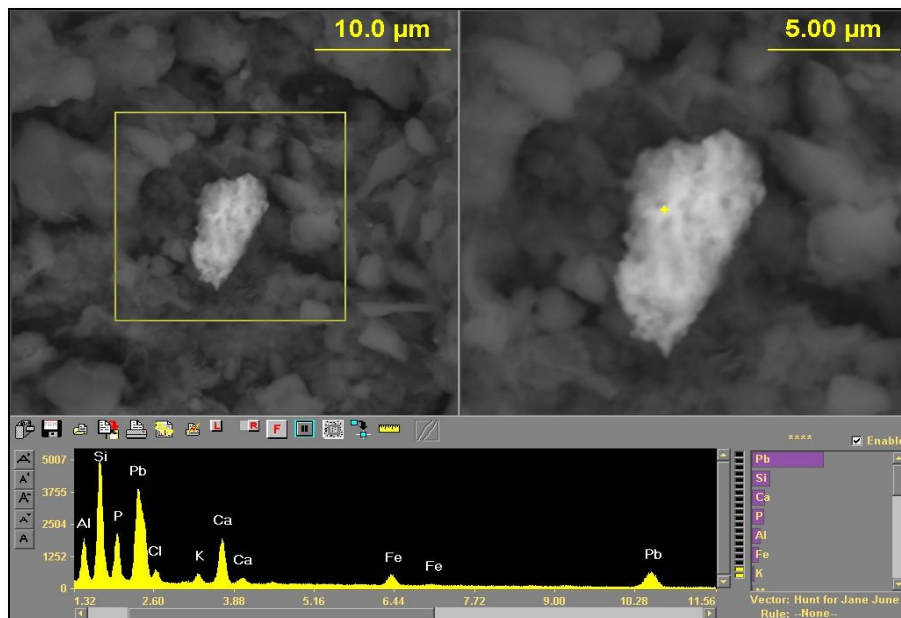


Figure G.18 SEM image shows PbP with Fe in Si Al Ca K particle determined in plot 3B quadrant a.

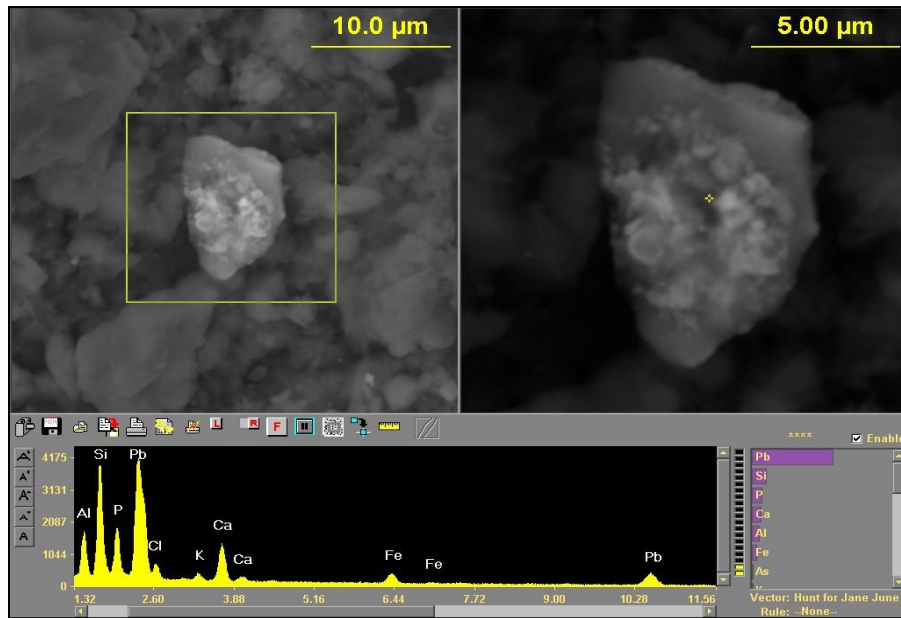


Figure G.19 SEM image shows PbP with Fe in Si Al Ca K particle determined in plot 3B quadrant b.

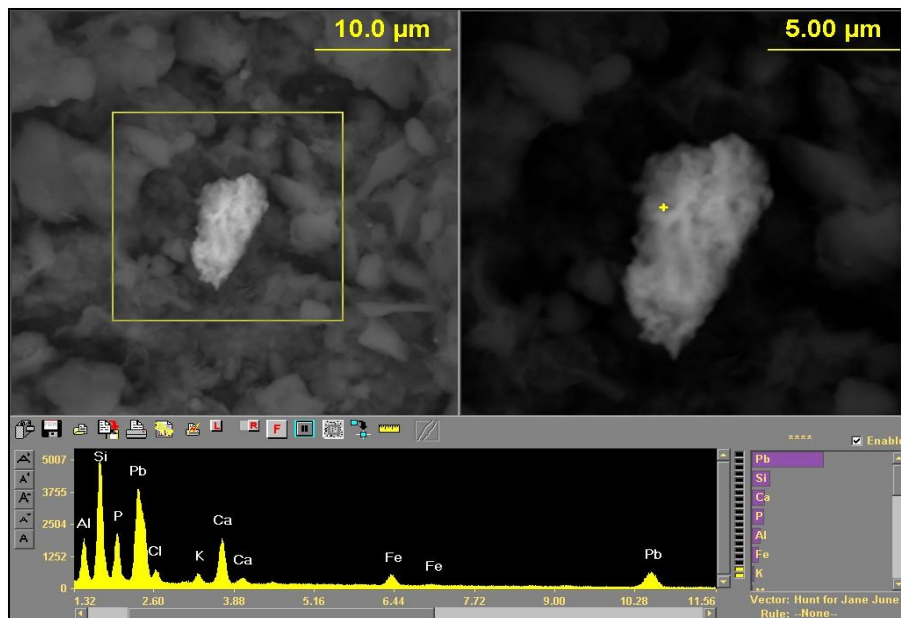


Figure G.20 SEM image shows PbP with Fe in Si Al Ca K particle determined in plot 3B quadrant b.

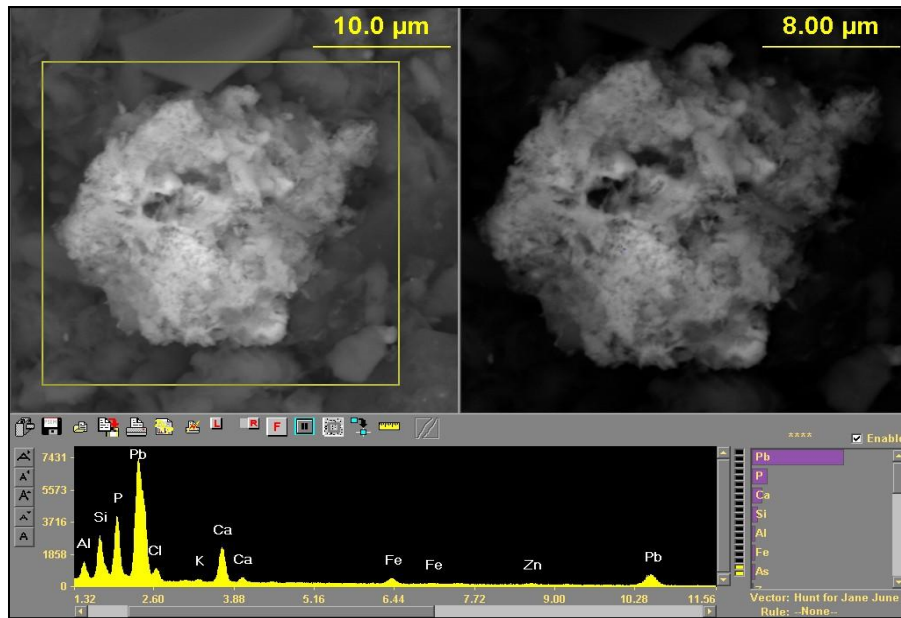


Figure G.21 SEM image shows PbP with Fe in Si Al Ca K particle determined in plot 3B quadrant c.

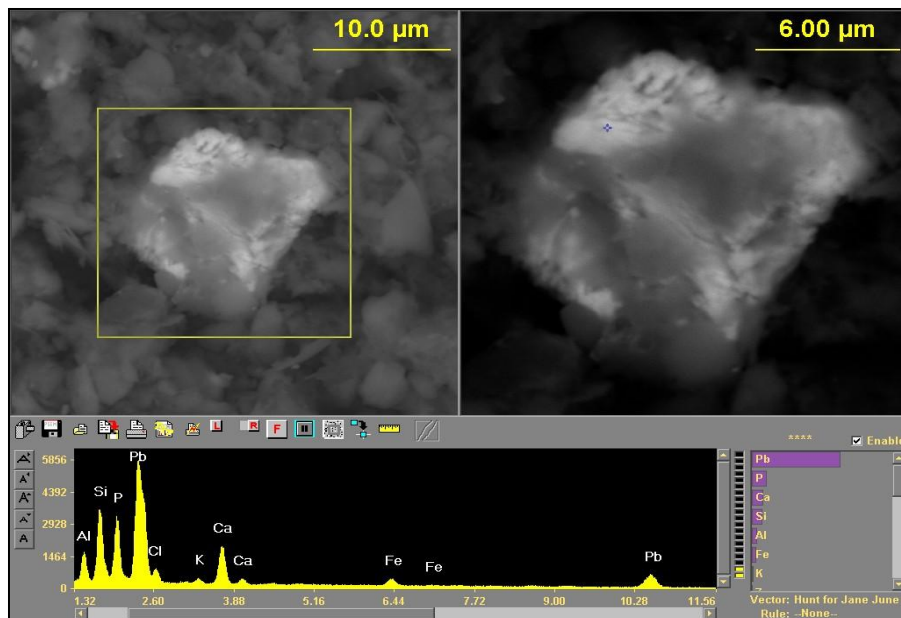


Figure G.22 SEM image shows PbP with Fe in Si Al Ca K particle determined in plot 3B quadrant c.

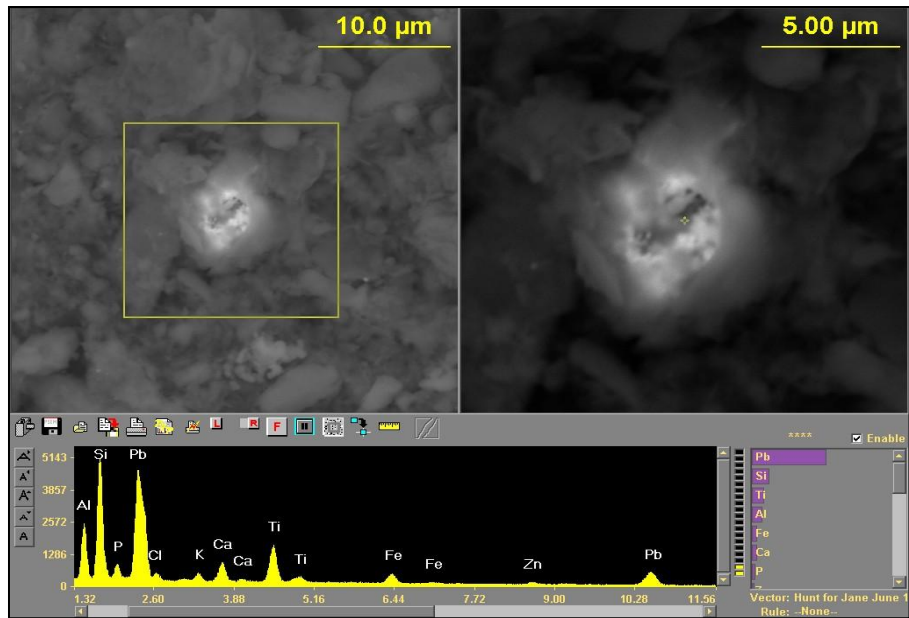


Figure G.23 SEM image shows PbP with Ti Fe Zn in Si Al Ca K particle determined in plot 3B quadrant d.

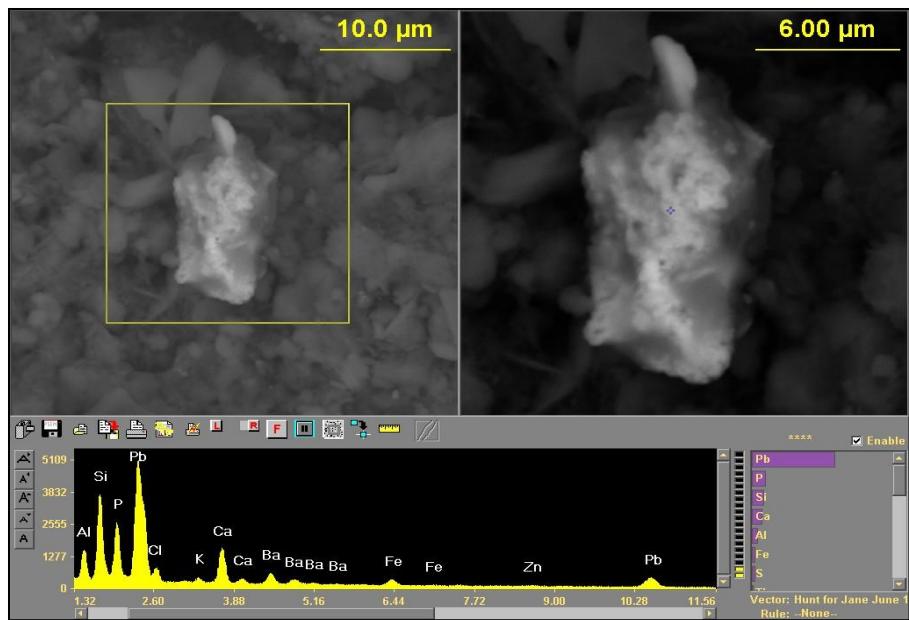


Figure G.24 SEM image shows PbP with Ba Fe in Si Al Ca K particle determined in plot 3B quadrant d.

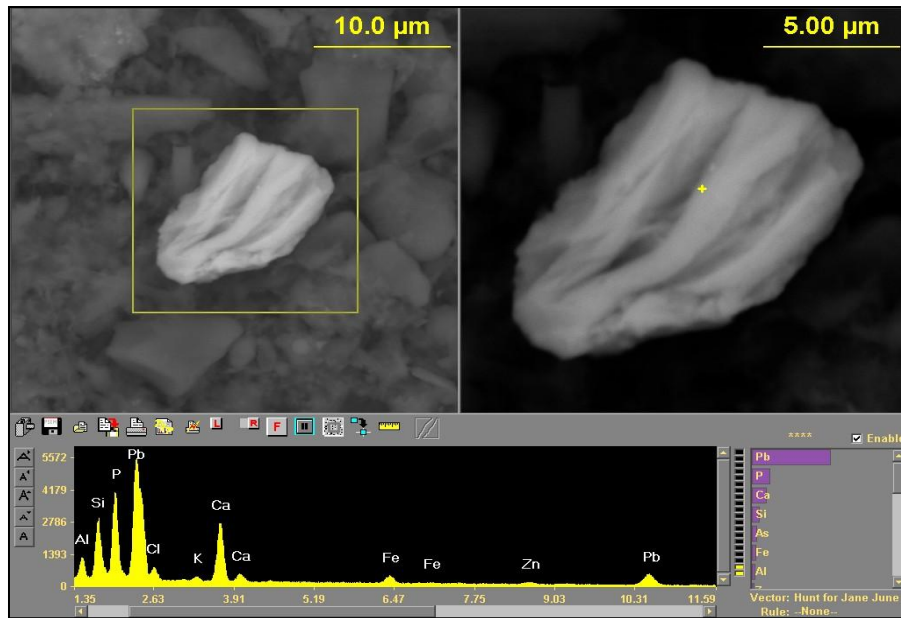


Figure G.25 SEM image shows PbP with Fe Zn in Si Al Ca K particle determined in plot 4B quadrant a.

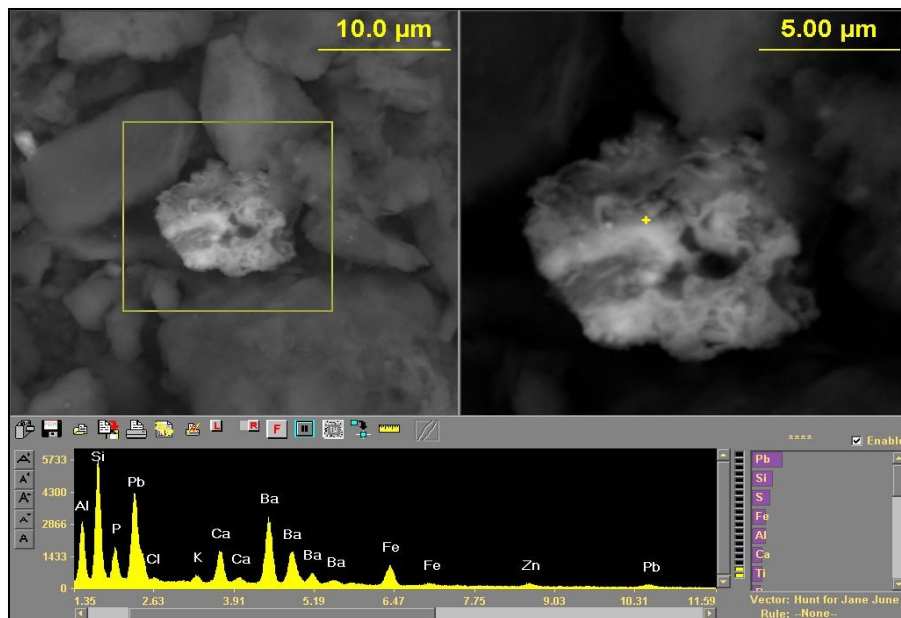


Figure G.26 SEM image shows PbP with Ba Fe Zn in Si Al Ca K particle determined in plot 4B quadrant a.

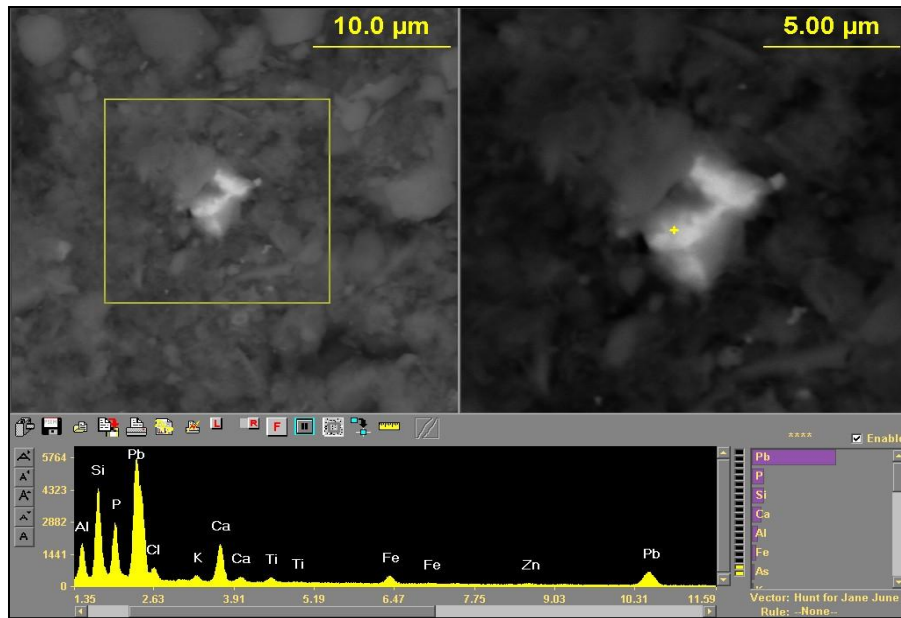


Figure G.27 SEM image shows PbP with Fe Ti Zn in Si Al Ca K particle determined in plot 4B quadrant b.

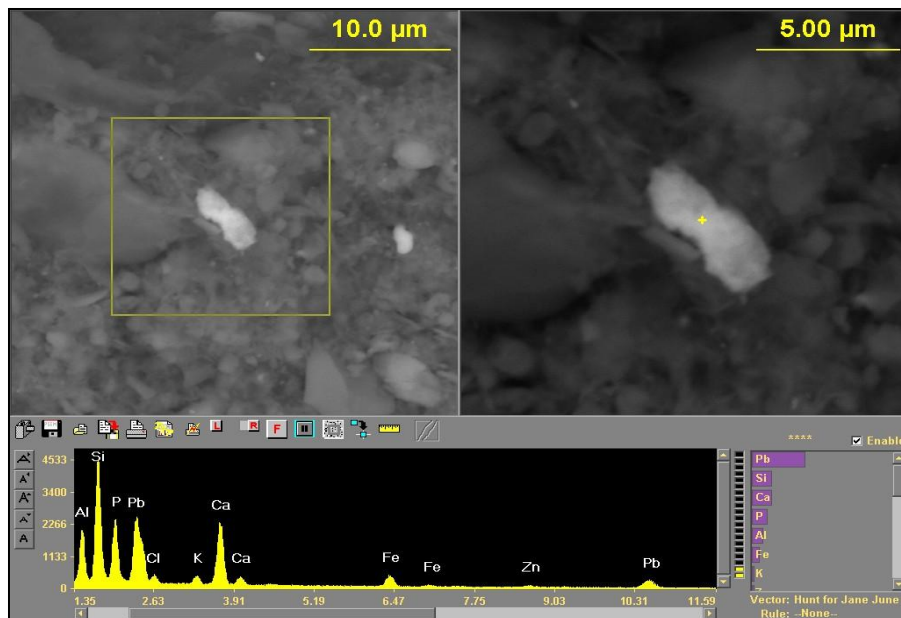


Figure G.28 SEM image shows PbP with Fe Ti Zn in Si Al Ca K particle determined in plot 4B quadrant b.

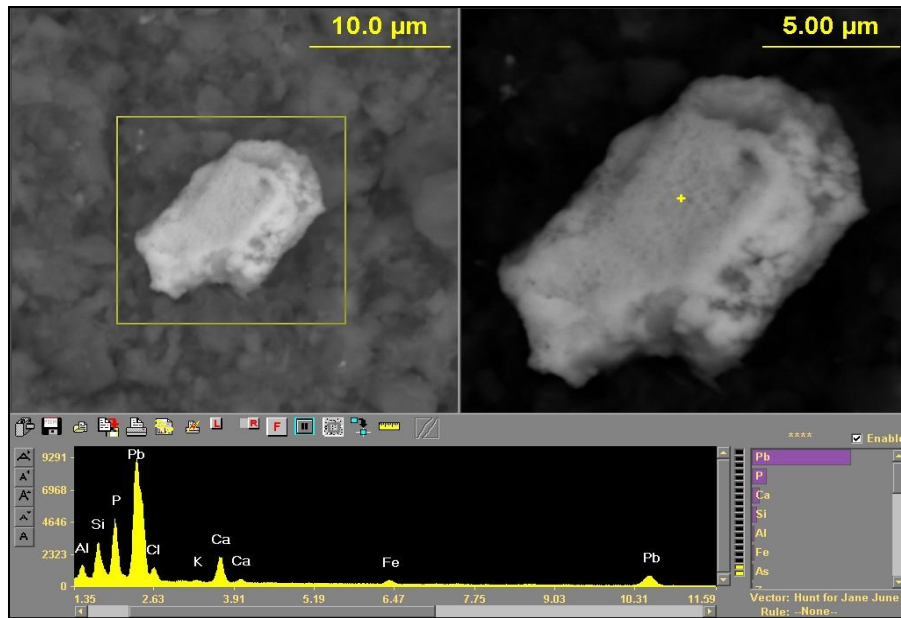


Figure G.29 SEM image shows PbP with Fe in Si Al Ca K particle determined in plot 4B quadrant c.

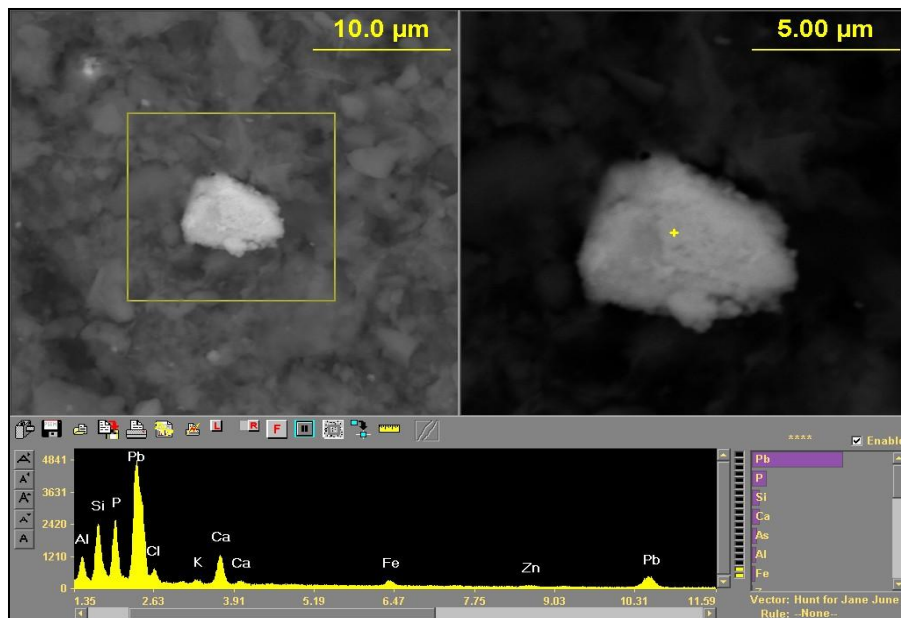


Figure G.30 SEM image shows PbP with Fe Zn in Si Al Ca K particle determined in plot 4B quadrant c.

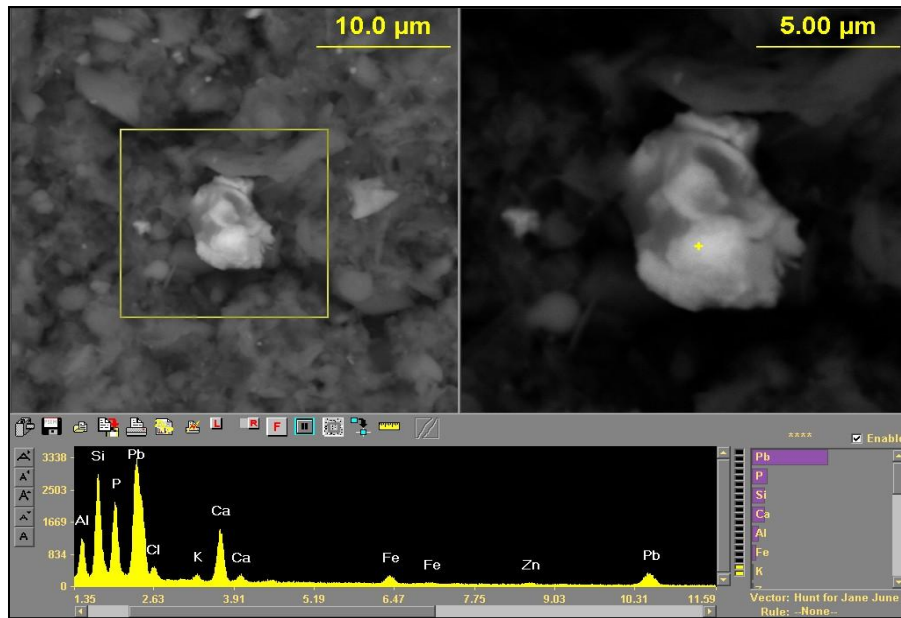


Figure G.31 SEM image shows PbP with Fe Zn in Si Al Ca K particle determined in plot 4B quadrant d.

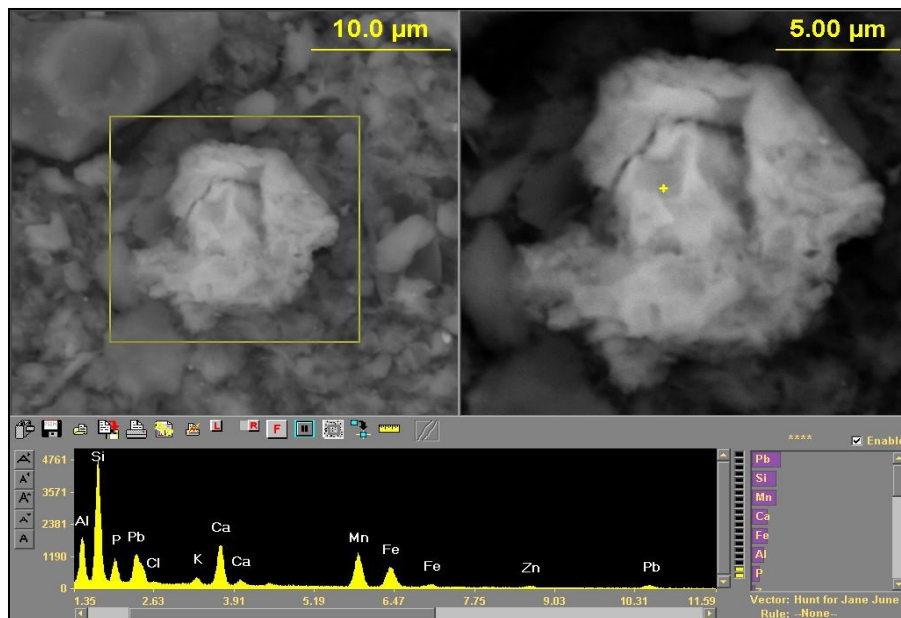


Figure G.32 SEM image shows PbP with Mn Fe Zn in Si Al Ca K particle determined in plot 4B quadrant d.

Appendix H

1613 St. Roche Ave. General Site Images



Figure H.1 Lysimeters installation into uncapped soil plots.



Figure H.2 deteriorated paints from exterior house walls.



Figure H.3 General view of the pre-treatment yard.



Figure H.4 General view of the backyard pre-treatment soil with deteriorated back house wall paint.



Figure H.5 Roto-tilling soil prior plants and rocks removal.



Figure H.6 Roto-tilling soil prior plants and rocks removal.



Figure H.7 Post-treatment installation of 6" clean soil cap.



Figure H.8 Post-treatment installation of 6" clean soil cap.



Figure H.9 Post-treatment installation of 6" clean soil cap.



Figure H.10 Watering Post-treatment 6" clean soil cap.



Figure H.11 Watering Post-treatment 6" clean soil cap.



Figure H.12 Installation of plastic barrier and centered hole for lysimeter installation into the uncapped plot.



Figure H.13 Centered hole for lysimeter installation into the uncapped plot.



Figure H.14 General view for the post-treatment capped (right) and uncapped (left) plots



Figure H.15 Examination of final post-treatment plots.



Figure H.16 Pre-treatment plots layout and heap of clean soil for capping.



Figure H.17 Pre-treatment plots layout and heap of clean soil for capping and part of tree as site obstacle.



Figure H.18 Post-treatment lysimeter installation with chicken wire and plastic barrier for animal protection and cross contamination.



Figure H.19 Heaps of fish bones ready for roto-till

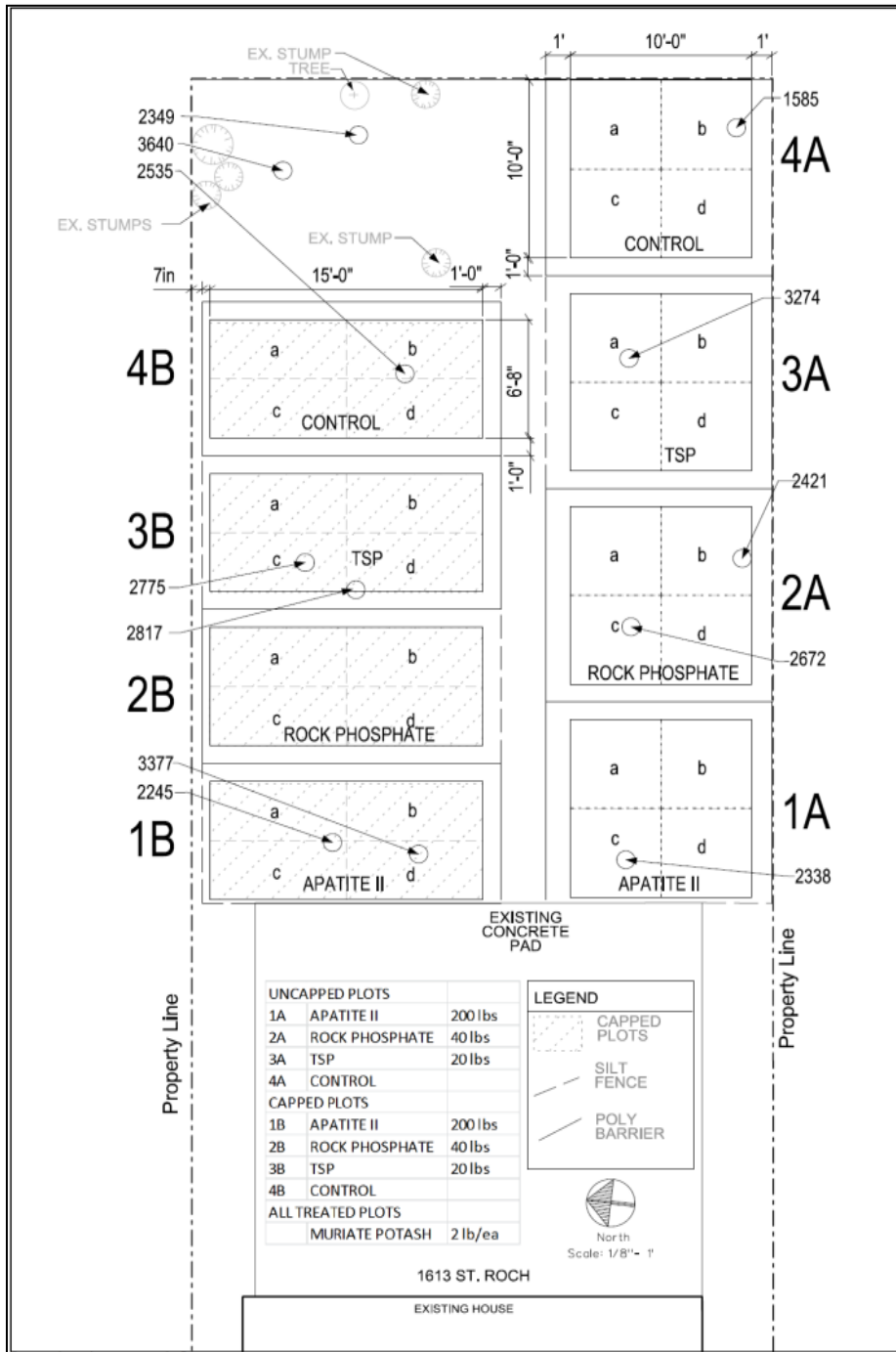


Figure H.20 1613 St. Roche Layout.

Appendix I

1818 Dumaine St. General Site Images



Figure I.1 General view of the yard and side house.



Figure I.2 Plot layout with phosphorous amendment.



Figure I.3 Plot layout with phosphorous amendment.



Figure I.4 Plot layout with phosphorous amendment.



Figure I.5 Pre-treatment Plot layout.



Figure I.6 Pre-treatment Plot layout with phosphorous amendments.



Figure I.7 Pre-treatment Plot layout.



Figure I.8 Pre-treatment Plot layout with phosphorous amendments.



Figure I.9 Pre-treatment Plot layout with phosphorous amendments.



Figure I.10 Spreading fish bones on plot before mixing with soil.



Figure I.11 Spreading fish bones on plot.



Figure I.12 Roto-tilling fish bones into the soil.



Figure I.13 Roto-tilling fish bones into the soil.



Figure I.14 Roto-tilling fish bones into the soil.



Figure I.15 General view of treated and un treated soil pots.



Figure I.16 Installation of protective chicken wire and plastic barriers for post-treatment plots.



Figure I.17 Installation of protective chicken wire and plastic barriers for post-treatment plots.



Figure I.18 Pre-treatment site cleanup of rocks and plants



Figure I.19 Pre-treatment site cleanup of rocks and plants



Figure I.20 Installation of protective chicken wire and plastic barriers for post-treatment plots and heap of clean soil cap.



Figure I.21 General view of treated and un treated soil pots.



Figure I.22 Installation of 6" clean cap soil.



Figure I.23 Transferring clean cap soil.



Figure I.24 Installation of 6" clean cap soil.



Figure I.25 Lysimeters installation into uncapped soil plots.



Figure I.26 General view of post-treatment uncapped (top) and capped (bottom) soil plots.



Figure I.27 Lysimeters installation into uncapped soil plots.



Figure I.28 Lysimeters installation into uncapped soil plots.

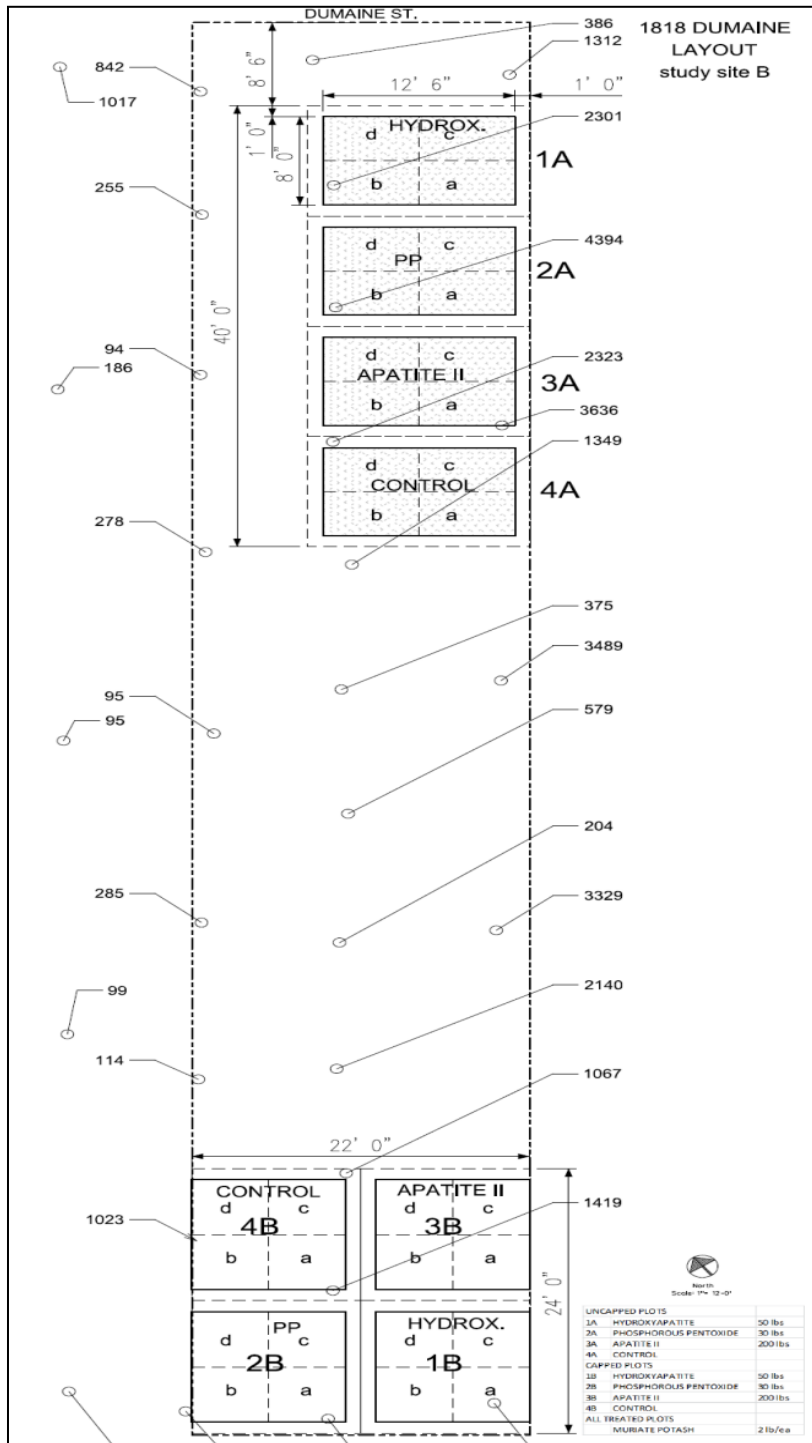


Figure I.29 1818 Dumaine St. layout.

Appendix J

2224 N. Prieur St. General Site Images



Figure J.1 General view of plant and rocks clean up pre-treatment plots.



Figure J.2 General view of plant and rocks clean up pre-treatment plots.



Figure J.3 General view of plant and rocks clean up pre-treatment plots.



Figure J.4 General view of plant and rocks clean up pre-treatment plots.



Figure J.5 Roto-tilling soil and fish bones.



Figure J.6 Mixing bone meal with soil.



Figure J.7 Roto-tilling soil and fish bones.



Figure J.8 Roto-tilling soil and fish bones.



Figure J.9 Roto-tilling soil and fish bones.



Figure J.10 Spreading out bone meal amendment into the plot.



Figure J.11 Removing Plants before adding the amendments.



Figure J.12 Removing Plants before adding the amendments.



Figure J.13 Removing Plants before adding the amendments.



Figure J.14 Removing Plants before adding the amendments.



Figure J.15 Roto-tilling soil for plants clean up.



Figure J.16 Roto-tilling soil for plants clean up.



Figure J.17 Spreading amendments on the plots.



Figure J.18 Spreading fish bones on the plots.



Figure J.19 Spreading amendments on the plots.



Figure J.20 Roto-till bone meal into the soil.



Figure J.21 Spreading bone meal on the plots.



Figure J.22 Plastic barrier installation for animal attack or water over flow.



Figure J.23 Lysimeters installation into pre-treatment un-capped plots.



Figure J.24 Post-treatment pre-capping plots.



Figure J.25 General view of post-treatment capped (top left) and un capped (bottom right) plots.



Figure J.26 Lysimeters installation into pre-treatment un-capped plots.



Figure J.27 Lysimeter installation into un-capped soil plot.



Figure J.28 Lysimeter installation into un-capped soil plot.



Figure J.29 Lysimeter installation into un-capped soil plot.



Figure J.30 Post-treatment pre-capping plots.



Figure J.31 General view of post-treatment capped (bottom) and uncapped (top) soil plots.



Figure J.32 Post-treatment capped soil plots after barriers installation.



Figure J.33 Post-treatment capped and uncapped soil plots before barriers installation.



Figure J.34 Post-treatment capped soil plots before barriers installation.



Figure J.35 Post-treatment capped soil plots before barriers installation.



Figure J.36 Post-treatment capped and uncapped soil plots before barriers installation.



Figure J.37 Post-treatment capped and uncapped soil plots before barriers installation.



Figure J.39 Post-treatment capped and uncapped soil plots before barriers installation.



Figure J.40 Post-treatment uncapped soil plots before barriers installation.



Figure J.41 Post-treatment capped soil plots before barriers installation.



Figure J.42 Post-treatment capped soil plots before barriers installation.



Figure J.43 Post-treatment capped and uncapped soil plots before barriers installation.



Figure J.44 Installing 6" of clean soil cap.



Figure J.45 Lysimeter installation into un-capped plots.



Figure J.46 Lysimeter installation into un-capped plots.



Figure J.47 Lysimeter installation into un-capped plots.



Figure J.48 Lysimeter installation into un-capped plots.



Figure J.49 Post-treatment site watering.



Figure J.50 Post-treatment site watering.



Figure J.51 Post-treatment site watering.



Figure J.52 Post-treatment site watering.



Figure J.53 Post-treatment site watering.



Figure J.54 Installation of chicken wire on soil plots.



Figure J.55 Installation of chicken wire on soil plots.



Figure J.56 Installation of chicken wire on soil plots.



Figure J.57 Installation of chicken wire on soil plots.



Figure J.58 Installation of chicken wire on soil plots.



Figure J.59 Installation of chicken wire on soil plots.



Figure J.60 Installation of chicken wire on soil plots.



Figure J.61 Installation of chicken wire on soil plots.



Figure J.62 Installation of chicken wire on soil plots.



Figure J.63 Installation of chicken wire on soil plots.



Figure J.64 Installation of chicken wire on soil plots.



Figure J.65 Pre-treatment plots layout.



Figure J.66 Pre-treatment plots layout.



Figure J.67 Pre-treatment plots layout.



Figure J.68 Pre-treatment plots layout.



Figure J.69 Pre-treatment plots layout.



Figure J.70 Pre-treatment plots layout.



Figure J.71 Pre-treatment plots layout.



Figure J.72 Pre-treatment plots layout.



Figure J.73 Pre-treatment plots layout.



Figure J.74 Pre-treatment plots layout.



Figure J.75 Pre-treatment plots layout.



Figure J.76 Pre-treatment plots layout.



Figure J.77 Pre-treatment plots layout.



Figure J.78 Pre-treatment plots layout.



Figure J.79 Pre-treatment plots layout.



Figure J.80 Pre-treatment plots layout.



Figure J.81 Pre-treatment plots layout.



Figure J.82 Pre-treatment plots layout.

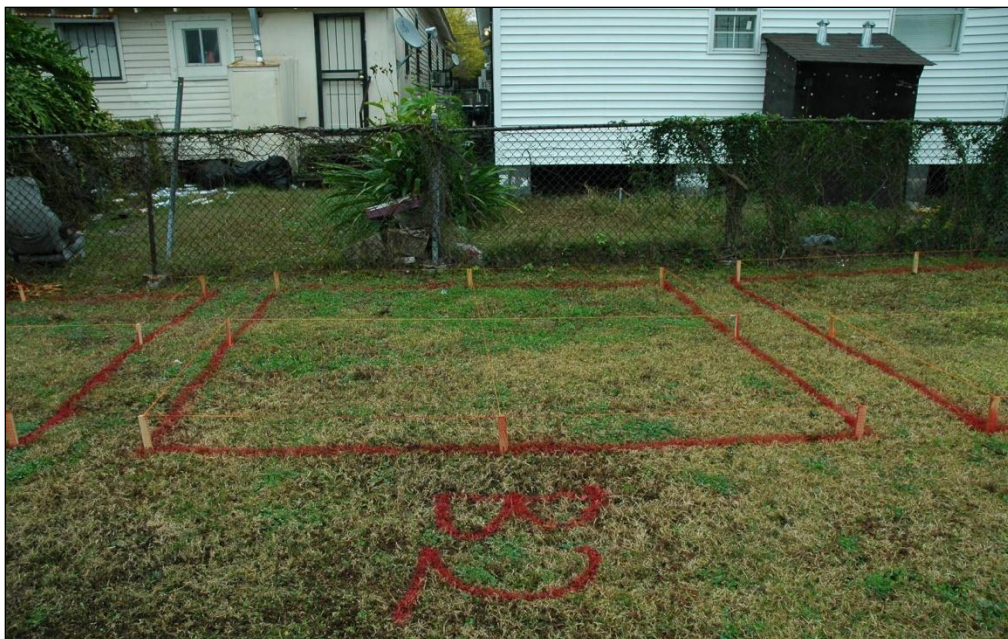


Figure J.83 Pre-treatment plots layout.



Figure J.84 Pre-treatment plots layout.



Figure J.85 Pre-treatment plots layout.



Figure J.86 Pre-treatment plots layout.



Figure J.87 Pre-treatment plots layout.



Figure J.88 Pre-treatment plots layout.



Figure J.89 Pre-treatment plots layout.



Figure J.90 Pre-treatment plots layout.



Figure J.91 Pre-treatment plots layout.



Figure J.92 Pre-treatment plots layout.



Figure J.93 Pre-treatment plots layout.



Figure J.94 Pre-treatment plots layout.



Figure J.95 Pre-treatment plots layout.



Figure J.96 Lysimeter installation into the post-treatment un-capped soil plots.

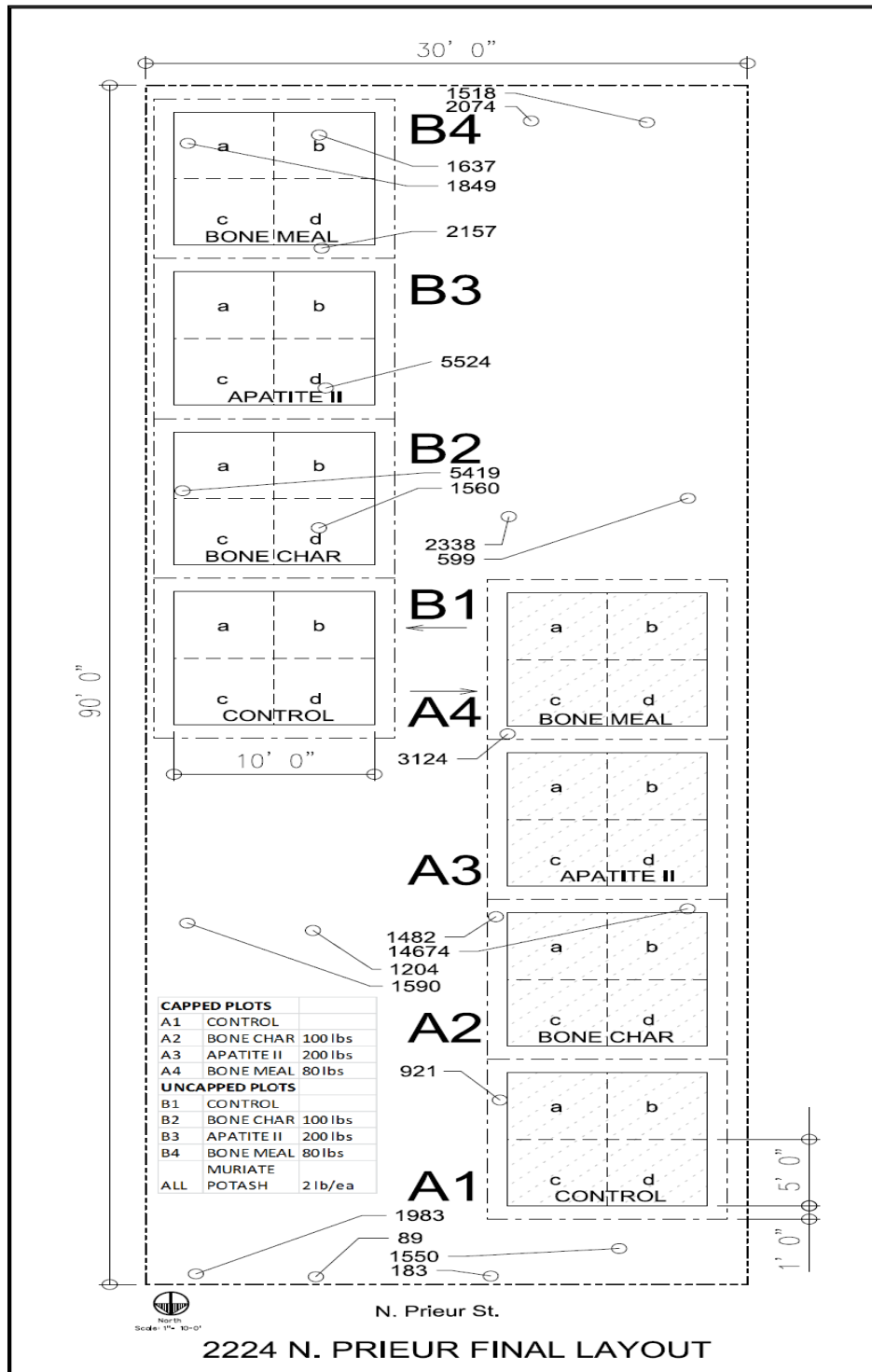


Figure J.97 2224 N. Prieur St. layout.

References

- Abdel Raouf, M.W. and Daifullah, A.A.M. (1997) Potential use of bone charcoal in the removal of antimony and europium radioisotopes from radioactive wastes. *Ads. Sci. Technol.*, 15, 559–569.
- Abel et al. (2012) Contribution of soil lead to blood lead in children: A study from New Orleans, LA. *Journal of Environmental Protection*, 3, 1704-1710.
- Abel et al. (2010) Lead distributions and risks in New Orleans following hurricanes Katrina and Rita. *Environmental Toxicology and Chemistry*, 29(7), 1429-1437.
- Admassu, W. and Breese, T. (1999) Feasibility of using natural fishbone apatite as a substitute for hydroxyapatite in remediating aqueous heavy metals. *J. Hazard Mater*, 69, 187–196.
- Abel, M.T., Cobb, G.P., Presley, S.M., Ray, G.L., Rainwater, T.R., Austin, G.P., Cox, S.B., Anderson, T., Leftwich, B., Kendall, R.J., and Suedel, B. (2010a) Lead distributions and risks in New Orleans following hurricanes Katrina and Rita. *Environ. Toxicol. Chem.*, 20, 1429-37.
- Abel, M.T., Suedel, B., Presley, S.M., Rainwater, T.R., Austin, G.P., Cox, S.B., McDaniel, L.N., Rigdon, R., Goebel, T., Zartman, R., Leftwich, B., Anderson, T., Kendall, R.J., and Cobb, G.P. (2010b) Spatial distribution of lead in urban surface soils of New Orleans Louisiana USA. *Environ. Geochem. Health.*, 32, 379-389.

- Arnich, N., Lanhers, M.C., Laurensot, F., Podor, R., Montiel, A. and Burnel, D. (2003) *In vitro* and *in vivo* studies of lead immobilization by synthetic hydroxyapatite. *Environ. Pollut.*, 124, 139–149.
- Aualiitia, P. (1987). The specific sorption of trace amounts of Cu, Pb, and Cd by inorganic particulates. *Water, Air, Soil Pollut.*, 35(1–2):172–185.
- Basta, N., Gradwohl, R., Snethen, K. and Schroder, J. (2001) Chemical immobilization of lead, zinc and cadmium in smelter contaminated soils using biosolids and rock phosphate. *J. Environ. Qual.*, 30, 1222–1230.
- Bellinger, D. (2008) Very low lead exposures and children’s neurodevelopment. *Curr. Opp. Pediatr.*, 20(2), 172-177.
- Bellinger, D.C. (2011) The protean toxicities of lead: new chapters in a familiar story. *Int. J. Environ. Res. Public Health*, 8, 2593-2628.
- Belluck, D.A., Benjamin, S.L., Baveye, P., Sampson, J. and Johnson, B. (2003) Widespread arsenic contamination of soils in residential areas and public spaces: an emerging regulatory or medical crisis?. *Int. J. Toxicol.*, 22, 109–128.
- Bennett, M.C. and Abram, J.C. (1967) Adsorption from solution on the carbon and hydroxyapatite components of bone char. *J. Colloid Interf. Sci.*, 23, 513–521.

- Berman, E. and McKiel, K. "Arch. Environ. Health," In: Nriagu, J.O., Ed., *The Biogeochemistry of Lead in the Environment, part A*. Elsevier/North Holland Biomedical Press, The Netherlands, 1978.
- Berti, W.R., and Cunningham, S.D. (1997) In-place inactivation of Pb in Pb-contaminated soils. *Environ. Sci. Technol.*, 31, 1359–1364.
- Berti, W.R., Cooper, E.M., Cunningham, S.D. and Vangronsveld, J. "Field Implementation-Practical Considerations," In: *Metal-Contaminated Soils: In Situ Inactivation and Phytoremediation*, Eds., Springer-Verlag and Landes Company, 1998.
- Bertinuson, J.R. and Clarck, C.S. "Interface," In: Nriagu, J.O., Ed., *The Biogeochemistry of Lead in the Environment, part A*. Elsevier/North Holland Biomedical Press, The Netherlands, 1978.
- Binns H., Gray, K.A., Chen, T., Finster, M.E., Peneff, N., Schaefer, P.D., Ovsey, V., Fernandes, J., Brown, M., and Dunlap B. (2004) Evaluation of landscape coverings to reduce soil lead hazards in urban residential yards: The Safer Yards Project. *Environ. Res.*, 96, 127-138.
- Blaylock, M.J., Salt, D.E., Dushenkov, S., Zakharova, O., Gussman, C., Kapulnik, Y., et al. (1997) Enhanced accumulation of Pb in Indian mustard by soil-applied chelating agents. *Environmental Science and Technology*, 31, 860-865.

- Bogden, J.D. and Louria, D.L. "Bull. Environ. Contam. Toxicol.," In: Nriagu, J.O., Ed., *The Biogeochemistry of Lead in the Environment, part A*. Elsevier/North Holland Biomedical Press, The Netherlands, 1978.
- Boisson, J., Mench, M., Vangronsveld, J., Ruttens, A., Kopponen, P., & De-Koe, T. (1999a) Immobilization of trace metals and arsenic by different soil additives: Evaluation by means of chemical extractions. *Communications in Soil Science and Plant Analysis*, 30, 365-387.
- Boisson, J., Ruttens, A., Mench, M., & Vangronsveld, J. (1999b) Evaluation of hydroxyapatite as a metal immobilizing soil additive for the remediation of polluted soils: Part 1. Influence of hydroxyapatite on metal exchangeability in soil, plant growth and plant metal accumulation. *Environmental Pollution*, 104, 225-233.
- Bostick, W.D. (2003) Use of apatite for chemical stabilization of subsurface contaminants: Final Report. U. S. Department of Energy; National Energy Technology Laboratory; COR: Richard Bush. 5-10.
- Bowen, H.J. "Trace Elements in Biochemistry," In: Nriagu, J.O., Ed., *The Biogeochemistry of Lead in the Environment, part A*. Elsevier/North Holland Biomedical Press, The Netherlands, 1978.
- Bradl, H. (2004) Adsorption of heavy metal ions on soils and soils constituents. *J Colloid Interface Sci*, 277, 1-18.

- Brown, S.L., Chaney, R. and Berti, B. (1999). Field test of amendments to reduce the in situ availability of soil lead. In W. W. Wenzel, D. C. Adrian, B. Alloway, H. E. Doner, C. Keller, M. Mench, R. Naidu, & G. M. Pierzynski (Eds.), Proceedings of the 5th International Conference on the Biogeochemistry of Trace Elements (pp. 506–507), Vienna, July 11–15.
- Brown, S.L., Chaney, R. L., Hallfrisch, J.G. and Xue, Q (2003a) Effect of biosolids processing on the bioavailability of lead in urban soils, *J. Environ. Qual.* 32, 100–108.
- Brown, S., Chaney, R., Hallfrisch, J., Ryan, J. and Berti, W. (2004) In situ soil treatments to reduce the phyto- and bioavailability of lead, zinc and cadmium. *J. Environ. Qual.*, 33, 522–531.
- Brown, S.L., Henry, C.L., Chaney, R.L., Compton, H. and DeVolder, P.S. (2003b) Using municipal biosolids in combination with other residuals to restore metal-contaminated mining areas, *Plant Soil* 249, 203–215.
- Brown, S.L., Chaney, R.L., Angel, J.S., & Baker, A.J.M. (1994a) Zinc and cadmium uptake by hyperaccumulator *Thlaspi caerulescens* grown in nutrient solution. *Soil Science Society of America Journal*, 59, p. 125-133.
- Brown, S.L., Chaney, R.L., Angel, J.S., & Baker, A.J.M. (1994b) Phytoremediation potential of *Thlaspi caerulescens* and bladder campion for zinc- and cadmium-contaminated soil. *Journal of Environmental Quality*, 23, p. 1151-1157.

- Bubb, J.M. and Lester, J.N. (1991) Impact of heavy metals on low land rivers and implications for the man and the environment. *Sci Total Environ*, 100, 207–258.
- Cao et al. (2008) Phosphate-induced lead immobilization from different lead minerals in soils under varying pH conditions. *Environmental Pollution*, 152, 184-192.
- Cao, R.X., Ma, L.Q., Chen, M., Singh, S. and Harris, W. (2003) Phosphate induced metal immobilization in a contaminated site. *Environ. Pollut.*, 122, 19–28.
- Cao, R.X., Ma, L.Q., Chen, M., Singh, S. and Harris, W. (2002) Impacts of phosphate amendments on lead biogeochemistry at a contaminated site. *Environ. Sci. Technol.*, 36, 5296–5304.
- Cao, R.X., Ma, L.Q., Rhue, D. and Appel, C. (2004) Mechanisms of lead, copper and zinc retention by phosphate rock. *Environ. Pollut.*, 131, 435–444.
- Cao, X., Ma, L.Q., Ming, C., Satya, S.P. and Harris W.G. (2002) Impacts of phosphate amendments on lead biogeochemistry at a contaminated site. *Environ. Sci. Technol.*; 36, 5296-5304.
- Cao, X., Ma, L.Q., Ming, C., Satya, S.P. and Harris W.G. (2003) Phosphate-induced metal immobilization in a contaminated site. *Environmental Pollution* 122, 19-28.

- Cao, X., Ma, L.Q., Singh, S.P. and Zhou, Q. (2008) Phosphate-induced lead immobilization from different lead minerals in soils under varying pH conditions. *Environmental Pollution*, 152, 184-192.
- Campanella, R. and Mielke H.W. (2008) Human geography of New Orleans' urban soil lead contaminated geochemical setting. *Environ Geochem Health*, 30(6), 531–40.
- Campbell, W.J. "Environ. Sci. Technol.," In: Nriagu, J.O., Ed., *The Biogeochemistry of Lead in the Environment, part A*. Elsevier/North Holland Biomedical Press, The Netherlands, 1978.
- Canfield, R.L., Henderson, C. R., Jr., Cory-Slechta, D. A., Cox, C.; Jusko, T. A., Lanphear, B. P. (2003) Intellectual impairment in children with blood lead concentrations below 10 µg per deciliter. *N. Engl. J. Med.* 348, 1517-1526.
- Cannon, H.L. and Bowels, J.M. "Science," In: Nriagu, J.O., Ed., *The Biogeochemistry of Lead in the Environment, part A*. Elsevier/North Holland Biomedical Press, The Netherlands, 1978.
- Casteel, S.W., Blanchar, R.W. and Yang, J. (1997) Effect of phosphate treatment on the bioavailability of lead from the Jasper County site— Joplin, Missouri. Missouri Department of Natural Resources, Jefferson City, MO.
- Casteel, S.W., Weis, C.P., Henningsen, G.M., et al. (2006) Estimation of relative bioavailability of lead in soil and soil like materials using young swine. *Environ Health Perspect*, 114, 1162–1171.

Center for Disease Control and Prevention (CDC) (2012) CDC updates guidelines for children's lead exposure. *Environmental Health Perspectives*, 120(7), A268.

Center for Disease Control and Prevention (CDC) (2012) CDC response to advisory committee on childhood lead poisoning prevention recommendations in "low lead level exposure harm children: a renewed call for primary prevention", Atlanta, GA:U.S. Centers for Disease Control and Prevention.

CDC (2004) Preventing lead exposure in young children: A housing-based approach to primary prevention of lead poisoning. Atlanta: US Department of Health and Human Services.

CDC (2005) Blood lead levels—United States, 1999–2002. *Morb. Mortal. Wkly. Rep.* 54(20), 513–516.

CDC (2009) Fourth National Report on Human Exposure to Environmental Chemicals. Atlanta,GA: CDC. <http://www.cdc.gov/exposurereport/>

Cecil, K.M., Brubaker, C.J., Adler, C.M., Dietrich, K.N., Altaye, M., Egelhoff, J.C., et al. (2008) Decreased brain volume in adults with childhood lead exposure. *PLoS Med.*, 5(5), 112.

Cecil, K.M., Dietrich, K.N., Altaye, M., Egelhoff, J.C., Lindquist, D.M., Brubaker, C.J., et al. (2011) Proton magnetic resonance spectroscopy in

- adults with childhood lead exposure. *Environ. Health Perspect.*, 119, 403-408.
- Chaney, R.L. and Ryan, J.A. (1994) Risk Based Standards for Arsenic, Lead and Cadmium in Urban Soils, Kreysa, G. and J. Wieser, Eds., DECHEMA, Frankfurt.
- Chaney, R., Malik, M., Li, Y.M., Brown, S.L., Brewer, E.P., Angle, J.S., et al. (1997) Phytoremediation of soil metals. *Current Opinion in Biotechnology*, 8, 279-284.
- Chaney, R.L., H.W. Mielke, and S.B. Sterrett (1989) Speciation, mobility, and bioavailability of soil lead, *Environ. Geochem. Health*, Suppl. 11, 109.
- Chaney, R.L., Mielke, H.W. and Sterrett, S.B.(1989) In lead in soil: issues and guidelines. Davies, B. E., Wixson, B. G., (Eds). *Environmental Geochemistry and Health*, 9 (Suppl.), 105-130.
- Chaney, R.L., Mielke, H.W. and Sterrett, S.B. (1989) Speciation, mobility, and bioavailability of soil lead. *Environmental Geochemistry and Health*, 11, 105-129.
- Chen, A., Cai, B., Dietrich, K., Radcliffe, J., and Rogan, W. (2007) Lead exposure, IQ, and behavior in urban 5-to 7-year-olds: does lead affect behavior only by lowering IQ? *Pediatrics* 119, e650.
- Chen et al. (1997) Effects of pH on heavy metal sorption on mineral apatite. *Environmental Science and Technology*, 31(3), 624–631.

- Chen et al. (2007) Evaluation of different phosphate amendments on availability of metals in contaminated soil. *Ecotoxicology and Environmental Safety*, 67, 278-285.
- Chen et al. (2006) The effect of grain size of rock phosphate amendment on metal immobilization in contaminated soils. *Journal of Hazardous Materials B*, 134, 74-79.
- Chen, H.M., Zheng, C.R., Tu, C., & Shen, Z.G. (2000) Chemical methods and phytoremediation of soil contaminated with heavy metals. *Chemosphere*, 41, 229-234.
- Chen, M., Ma, L.Q., Singh, S., Cao, R. and Melamed, R. (2003) Field demonstration of *in situ* immobilization of soil Pb using P amendments. *Adv Environ Res*, 8, 93–102.
- Chen, S., Zhu, Y. and Ma, Y. (2006) The effect of grain size of rock phosphate amendment on metal immobilization in contaminated soils. *J. Hazard Mater*, 134, 74–79.
- Chen, S.B., Zhu, Y.G., Ma, Y.B., and McKay, G. (2006) Effect of bone char application on Pb bioavailability in a Pb-contaminated soil. *Env. Pollut* 139(3), 433-439.
- Chen, T.C., Macauley, E., & Hong, A. (1995) Selection and test of effective chelators for removal of heavy metals from contaminated soils. *Canadian Journal of Civil Engineering*, 22(6), 1185-1197.

- Chen, X., Wright, J., Conca, J. and Peurrung, L. (1997a) Effects of pH on heavy metal sorption on mineral apatite. *Environ. Sci. Technol.*, 31, 624–631.
- Chen, X., Wright, J., Conca, J. and Perurrung, L. (1997b) Evaluation of heavy metal remediation using mineral apatite. *Water Air Soil Pollut.*, 98, 57–78.
- Chen, X., Wright, J., Conca J.L. and Peurrung, L.M. (1997) Evaluation of heavy metal remediation using mineral apatite. *Water, Air Soil Pollut.* 98, 57-78.
- Cheung, C.W., Porter, J.F. and McKay, G. (2001) Sorption kinetic analysis for the removal of cadmium ions from effluents using bone char. *Wat. Res.*, 35(3), 605-612.
- Chlopecka, A., & Adriano, D.C. (1997) Influence of zeolite, apatite and Fe-oxide on Cd and Pb uptake by crops. *The Science of the Total Environment*, 207(2-3), 195-206.
- Chiodo, L, Jacobson, S, Jacobson, L. (2004) Neurodevelopmental effects of postnatal lead exposure at very low levels. *Neurotox. Teratol.* 26, 359-371.
- Cholak, J., Schafer, L.J. and Sterling, T.D. "J. Air Pollut. Contr. Assoc.," In: Nriagu, J.O., Ed., *The Biogeochemistry of Lead in the Environment*, part A. Elsevier/North Holland Biomedical Press, The Netherlands, 1978.
- Choy, K.K.H. and McKay, G. (2005) Sorption of cadmium, copper, and zinc ions onto bone char using Crank diffusion model. *Chemosphere*, 60, 1141-1150.

- Chrysochoou, M., Dermatas, D. and Grubb, D. (2007) Phosphate application to firing range soils for Pb immobilization: the unclear role of phosphate. *J Hazard Mater*, 144, 1–14.
- Clapp, T.C., Umbreit, T.H., Meeker, R.J., Kosson, D.S. and Gray, D. (1991) Bioavailability of lead and chromium from encapsulated pigment materials. *Bull. Environ. Contam. Toxicol.*, 46, 271-275.
- Clark, S., Bornschein, R. Succop, P. Roda, S. and Peace, B.(1991) Urban lead exposures of children in Cincinnati, OH, *Chem. Speciation Bioavailability*, 3(3/4), 163.
- Conca, J.L., Ping, L.N., Parker, B., Moore, B., Adams, A., Wright, J. and Heller, P. (2000) PIMS – Remediation of metal contaminated waters and soils. Proc. Second Int. Conf. Remediation of Chlorinated and Recalcitrant Compounds (May 2000) with an addendum from ICAM 2000.
- Cotter-Howells, J. (1996) Lead phosphate formation in soil. *Environmental Pollution*, 93(1), 9-16.
- Cotter-Howells J., Champness P.E., Charnock J.M., and Pattrick R.A.D. (1994) Identification of pyromorphite in mine-waste contaminated soils by ATEM & EXAFS. *Eur. J. Soil Sci.*, 45, 393-402.
- Cotter-Howells, J. (1996) Lead phosphate formation in soils. *Environ. Pollut.*, 93(1), 9-16.

- Cotter-Howells, J., and Caporn, S. (1996). Remediation of contaminated land by formation of heavy metal phosphates. *App. Geochem.*, 11, 335–342.
- Cotter-Howells, J. and Thornton, L. (1991) Source and pathways of environmental lead to children in a Derbyshire mining village. *Environmental Geochemistry and Health*, 13(2).
- Cotter-Howells, J.D., Champness, P.E., Charnock, J.M. and Patrick, R.A.P. (1994) Identification of pyromorphite in mine-waste contaminated soils by ATEM and EXAFS. *Eur. J. Soil Sci.*, 45, 393-402.
- Davies, D.J.A., Thornton, I., Watt, J.M., Culbard, E.B., Harvey, P.G., Delves, H.T., Sherlock, J.C., Smart, G.A., Thomas, J.F.A. and Quinn, M.J. (1990) Lead intake and blood lead in two-year-old U.K. urban children. *Science of the Total Environment*, 90, 13-29.
- Davis, A., Drexler, J.W., Ruby, M.V. and Nicholson, A. (1993) Micromineralogy of mine wastes in relation to lead bioavailability. *Environ Sci. Technol.*, 27, 1415-1425.
- Danny, C.K.K., Cheung, C.W., Choy, K.K.H., Porter, J.F. and McKay, G. (2004) Sorption equilibria of metal ions on bone char. *Chemosphere*, 54, 273-281.
- Davis, B.E. (1995) Lead. In: Alloway, B. J. (eds) *Heavy metals in soil*. Blackie Academic and Professional, Glasgow, 208–223.

- Davis, J.G., Weeks, G., and Parker, M.B. (1995) Use of deep tillage and liming to reduce zinc toxicity in peanuts grown on flue dust contaminated land. *Soil Technology*, 8(2), 85-95.
- DeTreville, R.T.P. (1964) *Arch. Environ. Health*, 8, 212.
- Dieter, M.P., Matthews, H.B., Jeffcoat, R.A. and Moseman, R.F. (1993) *J. Toxicol. Environ. Health*, 39, 79.
- Drexler, J.W., & Brattin, W.J. (2007) An in vitro procedure for estimation of lead relative bioavailability: With validation. *Human and Ecological Risk Assessment*, 13, 383-401.
- Dudka, S., Piotrowska, M. and Terelak, H. (1996) Transfer of cadmium, lead, and zinc from industrially contaminated soil to crop plants: A field study. *Environmental Pollution*, 94, 181-188.
- Durum, W.H., Hem, J.D. and Heidel, S.G. "U.S. Geol. Survey Circular," In: Nriagu, J.O., Ed., *The Biogeochemistry of Lead in the Environment*, part A. Elsevier/North Holland Biomedical Press, The Netherlands, 1978.
- Edwards, R., Rebedda, I., Lepp, N.W., and Lovell, A.J. (1999) An investigation into the mechanism by which synthetic zeolites reduce labile metal concentrations in soils. *Journal of Environmental Geochemistry and Health*, 21(2), 157-173.
- Elias, R. (1989) Soil-lead abatement overview: alternatives to soil replacement. *Environ. Geochem. Health Suppl* 9, 301-305.

Environmental Security Technology Certification Program (ESTCP) (2006)

PIMSTTM: remediation of soil and groundwater contaminated with metals.

Cost and performance report.

Eric Deydier, E., Guilet, R., Sarda, S. and Sharrock, P. (2005) Physical and chemical characterisation of crude meat and bone meal combustion residue: "waste or raw material. *J. Hazard Mater.* 121(1-3):141-8.

Eusden, J.D., Gallagher, L., Eighmy, T.T., Crannell, B.S., Krzanowski, J.R., Butler, L.G., Cartledge, F.K., Emery, E.F., Shaw, E.L. and Francis, C.A. (2002) Petrographic and spectroscopic characterization of phosphate-stabilized mine tailings from Leadville, Colorado. *Waste Manage.*, 22, 117–135.

Evanko, F.R., & Dzombak, D.A. (1997) Remediation of metals-contaminated soils and groundwater. Technology Evaluation Report prepared for Ground Water Remediation Technologies Analysis Center, TE-97-01. Pittsburgh, PA: Author.

Everett, J.C., Day, C.L. and Reynolds, D. "Food Cosmet. Toxicol.," In: Nriagu, J.O., Ed., *The Biogeochemistry of Lead in the Environment, part A*. Elsevier/North Holland Biomedical Press, The Netherlands, 1978.

Farfel, M.R., Orlova, A., Chaney, R.L., Lees, P.S/J. Rhode, C. and Ashley, P.J. (2005) Biosolids compost amendment for reducing soil lead hazards: a

- pilot study of Orgro amendment and grass seeding in urban yards. *Sci. Total Env.*, 340, 81-95.
- Federal Remediation Technologies Roundtable (FRTR) (2001) Retrieved September 28, 2011, from http://www.frtr.gov/matrix2/top_page.html
- Fransworth et al. (2003) Dissolution of lead phosphate. Research Experience for Undergraduates, 1-13.
- Gabalton, C., Marzal, P., Ferrer, J. and Seco, A. (1996) Single and competitive adsorption of Cd and Zn onto a granular activated carbon. *Water Res.*, 30, 3050–3060.
- Garcia-Sanchez, A., Alastuey, A., and Querol, X. (1999) Heavy metal adsorption by different minerals: Application to the remediation of polluted soils. *Science of the Total Environment*, 242(1-3), 179-188.
- Giammar et al. (2000) Lead phosphate solubility in water and soil suspensions. *Environmental Science & Technology*, 32(3), 388-393.
- Gilbert, S.G. and Weiss, b. (2008) A rationale for lowering the blood lead action level from 10 to 2 µg/dL *Neurotox.*, 27(5) 693-701.
- Girgis, B.S., Abdel Kader, A. and Aly, A.N.H. (1997) Development of porosity in bone char during decolourization of sugar syrup. *Ads. Sci. Technol.*, 15, 277–287.

- Cordell, Dana; Drangert, Jan-Olof; White and Stuart (2009) The story of phosphorus: Global food security and food for thought. *Global Environmental Change*, 19(2), 292–305.
- Gould, E. (2009) Childhood lead poisoning: Conservative estimates of the social and economic benefits of lead hazard control. *Environmental Health Perspective*, 117(7), 1162-1167.
- Goyer, R.A. "Toxic Effects of Metals," In: C.D. Klaassen, Ed., *Cassarett and Doull's Toxicology, The Basic Science of Poisons*, 5th Edition, McGraw-Hill, New York, 1996.
- Graziano, J.H., Lolocono, N.J., Maddaloni, M., Chillrud, S., and Blum, C.B. (2001) Assessing the oral bioavailability of lead in soil in humans. Presented at the Annual Meeting of the Society of Toxicology, San Francisco, CA.
- Grewe, K. (1985) Planung und Trassierung römischer Wasserleitungen, Wiesbaden: Chmielorz, ISBN 3-87124-025-7.
- Gworek, B. (1992) Lead inactivation in soils by zeolites. *Plant and Soil*, 143, 71-74.
- Hamon, R.E., Mclaughlin, M.J., and Cozens, G. (2002) Mechanisms of attenuation of metal availability in in situ remediation treatments. *Environmental Science and Technology*, 36, 3991-3996.

- Harter, R.D. (1983) Effect soil pH on adsorption of lead, copper, zinc, and nickel. *Soil Sci. Soc. Am. J.*, 47, 47-51.
- Harvey et al. (1983) *Devel. Psychol.*, 6, 145-156.
- Hashimoto, Y., Takaoka, M., Oshita, K. and Tanida, H. (2009) Incomplete transformation of Pb to pyromorphite by phosphate-induced immobilization investigated by X-ray absorption fine structure (XAFS) spectroscopy. *Chemosphere*, 76, 616-622.
- Hawkes, H.E. and Webb, J.S. "Geochemistry in Mineral Exploration," In: Nriagu, J.O., Ed., *The Biogeochemistry of Lead in the Environment, part A*. Elsevier/North Holland Biomedical Press, The Netherlands, 1978.
- Hayes, K.F. and Katz, L.E. (1996) Application of X-ray absorption spectroscopy for surface complexation modeling of metal ion sorption. In: *Brady PV*, editor. *Physics and Chemistry of Mineral Surfaces*. CRC Press.
- Hettiarachchi, G.M. and Pierzynski, G.M. (2004) Soil lead bioavailability and in situ remediation of lead-contaminated soils: a review. *Environmental Progress*, 23, 78-93.
- Hettiarachchi, G.M., and Pierzynski, G.M. (2002) In situ stabilization of soil lead using phosphorous and manganese oxide: Influence of plant growth. *Journal of Environmental Quality*, 31, 564-572.

- Hettiarachchi, G.M., Pierzynski, G.M. and Ransom, M.D. (2000) In situ stabilization of soil lead using phosphorus and manganese oxide. *Environ. Sci. Technol.*, 34, 4614–4619.
- Higgs, F.J., Mielke, H.W. and Brisco, M. (1999) Soil Lead at Elementary Public Schools: Comparison between School Properties and Residential Neighbourhoods of New Orleans. *Environ. Geochem. Health* 21, 27-36.
- Hirschler, D.A., Gilbert, L.F., Lamb, F.W. and Niebylski, L.M. (1957) *Ind. Eng. Chem.*, 49, 1131.
- Hirschler, D.A. and Gilbert, L.F. (1964) Nature of lead in automotive exhaust gas. Archives of environmental health, symposium of lead.
- Hodge, A. Trevor (1992) Roman Aqueducts & Water Supply. London: Duckworth, ISBN 0-7156-2194-7.
- Hodson, M.E.; Valsami-Jones, E.; Cotter-Howells, J.D. (2000), “Bonemeal Additions as a Remediation Treatment for Metal Contaminated Soil,” *Environ. Sci. Technol.*, 34, 3501-3507.
- Hodson, M.E., Valsami-Jones, E., Cotter-Howells, J.D., Dubbin, W.E., Kemp, A.J., Thornton, I., and Warren, A. (2001) Effect of bone meal (calcium phosphate) amendments on metal release from contaminated soils- a leaching column study. *Environ. Pollut.*, 112, 233-243.
- Hooda, P.S. (2010) Assessing bioavailability of soil trace elements. In: Hooda, P. S. (Ed.), *Trace Elements in Soils*. John Wiley & Sons Ltd, UK, 229-266.

- Hunt, A., Johnson, D.L., Thornton, I. and Watt, J.M. (1993) Apportioning the sources of lead in house dusts in the London Borough of Richmond, England. *Sci. Total Environ.*, 138, 183–206.
- Hunt, A., Johnson, D.L., Watt, J.M. and Thornton, I. (1992) Characterizing the sources of particulate lead in house dust by automated scanning electron microscopy. *Environmental Science and Technology*, 26, 1513-1523.
- Johnson, D.L. and Bretsch J.K. (2002) Soil lead and children's blood lead levels in Syracuse, NY, USA. *Environ Geochem Health*, 24, 375–85.
- Jones, R.L., Homa, D.M., Meyer, P.A., Brody, D.J., Caldwell, K.L., Pirkle, J.L., Brown, M.J. (2009) Trends in blood lead levels and blood lead testing among US children aged 1 to 5 years, 1988-2004. *Pediatrics*, 123(3), 376-85.
- Jordan, L.D. and Hogan, D.J. "N.Z.J. Sci.," In: Nriagu, J.O., Ed., *The Biogeochemistry of Lead in the Environment, part A*. Elsevier/North Holland Biomedical Press, The Netherlands, 1978.
- Joselow, M.M. and Bogden, J.D. "Am. J. Public Health," In: Nriagu, J.O., Ed., *The Biogeochemistry of Lead in the Environment, part A*. Elsevier/North Holland Biomedical Press, The Netherlands, 1978.
- Juhasz, A.L., Weber, J. and Smith, E. (2011) Impact of soil particle size and bioaccessibility on children and adult lead exposure in peri-urban contaminated soils. *Journal of Hazardous Materials*, 186, 1870-1879.

- Jusko, T, Henderson, C., Lanphear, B., Cory-Slechta, D., Parsons, P., and Canfield, R. (2008) Blood lead concentrations < 10 g/dL and child intelligence at 6 years of age. *Environ. Health Perspect.*, 116, 243-248.
- Kabata-Pendias, A. (1980). Heavy metals sorption by clay minerals and oxides of iron and manganese. *Mineralogia Polonica*, 11(2):3–13.
- Kloke, A. and Riebartsch, K. "Naturwissenschaften," In: Nriagu, J.O., Ed., *The Biogeochemistry of Lead in the Environment, part A*. Elsevier/North Holland Biomedical Press, The Netherlands, 1978.
- Knox, A., Kaplan, D., Adriano, D., Hinton, T. and Wilson, M. (2003) Apatite and phillipsite as sequestering agents for metals and radionuclides. *J. Environ. Qual.*, 32, 515–525.
- Kotuby-Amacher, J. and Gambrell, R.P. (1988) Factors affecting trace metal mobility in subsurface soils. Editor. Factors affecting trace metal mobility in subsurface soils. U. S. Environmental Protection Agency. EPA/600/2-88/036.
- Laidlaw, M.A.S. Association between soil lead and blood lead — evidence. website [http:// www.urbanleadpoisoning.com/](http://www.urbanleadpoisoning.com/).
- Laidlaw, M.A.S., Mielke H.W., Filippelli G.M., Johnson D.L. and Gonzales C.R. (2005) Seasonality and children's blood lead levels: developing a predictive model using climatic variables and blood lead data from

- Indianapolis, Indiana, Syracuse, New York and New Orleans, Louisiana (USA). *Environ Health Perspect*, 113(6), 793–800.
- Laidlaw, M.A.S., Zahran S., Mielke H.W., Taylor M.P. and Filippelli G.M. (2012) Re-suspension of lead contaminated urban soil as a dominant source of atmospheric lead in Birmingham, Chicago, Detroit and Pittsburgh, USA. *Atmos Environ*, 49, 302–10.
- Landsdown, R., Yule, W., Urbanowicz, M.A. and Hunter, J. (1986) *Int. Arch. Occup. Environ. Health*, 57, 225-235.
- Lanphear, B.P., Hornung, R., Khoury, J., Yolton, K., Baghurst, P., Bellinger, D.C., Canfield, R.L., Dietrich, K.N., Bornschein, R., Greene, T., Rothenberg, S.J., Needleman, H.L., Schnaas, L., Wasserman, G., Graziano, J., and Roberts, R. (2005) Low-level environmental lead exposure and children's intellectual function: an international pooled analysis. *Environ. Health Perspect.*, 113, 894-899.
- Laperche, V. and Traina, S. (1998) Immobilization of Pb by hydroxyapatite. In: Jenne E (ed) *Adsorption of metals by geomedia*. Academic, London, 255–276.
- Laperche, V., Logan, T.J., Gaddam, P., and Traina, S.J. (1997) Effect of apatite amendments on plant uptake of lead from contaminated soil. *Environmental Science and Technology*, 31, 2745-2763.

- Laperche, V., Traina, S.J. Gaddham,P., and Logan, T. (1996) Chemical and mineralogical characterizations of Pb in a contaminated soil: reactions with synthetic apatite. *Environ. Sci. Technol.*, 30, 3321-3326.
- Laperche (2000) Immobilization of lead by in situ formation of lead phosphates in soils. Environmental Restoration of Metals-Contaminated Soils. *CRC Press*. p.61.
- Laperche, V., Traina, S.J. Gaddham,P., and Logan, T. (1996) Chemical and mineralogical characterizations of Pb in a contaminated soil: reactions with synthetic apatite. *Environ. Sci. Technol.*, 30, 3321-3326.
- Leh, H.O. "Gesunde Pflanz," In: Nriagu, J.O., Ed., *The Biogeochemistry of Lead in the Environment, part A*. Elsevier/North Holland Biomedical Press, The Netherlands, 1978.
- Levin, R., Brown, M.J., Kashtock, M.E., Jacobs, D.E., Whelan, E.A., Rodman, J., Schock, M.R., Padilla, A. and Sinks, T. (2008) Lead exposures in U.S. children, 2008: implications for prevention. *Environmental Health Perspective*, 116, 1285-1293.
- Li, Y., Chaney, R., Siebielec, G. and Kerschner, B. (2000) Response of four turf grass cultivars to limestone and biosolids-compost amendment of a zinc and cadmium contaminated soil at Palmerton, PA. *J. Environ. Qual.*, 29, 1440–1447.

- Lin, C., Lian, J. and Fang, H. (2005) Soil lead immobilization using phosphate rock. *Water Air Soil Pollut.*, 161, 113–123.
- Lindsay, W.L. (1979) Lead. In: *Chemical Equilibria in Soils*. John Wiley & Sons, Inc., New York, 329-342.
- Litt, J.S., Hynes, H.P., Carroll, P., Maxfield, R., McLaine, P. and Kawecki, C. (2002) Lead safe yards,; a program for improving health in urban neighborhoods, *J. Urban Technol.*, 9(2), 71-93.
- Lower, S., Maurice, P. and Traina, S.J. (1998) Simultaneous dissolution of hydroxylapatite and precipitation of hydroxypyromorphite: direct evidence of homogeneous nucleation. *Geochim Cosmochim Acta*, 62, 1773–1780.
- Lothenbach, B., Furrer, G. and Schulin, R. (1997) Immobilization of heavy metals by polynuclear aluminum and montmorillonite compounds. *Environmental Science and Technology*, 1452-1462.
- Ma et al. (1994) Effects of NO_3^- , Cl^- , F^- , SO_4^{2-} , and CO_3^{2-} on Pb^{2+} immobilization by hydroxyapatite. *Environmental Science & Technology*, 28(3), 408-418.
- Ma et al. (1993) In situ lead immobilization by apatite. *Environmental Science & Technology*, 27(9), 1803-1810.
- Ma, L.Q. and Rao, G. (1999) Aqueous Pb reduction in Pb-contaminated soils by phosphate rocks. *Water Air Soil Pollut.*, 110, 1–16.
- Ma, L.Q. and Rao, G.N. (1997) Effects of phosphate rock on sequential chemical extraction of lead in contaminated soils. *J. Environ. Qual.*, 26, 788-794.

- Ma, Y.Q., Logan, T.J. and Traina, S.J. (1995) Lead immobilization from aqueous solutions and contaminated soils using phosphate rocks. *Environ. Sci. Technol.*, 29, 1118–1126.
- Ma, Y.Q., Traina, S.J., Logan, T.J. and Ryan, J.A. (1993) In situ lead immobilization by apatite. *Environ. Sci. Technol.*, 27, 1803–1810.
- Ma, Y.Q., Traina, S.J., Logan, T.G. and Ryan J.A. (1994) Effects of Aqueous Al, Cd, Cu, Fe(II), Ni and Zn on Pb Immobilization by Hydroxyapatite. *Environ. Sci. Technol.*, 28, 1219-1228.
- Ma, Y.Q., Traina, S.J., Logan, T.G. and Ryan J.A. (1993) *In situ* immobilization by apatite. *Environ. Sci. Technol.*, 28, 1803-1610.
- Macher, S.D. and Hosick, T.J. (2004) Determination of soil lead variability in residential soil for remediation decision making. *Water Air Soil Pollut.*, 151, 305-322.
- Martin T.A. and Ruby M.V. (2004) Review of in situ remediation technologies for lead, zinc, and cadmium in soil. Wiley Periodicals, Inc., 35-53. DOI: 10.1002/rem.20011.
- Mavropoulos, E., Rocha, N., Morieira, J., Rossi, A. and Soares, G. (2004) Characterization of phase evolution during lead immobilization by synthetic hydroxyapatite. *Mater Charact.*, 53, 71–78.

- Mavropoulos, E., Rossi, A., Costa, A., Perez, C., Moreira, J. and Saldanha, M. (2002) Studies on the mechanisms of lead immobilization by hydroxyapatite. *Environ. Sci. Technol.*, 36, 1625–1629.
- McGowen, S.L., Basta, N.T. and Brown, G.O. (2001) Use of diammonium phosphate to reduce heavy metal solubility and transport in smelter-contaminated soil. *J. Environ. Qual.*, 30, 493–500.
- McGrath, S.P. and Cunliffe, C.H. (1985) A simplified method for the extraction of the metals Fe, Zn, Cu, Ni, Cd, Pb, Cr, Co and Mn from soils and sewage sludges. *Journal of Science Food and Agriculture*, 36, 794-798.
- McKay, G. and Bino, M.J. (1990) Simplified optimization procedure for fixed bed adsorption systems. *Water, Air, Soil Pollution*, 51, 33-41.
- McKay, G. and Bino, M.J. (1987) Adsorption of pollutants onto activated carbon in fixed beds. *J. Chem. Technol. Biotechnol.*, 37, 81–93.
- McKenzie, R. M. (1980) The adsorption of Pb and other heavy metals on oxides of manganese and iron. *Aust. J. Soil Res.*, 18(1): 61-73.
- McLean, J.E. and Bledsoe, B.E. (1992) Behavior of metals in soil. *USEPA, ground water issue*, 1-25.
- Medlin, E.A. (1997) An *In Vitro* Method for Estimating the Relative Bioavailability of Lead in Humans; MS Thesis. University of Colorado, Boulder, CO, USA.

- Melamed, R., Cao, X., Chen, X., Ma, L.Q. (2003) Field assessment of lead immobilization in a contaminated soil after phosphate application. *Sci. Total Environ*; 305, 117-127.
- Mench, M.J., Didier, V.L., Loffler, M., Gomez, A. and Masson, P. (1994) A mimicked in-situ remediation study of metal-contaminated-soils, with emphasis on cadmium and lead. *Journal of Environmental Quality*, 23, 58-63.
- Mielke, H.W. (1994) Lead in New Orleans Soils: New Images of an Urban Environment. *Environ. Geochem. Health* 16(3/4), 123-128.
- Mielke, H.W. (1993) Lead dust contaminated U.S.A. Communities: comparison of Louisiana and Minnesota. *Appl. Geochem. Suppl.*, 2, 257-261.
- Mielke, H.W. (1991) Lead in residential soils: background and preliminary results of New Orleans. *Water, Air, and Soil Pollution*, 57-58, 111-119.
- Mielke, H.W., Anderson, J., Berry, K., Mielke Jr., P.W., Chaney, R.L. and Leech, M. (1983) Lead concentrations in inner-city soils as a factor in the child lead problem. *American Journal of Public Health*, 73, 1366-1369.
- Mielke, H.W. and Reagan, P.L. (1998) Soil is an important source of childhood lead exposure. *Environmental Health Perspectives*, 106(1), 217-229.
- Mielke, H.W. and Zahran, S., (2012) The urban rise and fall of air lead (Pb) and the latent surge and retreat of societal violence. *Environ. Int.*, 43, 48-55.

- Mielke, H.M., Dugas, D., Mielke, P.W., Smith, K.S., Smith, S.L., and Gonzales C.R. (1997) Associations between lead dust contaminated soil and childhood blood lead: a case study of Urban New Orleans and Rural Lafourche Parish, Louisiana, USA. *Environ. Health Perspect.*, 105(9), 950-954.
- Mielke, H.W., Gonzales, C.R. and Mielke, P.W. (2011) The continuing impact of lead dust on children's blood lead: Comparison of public and private properties in New Orleans. *Environmental Research.*, 111, 1164-1172.
- Mielke, H.W., Gonzalez, C.R., Powell, E., Jatun, M., and Mielke, P. W. (2007) Nonlinear association between soil lead and blood lead of children in metropolitan New Orleans, Louisiana: 200-2005. *Sci. Total Environ.*, 388, 45-53.
- Mielke, H.W., Gonzales, C.R., Powell, E.T. and Mielke, P.W. (2013) Environmental and health disparities in residential communities of New Orleans: the need for soil lead intervention to advance primary prevention. *Environmental International*, 51, 73-81.
- Mielke, H.W., Gonzales, C., Powell, E. and Mielke Jr., P.W. (2005b) Changes of multiple metal accumulation (MMA) in New Orleans soil: preliminary evaluation of differences between survey I (1992) and survey II (2000). *Int. J. Environ. Res. Public Health*, 2, 84-90.

- Mielke H.W., Gonzales C.R. and Mielke P.W. (2011b) The continuing impact of lead (Pb) dust on children's blood lead: comparison of public and private properties in New Orleans. *Environ Res*, 111(8), 1164–72.
- Mielke H.W., Gonzales C.R., Smith M.K. and Mielke P.W. (2000) Quantities and associations of lead, zinc, cadmium, manganese, chromium, nickel, vanadium, and copper in fresh Mississippi alluvium and New Orleans alluvial soils. *Sci Total Environ*, 246, 249–59.
- Mielke, H.W., Gonzales, C.R., Smith, M.K. and Mielke, P.W. (1999) The urban environment and children's health: Soils as an integrator of lead, zinc, and cadmium in New Orleans, Louisiana, USA. *Environmental Research Section A*, 81(2), 117-129.
- Mielke H.W., Laidlaw M.A.S. and Gonzales C.R. (2011a) Characterization of lead (Pb) from traffic in 90 U.S.A. urbanized areas: review of urban lead dust and health. *Environ. Int.*, 37, 248–57.
- Mielke, H.W., Laidlaw, M.A.S. and Gonzales, C.R. (2011) Estimation of leaded (Pb) gasoline's continuing material and health impacts on 90 US urbanized areas. *Environment International*, 37, 248-257.
- Mielke, H.W., Powell, E.T., Gonzales, C.R., Mielke, P.W. Jr, Ottesen, R.T., Langedal, M. (2006) New Orleans soil lead (Pb) cleanup using Mississippi River alluvium: need, feasibility, and cost. *Environ. Sci. Technol.*, 40, 2784-2789.

- Mielke, H.W., Powell, E.T., Gonzales, C.R., and Mielke, P.W. (2006) Hurricane Katrina's impact on New Orleans soils treated with low lead Mississippi river alluvium. *Environ. Sci. Technol.* 40 (24), 7623-7628.
- Mielke, H.W., Powell, E.T., Gonzales, C.R., Mielke, P.W., Ottesen, R.T., and Langedal M. (2006) New Orleans Soil Lead (Pb) Cleanup Using Mississippi River Alluvium: Need, Feasibility and Cost. *Environ. Sci. Technology.*, 40(08), 2784-9.
- Mielke, H.W., Powell, E.T., Shah, A., Gonzales, C.R. and Mielke, P.W. (2001) Multiple Metal Contamination from house paints: Consequences of power sanding and paint scraping in New Orleans. *Environmental Health Perspective*, 109(9), 973-978.
- Mielke H.W., Smith M.K., Gonzales C.R. and Mielke P.W. (1999) The urban environment and children's health: soils as an integrator of lead, zinc and cadmium in New Orleans, Louisiana, USA. *Environ Res*, 80(2), 117–29.
- Mielke Jr., P.W. and Berry, K.J. (2007) Permutation Methods: a Distance Function Approach, second ed. *SpringerVerlag*, New York.
- Miinyev, V.G., Kocketavkin, A., and Nguyen, V.B. (1990) Use of natural zeolites to prevent heavy metal pollution of soils and plants. *Soviet Soil Science*, 22, 72-79.

- Miller, D.D. and Schriker B.R. (1982) In vitro estimation of food iron bioavailability. In: *Nutritional bioavailability of iron. ACS Symp Ser*, 203, 10–25.
- Mitchell, R.L. "In: Trace Elements in Soils and Crops (Tech. Bull. 21)," In: Nriagu, J.O., Ed., *The Biogeochemistry of Lead in the Environment*, part A. Elsevier/North Holland Biomedical Press, The Netherlands, 1978.
- Miranda, M., Kim, D., Galeano, M., Paul, C., Hull, A., and Morgan, S. (2007). The relationship between early childhood blood lead levels and performance on end-of-grade tests. *Environ. Health Perspect.*, 115, 248-1253.
- Miretzky, P. and Fernandez-Cirelli, A. (2008) Phosphates for immobilization in soils: a review. *Environ. Chem. Lett.*, 6, 121-133.
- Miretzky, P. and Fernandez-Cirelli (2007) A Phosphates for Pb immobilization in soils: a review, *Environmental Chem. Lett*, Springer-Verlag.
- Morrison et al. (2013) Spatial relationships between lead sources and children's blood lead levels in the urban center of Indianapolis (USA). *Environ. Geochem. Health*, 35, 171-183.
- Mosby, D.E. (2000) Reductions of lead bioavailability in soil to swine and fescue by addition of phosphate. Unpublished master's thesis, University of Missouri-Columbia.

- Mukerjee, D. (1998) Assessment of risk from multimedia exposures of children to environmental chemicals, *Air Waste Manage. Assoc.*, 48, 483–501.
- Namasivayam, C. and Kadirvelu, K. (1997) Agricultural solid wastes for the removal of heavy metals: Adsorption of Cu(II) by coirpith carbon. *Chemosphere*, 34, 377–399.
- Netzer, A. and Hughes, D.E. (1984) Adsorption of copper, lead and cobalt by activated carbon. *Water Res.*, 18, 927–933.
- Nevin, R. (2000) How lead exposure relates to temporal changes in IQ, violent crime, and unwed pregnancy. *Environ Res.*, 83, 1–22.
- Nigg, J., Knottnerus, G., Martel, M., Nikolas, M., Cavanagh, K., Karmaus, W., and Rappley, M. (2008) Low blood lead levels associated with clinically diagnosed attention-deficit/hyperactivity disorder and mediated by weak cognitive control. *Biol. Psych.*, 63, 325-331.
- Nigg, J., Nikolas, M., Knottnerus, G., Cavanagh, K., and Friderici, K. (2010) Confirmation and extension of association of blood lead with attention-deficit/hyperactivity disorder (ADHD) and ADHD symptom domains at population-typical exposure levels. *J. Child Psychol. Psychiat. Allied Disciplin.*, 51, 58-65.
- Nriagu, J.O. (1974) Lead orthophosphates—IV. Formation and stability in the environment. *Geochimica et Cosmochimica Acta*, 38, 887–898.

- Nriagu, J.O., Ed., *The Biogeochemistry of Lead in the Environment, part A*. Elsevier/North Holland Biomedical Press, The Netherlands, 1978.
- Nriagu, J.O., P.B., Moore. Eds., *Phosphate Minerals*. Springer-Verlag, Burlington, 1984.
- OEHHA (2007) Development of Health Criteria for Schools Site Risk Assessment Pursuant to Health and Safety Code Section 901(g): Proposed Child-Specific Benchmark Change in Blood Lead Concentration for School Site Risk Assessment.
- OEHHA (2009) Revised California Human Health Screening Level for Lead in Soil. California Office of Environmental Health Hazard Assessment.
- Olson, Kelly. Cosmetics in Roman Antiquity: Substance, Remedy, Poison. *The Classical World* , 102(3) (SPRING 2009), 294-298.
- Olson, K.W. and Skogerboe, R.K. (1975) Identification of soil lead compounds from automotive sources. *Environmental Science and Technology*, 9(3), 227-230.
- Oomen, A.G., Hack, A., Minekus, M., Zeijdner, E., Cornelis, C., Schoeters, G., et al. (2002) Comparison of five in vitro digestion models to study the bioaccessibility of soil contaminants. *Environmental Science and Technology*, 36, 3326-3334.

- Owenby, D.R., Galvan, K.A., and Lydy, M.J. (2005) Lead and zinc bioavailability to *Eisenia fetida* after phosphate amendment to repository soils. *Env. Pollut.*, 136, 315-321.
- Paustenbach, D. (2000) The practice of exposure assessment: a state-of-the-art review. *Journal of Toxicology and Environmental Health B* 3, 179-291.
- Pearson, M.S., Maenpaa, K., Pierzynski, G.M. and Lydy, M.J. (2000) Effects of soil amendments on the bioavailability of lead, zinc, and cadmium to earthworms. *J. Environ. Qual.*, 29, 1611–1617.
- Phosphate Induced Metal Stabilization (PIMS) (2000) Summary of apatite remediation results from Bunker Hill and Success Mine for Pb, Cd, Zn and Cu. Retrieved September 23, 2011, from www.ufaventures.com/ufa_ventures/tech_briefs/apatite.html
- Pierzynski, G.M. and Schwab, A.P. (1993) Bioavailability of zinc, cadmium, and lead in a metal contaminated alluvial soil. *Journal of Environmental Quality*, 22, 247-254.
- Porter, S.K., Scheckel, K.G., Impellitteri, C.A., and Ryan, J.A. (2004) Toxic metals in the environment: thermodynamic considerations for possible immobilization strategies for Pb, Cd, As, and Hg. *Crit. Rev. Env. Sci. Technol.*, 34, 495-604.

- Puls, R.W., Powell, R.M., Clark, D. and Eldred, C.J. (1991) Effect of pH, solid/solution ratio, ionic strength, and organic acids on Pb and Cd sorption on kaolinite. *Water, Air, and Soil Pollution*, 57-58, 423-430.
- Rabinowitz, M.B. (1993) Modifying soil lead bioavailability by phosphate addition. *Bull. Environ. Contam. Toxicol* 51, 438-444.
- Reagan P.L. and Silbergeld E.K. (1990) Establishing a health based standard for lead in residential soils. In: Hemphill, Cothorn, editors. *Trace Subst. Environ. Health*, Supplement, *Environ Geochem Health*, 12, 199–238.
- Rebedda, I. and Lepp, N.W. (1994) The use of synthetic zeolites to reduce plant metal uptake and phytotoxicity in two polluted soils. In D. C. Adriano, Z. S. Chen, & S. S. Yang (Eds.), *Biogeochemistry of trace elements Northwood, England: Science Reviews*, 81-87.
- Rodriguez, R.R., Basta, N.T., Casteel, S.W., et al. (1999) An in vitro gastrointestinal method to estimate bioavailable arsenic in contaminated soils and solid media. *Environ Sci Technol*, 33, 642–649.
- Rosner, D. and Markowitz, G. (2012) With the best intentions lead research and the challenge to public health, *American Journal of Public Health*, 102(11), 19-33.
- Roy, A., Bellinger, D., Hu, H., Schwartz, J., Wright, R., Palaniappan, K., Balakrishnan, K. (2008). Lead associated deficits in executive function

and behavior in 3-7 year old children in Chennai, India. *Epidemiology* 19, S306.

Royal Commission on Environmental Pollution (RCEP) (1983) Lead in the environment ninth report. HMSO, London.

Ruby, M.V. (2004) Bioavailability of soil-borne chemicals: Abiotic assessment tools. *Human and Ecological Risk Assessment*, 10, 647-656.

Ruby, M.V., Davis, A. and Nicholson, A. (1994) In situ formation of lead phosphates in soils as a method to immobilize lead. *Environ Sci. Technol.* 28, 646-654.

Ruby, M.V., Davis, A., Link, T.E., et al. (1993) Development of an in vitro screening test to evaluate the in vivo bioaccessability of ingested mine-waste lead. *Environ Sci Technol*, 27, 2870–2877.

Ruby, M.V., Davis, A., Schoof, R., Eberle S. and C.M. Sellstone (1996) Estimation of lead and arsenic bioavailability using a physiologically-based extraction test, *Environ. Sci. Technol.* **30(2)**, 422–430.

Ruby, M.V., Schoof, R., Brattin, W., Goldade, M., Post, G. Harnois M., et al. (1999) Advances in evaluating the oral bioavailability of inorganics in soil for use in human health risk assessment, *Environ. Sci. Technol.* **33**, 3697–3705.

Ryan, J. and Berti, W. (2001) Conclusions from the In-Place Inactivation and Natural Ecological Restoration (IINERT) Joplin Field Trial. Presented at

the Annual Meeting of the Soil Science Society of America, Charlotte, NC.

Ryan, J.A., Berti, W.R., Brown, S.L., Casteel, S.W., Chaney R.L. and Doolan M. *et al.* (2004) Reducing children's risk from soil lead: Summary of a field experiment, *Environ. Sci. Technol.* **38**, 18A–24A.

Ryan, J.A., Zhang, P.C., Hesterberg, D., Chou, J. and Sayers, D.E. (2001) Formation of chloropyromorphite in a lead-contaminated soil amended with hydroxyapatite. *Environ. Sci. Technol.*, *35*, 3798–3803.

Ryan, K., Zhang, P., Hesterberg, D., Chou, J. and Sayers, D. (2001) Formation of chloropyromorphite in a lead-contaminated soil amended with hydroxyapatite. *Environ. Sci. Technol.*, *35*, 3798–3803.

Salt, D.E., Prince, R.C., Pickering, I.J. and Raskin, I. (1995) Mechanisms of cadmium mobility and accumulation in Indian mustard. *Plant Technology*, *109*, 1427-1433.

Sappin-Didier, V., Mench, M., Gomez, A. and Lambrot, C. (1997) Use of inorganic amendments for reducing metal bioavailability to ryegrass and tobacco in contaminated soils. In A. Iskandar & D. C. Adriano (Eds.), *Remediation of soils contaminated with metals* Northwood, England: Science Reviews, 85-98.

- Sauve', S., Marti'nez, C., McBride, M. and Hendershot, W. (2000) Adsorption of free lead (Pb^{2+}) by pedogenic oxides, ferrihydrite and leaf compost. *Soil Sci Soc Am J*, 64, 595–599.
- Scheinost, A., Abend, S., Pandya, K. and Sparks, D. (2001) Kinetic controls on Cu and Pb sorption by ferrihydrite. *Environ. Sci. Technol.*, 35, 1090–1096.
- Scheckel, K.G., and Ryan, J.A. (2002) Effects of aging and pH on dissolution kinetics and stability of chloropyromorphite. *Environ. Sci. Technol.*, 36, 2198-2204.
- Scheckel, K.G., and Ryan, J.A. (2004) Spectroscopic speciation and quantification of lead in phosphate-amended soils. *J. Environ. Qual.*, 33, 1288–1295.
- Schofield, P.F., Valsami-Jones, E., Hodson, M.E. and Mosselmans, J.F.W. (2001) Identification of metal phosphates in bone meal remediated contaminated soil using EXAFS. SRS, 1-4.
- Schoof et al. (1995) An assessment of lead absorption from soil affected by smelter emissions. *Environmental Geochemistry and Health*, 17(4), 189-199.
- Schoof, R.A. and Freeman, G.B. (1995) Poster presented at the Seventh International Congress of Toxicology, Seattle, WA.
- Schwartz, J. (1994) Low-level lead exposure and children's IQ: a meta-analysis and search for a threshold. *Environ. Res.*, 65(1), 42-5.

- Seaman, J., Arey, J. and Bertsch, P. (2001) Immobilization of Ni and other metals in contaminated sediments by hydroxyapatite addition. *J. Environ. Qual.*, 30, 460–469.
- Shashkova, I., Rat'Ko, A. and Kitikova, N. (1999) Removal of heavy metal ions from aqueous solutions by alkaline-earth metal phosphates. *Colloids Surf A Physicochem Eng Asp*, 160, 207–215.
- Shevade, A.V., Erickson, L., Pierzynski, G., and Jiang, S. (2001) Formation and stability of substituted pyromorphite: a molecular modeling study. *J. Hazard. Subst. Res.*, 3, 2.1-2.12.
- Shuman, L.M. (1997) Amelioration of zinc toxicity in cotton using lime or mushroom compost. *Journal of Soil Contamination*, 6, 425-438.
- Simon, D.L., Maynard, E.J. and Thomas, K.D. (2007) Living in a sea of lead – changes in blood and hand-lead of infants living near a smelter. *J. Expo. Sci. Environ. Epidemiol.*, 17, 248–259.
- Skerfving, S. and Bergdahl, I.A. "Lead," In: G.F. Nordberg, B. A. Fowler, M. Nordberg and L. T. Friberg, Eds., *Handbook on the Toxicology of Metals*, 3rd Edition, Academic Press, Burlington, 2007.
- Smith, W.H. "J. Air Pollut. Control Assoc.," In: Nriagu, J.O., Ed., *The Biogeochemistry of Lead in the Environment, part A*. Elsevier/North Holland Biomedical Press, The Netherlands, 1978.

- Sneddon, I., Orueetxebarria, M., Hodson, M., Schofield, P. and Valsami-Jones, E. (2006) Use of bone meal amendments to immobilize Pb, Zn and Cd in soil: a leaching column study. *Environ Pollut.*, 144, 816–825.
- Srinivasan, M., Ferraris, C. and White, T. (2006) Cadmium and lead ion capture with three dimensionally ordered macroporous hydroxyapatite. *Environ. Sci. Technol.*, 40,7054–7059.
- Surkan, P., Zhang, A., Trachtenberg, F., Daniel, D., McKinlay, S., and Bellinger, D. (2007) Neuropsychological function in children with blood lead levels < 10 µg/dL. *Neurotoxicology* 28, 1170-1177.
- Suzuki, Y., Kyoichi, I. and Miyake, M. (1981) Synthetic hydroxyapatites employed as inorganic cation-exchangers. *J Chem. Soc Faraday Trans.*, 77, 1059–1062.
- Swaine, D.J., and Mitchell, R.L. (1960) Trace-element distribution in soil profiles. *J. Soil Sci.*, 11, 347-387.
- Takeuchi, Y. and Arai, H. (1990) Removal of coexisting Pb²⁺, Cu²⁺ and Cd²⁺ ions from water by addition of hydroxyapatite powder. *J. Chem. Eng. Jpn.*, 23, 75–80.
- Tang, X.Y., Zhu, Y.G., Chen, S.B., Tang, L.L., and Chen, X.P. (2004) Assessment of the effectiveness of different phosphorous fertilizers to remediate Pb-contaminated soil using in vitro test. *Environment International*, 30, 531-537.

- Téllez-Rojo, M. M., Bellinger, D. C., Arroyo-Quiroz, C., Lamadrid-Figueroa, H., Mercado-García, A., Schnaas-Arrieta, L., Wright, R. O., Hernández-Avila, M., and Hu, H. (2006) Longitudinal associations between blood lead concentrations < 10 µg/dL and neurobehavioral development in environmentally-exposed children in Mexico City. *Pediatrics* 118, 323-330.
- Ter Harr, G. and Aronow, "Environ. Health Prespect.," In: Nriagu, J.O., Ed., *The Biogeochemistry of Lead in the Environment, part A*. Elsevier/North Holland Biomedical Press, The Netherlands, 1978.
- Ter Harr, G.L. and Bayard, M.A. (1971) *Nature*, 232, 553.
- Thornton, I., Davies, D.J.A., Watt, J.M. and Quinn, M.J. (1990) Lead exposure in young children from dust and soil in the United Kingdom. *Environmental Health Perspectives*, 89, 43-48.
- Tornabene, T.G. and Edwards, H.W. (1972) *Science*, 176, 1334.
- Traina, S.J. and Laperche, V. (1999) Contaminant bioavailability in soils, sediments, and aquatic environments. *Proc. Natl. Acad. Sci. USA*, 96, 3365–3371.
- U.S. Department of Agriculture (USDA) (1999). Soil taxonomy a basic system of soil classification for making and interpreting soil surveys by Soil Survey Staff. 2nd Edition. Washington, DC.

U.S. Department of Health and Human Services (2000) Healthy People 2010, Understanding and improving health, Washington, DC: US Department of Health and Human Services.

United States Environmental Protection Agency (USEPA) (2014). Human exposure and atmospheric sciences. CHAD-2000 retrieved 10/28/2014 from <http://www.epa.gov/heads/chad2000.html>.

United States Environmental Protection Agency (USEPA) (2007) Guidance for evaluating the oral bioavailability of metals in soils for use in human health risk assessment. pp. 1-18.

United States Environmental Protection Agency (US EPA) (1991) Leachability phenomena. Recommendations and rationale for analysis of contaminant release by the Environmental Engineering Committee. EPA-SAB-EEC-92-003. Washington, DC: Author.

United States Environmental Protection Agency (US EPA) (1997b, March) Recent developments for in situ treatment of metal contaminated soils. EPA-542-R-97-004. Washington, DC: Author.

United States Environmental Protection Agency (US EPA) (2008) Standard operating procedure for an in vitro bioaccessibility assay for lead in soil. EPA 9200, 1-86.

- United States Environmental Protection Agency (USEPA) (2013). Technical review workgroup recommendations regarding gardening and reducing exposure to lead-contaminated soils. p. 2-23.
- United States Environmental Protection Agency (US EPA) (2000a) Technology alternatives for the remediation of soils contaminated with As, Cd, Cr, Hg, and Pb. Engineering Bulletin. Washington, DC: Author. Retrieved September 27, 2011, from <http://www.epa.gov/swertio1/download/remed/tdtchalt.pdf>
- USEPA (1986) Test Methods for the Evaluation of Solid Waste: Laboratory Manual Physical Chemical Methods: Method 3051: Microwave Assisted Acid Digestion of Sediments, Sludges, Soil and Oils, vol. IA. Washington, DC 204607 Office of Solid Waste.
- United States Environmental Protection Agency (US EPA) (1997a) Test methods for evaluating solid waste physical/chemical methods, SW-846. Revised methods. Version 2. Integrated Manual/Update III. Washington, DC: Author.
- USEPA (1993) Urban Soil Lead Abatement Demonstration Project Volume I: integrated report. EPA 600/AP-93/001a.
- USEPA (2001a) Lead-Safe Yards developing and implementing a monitoring, assessment, and outreach program for your community. EPA/625/R-00/012.

- USEPA (2001b) Requirements for QAPPs. EPA QA/R 5, EPA/240/B 01/003.
- USEPA (2006) Air Quality Criteria for Lead, Volume I. Research Triangle Park, NC: National Center for Environmental Assessment – RTP Office.
EPA/600/R-5/144aF. October. Available at:
<http://cfpub.epa.gov/ncea/cfm/recordisplay.cfm?deid=158823>.
- U.S. Federal Register (2001) Part III, *Environmental Protection Act*, 40 CFR Part 745. Lead: Identification of Dangerous Levels of Lead; Final Rule. Vol 66, No 4, January 5, 2001/Final Rules and Regulations.
- Van Borm, W., Wouters, L., Van Grieken, R. and Adams, F. (1990) Lead particles in an urban atmosphere: An individual particle approach. *The Science of the Total Environment*, 90, 55-66.
- Vangronsveld, J. and Cunningham, S. (Eds.). (1998) *Metal-contaminated soils: In situ inactivation and phytoremediation*. Georgetown, TX: Springer-Verlag and R.G. Landes Company.
- Warren, H.V., Delavault, R. E. and Cross, C.H. "Trace Substances in the Environ. Health," In: Nriagu, J.O., Ed., *The Biogeochemistry of Lead in the Environment, part A*. Elsevier/North Holland Biomedical Press, The Netherlands, 1978.
- Weber, M. A., K. A. Barbarick, and D. G. Westfall. 1984. Application of clinoptilolite to soil amended with sewage sludge. *Zeo-Agriculture: Use of*

- Natural Zeolites in Agriculture and Aquaculture. W. F. Pond and F. A. Mumpton (Eds.) Westview Press, Boulder, CO.
- Weis, C.P. and LaVelle, J.M. (1991) Characteristics to consider when choosing an animal model for the study of lead bioavailability. *Chemical Speciation and Bioavailability*, 3, 113-119.
- Weatherbill (2014). Top 10 rainiest US cities and the one billion dollar question. www.weatherbill.com/reports/rainstudy. Retrieved from internet in November 4/2014.
- Wixson, B.G. and Davies, B.E. (1994) Guidelines for lead in soil. *Environ. Sci. Technol.*, 28(1), 26A-31A.
- Wragg, J. and Cave, M.R. (2002) In-vitro methods for the measurement of the oral bioaccessibility of selected metals and metalloids in soil. Crit Rev R&D Technical Report P5-062/TR/01.
- Wright, J, Rice, K.R., Murphy, Brain., and Conca, J.L, (2004) PIMS Using Apatite II: Remediation of Pb-Contaminated Range Soil At Camp Stanley Storage Activity, TX. In Sustainable Range Management - 2004. Proceedings of the Conference on Sustainable Range Management. January 5-8, 2004, New Orleans.
- Wright, J.P., Dietrich, K.N., Ris, M.D., Hornung, R.W., Wessel, S.D., Lanphear, B.P., et al. (2008) Association of prenatal and childhood blood lead

- concentrations with criminal arrests in early adulthood. *PLoS Med.*, 5(5), 101.
- Wu, J., Edwards, R., He, X.E., Liu, Z. and Kleinman M. (2010) Spatial analysis of bioavailable soil lead concentrations in Los Angeles, California. *Environ Res*, 110, 309–17.
- Xenidis, A., Stouraiti, C. and Paspaliaris, I. (1999) Stabilization of oxidic tailings and contaminated soils by calcium oxyphosphate addition: The case of Montevecchio (Sardinia, Italy). *Journal of Soil Contamination*, 8, 681-697.
- Xiong, Z.T. (1997) Bioaccumulation and physiological effects of excess lead in a roadside pioneer species, *Sonchus oleraceus*. *Environmental Pollution*, 97(3), 275.
- Xu, Y. and Schwartz, F.W. *J. Contam. Hydrol.*, in press.
- Xu, Y. and Schwartz, F.W. (1994) Lead immobilization by hydroxyapatite in aqueous solutions. *J. Contam. Hydrol.*, 15, 187-206.
- Yang, J., Mosby, D.E., Casteel, S.W. and Blanchard, R.W. (2001) Lead immobilization using phosphoric acid in a smelter-contaminated urban soil. *Environ. Sci. Technol.*, 35, 3553-3559.
- Yang, J., and Mosby, D.E. (2006) Field assessment of treatment efficacy by three methods of phosphoric acid application in lead-contaminated urban soil. *Sci. Total Environ.*, 366, 136-142.

- Zahran, S., Mielke, H.W., Gonzales, C.R., Powell, E.T., and Weiler, S. (2010)
New Orleans after hurricanes Katrina/Rita: a quasi-experiment of the
associations between soil lead and children's blood lead. *Environ. Sci.
Technol.* 33, 4433-4440.
- Zahran, S., Mielke, H.W., Weiler, S., Berry, K.J. and Gonzales, C. (2009)
Children's blood lead and standardized test performance response as
indicators of neurotoxicity in metropolitan New Orleans elementary
schools. *Neurotoxicol.*, 30, 888-897.
- Zahran, S., Mielke, H.W., Weiler, S. and Gonzales, C.R. (2011) Nonlinear
associations between blood lead in children, age of child, and quantity of
soil lead in metropolitan New Orleans. *Sci. Total Environ.*, 7, 1211-1218.
- Zahran, S., Mielke, H.W., Weiler, S., Hempel, L. and Berry, K.J. (2012)
Associations between standardized school performance tests and mixtures
of Pb, Zn, Cd, Ni, Mn, Cu, Cr, Co, and V in community soils of New
Orleans. *Environmental Pollution*, 169, 128-135.
- Zhang, P. and Ryan, J.A. (1999a) Transformation of Pb(II) from cerrusite to
chloropyromorphite in the presence of hydroxyapatite under varying
conditions of pH. *Environmental Science & Technology*, 33, 625-630.
- Zhang, P. and Ryan, J.A. (1999b) Formation of chloropyromorphite from galena
(PbS) in the presence of hydroxyapatite. *Environmental Science &
Technology*, 34, 618-624.

- Zhang, P., Ryan, J.A. and Bryndzia, L.T. (1997) Pyromorphite formation from goethite adsorbed lead. *Environ Sci Technol.*, 31, 2673-2678.
- Zhang, P., Ryan, J.A., and Yang, J. (1998) In Vitro Soil Pb in the presence of Hydroxyapatite. *Environ. Sci. Technol.*, 32, 318–332.
- Zia, M.H., Codling, E.E., Scheckel, K.G. and Chaney, R.L. (2011) *In vitro* and *in vivo* approaches for the measurement of oral bioavailability of lead (Pb) in contaminated soils: a review. *Environmental Pollution*, 159, 2320-2327.
- Ziegler et al. (1978) Absorption and retention of lead by infants. *Pediat. Res.*, 12, 29-34.
- Zimdahl, R.L. and Skogerboe, R.K. (1977) Behavior of lead in soil. *Environmental Science and Technology*, 11(13), 1202-1207.

Biographical Information

Dhary Saad Alkandary was born on January 30, 1982 in Kuwait City, Kuwait. Dhary grew up in AlSha'ab area, Kuwait City and graduated from Ahmed Al Basher Al Romi high school in 1999. He attended the Kuwait University where he earned a bachelor of Earth and Environmental Science degree in geology in June 2006. After graduation, he worked for the Ministry of Interior for a year. In 2007, Dhary worked for Kuwait Oil Company (KOC) for a year as a geologist and in 2008 he worked as a teacher assistant in the Department of Earth and Environmental Science for a year. Returning to full-time university studies in 2009, Dhary entered the Master of Science program at the University of Texas at Arlington under the supervision of Dr. Andrew Hunt. He earned his Master's degree in Earth and Environmental in 2010. He joined the Ph.D. program and worked on his research for four years. He earned his doctoral degree in Earth and Environmental Science in 2014. Dhary will teach at Kuwait University and continue his publications and research in land deterioration and soil remedy.